REGIONAL EARTHQUAKE LOSS ESTIMATION: ROLE OF TRANSPORTATION NETWORK, SENSITIVITY AND UNCERTAINTY, AND RISK MITIGATION

by

Erdem Karaca

B.S., Civil Engineering,
Bogazici University, Istanbul, Turkey (1999)

M.S., Civil Engineering,
Massachusetts Institute of Technology, Cambridge, Massachusetts (2002)

Submitted to the Department of Civil and Environmental Engineering
in Partial Fulfillment of the Requirements for the Degree of

DOCTOR OF PHILOSOPHY IN CIVIL ENGINEERING

at the

Massachusetts Institute of Technology

June 2005

Signature of Author .....
Department of Civil and Environmental Engineering
May 19, 2005

Certified by .....
Daniele Veneziano
Professor of Civil and Environmental Engineering
Thesis Supervisor

Accepted by .....
Andrew J. Whittle
Chairman, Departmental Committee for Graduate Students

Regional Earthquake Loss Estimation: Role of Transportation Network, Sensitivity and Uncertainty, and Risk Mitigation

by

Erdem Karaca

Submitted to the Department of Civil and Environmental Engineering on May 19, 2005
in Partial Fulfillment of the Requirements for the
Degree of Doctor of Philosophy in the Field of Civil Engineering

ABSTRACT

Large earthquakes near densely populated areas such as the 1994 Northridge and 1995 Kobe events have caused extensive damage to the physical infrastructure and losses to the regional and national economies. Economic losses are due in part to direct damage and in part to business interruption caused by non-functioning infrastructure and interdependencies among industrial sectors.

We developed a regional earthquake loss methodology that emphasizes economic interdependencies at regional and national scales and the mediating role of the transportation network. In an application to the Central U.S. under threat from earthquakes from the New Madrid Seismic Zone, we (1) evaluate regional and national losses from scenario earthquakes, (2) quantify uncertainty on the losses through loss risk curves including contributions from seismicity, attenuation, fragilities, etc. and (3) assess the effectiveness of alternative mitigation strategies. The loss assessment methodology includes spatial interactions (through the transportation network) and business interaction (through an input-output model) and extends geographically to the entire conterminous U.S. The losses reflect damage to buildings and transportation components, reduced functionality, changes in the level of economic activity in different economic sectors and geographical regions, and the speed of the reconstruction/recovery process.

Evaluation of losses for a number of scenario earthquakes indicates that losses from business interruption may be as significant as infrastructure repair costs. The overall loss is also contributed by the increase in transportation costs due to network damage. As part of the uncertainty evaluation, we assess the sensitivity of earthquake losses to various component models and model parameters. Using a detailed model of regional seismicity, scenario earthquake building losses, and a relation between business losses and building losses, we develop risk curves for building losses, business losses, and total economic losses. The results underline the importance of considering uncertainty in risk assessment. Finally, we investigate the effectiveness of alternative loss mitigation strategies such as retrofitting of buildings or bridges and faster recovery of functionality for various occupancy classes or bridges. For a number of cases, we develop loss risk curves for mitigated conditions and calculate expected annual losses, which might be used for rational decision making e.g. through cost-benefit comparison.

Thesis Supervisor: Daniele Veneziano
Title: Professor of Civil and Environmental Engineering

ACKNOWLEDGMENTS

I would like to express my sincerest gratitude to my thesis supervisor Prof. Daniele Veneziano for his invaluable guidance and support throughout these years. It has been a privilege and my good fortune to work under his supervision. His constant encouragement, friendliness, and most importantly patience made this endeavor possible. I sincerely thank him for sharing his wealth of knowledge and expertise. His inspiration and motivation will guide me for the rest of my life.

I would like to also thank Prof. Joseph Sussman and Prof. Robert V. Whitman for taking the time to serve in my thesis committee and for their valuable comments and suggestions.

I gratefully acknowledge the financial support provided by the National Science Foundation through the Mid-America Earthquake Center.

Special thanks are extended to the staff of the Department of Civil and Environmental Engineering at MIT for their support and friendship over the years.

There are numerous friends and coworkers that made the MIT experience more bearable and enjoyable. I would like to thank Alberto, Basak, Cagatay, Ching, David, Emre, Isil, Julija, Karim, Kartal, Maria, Metin, Namik, Oguz, Onnik, Ozgun, Phani, Tzu-Yang, and many others for their friendship over the years. I will always remember your kindness and support.

I am grateful to my parents for everything they have done for me. It is not possible for me to express my gratitude to them. I also thank my brother Ersin for his love and support. I miss you all.

Finally, I am most grateful to my wife Zekiye for her constant encouragement, support, and love. Thank you for your patience and many sacrifices you have endured over the years. I am so lucky to have you with me at every important step of my personal and professional life. Thank you for believing in me and always being there.

TABLE OF CONTENTS

1 INTRODUCTION 19

1.1 Objectives 20

1.2 Thesis Organization 21

2 REGIONAL SEISMIC LOSS ESTIMATION: A LITERATURE REVIEW 23

2.1 General Methodology of Seismic Loss Estimation 23

2.1.1 Hazard Analysis 24

2.1.2 Local Site Effects 25

2.1.3 Exposure Information 26

2.1.4 Vulnerability Analysis 26

2.1.5 Determination of Seismic Risk 28

2.2 Seismic Loss Estimation for Building Stocks 29

2.2.1 Loss Estimation through Visual Screening 30

2.2.2 Loss Estimation through Approximate Structural Analyses 30

2.2.3 Detailed Loss Estimation through Linear Analyses Methods 31

2.2.4 Detailed Loss Estimation using Nonlinear (Pushover) Analysis Methods 32

2.3 Regional Loss Estimation Including Transportation Network 33

2.4 Sensitivity and Uncertainty in Loss Estimation 37

2.4.1 Losses from a Single Building 37

2.4.2 Losses from a Portfolio of Buildings 38

2.4.3 Regional Losses 39

2.5 Concluding Remarks 41

3 SEISMIC LOSS ESTIMATION METHODOLOGY 43

3.1 General Framework 43

3.2 Analysis Regions and Transportation Network 46

3.2.1 Building Analysis Regions 46

3.2.2 Transportation Network 48

3.2.3 Economic Analysis Regions 56

3.3 Inventory, Classifications, and Other Data 57

3.3.1 Building Inventory 57

3.3.2 Bridge Inventory 65

3.3.3 Soil Conditions 66

3.3.4 Economic Data 69

3.4 Component Models 81
3.4.1 Ground Motion Attenuation Relationships 83
3.4.2 Site Amplification Model 97
3.4.3 Building Vulnerability Model 106
3.4.4 Bridge Vulnerability Model 128
3.4.5 Loss of Functionality and Recovery Model 129
3.4.6 Transportation Network and Regional Economic Analysis Model 137
3.4.7 Economic losses 144
3.5 Concluding Remarks 146

4 SCENARIO EARTHQUAKE LOSSES AND SENSITIVITY ANALYSIS 149
4.1 Scenario Earthquake Loss 149
4.1.1 Ground Motion Intensity 149
4.1.2 Building Damage and Loss 152
4.1.3 Bridge Damage and Loss 158
4.1.4 Transportation Link Functionality and Flows 160
4.1.5 Economic Losses 163
4.2 Sensitivity analysis 165
4.2.1 Sensitivity to Earthquake Location 166
4.2.2 Sensitivity to Earthquake Magnitude 174
4.2.3 Sensitivity to Ground Motion Attenuation 178
4.2.4 Sensitivity to Site Amplification 184
4.2.5 Sensitivity to Soil Conditions 189
4.2.6 Sensitivity to Building Code Levels 195
4.2.7 Sensitivity to Expected Mean Building Vulnerability 199
4.2.8 Sensitivity to Variation in Mean Building Vulnerability 200
4.2.9 Sensitivity to Functionality of Structural and Nonstructural Building Components 208
4.2.10 Sensitivity to Functionality and Recovery Interactions 210
4.2.11 Sensitivity to Rerouting 213
4.2.12 Sensitivity to Reconstruction Spending 213
4.2.13 Sensitivity to Cost of Borrowing 213
4.2.14 Sensitivity to Slack in Production Capacity 217
4.3 Concluding Remarks 220

5 UNCERTAINTY ASSESSMENT AND LOSS-RISK CURVES 223
5.1 Risk Curves for Building Losses 223
5.1.1 Uncertainty of Scenario Earthquake Losses 223
5.1.2 Building Loss Risk Curves from Regional Seismicity 226
5.1.3 Building Loss Risk Curves Including Model and Parameter Uncertainty 234

5.2 Risk Curves for Business Losses 236
5.2.1 Relation between Business and Building Losses 238
5.2.2 Business Loss Risk Curves 240
5.2.3 Total Loss Risk Curves 242
5.3 Assigning Hazard Consistent Rates to Scenario Earthquakes 244
5.3.1 Proposed Methodology 246
5.3.2 Application to NMSZ and Shelby County 250
5.3.3 Results for Shelby County and the NMSZ Region 250
5.4 Concluding Remarks 256

6 EVALUATION OF MITIGATION STRATEGIES 259
6.1 Pre-Earthquake Mitigation Strategies 259
6.1.1 Retrofitting of Buildings 259
6.1.2 Retrofitting of Bridges 270
6.2 Post-Earthquake Mitigation Strategies 272
6.2.1 Faster Recovery of Buildings 273
6.2.2 Faster Recovery of Bridges 275
6.3 Concluding Remarks 276

7 SUMMARY, CONCLUSIONS AND FUTURE WORK 279
7.1 Summary and Conclusions 279
7.2 Future Research Directions 284

REFERENCES 287

LIST OF FIGURES

Figure 2-1: Deterministic Hazard Analysis 24
Figure 2-2: Probabilistic Hazard Analysis 25
Figure 2-3: Site-Specific Response Spectra Based on Soil Shear Wave Velocity 26
Figure 2-4: A Structural Inventory Classification System (ATC, 1985; NIBS, 2000) 27
Figure 2-5: Structural Vulnerability and Damage States for Various Levels of Seismic Demand 28
Figure 2-6: Uncertainties in Seismic Performance and Use of Fragility Curves 29
Figure 2-7: Data Needed for Various Levels of Analysis and Risk Assessment 30
Figure 2-8: Seismic Evaluation of Buildings Using Nonlinear Analysis 32
Figure 2-9: Tornado Diagram Showing Results of Sensitivity Analysis from Porter et al (2002) 38
Figure 2-10: Mean Return Period of Losses for a Portfolio of Structures from Bazzurro and Luco (2004) 40
Figure 3-1: CUS Analysis Regions Used in Model 1 49
Figure 3-2: Close up of the NMSZ Analysis Regions Used in Model 1 49
Figure 3-3: Close up of the NMSZ Analysis Regions Used in Model 2 50
Figure 3-4: Close up of the NMSZ Analysis Regions Used in Model 3 50
Figure 3-5: Comparison of Population, Total Square Footage, and Area Weighted Centroids of NMSZ Counties 52
Figure 3-6: Highway Links around NMSZ Included both in Model 1 and Model 2 52
Figure 3-7: Transportation Network Links and Nodes Used in Transportation Network Model 1 53
Figure 3-8: Transportation Network Links and Nodes Used in Transportation Network Model 2 53
Figure 3-9: Transportation Network Model 1 Links and Nodes around CUS 54
Figure 3-10: Transportation Network Model 2 Links and Nodes around CUS 54
Figure 3-11: Transportation Network Model 1 Highway Bridges 55
Figure 3-12: Transportation Network Bridges around Shelby County 55
Figure 3-13: Economic Analysis Regions in CUS for Transportation Network 1 58
Figure 3-14: Economic Analysis Regions in CUS for Transportation Network 2 58
Figure 3-15: Economic Analysis Regions in NMSZ for Building Analysis Region Model 1 59
Figure 3-16: Economic Analysis Regions in NMSZ for Building Analysis Region Model 3 59
Figure 3-17: Economic Analysis Regions outside CUS for Transportation Network 1 60
Figure 3-18: Economic Analysis Regions outside CUS for Transportation Network 2 60
Figure 3-19: CUS Coverage of Soil Classification Maps (Bauer, 1997) 68
Figure 3-20: NMSZ Coverage of Soil Classification Maps (Bauer, 1997) 68
Figure 3-21: Comparison of CEUS Attenuation Relations for PGA, M=8.0 94
Figure 3-22: Comparison of CEUS Attenuation Relations for Sa(1.0sec), M=8.0 94
Figure 3-23: Comparison of Attenuation Relations for PGA, M=8.0 95
Figure 3-24: Comparison of Attenuation Relations for Sa(1.0sec), M=8.0 95
Figure 3-25: Comparison of Attenuation Relations for PGA, M=7.0 96
Figure 3-26: Comparison of Attenuation Relations for Sa(1.0sec), M=7.0 96
Figure 3-27: Comparison of Short Period Spectral Acceleration Factors for Site Class C 107

Figure 3-28: Comparison of Short Period Spectral Acceleration Factors for Site Class D 107
Figure 3-29: Comparison of Long Period Spectral Acceleration Factors for Site Class C 108
Figure 3-30: Comparison of Long Period Spectral Acceleration Factors for Site Class D 108
Figure 3-31: Example Building Capacity, Demand, and Fragility Curves 109
Figure 3-32: Example Building Capacity Curve and Control Points (Kircher et al, 1997a) 110
Figure 3-33: Example Intersection of Building Capacity Curves and Demand Spectra (Kircher et al, 1997a) 112
Figure 3-34: Joint Probability Surface of Demand and Capacity Intersection Points (Kircher et al, 1997a) 118
Figure 3-35: Representation of the Vulnerability Model Used 124
Figure 3-36: Comparison of HAZUS and Derived Fragility Curves (Low Code URML) 127
Figure 3-37: Comparison of Mean Damage Factors (Low Code URML) 127
Figure 3-38: Comparison of Attenuation of Damage for an NBI Material Class 2 Bridge 132
Figure 3-39: Comparison of Attenuation of Damage for an NBI Material Class 1 Bridge 132
Figure 4-1: Location of Scenario Earthquake 150
Figure 4-2: Estimated (a) Sa(0.3sec) and (b) Sa(1.0sec) in CUS for Scenario Earthquake 151
Figure 4-3: Estimated (a) Sa(0.3sec) and (b) Sa(1.0sec) in NMSZ for Scenario Earthquake 151
Figure 4-4: Estimated (a) Sa(0.3sec) and (b) Sa(1.0sec) in Shelby County for Scenario Earthquake 151
Figure 4-5: Ratio of Sa(1.0sec) to Sa(0.3sec) for Scenario Earthquake 152
Figure 4-6: Distribution of Building Losses with Distance for Scenario Earthquake 155
Figure 4-7: Distribution of Normalized Building Losses with Distance for Scenario Earthquake 155
Figure 4-8: Spatial Distribution of Building Losses in NMSZ 156
Figure 4-9: Spatial Distribution of Normalized Building Losses in NMSZ 156
Figure 4-10: Spatial Distribution of Building Losses in Shelby County 157
Figure 4-11: Spatial Distribution of Normalized Building Losses in Shelby County 157
Figure 4-12: Bridge Damage around NMSZ 159
Figure 4-13: Bridge Damage around Shelby County 159
Figure 4-14: Functionality of Links around NMSZ at (a) Day 1, (b) Day 7, (c) Day 30, and (d) Day 180 160
Figure 4-15: Functionality of Links around Shelby County at (a) Day 1, (b) Day 7, (c) Day 30, and (d) Day 180 161
Figure 4-16: Pre-Earthquake Link Capacity Utilization around (a) NMSZ Region and (b) Shelby County 162
Figure 4-17: Link Capacity Utilization around Shelby County at (a) Day 1, (b) Day 7, and (c) Day 180 163
Figure 4-18: Distribution of Building Losses with Distance for Different Scenario Earthquakes 172
Figure 4-19: Distribution of Normalized Building Losses with Distance for Different Scenario Earthquakes 172
Figure 4-20: Distribution of Value Added Losses with Distance for Different Scenario Earthquakes 173
Figure 4-21: Distribution of Normalized Value Added Losses with Distance for Different Scenario Earthquakes 173
Figure 4-22: Distribution of Building Losses with Distance for Different Earthquake Magnitudes 177

Figure 4-23: Distribution of Normalized Building Losses with Distance for Different Earthquake Magnitudes 177
Figure 4-24: Distribution of Value Added Losses with Distance for Different Earthquake Magnitudes 179
Figure 4-25: Distribution of Direct Value Added Losses with Distance for Different Earthquake Magnitudes 179
Figure 4-26: Distribution of Normalized Value Added Losses with Distance for Different Earthquake Magnitudes 180
Figure 4-27: Distribution of Building Losses with Distance for Different Attenuation Relations 183
Figure 4-28: Distribution of Normalized Building Losses with Distance for Different Attenuation Relations 183
Figure 4-29: Distribution of Value Added Losses with Distance for Different Attenuation Relations 185
Figure 4-30: Distribution of Normalized Value Added Losses with Distance for Different Attenuation Relations 185
Figure 4-31: Distribution of Building Losses with Distance for Different Soil Amplification Models 188
Figure 4-32: Distribution of Normalized Building Losses with Distance for Different Soil Amplification Models 188
Figure 4-33: Distribution of Value Added Losses with Distance for Different Soil Amplification Models 190
Figure 4-34: Distribution of Normalized Direct Value Added Losses with Distance for Different Soil Amplification Models 190
Figure 4-35: Ratio of NEHRP Short Period Soil Amplification Factors 194
Figure 4-36: Ratio of NEHRP Long Period Soil Amplification Factors 194
Figure 4-37: Distribution of Building Losses with Distance for Different Building Code Levels 198
Figure 4-38: Distribution of Normalized Building Losses with Distance for Different Building Code Levels 198
Figure 4-39: Comparison of Building Losses for Different Code Levels to Baseline Scenario at Different Distances 199
Figure 4-40: Distribution of Building Losses with Distance for Different Mean Seismic Vulnerability 203
Figure 4-41: Distribution of Normalized Building Losses with Distance for Different Mean Seismic Vulnerability 203
Figure 4-42: Comparison of Building Losses for Different Mean Seismic Vulnerability 204
Figure 4-43: Distribution of Building Losses with Distance for Different Variance in Mean Seismic Vulnerability 207
Figure 4-44: Comparison of Building Losses for Different Variance in Mean Seismic Vulnerability 207
Figure 4-45: Total Slack Used in Pre-earthquake state 219
Figure 5-1: Importance Factors for Scenario Earthquake M700_3550_9000 227
Figure 5-2: Importance Factors for Scenario Earthquake M750_3550_9000 227
Figure 5-3: Importance Factors for Scenario Earthquake M800_3550_9000 228
Figure 5-4: Importance Factors for Scenario Earthquake M750_3600_9000 228
Figure 5-5: Loss Risk Curves for Shelby County and the NMSZ Region - Partial Rupture of NMSZ Faults 232
Figure 5-6: Loss Risk Curves for Shelby County and the NMSZ Region– Complete Rupture of NMSZ Faults 232
Figure 5-7: Relative Contribution of Seismic Sources to EAL of Shelby County and the NMSZ Region. 234

Figure 5-8: Relative Contribution of Distributed Seismicity to EAL of Shelby County and the NMSZ Region 234
Figure 5-9: Relative Contribution of NMSZ Characteristic Earthquakes to EAL of Shelby County – Partial Rupture of NMSZ Faults 235
Figure 5-10: Relative Contribution of NMSZ Characteristic Earthquakes to EAL of the NMSZ Region – Partial Rupture of NMSZ Faults 235
Figure 5-11: Relative Contribution of NMSZ Characteristic Earthquakes to EAL of Shelby County – Complete Rupture of NMSZ Faults 235
Figure 5-12: Building Loss Risk Curves for Shelby County and the NMSZ Including Parameter/Model Uncertainty (Point Source Distributed Seismicity, Partial Rupture of NMSZ Faults) 237
Figure 5-13: Building Loss Risk Curves for Shelby County and the NMSZ Including Parameter/Model Uncertainty (Point Source Distributed Seismicity, Complete Rupture of NMSZ Faults) 237
Figure 5-14: Total Value Added Loss vs Total Building Loss in Shelby County 239
Figure 5-15: Total Value Added Loss vs Total Building Loss in NMSZ Region 239
Figure 5-16: Value Added Loss Risk Curves for Shelby County and the NMSZ Including Parameter/Model Uncertainty (Point Source Distributed Seismicity, Partial Rupture of NMSZ Faults) 241
Figure 5-17: Value Added Loss Risk Curves for Shelby County and the NMSZ Including Parameter/Model Uncertainty (Point Source Distributed Seismicity, Complete Rupture of NMSZ Faults) 241
Figure 5-18: Total Loss Risk Curves for Shelby County and the NMSZ Including Parameter/Model Uncertainty (Point Source Distributed Seismicity, Partial Rupture of NMSZ Faults) 243
Figure 5-19: Total Loss Risk Curves for Shelby County and the NMSZ Including Parameter/Model Uncertainty (Point Source Distributed Seismicity, Complete Rupture of NMSZ Faults) 243
Figure 5-20: Seismic Hazard Curve for Memphis, TN 253
Figure 5-21: Building Loss Risk Curves for Shelby County and the NMSZ Region, Case 1 254
Figure 5-22: Value Added Loss Risk Curves for Shelby County and the NMSZ Region, Case 1 255
Figure 6-1: Reduced Loss Risk Curves for Shelby County and the NMSZ Region, All Buildings Upgraded to High-Code Level, Complete Rupture of NMSZ Faults 262
Figure 6-2: Reduced Loss Risk Curves for Shelby County and the NMSZ Region Including Parameter Uncertainty, All Buildings Upgraded to High-Code Level, Complete Rupture of NMSZ Faults 262
Figure 6-3: Retrofitted Routes (a) Route 1, Memphis Interstate Highway Links, (b) Route 2, Section of I-40 Connecting Memphis to Nashville, (c) Route 3, Section of I-40 Connecting Memphis to Little Rock, AR, and (d) Route 4, Section of I-55 Connecting Memphis to St. Louis, MO. 271
Figure 6-4: Link Capacity Utilization Ratios around Shelby County in Pre-Earthquake State 273

LIST OF TABLES

Table 2-1: Comparison of Seismic Loss Estimation Models 36
Table 3-1: Number of Building Analysis Regions in CUS 47
Table 3-2: Number of Economic Analysis Regions 57
Table 3-3: Building Occupancy Classes (HAZUS) 62
Table 3-4: Building Structure (Model Building) Types (HAZUS) 63
Table 3-5 : Distribution Percentage of Floor Area for Model Building Types within Each Building Occupancy Class, Low-Rise, Tennessee (HAZUS, 2000) 64
Table 3-6: Distribution Percentage of Floor Area for Model Building Types within RES1 Building Occupancy Class for Seven CUS States (HAZUS) 65
Table 3-7: Site Classes (from the 1997 NEHRP Provisions) 67
Table 3-8: Economic Sectors Used (Okuyama et al, 1999) 70
Table 3-9: The Make of Commodities by Industries, 1997 ($B/year) 71
Table 3-10: The Use of Commodities by Industries, 1997 ($B/year) (cont. in next page) 72
Table 3-11: The Use of Commodities by Industries (after Modification), 1997 ($B/year) 75
Table 3-12: The Input-Output Matrix, A 77
Table 3-13: Mapping of CFS Commodities to Economic Sectors 82
Table 3-14: Mapping of Economic Sectors into Building Occupancy Classes 82
Table 3-15: Ground Motion Relations Used in 2002 USGS National Seismic Hazard Maps (Campbell, 2004) 85
Table 3-16: Coefficients for Atkinson and Boore (1995, 1997) Attenuation Relation 90
Table 3-17: Log of Ground Motion Parameters in g for M=8.0 as a Function of log Distance (Frankel et al., 1996) 90
Table 3-18: Coefficients for Toro et al (1997) Attenuation Relation 90
Table 3-19: Coefficients for Somerville et al (2001) Attenuation Relation 93
Table 3-20: Coefficients for Campbell (2003) Attenuation Relation 93
Table 3-21: NEHRP Short Period Soil Amplification Factors, F_A 100
Table 3-22: NEHRP Long Period Soil Amplification Factors, F_V 100
Table 3-23: Modified Amplification Factors for Dobry et al (2000) 103
Table 3-24: Modified Amplification Factors for Hwang et al (1997) 104
Table 3-25: Modified Amplification Factors for Borcherdt (2002) 105
Table 3-26: Mean Damage/Loss Factors (HAZUS, 2000) 116
Table 3-27 : Unit Building Replacement Costs (NIBS, 2000) 120
Table 3-28 : Relative Percentages of Building Replacement Costs (HAZUS, 2000) 121
Table 3-29: Bridge Classification Used in HAZUS for Non-California Bridges 130
Table 3-30: Bridge Classification Used in Hwang et al (2000) 131
Table 3-31: Bridge Classification Used in Desroches (2002) 131
Table 3-32: Mapping of NBI Material Classes to Classifications in Different Bridge Fragility Evaluation Studies 131
Table 3-33 : Functionality Interaction Coefficients 138

Table 3-34 : Recovery Interaction Coefficients 139
Table 4-1: Building Losses for Scenario Earthquake 154
Table 4-2: Percent Building Losses for Scenario Earthquake 154
Table 4-3: Bridge Losses for Scenario Earthquake 158
Table 4-4: Economic Losses for Scenario Earthquake 164
Table 4-5: Percent Economic Losses for Scenario Earthquake 164
Table 4-6: Component Models and Parameters Considered in Sensitivity Analysis 167
Table 4-7: Sensitivity of Building Losses to Earthquake Location 169
Table 4-8: Sensitivity of Bridge Losses to Earthquake Location 169
Table 4-9: Sensitivity of Economic Losses to Earthquake Location 170
Table 4-10: Sensitivity of Building Losses to Earthquake Magnitude 175
Table 4-11: Sensitivity of Bridge Losses to Earthquake Magnitude 175
Table 4-12: Sensitivity of Economic Losses to Earthquake Magnitude 176
Table 4-13: Sensitivity of Building Losses to Attenuation Relations 181
Table 4-14: Sensitivity of Bridge Losses to Attenuation Relations 181
Table 4-15: Sensitivity of Economic Losses to Attenuation Relations 182
Table 4-16: Sensitivity of Building Losses to Soil Amplification 186
Table 4-17: Sensitivity of Bridge Losses to Soil Amplification 186
Table 4-18: Sensitivity of Economic Losses to Soil Amplification 187
Table 4-19: Sensitivity of Building Losses to Soil Conditions 191
Table 4-20: Sensitivity of Bridge Losses to Soil Conditions 191
Table 4-21: Sensitivity of Economic Losses to Soil Conditions 192
Table 4-22: Sensitivity of Building Losses to Building Code Level 196
Table 4-23: Sensitivity of Economic Losses to Building Code Level 197
Table 4-24: Sensitivity of Building Losses to Mean Building Vulnerability 201
Table 4-25: Sensitivity of Economic Losses to Mean Building Vulnerability 202
Table 4-26: Sensitivity of Building Losses to Variation in Mean Building Vulnerability 205
Table 4-27: Sensitivity of Economic Losses to Variation in Mean Building Vulnerability 206
Table 4-28: Sensitivity of Economic Losses to Weights Assigned to Functionality of Structural and Nonstructural Components 209
Table 4-29: Sensitivity of Economic Losses to Functionality and Recovery Interactions 211
Table 4-30: Sensitivity of Economic Losses to Selected Functionality and Recovery Interactions 212
Table 4-32: Sensitivity of Economic Losses to Rerouting 214
Table 4-33: Sensitivity of Economic Losses to Reconstruction Spending and Repayment 215
Table 4-34: Sensitivity of Economic Losses to Total Borrowing Costs 216
Table 4-35: Sensitivity of Economic Losses to Available Slack in Production 218
Table 4-36: Summary of Sensitivity Results for Building Losses 222
Table 5-1: Scenario Earthquakes Used in ANOVA 224
Table 5-2: Factors Considered in ANOVA 225
Table 5-3: Summary of Results for Scenario Earthquake Uncertainty Assessment 226
Table 5-4: EAL for Shelby County and the NMSZ Region 233

Table 5-5: Hazard Consistent Scenario Earthquake Probabilities 251
Table 5-6: Ratios of Calculated to Given Ground Motion Exceedance Frequencies 252
Table 5-7: Summary of EALs for Shelby County and the NMSZ Region 257
Table 6-1: Building Inventory Value for Different Building Occupancy and Structural Classes 260
Table 6-2: Building Losses for Retrofitted Buildings 261
Table 6-3: Business Losses for Retrofitted Building Structural Classes 264
Table 6-4: Building Losses for Retrofitted Building Occupancy Classes 265
Table 6-5: Business Losses for Retrofitted Building Occupancy Classes 266
Table 6-6: Building Losses for Retrofitted Building Structural Classes 268
Table 6-7: Business Losses for Retrofitted Building Structural Classes 269
Table 6-8: Transportation Losses for Retrofitted Bridges on Selected Links 272
Table 6-9: Business Losses for Faster Recovery of Building Occupancy Classes 274
Table 6-10: Transportation Losses for Faster Recovery of Bridges on Selected Links 275

1 Introduction

Recent earthquakes near urban areas, such as 1994 Northridge and 1995 Kobe earthquakes, have caused extensive physical damage to buildings and utility networks (Chang and Nojima, 2001). Damage to the built environment resulted in significant direct losses (e.g. repair and replacement costs) and indirect losses (e.g. losses due to decrease in economic activity). The performance of lifelines such as the transportation, water, and electricity networks both immediately after the earthquake and over time has affected the indirect economic losses. Among these lifelines, the transportation network is of critical importance since it provides the medium for transfer of personnel and materials required for recovery, repair and reconstruction. Moreover, recent earthquakes have shown that transportation networks, in particular bridges, have high seismic vulnerability (Caltrans, 1994; BTS, 1998; Chang and Nojima, 2001).

Although California and the Pacific Northwest constitute major earthquake concerns in United States due to their known seismicity, the Central United States (CUS) region is also at risk due to relatively infrequent but high magnitude characteristic events. Some of the greatest earthquakes in the U.S. history occurred in 1811-1812 near New Madrid, Missouri with estimated moment magnitudes between M7.0 and M8.0, causing extensive damage and loss of lives (Johnston, 1996). In general, it is more difficult to quantify seismic risk in the CUS than in the Western U.S. due to low seismicity and limited knowledge on intra-plate earthquakes compared to plate boundary earthquakes. An important difference between the two regions is the lower attenuation of seismic waves in the CUS, which for the same earthquake magnitude tends to cause more widespread damage. Moreover, buildings and bridges in the CUS were not generally designed for seismic resistance until the 1990s; hence, there is a large inventory of vulnerable structures in the CUS, which might suffer damage also from moderate and large magnitude earthquakes. The CUS is an important economic center for commodity trade and flow. Based on 1993 Commodity Flow Survey data, the value of annual commodity shipments related to nine Midwest states is estimated to be about $2,000-4,000B with about 40-45 percent of the exports/imports taking

place among these states (Okuyama et al, 1999; BTS, 1997). In addition, important highway connections between the Northeast U.S. to Western U.S. pass through this region; hence interruption of the highway network in CUS would have negative effects on the economies of these regions as well.

Due to the relatively large inventory of seismically vulnerable structures and the amount of economic activities in the region, there is the potential of having major economic losses from future seismic events in the CUS region. In order to get better prepared for such events and reduce the resulting economic losses, it is important be able to reliably estimate the physical damage and economic losses from possible earthquakes. This is a challenging task, especially when networks are considered due to the nonlinear dependence of their functionality on damage. Earthquake loss estimation involves many complexities and uncertainties related to earthquake occurrence, the effects of ground motion on the built environment, and the resulting direct and indirect economic losses. The indirect economic losses depend not only on induced damage, but also on the post-earthquake recovery rate, which in turn is affected by the capacity limitations of the damaged transportation network. Finally, the interaction among different economic sectors and geographic regions (mediated by the transportation network) makes it difficult to isolate regions or components of the system for analysis purposes. Due to these complexities, previous loss estimation studies have generally limited their scope and approach or confined themselves to a specific geographical scale.

1.1 Objectives

There are three main objectives of this study: (1) to evaluate economic losses from scenario earthquakes at regional/national scales with special consideration for the effect of the transportation network vulnerability; (2) to assess earthquake loss uncertainties at different temporal and spatial scales, and (3) to evaluate pre- and post-earthquake loss mitigation measures. While the methodology is conceptually applicable to any region, applications are specifically developed for the Central U.S. (CUS) region using corresponding data and parameters. It models regional economy and transportation network in an integrated manner. A variety of loss measures including building losses, business losses, and increased transportation costs are evaluated. The methodology is modular, flexible, and computationally efficient. Numerical efficiency allows one to use this methodology for sensitivity and uncertainty analysis.

Using scenario earthquake losses, their uncertainty, and a model of regional seismicity, we develop loss risk curves for building losses, business losses, and total economic losses.

Finally, we evaluate the effectiveness of pre- and post-earthquake mitigation strategies. Pre-earthquake mitigation alternatives studied include retrofitting of different types of buildings and the strengthening of bridges on selected links. Post earthquake mitigation strategies considered are faster recovery for various building occupancy classes or for bridges on selected transportation routes.

1.2 Thesis Organization

The remainder of this thesis is organized as follows:

Chapter 2 provides a review of the literature on seismic loss estimation. Methodologies that use different levels of analysis detail are presented. This is followed by a review of regional loss estimation studies that consider losses due to business interruption or transportation network damage in addition to building losses. Finally, work on uncertainty in seismic losses assessment is summarized.

Chapter 3 describes the general framework and component models of the seismic loss estimation methodology developed in this study. The methodology is based on HAZUS (NIBS, 2000) and the work of Kunnumkal (2002), Veneziano et al. (2002), and Jammalamadaka (2003), although some modifications and additions have been made in many areas. The resulting methodology is more comprehensive than many existing ones and includes: (1) damage to buildings and road transportation system components, (2) functionality of buildings, industrial sectors, and road transportation system components and their recovery over time, (3) economic losses associated with repair/restoration of damaged structures, (4) economic losses due to business interruption and economic gains from increased production, and (5) increased costs due to damage to the transportation system.

Chapter 3 describes the sources of data and classification schemes used in this study, including building inventory, bridge inventory, soil classification maps, economic data, and related classifications. The chapter also provides a detailed explanation of the component models used in the loss estimation methodology: the attenuation relationships, soil amplification model, building vulnerability model, bridge vulnerability model, loss of functionality and recovery model, and

the transportation network and regional economic analysis model. For each component, we first provide a general description of the model and then give details on the data and parameters selected for application to New Madrid Seismic Zone (NMSZ) earthquakes.

In **Chapter 4**, we apply the loss estimation methodology of Chapter 3 to a scenario earthquake and assess the sensitivity of the losses to various components or parameters of the methodology. We first present the results for a moment magnitude M7.5 NMSZ earthquake. We specifically discuss the level and spatial distribution of: ground motion intensity, building damage and loss, bridge damage and loss, transportation link functionality and flows, and business interruption losses. Next, we investigate the sensitivity of the losses to alternative models and parameters in various parts of the loss estimation methodology with the objective of identifying the models/variables that most significantly affect the results or contribute to the overall uncertainty in the loss. The models/variables considered are related to the earthquake scenario, ground motion intensity, building vulnerability, transportation network, functionality of industrial facilities, and economic analysis.

In **Chapter 5**, we quantify uncertainty in the losses for various regions in the CUS and in the nation as a whole. We first quantify uncertainty in the building losses under scenario earthquakes. Then we include uncertainty in future earthquake occurrences and develop loss risk curves for building losses. Based on the observation that business losses are closely related to building losses, we generate loss risk curves for value added losses using the risk curves for building losses. These loss risk curves are used to quantify expected annual losses. Finally, we assess a simplified methodology to generate loss risk curves using a limited number of scenario earthquakes and regional seismic hazard data.

Chapter 6 evaluates the effectiveness of alternative pre- and post-earthquake loss mitigation strategies. Pre-earthquake mitigation strategies include retrofitting of different types of buildings and the hardening of bridges on selected transportation links. Retrofitted buildings may belong to a certain structural type or to a certain building occupancy class. Post-earthquake mitigation strategies considered include faster recovery of buildings and bridges.

Chapter 7 summarizes our main findings and conclusions and makes recommendations for future work.

2 Regional Seismic Loss Estimation: A Literature Review

Recently, large earthquakes near urban areas, such as the 1994 Northridge and 1995 Kobe earthquakes, have caused extensive physical damage to buildings and utility networks. In addition to the direct costs due to damage to the built environment, these events have caused substantial economic losses due to disruption of regional economic activities over a period of time following their occurrence. Due to interregional and inter-industrial dependencies, the consequences of such damaging events may extend far beyond the immediately damaged region. Although there is a growing interest in these broader economic and social consequences of earthquakes, the literature has generally focused on the estimation of the direct losses from repair/restoration of structures and their contents.

This chapter reviews the literature on seismic loss estimation. First, a general overview of seismic loss estimation and its basic components is given. Then, estimation methodologies for building losses with different levels of detail are presented. This is followed by a review of studies regional loss studies. Finally, past work on uncertainty in seismic loss assessment is summarized.

2.1 General Methodology of Seismic Loss Estimation

Seismic risk assessment and loss estimation are essential tools for seismic hazard mitigation at regional and national scales. Knowing the seismic risk and potential losses of a region helps in raising public awareness and preparedness, allocating resources for mitigation and disaster management and prioritizing retrofit operations (EERI, 1997).

Components of seismic risk and loss estimation are (1) Hazard analysis; (2) Local site effects (microzonation); (3) Exposure information (structural inventory); (4) Vulnerability analysis; and

(5) Estimation of risk and loss (Coburn et al, 1994; CSSC, 1999; Chandler and Nelson, 2001; Bendimerad, 2001). These components are briefly described in the following subsections.

2.1.1 Hazard Analysis

Hazard analysis is the process of quantitatively estimating the likelihood of different ground motions at a site or in a region of interest based on the characteristics of surrounding seismic sources and the seismic wave propagation in geologic media. The study of earthquake hazard thus falls primarily within the disciplines of geology and seismology, with input from civil engineering (FEMA, 1989). In this respect, the term seismic hazard has a technical meaning restricted to the behavior of the ground, apart from any effects on the built environment. The basic methodology of hazard analysis comprises source modeling, wave attenuation, and local ground amplification. Seismic hazard may be analyzed deterministically (see Figure 2-1) for scenario earthquakes or probabilistically (see Figure 2-2) by explicitly considering the occurrence rate of earthquakes of different sizes and locations and the attenuation of ground motion with distance from the source (Kramer, 1996; Marcellini et al, 2001). Probabilistic seismic hazard analysis involves determining the probability of exceeding various specified

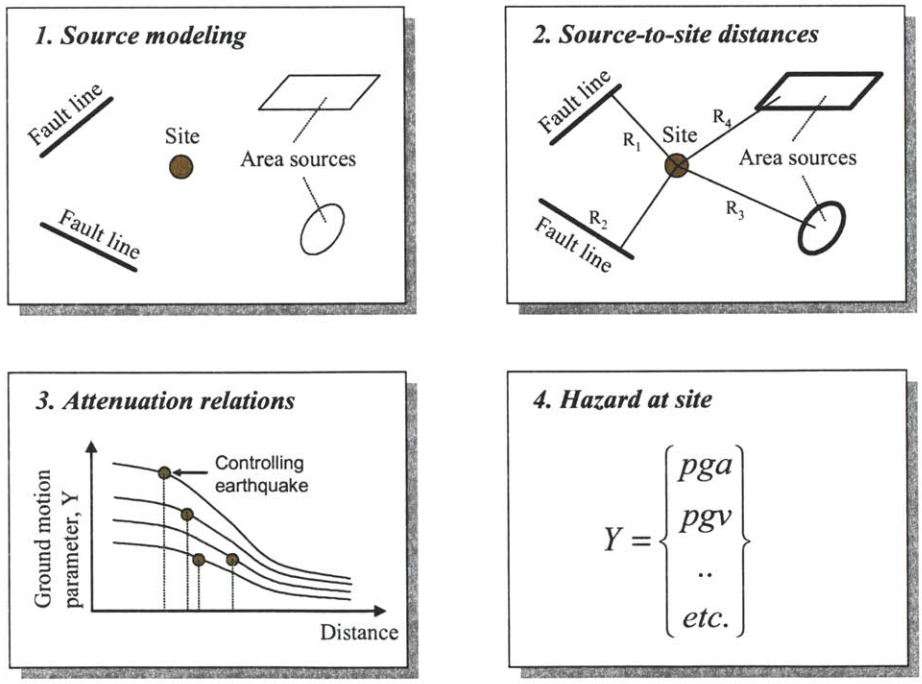

Figure 2-1: Deterministic Hazard Analysis

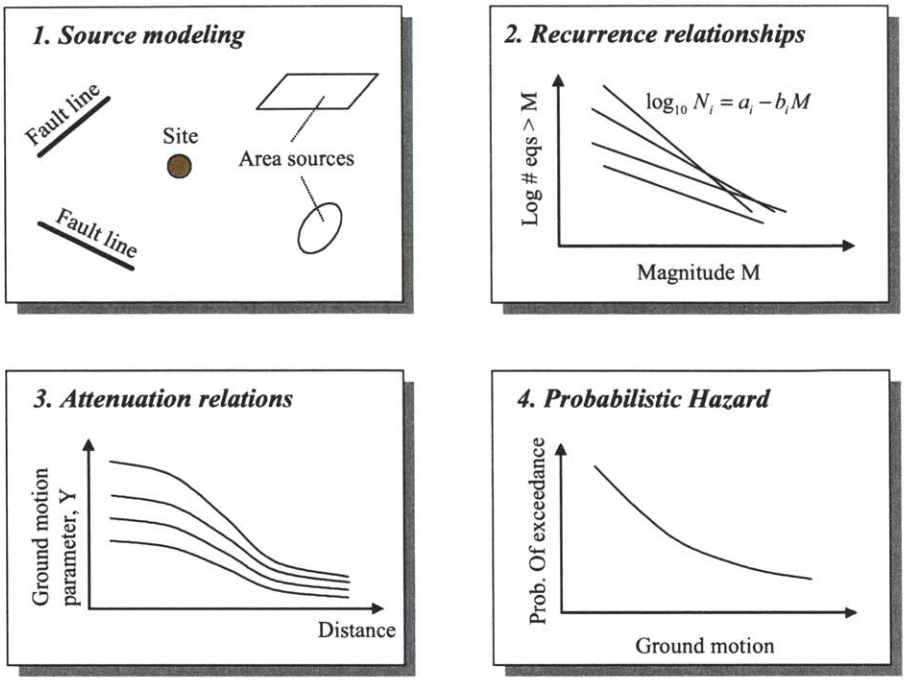

Figure 2-2: Probabilistic Hazard Analysis

ground motions. Accordingly, the output of hazard analysis is typically a curve showing the exceedance probabilities of various ground motions at a site or a hazard map showing the ground motion with a specific exceedance probability over a given time period in a region.

2.1.2 Local Site Effects

Local geologic and soil conditions can significantly influence ground motion characteristics such as the amplitude, frequency content, and duration of ground motion (Kramer, 1996, Marcellini et al., 2001). Therefore, the accurate assessment of local site conditions is essential to accurately determine the hazard curve. Consideration of the local site conditions results in the development of site-specific response spectra to be used for structural analysis and design. Figure 2-3(b) shows are typical response spectra for different soil conditions, which were determined based on the average soil shear wave velocity as illustrated in Figure 2-3(a). Seismic design codes including the International Building Code (IBC, 2000) classify soils into groups according to properties such as strength, penetration resistance, and shear wave velocity. Measuring these properties over a dense grid and combining them with hazard analysis on reference soil provides a detailed map that reveals not only the soil parameters required to obtain site-specific response

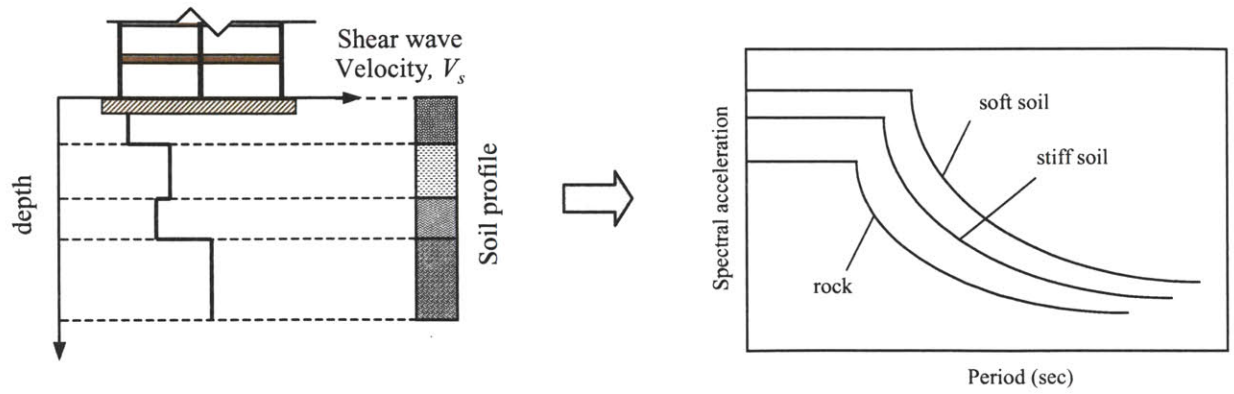

(a) Subsurface soil profile and shear wave velocity (b) Schematic response spectra for different soil conditions

Figure 2-3: Site-Specific Response Spectra Based on Soil Shear Wave Velocity

spectra, but also the potential for liquefaction and ground failure. The process of developing such detailed maps is called microzonation.

2.1.3 Exposure Information

By exposure we mean the value of structures and contents, business activities, lives and other valuables that may be subject to losses in a seismic event. Depending on the scope of the risk assessment study, exposure may include a single building with its occupants and contents, or at the other extreme all constructed facilities in a region including all buildings with their occupants and contents, lifelines, and utility systems. Building exposure information for a region requires the use of a systematic inventory system that classifies structures according to type and occupancy. Such data collection and classification system was developed for California and reported in ATC-13 (ATC, 1985). The same system was used in the HAZUS Earthquake Loss Estimation Methodology (NIBS, 2000); see summary in Figure 2-4.

2.1.4 Vulnerability Analysis

The vulnerability of a building or system measures the sensitivity of the building or system to exposure to seismic ground motion. The vulnerability of an element is usually expressed as a percentage loss (or as a value between zero and one) for a given hazard severity level (Coburn et al., 1994).

Multiple damage states are typically considered in a vulnerability analysis. Figure 2-5(a) shows the damage states of a building based on the applied base shear. The roof displacement – base

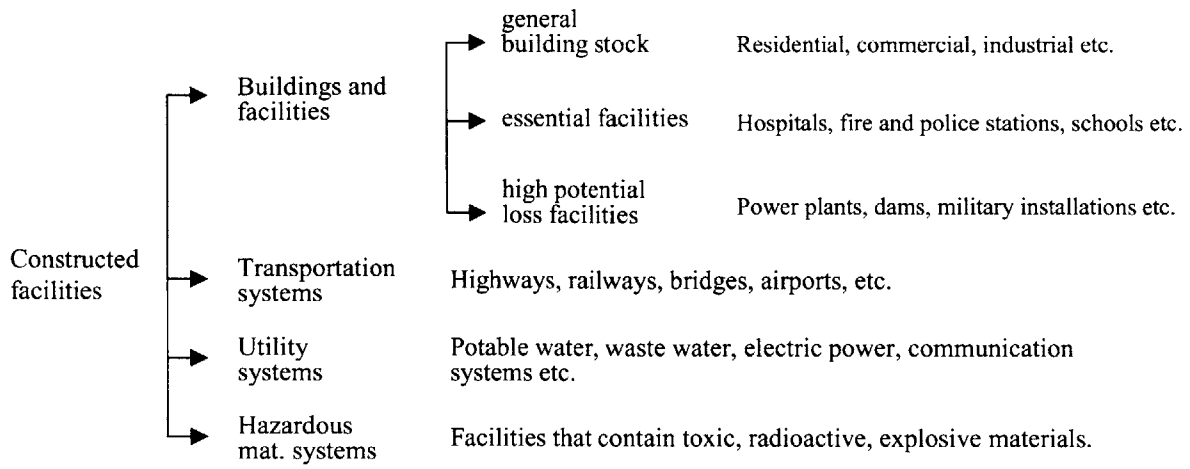

Figure 2-4: A Structural Inventory Classification System (ATC, 1985; NIBS, 2000)

shear curve, called the capacity curve, is also shown in this figure. The shape of the capacity curve reflects the nonlinear behavior of a building under increasing earthquake loads. A more convenient representation of the damage states is provided in Figure 2-5(b) where the building capacity and seismic demand curves are shown superposed. The intersection of the capacity and demand curves is the damage state likely to be experienced by the structure. As can be seen from the figure, a strong structure is likely to suffer light or moderate damage under low seismic demand, and moderate to extensive damage under high seismic demand. On the other hand, a weak structure is expected to suffer moderate to extensive damage under low seismic demand and collapse under high demand.

Methods of vulnerability analysis vary defending on the exposure information and the complexity of the approach they use. The seismic vulnerability of structures is often expressed in terms of fragility curves or damage functions that take into account the uncertainties in the seismic demand and capacity. Fragility functions can be developed for entire buildings or for individual structural components depending on the level of detail at which the analysis is performed. Early forms of fragility curves used qualitative ground motion intensities largely based on expert opinion. Recent advances in nonlinear structural analysis have enabled the development of fragility curves in terms of response spectrum parameters. Figure 2-6(a) shows typical seismic demand and structural capacity curves together with their uncertainties. Based on these curves and uncertainties, fragility curves of the type shown in Figure 2-6(b) can be constructed for various damage states. Since each damage level is associated with a

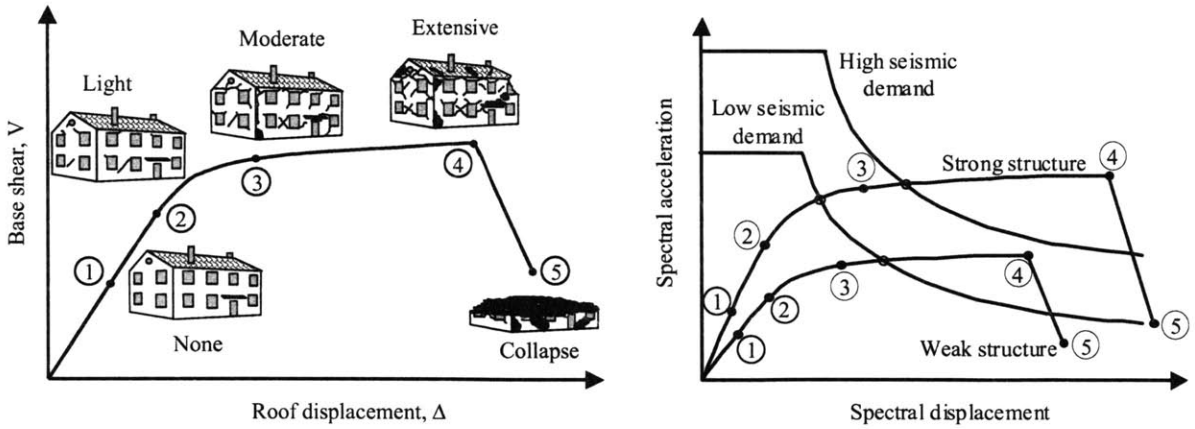

(a) Damage states shown on V-Δ curve (b) Damage levels based on seismic demand

Figure 2-5: Structural Vulnerability and Damage States for Various Levels of Seismic Demand

repair/replacement cost, the probabilistic estimates of the total cost can be estimated using these curves once the building response for a given hazard is evaluated. For this purpose, one may use representative fragility curves for structures in a given class, or custom damage curves for individual structures developed through nonlinear analysis.

The construction of fragility or damage curves is the key step in estimating the probability of various damage states for buildings or building components as a function of seismic demand on structure. Thus, the development of realistic fragility curves for buildings and lifelines in seismic regions constitutes an essential part of seismic risk analysis.

2.1.5 Determination of Seismic Risk

The standard definition of risk is the probability of damage or loss to a given element or facility, during a specified period of time. It is important to distinguish between risk and vulnerability. Risk combines the expected losses from all levels of ground motion severity whereas vulnerability is usually expressed as a function of ground motion severity (Coburn et al., 1994). Loss is defined as the human and financial consequences of damage, including injuries or deaths, monetary costs of repair, and the loss of revenue.

Hazard and risk are often used in the literature with different meanings. Here we adopt the standard terminology of the EERI Committee on Seismic Risk (1984). Specifically, seismic risk is the probability that social or economic consequences of earthquakes will equal or exceed specified values at a site, at several sites, or in an area, during a specified exposure time (EERI,

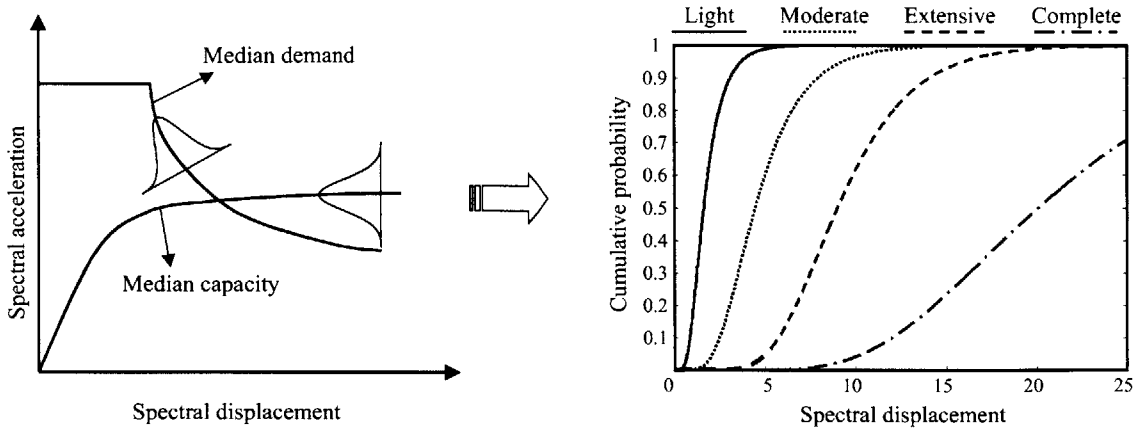

(a) Uncertainties in seismic capacity and demand (b) fragility curves for various damage states

Figure 2-6: Uncertainties in Seismic Performance and Use of Fragility Curves

1984). On the other hand, seismic hazard is any physical phenomenon associated with an earthquake that may produce adverse affects on human activities and vulnerability is the amount of damage or loss induced by a given level of hazard. Thus, while seismic hazard is purely a product of natural processes, seismic risk depends on the vulnerability and societal exposure (the built environment, population density, and the value of operations) (Dowrick, 2003).

2.2 Seismic Loss Estimation for Building Stocks

Seismic risk assessment and loss estimation for large building stocks can be conducted at various levels of detail depending on the objectives, size of the building stock, available time, and economic constraints. For a rapid and approximate assessment of general seismic risk and probable loss, a rapid visual screening of the building stock is sufficient to gather the necessary data. As the accuracy and reliability of the desired risk assessment study increases, more detailed soil and structural data become necessary. Figure 2-7 summarizes the site and structural information needed to conduct various levels of seismic risk assessment. In the following subsections, structural evaluation approaches of increasing accuracy and complexity are briefly described.

2.2.1 Loss Estimation through Visual Screening

Visual screening leads to a rapid evaluation of building stocks with minimal information requirement, suitable for an overall approximate risk assessment. In such a methodology, as

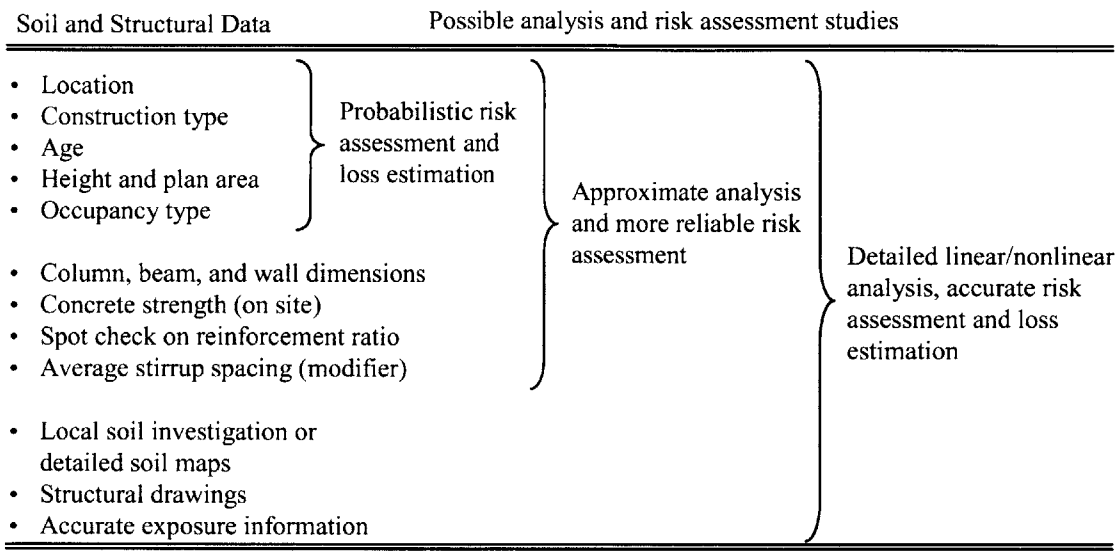

Figure 2-7: Data Needed for Various Levels of Analysis and Risk Assessment

reported in FEMA 154 (FEMA, 1988), the screened structures are assigned a score based on location, structural type, age, height, occupancy type, and visible irregularities. Subsequent risk assessment relies on statistical damage data from previous seismic events for various building classes. This methodology provides general information about the building stock, identifies buildings requiring priority attention due to serious structural irregularities, and allows for approximate risk and loss estimation. The main disadvantage is that little information can be obtained about the risk of individual buildings since the general risk assessment is based on statistical data.

2.2.2 Loss Estimation through Approximate Structural Analyses

Approximate structural analysis requires basic structural information such as the dimensions of columns, beams and shear walls, which can be determined from building drawings or measurements, usually on the ground floor. Where building drawings are not available, minimum reinforcement is assumed in the structural elements. Concrete strength is usually set to a conservative value, however, on site or laboratory measurement of concrete strength is more appropriate for buildings in areas known for variability in material properties. The lateral seismic design loads on the building are calculated using the static equivalent load method and distributed to the floors according to seismic codes. The calculated load demand is compared with the lateral load capacity of the floor determined either from individual analysis of each

member, or as a whole through a simplified analysis of the entire building system. The former requires distribution of the floor load to members according to their rigidities. Evaluation of the building is performed by means of a seismic index, I_s, determined as the ratio between the total allowable lateral load and the probable lateral seismic load demand

$$I_s = \frac{V_{all}}{V} \tag{2.1}$$

To save time, this evaluation is generally performed only for the ground floor. If it is performed for each floor, the most critical index among all floors is assigned for the building. Detailed information on approximate structural evaluation methods can be found in FEMA (1992, 1998), Scarlat (1996), and Hawkins (1986). An advantage of using an approximate structural evaluation, in addition to time saving compared to detailed analysis is the ability to perform a first level prioritization, based on the level of lateral load resistance, for subsequent more detailed analysis or retrofit application.

2.2.3 Detailed Loss Estimation through Linear Analyses Methods

Detailed evaluation through linear analysis is the most commonly used approach since most seismic codes (e.g. IBC, 2000) require these methods. Based on detailed structural information, member forces under design loads are determined and compared with their ultimate strength. It is thus possible to accurately determine the overstressed members under the design loads. However, it is difficult to assess the seismic risk of the entire building. Although this method is useful to prioritize deficient structures, it usually is insufficient to determine optimum retrofit strategies. The current trend is to use nonlinear analysis, which requires approximately the same amount of data, but more engineering effort and expertise compared to the approaches based on linear analysis.

2.2.4 Detailed Loss Estimation using Nonlinear (Pushover) Analysis Methods

Detailed evaluation using nonlinear analysis provides the most accurate assessment of risk and loss, at the expense of detailed site investigation, longer computation times, and a higher level of technical expertise. By considering the nonlinear inelastic behavior of structural members under increasing loads, this methodology can predict the nonlinear behavior of the structural system much more accurately than linear analysis. Figure 2-8(a) shows typical roof displacement vs.

base shear curve obtained from nonlinear pushover analysis of buildings. Using this curve alone, one can perform a preliminary evaluation of the structure's seismic safety by comparing its capacity with the seismic demand determined using the equivalent static load method of seismic codes. A better performance evaluation can be made by converting both the capacity curve and the seismic demand spectrum to the acceleration-displacement response spectrum (ADRS) format as shown in Figure 2-8 (b). A further improved evaluation can be achieved by obtaining a reduced inelastic response spectrum for the seismic demand to consider the increased damping due to inelastic deformations in the building (ATC, 1996).

The intersection of the capacity and demand curves shown in Figure 2-8 (b) is called the performance point of the building. Based on the location of this point, the performance level of the building is determined. Intervals of spectral displacement that correspond to different performance levels are shown in Figure 2-8 (b). The limits of the performance levels are usually in terms of interstory drift. If the performance point is located in the initial portion of the capacity curve where the inelastic deformations are not significant, (this corresponds to an interstory drift less than 0.01), the performance level of the building is "immediate occupancy". For interstory drift values between 0.01-0.02, the limits of which correspond to immediate occupancy and life safety levels, the performance level of the building is "damage control". In this region, inelastic deformations are expected but pose no significant threat to the stability of the building and the safety of its occupants. Between the life safety and structural stability levels,

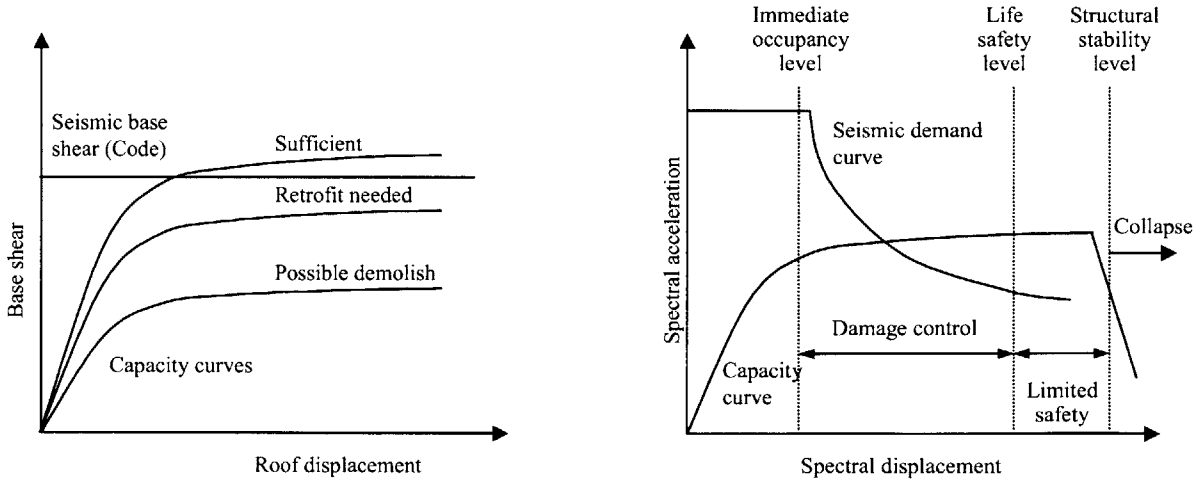

(a) Evaluation based on equivalent static load (b) Evaluation based on performance level

Figure 2-8: Seismic Evaluation of Buildings Using Nonlinear Analysis

the building performance level is described as "limited safety". Large inelastic deformations are expected, which may result in excessive cracking and failure of some structural members, posing threat to occupants or resulting in local failures. Beyond the structural stability level, the collapse of the building is imminent. From this discussion, it is apparent that nonlinear analysis is a very convenient methodology for the development of fragility curves as shown in Figure 2-6(b). However, nonlinear analysis methods are known to provide the most detailed information about structural performance. However, these methods also suffer from certain drawbacks, (Krawinkler and Seneviratna, 1997; Ghobarah, 2000).

2.3 Regional Loss Estimation Including Transportation Network

In contrast to loss estimation methods for individual structures, the level of detail that can be accomplished in regional seismic loss analysis is limited as a result of system size, computational requirements, limitations on available data, lack of complete knowledge, and other factors. This section reviews some of the previous studies on regional loss estimation, especially those that involve transportation network components and resulting losses. Some methodologies (e.g. ATC, 1985; NIBS, 2000) are comprehensive as they consider damage to buildings, bridges and utility network components and not limited to building losses. Others concentrate on specific systems such as the transportation network or consider only selected loss components depending on the objective of the study.

One of the earliest attempts of a comprehensive seismic loss estimation methodology is ATC-13, (ATC, 1985) which was developed for California. The ATC-13 methodology estimates earthquake damages and direct economic losses based on macroseismic intensity data and expert opinion. Although the methodology is relatively comprehensive, some of the classifications used are coarse. For example, only two types of bridges, major and minor, are considered regardless of structural type or material. Moreover, ATC-13 concentrates on the estimation of damages and direct economic losses and does not deal with indirect losses or the effect of damage to the transportation network (although it considers recovery over time). Rojahn et al. (1997) used an updated version of the ATC-13 methodology to evaluate seismic losses for Salt Lake County, Utah. ATC-13 also serves as the basis of more recent methodologies such as HAZUS (NIBS, 2000)

HAZUS (NIBS, 2000; Whitman et al, 1997) is one of the most comprehensive regional loss estimation methodologies with the capability of application at different geographic scales. Rather detailed methods have been implemented to model ground motion, ground failures, and structural and nonstructural damages to buildings, the transportation network, and lifeline components. HAZUS also evaluates induced social and indirect economic losses. Indirect economic losses include changes in employment, loss in tax revenue, and production losses due to reduced demand. The only transportation related loss considered is the direct loss from damage to the transportation network. HAZUS lacks the capability to perform a transportation network analysis. Since transportation capacity constraints are not considered in the economic balancing process, indirect losses from commodity flow disruption, increased travel distances, and their evolution over time during the recovery phase are not evaluated. HAZUS is being increasingly used by the public sector in seismic risk analysis and policy decisions. For example, FEMA (2000) used HAZUS to evaluate the annualized losses for buildings in the US (FEMA-366). The study used USGS seismic hazard maps and default parameters of HAZUS in calculating annualized losses.

Werner et al. (2000) use a detailed transportation network model to estimate direct losses and indirect losses due to increased travel times. Engineering models are used to estimate damage and its uncertainty through Monte Carlo simulation. The developed methodology is applied to estimate increased travel times within Shelby County, TN. Probability distributions of economic losses resulting from increased travel costs are developed by generating a large number of seismic events that affect region and by calculating the corresponding losses using Monte Carlo simulation. Although the recovery of transportation capacity over time is included, the methodology does not consider damage to the remaining built environment and the associated changes in supply and demand in different economic sectors. Computational and data requirements limit the scope of the approach to small geographical regions.

Cho et al. (2001) developed a loss estimation methodology for the Los Angeles metropolitan region, in which the earthquake impact on the transportation network and industrial sectors are modeled in an integrated manner. Economic sectors within the affected region are assumed to interact through commodity flows on the urban transportation network. The reduced capacity of the transportation network as well as the reduced transportation demand due to reduced economic activity are considered. However, only recovery of the business firms is considered

and recovery of the transportation network over time is coarsely modeled by assuming that damaged bridges will remain closed for a period of one year. Use of models and data specific to southern California limits applicability beyond the Los Angeles region.

Sohn et al (2001) and Kim et al. (2002) used a multi-regional input-output model together with a regional commodity flow model to estimate the economic impact of scenario earthquakes. Following an earthquake, the decrease in the final demand for commodities is estimated based on resiliency of the economic sectors and the degree of network disruption. A multi-regional input-output model is used to estimate exports/imports by commodity type for each analysis region and a commodity flow model is used to allocate flows over the transportation network for minimum cost. However, the reduction in production capacity of different economic sectors and the associated change in transportation demand are not included in the model. Moreover, only bridge damage is taken into account for evaluating link capacity and damaged links are assumed to remain in the damaged state for a period of one year. Thus, recovery of the transportation network and the economic sectors is not modeled in this approach.

A comparison of the main features of the above loss estimation studies is provided in Table 2-1. All methodologies except that of Kim et al (2002) are applicable at the regional or metropolitan level. Kim et al (2002) and Werner et al (2000) do not consider damage to buildings or facilities and only models damage to bridges. The closure time of bridges in Cho et al (2001) and Kim et al (2002) is assumed to be one year, which is quite long for non-major bridges. Also, Werner et al (2000) calculate only increased travel times due to transportation network damage, while no network analysis is performed in HAZUS (NIBS, 2000). Finally, the methodologies of Werner et al and Cho et al require specific data on the transportation network and traffic flows, which limits their application to the metropolitan scale.

Table 2-1: Comparison of Seismic Loss Estimation Models

	HAZUS (2000)	Werner et al. (2000)	Cho et al. (2000)	Kim et al. (2002)
Geographic scale	Regional	Metropolitan	Metropolitan	National
Lowest geographical unit	Census tract	Traffic Analysis Zone	Traffic Analysis Zone	EQAZ, 2-5 EQAZ's per state
Detail in transportation network	None included for transportation network flow modeling	Detailed inventory of urban road system	Detailed inventory of L.A. region roads	Interstate highway network
Infrastructure earthquake vulnerability	For most building infrastructure including lifelines	Only for highway bridges, approach fills, and roadways	Explicitly modeled for highway bridges and industries	Only for highway bridges
Recovery of components	Yes, detailed recovery models	Yes, for highway components only	Yes, for economic sectors only	No
Direct losses	Yes	Yes, only for highway components	Yes	No
Losses due to business interruption	Yes	Yes, limited to costs of travel delays	Yes	Yes, excluding indirect losses due to the damage to the economic sectors
Industrial interactions (through input-output models)	Yes, detailed input-output modeling for indirect losses	None, transportation demand is assumed to be exogenous	Yes, detailed input-output models	Yes, input-output models for industrial interactions
Prediction of network flows	None, there is no transportation flow modeling involved	Yes, detailed artificial intelligence approach	Yes, urban transportation planning method	Yes, optimization based algorithms minimizing transportation costs
Freight/Traveler	None	Both	Both	Freight
Losses in transportation network	None	Increase in travel time	Increase in travel cost and effect on the economy	Increase in travel cost and effect on economy

2.4 Sensitivity and Uncertainty in Loss Estimation

While progress has been made in the development of formal quantitative loss estimation methodologies in recent years, a common limitation is that the economic losses are evaluated deterministically, neglecting uncertainty in data and models. As a consequence, the loss estimates fail to provide the decision makers with important information on the uncertainty or the likely range of losses that could occur. There are only a few limited studies on the assessment of earthquake loss uncertainty. The main obstacle is the computational effort required. In this section, we summarize previous studies on sensitivity and for uncertainty for single buildings, a portfolio of buildings, or the building inventory in a region.

2.4.1 Losses from a Single Building

A number of sensitivity studies have considered the losses from individual buildings. These studies involve more detailed structural characterization and analysis than regional loss estimation studies.

Porter et al (2002) investigated the sensitivity of building losses to major uncertain variables for a high-rise nonductile reinforced concrete frame building using assembly based vulnerability method (Porter et al, 2001). Variables included in the study are spectral acceleration, ground motion details, mass, damping, structural force-deformation behavior, building component fragility, contractor costs, and the contractor's overhead and profit. The study assesses the variability in repair cost by setting the variables to their 10^{th} and 90^{th} percentile values one at a time while setting the remaining parameters to median values. The assembly capacity/fragility, shaking intensity, and details of the ground motion are the parameters that affect the losses most; see Figure 2-9. Uncertainty in variables related to structural response, such as mass and damping, contribute less to the overall uncertainty.

In a similar study, Lee and Mosalam (2003) investigated the sensitivity of seismic demand, not the losses, to several variables including ground shaking, ground motion profile, structural strength and stiffness, mass, and damping. The study uses a reinforced concrete shear wall building and the sensitivity analysis results are in general agreement with those of Porter et al (2002). The seismic demand was found to be most sensitive to ground motion variables, ground

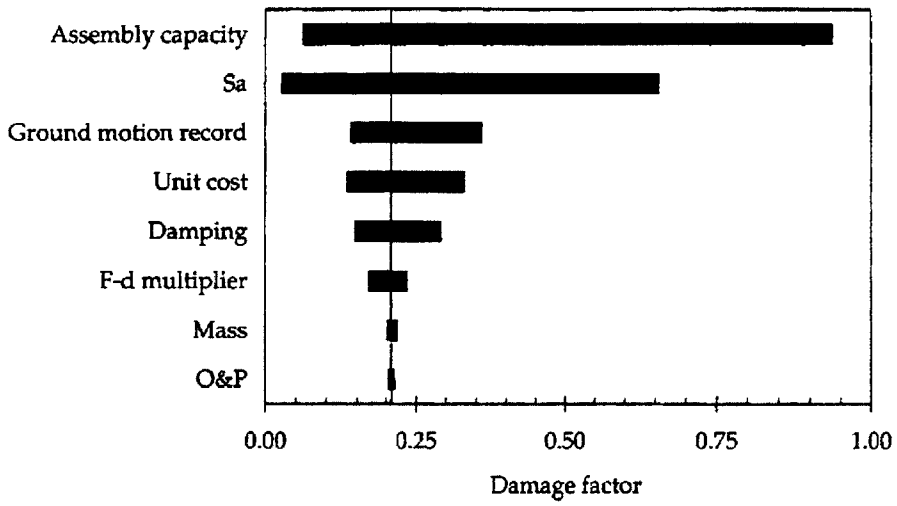

Figure 2-9: Tornado Diagram Showing Results of Sensitivity Analysis from Porter et al (2002)

shaking intensity and ground motion profile. Again, sensitivity to variables such as stiffness, strength, damping and mass was found to be small.

Neither of the above two studies considered interaction among the uncertain variables, which might affect the results. For example, building mass and stiffness determines the fundamental period of a structure which is used in the selection of ground motion level and profile. Therefore, these two parameters may also indirectly affect the seismic demand through correlation with ground motion parameters. Even for a single building quantification of the correlations among these variables is a difficult task.

2.4.2 Losses from a Portfolio of Buildings

With few exceptions, the loss sensitivity analysis for a portfolio of buildings is similar to that for single buildings. For a single structure, the seismic hazard is computed by considering all the seismic sources that pose a threat. In the case of a portfolio of structures, the number of seismic events used in the analysis may be reduced to limit the computational requirements. A second difference is that, for a given earthquake, the ground motions at different sites are correlated (McGuire, 2004). The exact or even approximate calculation of these correlations is a formidable task. Thirdly, the seismic resistance of structures at different sites may be correlated due to similarities in design and construction practices. Although some of these correlations are

captured by grouping similar structures into the same class, the quantification of building-to-building damage and loss correlation is very difficult. Due to these difficulties, the correlations are either neglected or modeled through Monte Carlo analysis.

Bazurrro and Luco (2004) studied the effect of neglecting various sources of uncertainty and correlation on the losses from single buildings and a portfolio of buildings. They considered ground motion uncertainty for a given set of earthquake source parameters, ground motion correlation at different sites, uncertainty in structural response given the ground motion level, uncertainty in loss given structural response, and correlation between losses from similar buildings in the same portfolio. Figure 2-10 shows loss exceedance probability curves obtained for a portfolio of 39 structures located at 5 different sites. The figure shows curves for different cases including a deterministic scenario (black line); with ground motion variability included (blue line); with ground motion, building response, and loss variability included (green line); and with the above uncertainties and building-to-building loss correlation included (red line). Uncertainty on the losses conditional on the level of ground motion has a large effect on the final loss exceedance curves, partly due to limited information on the buildings considered in the study. The loss correlation between similar buildings at the same site also increases the seismic risk. However, the average annual losses calculated by the latter three cases are all about the same, which is attributed to the fact that the curves cross each other at a mean return period of 100 years.

The loss estimates for the deterministic case are significantly lower than those from probabilistic analysis. For example, very large losses occur only in the probabilistic analysis. This may significantly affect decisions about a building portfolio. Moreover, the exceedance probability curves are affected more significantly by the different sources of uncertainty than the average annual loss is.

2.4.3 Regional Losses

The study of loss sensitivity and uncertainty for extended geographical regions are more limited. Regional loss estimation studies involve building inventories composed of a number of different structural types distributed geographically. Building damages and losses have to be evaluated for all structural building types rather than for a single building type, at an appropriate level of

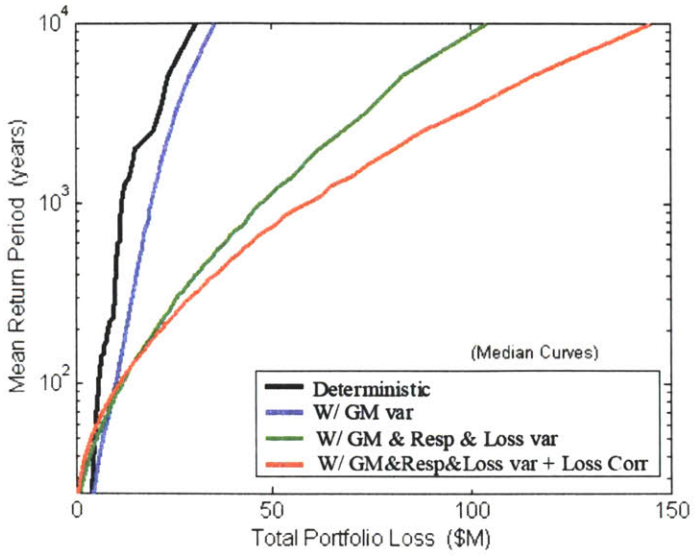

Figure 2-10: Mean Return Period of Losses for a Portfolio of Structures from Bazzurro and Luco (2004)

detail. The necessity to evaluate damages and losses at a large number of sites and for different structural types increases the computational requirements. Building characterization and response analysis are not as detailed as those for single buildings. Hence, the parameters that can be included in the sensitivity/uncertainty analysis are different from those for individual buildings.

Grossi (2000) performed a sensitivity analysis of residential building losses in Oakland, CA using the HAZUS program. They investigate the residential building losses in mitigated and unmitigated conditions, which are represented by moderate-code and high-code structures, respectively. The parameters considered in the sensitivity analysis are earthquake recurrence period, ground motion attenuation, soil classification, the inventory of residential buildings, and the fragility of mitigated and unmitigated structures. The study considers two alternatives for each parameter and performs 64 (2^6) runs for each of the 46 earthquakes scenarios considered. Average annual losses and loss exceedance probability curves were obtained by assigning equal weight to each of the parameter value alternatives. Maximum average annual losses are about 3 times the minimum annual losses. Ground motion attenuation and earthquake recurrence are found to be the most influential parameters, while soil mapping and fragility relations for mitigated structures are the least influential ones.

In another study, Al-Momani and Harrald (2003) used HAZUS to study the sensitivity of earthquake losses in San Francisco. These authors considered scenario earthquakes with magnitudes M5.5 to M7.5 on two faults with epicenters corresponding to historical earthquakes. The variables included in the sensitivity analysis are attenuation relation, soil classification, ground failure due to liquefaction, and building code level. For each earthquake location and magnitude, 24 runs were performed using different values of the above variables. The results include losses from residential buildings, and the number of people killed, hospitalized, or displaced. Comparing the building losses, the study concludes that ground failure effects are most influential, especially at lower magnitudes, followed by the attenuation relation and soil conditions. Losses are least sensitive to building construction parameter. The ratio between maximum and minimum losses from residential buildings is 2.0-3.0. The same ratio for the number of people killed, hospitalized, or displaced is higher, ranging between 4.0 and 7.0.

The above studies concentrated mainly on building losses since methods for the estimation of these losses are better established compared to business losses and are computationally less intensive as no time element is involved. The sensitivity studies are limited to County level spatial resolution and include only a small number of variables. Both studies consider regions in California; results might be different for other US regions due to differences in building inventory, soil conditions, attenuation, etc.

2.5 Concluding Remarks

In this chapter, we have reviewed the literature on seismic loss estimation starting with a general overview of the main components of a loss estimation methodology (hazard analysis, site effects, exposure information, vulnerability analysis, and determination of seismic risk). The amount of effort required by each component depends on the size and properties of the system and the accuracy and resolution of the analysis. The required effort increases when losses other than those due to physical damage are included.

A number of loss estimation methodologies include the loss contributions from business interruption and transportation network damage, in addition to building losses. However, there are limitations in each of the studies reviewed. Some studies are limited to the metropolitan scale due to intensive data and computational needs; see for example Cho et al (2001). Others concentrate only on transportation system and transportation cost increases following an

earthquake e.g Werner et al (2000). HAZUS (NIBS, 2000) does not include transportation system analysis and calculated only regional business losses. Kim et al (2002), model only damage to interstate highways and do not consider damage to industrial facilities. Cho et al (2001) and Kim et al (2002) assume that damaged bridges remain closed for one year.

There is a need for a more comprehensive methodology that models buildings, the transportation network, and the economy in an integrated manner, including the recovery period following the earthquake. The methodology should include building and business losses, the latter due to the reduced functionality of facilities. Also there is a need to evaluate economic losses at both the regional and national level, as the two values may be quite different.

In addition, an understanding on the range of losses that might be observed for given seismic events is required for more informed decision making. It is important to understand the model parameters that significantly affect the loss estimates or contribute the most to the overall uncertainty so that they can be studied in greater detail. These most sensitive parameters can be identified through sensitivity analysis. The limited number of studies that deal with uncertainties in building losses mainly concentrate on building losses and include a small number of model parameters to include computational requirements. Development of a modular and computationally efficient regional loss estimation methodology would allow one to include the effect of a larger number of variables and increase the spatial and temporal resolution of the results.

In the following chapter, we present a comprehensive methodology developed for estimation of regional building, business, and transportation losses from scenario earthquakes. The methodology considers damage to buildings and transportation network and performs an integrated analysis of regional economies and transportation system. The losses are evaluated at both regional and national level. The methodology is applied to events in NMSZ and used for sensitivity analysis, risk assessment and evaluation of retrofit strategies as described in following chapters.

3 Seismic Loss Estimation Methodology

This chapter describes the general framework and component models of the seismic loss estimation methodology used in this study. The methodology is mainly based on HAZUS (NIBS, 2000) and the work of Kunnumkal (2002), Veneziano et al. (2002), and Jammalamadaka (2003). Most of the component models used are based on these previous studies, although some modifications and additions have been made. These include: a new representation of the analysis regions and transportation network including bridges; use of more recent demographic, economic, and physical data; a more detailed classification of buildings; consideration of several additional attenuation relations; implementation of linear seismic sources; ability to use a probabilistic representation of seismicity for risk evaluation; used a new model for regional economic analysis considering damage to transportation network; and calculation of different types of economic losses in addition to production losses.

First the general analysis framework is introduced in Section 3.1. Section 3.2 describes the analysis regions and transportation network used in loss estimation. Section 3.3 identifies the sources of data and classification schemes used by the various component models. The component models, which include the seismicity model, ground motion attenuation, soil amplification, building and bridge vulnerability, building and bridge functionality, and transportation network and regional economic analysis, are described in detail in Section 3.4. Comments on various issues related to loss estimation are provided in Section 3.5.

3.1 General Framework

The earthquake loss estimation methodology developed here is more comprehensive than many existing ones. It includes:

(1) damage to buildings and road transportation system components,

(2) functionality of buildings, industrial sectors, and road transportation system components and its recovery over time,

(3) economic losses associated with repair/restoration of damaged structures,

(4) economic losses due to business interruption, and economic gains from increased production.

(5) increased costs due to damage to the transportation system.

The conterminous U.S. is divided into economic analysis regions, which are connected by main roads. The nodes of the transportation network are highway intersections and the links are the highway segments connecting the nodes, along with the bridges on them. Each county (or each census tract near the New Madrid Seismic Zone (NMSZ)) is assigned to the highway node that is closest to its centroid. All the counties (census tracts) that are associated with the same highway node form an economic analysis region or EAR. The exports from/imports to an EAR are assumed to be transported through the node associated with that EAR. Building damage is evaluated only within the seven CUS states of Arkansas, Illinois, Indiana, Kentucky, Mississippi, Missouri, and Tennessee. Building analysis regions (BAR) consist of a single county or census tract and all the building stock in a BAR is assumed to be concentrated at the centroid of the BAR.

Following a scenario earthquake, ground motion attenuation and infrastructure vulnerability models are used to assess the damage and functionality of the building infrastructure and road transportation network components in each EAR. Immediately after the earthquake, the production and consumption rates in different economic sectors are estimated under the constraints of the damaged transportation network and reduced economic sector functionalities. The functionalities of the various economic sectors are updated over time, considering dependence on the functionalities of lifelines and residential buildings. During the recovery period, economic losses due to reduced productions and consumptions in different economic sectors and the increased transportation costs are estimated. Economic losses due to building and transportation network damage are also calculated and reported.

The main steps of the loss estimation methodology are as follows:

Step 1: Estimation of initial damage and functionalities

Local ground motion intensities for each analysis region and transportation link are calculated using scenario earthquake parameters (e.g. magnitude and epicentral location) and attenuation relations. The ground motions are amplified based on soil class using soil amplification factors. The consequent damage to buildings, lifelines, highway pavements and bridges is calculated using capacity and fragility relationships. Then, initial functionalities of all the economic sectors and the transportation network components are calculated using damage-functionality relationships.

Step 2: Estimation of post-earthquake economic activities and link flows:

At discrete time intervals, the reduced production capacities of different economic sectors in different analysis regions and the reduced capacity of the transportation links are calculated. An integrated linear programming approach is used to optimize regional productions/consumptions, regional imports/exports and transportation link flows.

Increased demand in the construction sector due to reconstruction spending and consequent reduction in consumption due to repayment of reconstruction expenditures are considered in the model. We assume that the buildings in the damaged regions are repaired or reconstructed in a 3 year period, 50% in year 1, 30% in year 2, and %20 in year 3. This reconstruction spending is included in the economic analysis as an additional demand in the construction sector, which creates a stimulus to the regional economies. However, the repayment of construction expenditures will result in reduced demand in other sectors over a longer time horizon, especially in the financial, insurance, and governmental sectors due to loan payments, decline in personal savings, or reduced government expenditures. Assuming all loans will mature in 15 years, we include the effect of reconstruction payments as a reduced demand in the services and government sector over a 15 year period following the earthquake. We do not include any borrowing costs in this accounting as it is not clear whether the construction expenditures are paid by loans, private savings, or government. Any combination of these is possible with private loans having higher associated borrowing costs.

Step 3: Calculation of economic losses:

Direct and indirect business interruption losses incurred during the current time step are calculated by comparing the production and consumption levels to those in the pre-earthquake state. Economic losses due to repair/restoration costs of structures are calculated in step 1.

Step 4: Functionality update:

A recovery model is used to update the functionality of infrastructure components taking into account the effects of interactions among the functionalities of different systems over time.

Steps 2 to 4 are repeated for subsequent time intervals for over a time period of 15 years. Economic losses for each analysis region are aggregated during this 15-year period. These losses include loss in production, consumption, and value-added for different economic sectors in different economic analysis regions. In regions that are not damaged by the earthquake the losses may be negative; i.e. such regions may experience net gains. Increased transportation costs due to rerouting caused by reduced transportation capacity are also calculated.

In the next two sections, we provide details on the data sources and component models used in applying the earthquake loss estimation methodology to earthquakes in the New Madrid Region.

3.2 Analysis Regions and Transportation Network

The model used in this study covers the entire conterminous US. The conterminous US is divided into a number of analysis regions, which are connected to each other by a highway network. Analysis regions are selected to be census tracts or counties in the CEUS or a number of aggregated counties in other regions of the US. The transportation network consists of highway segments, along with bridges on them, and transportation nodes at highway intersection points or at points where the number of lanes along a link changes.

3.2.1 Building Analysis Regions

The analysis regions used in this study are census tracts, counties, or an aggregation of counties depending on location relative to the NMSZ. A finer spatial discretization is used within about 100 km from the center of the NMSZ to better represent the geographical distribution of

structures, facilities, and activities and better account for local ground motion, damage, and loss distribution.

In applying the methodology to the CUS, building damage and the corresponding direct loss are limited to the 7 CUS states that are close to the NMSZ, i.e. to Arkansas, Illinois, Indiana, Kentucky, Mississippi, Missouri, and Tennessee. In these states, the largest unit of spatial aggregation used in analysis is the county and the smallest unit is the census tract (the building inventory and other related parameters are provided at the census tract level).

To investigate the sensitivity of the estimated damages and losses to the size of the analysis regions, models with three different spatial resolution are considered. In model 1, each analysis region in the seven CUS states consists of a single county. In model 2, the spatial resolution in Shelby County is increased to the census tract level while keeping the rest of the analysis regions at the county level. As Memphis and a significant portion of the building inventory with in NMSZ is located in Shelby County, this model is expected to provide more accurate damage and loss estimates. In model 3, the spatial discretization of the analysis is increased to the census tract level not only in Shelby County but also in other counties around NMSZ. The region where the spatial discretization is increased includes 90 counties between latitudes 88.0 and 92.0 and longitudes 34.0 and 38.0. We call this the NMSZ region. Table 3-1 provides the number of analysis regions in Shelby County, the NMSZ region, and the seven CUS states for the three models.

Figure 3-1 shows the analysis regions used in model 1 for the seven CUS states. Figure 3-2 provides a close up of the analysis regions in the NMSZ. Shelby County and the counties close to NMSZ are highlighted in both figures. Also shown in the figures are the three NMSZ faults used by USGS to produce seismic hazard maps and the rectangular area where the resolution of the

Table 3-1: Number of Building Analysis Regions in CUS

Region	Model 1	Model 2	Model 3
Shelby County	1	216	216
NMSZ (excluding Shelby County)	89	89	566
CUS (excluding NMSZ)	591	591	591
Total	681	896	1373

model is increased to the census tract level in model 3.

The analysis regions used in models 2 and 3 are shown in Figure 3-3 and Figure 3-4, respectively. As noted above, in model 2 the resolution of the analysis in Shelby County is increased to the census tract level. In model 3, all the counties within the above mentioned latitudes and longitudes are analyzed at the census tract level.

Inventories of buildings, population, economic activity, and local soil conditions for each analysis region are obtained from various sources as explained in Section 3.3. All these spatially distributed quantities are treated as being concentrated at the population centroid of the associated analysis region. The population centroid of an analysis region is the population-weighted average of the geometric centroids of the census tracts comprising the region. Figure 3-5 compares the population centroid, square footage of building centroid, and area-weighted (geometric) centroid for the counties in NMSZ. In general, the population and square footage weighted centroids are much closer to each other than the area weighted centroids. As mentioned above, the population centroids are used in this study unless otherwise specified. The population centroid in a better representation of the local building inventory and economic activities than the geometric centroid of the analysis region. Sensitivity of the results to using the geometric and building area weighted centroids is discussed in Chapter 4.

3.2.2 Transportation Network

The transportation links used in this study are extracted from the 2002 National Transportation Atlas Database (NTAD) (BTS, 2002). NTAD provides data on the National Highway Planning Network (NHPN), which is a comprehensive database of the US major highway system. It consists of the US highways including rural arterials, urban principal arterials, and all National Highway System (NHS) routes. The 2002 NTAD provides data not only on the location of highways but also on properties of the highway links such as length, number of lanes, NHS link classification and Strategic Highway Corridor Network (STRAHNET) link classification. Using these data, two different versions of the transportation network have been developed and used in this study. The resolution of the two models inside the NMSZ region is the same. The models only differ in the links included the NMSZ.

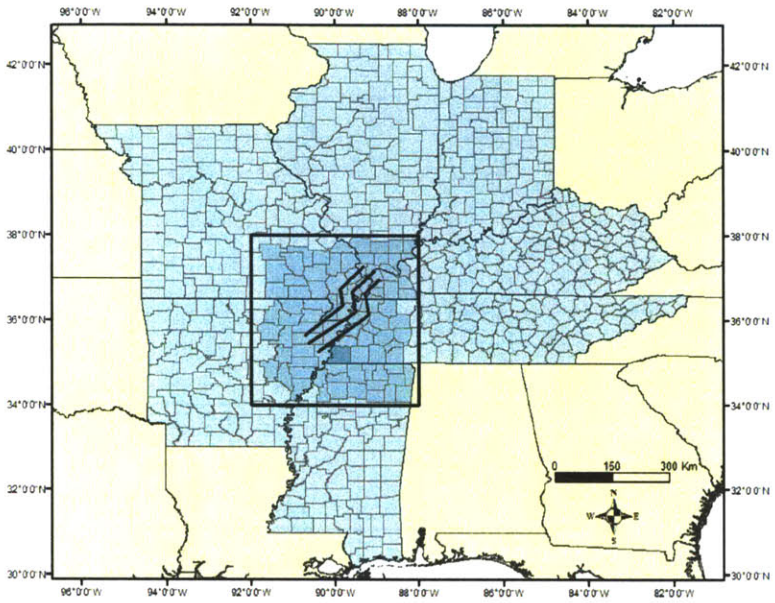

Figure 3-1: CUS Analysis Regions Used in Model 1

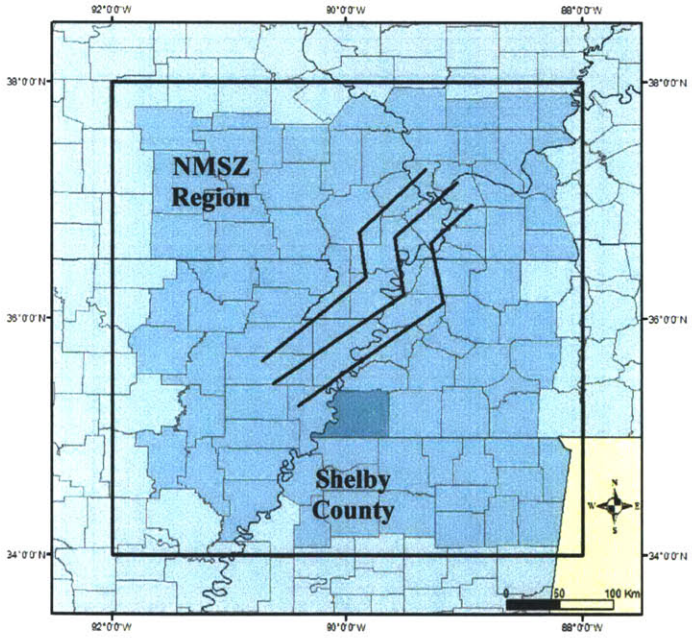

Figure 3-2: Close up of the NMSZ Analysis Regions Used in Model 1

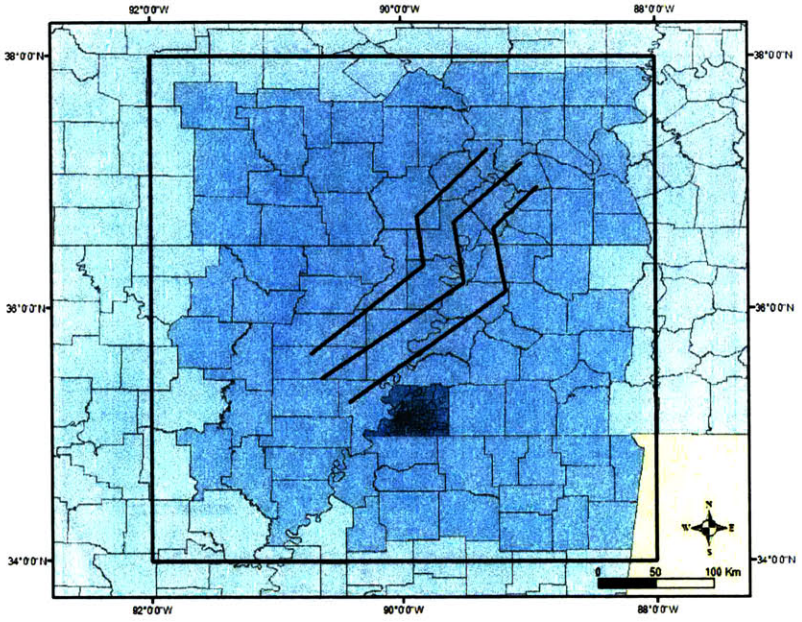

Figure 3-3: Close up of the NMSZ Analysis Regions Used in Model 2

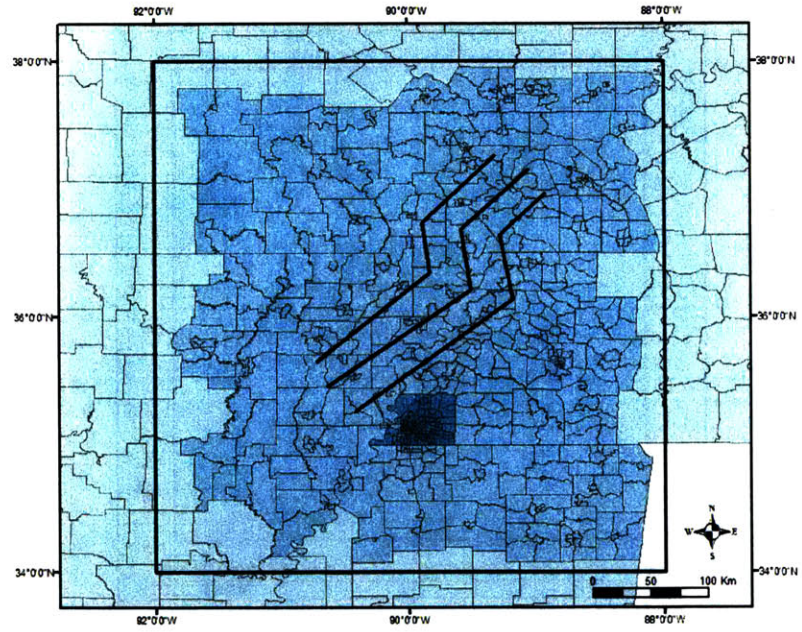

Figure 3-4: Close up of the NMSZ Analysis Regions Used in Model 3

Inside the NMSZ region, both models include all the highway links that are on the NHS and STRAHNET networks. Figure 3-6 shows the boundary of the region where the resolution of the two models is the same and the highway links within the region. Outside the NMSZ region, model 1 includes only the interstate highways, whereas model 2 includes both interstate highways and highways on the STRAHNET network. The transportation network links used in models 1 and 2 are shown in Figures 3-7 and 3-8, respectively, together with the nodes. The nodes are located at link intersections, at the end point of terminal links, and at locations where the number of lanes along a link changes. Transportation network model 1 has 2135 links and 1525 nodes, whereas model 2 has 2716 links and 1983 nodes.

The links and nodes in the seven CUS states for models 1 and 2 are shown in Figures 3-9 and 3-10, respectively. The extended NM region (ENMR), rectangular NMSZ region, and NMSZ faults are also shown in these figures. Finally, Figures 3-11 and 3-12 provide a close up view of the same figures around the NMSZ.

Highway bridges are considered only within the ENMR, where there is the possibility of highway closures due to bridge damage. Among the highway bridges on the NHS and STRAHNET networks inside the ENMR, only those along highway links are included in the model. All other bridges including pedestrian bridges crossing highways or overpass bridges carrying links not included in the network are excluded. The damage to these overpass bridges might cause closure of highway sections due to falling debris or collapsed components, but the debris can be cleared in a fairly short amount of time compared to the time required for repair of a highway bridge.

The bridges on the links bordering the ENMR are not included in the analysis. Hence traffic flow around and outside the ENMR is assumed not interrupted. The transportation and bridge network in the ENMR are the same in both models and include 4651 bridges. Bridge information has been extracted from the 2000 National Bridge Inventory (NBI) (FHWA, 2000), which provides data on physical, structural and traffic characteristics of bridges throughout the US. Figure 3-11 shows the location of the 4651 highway bridges. As mentioned above, the number of bridges considered in models 1 and 2 are the same as the links included within the ENMR in both models are identical. 184 of the 4651 bridges are located within Shelby County (See Figure 3-12).

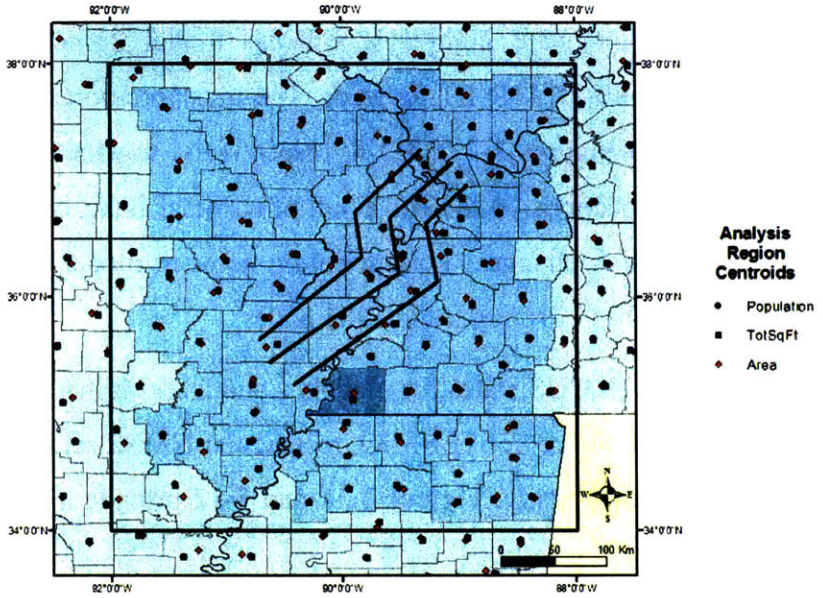

Figure 3-5: Comparison of Population, Total Square Footage, and Area Weighted Centroids of NMSZ Counties

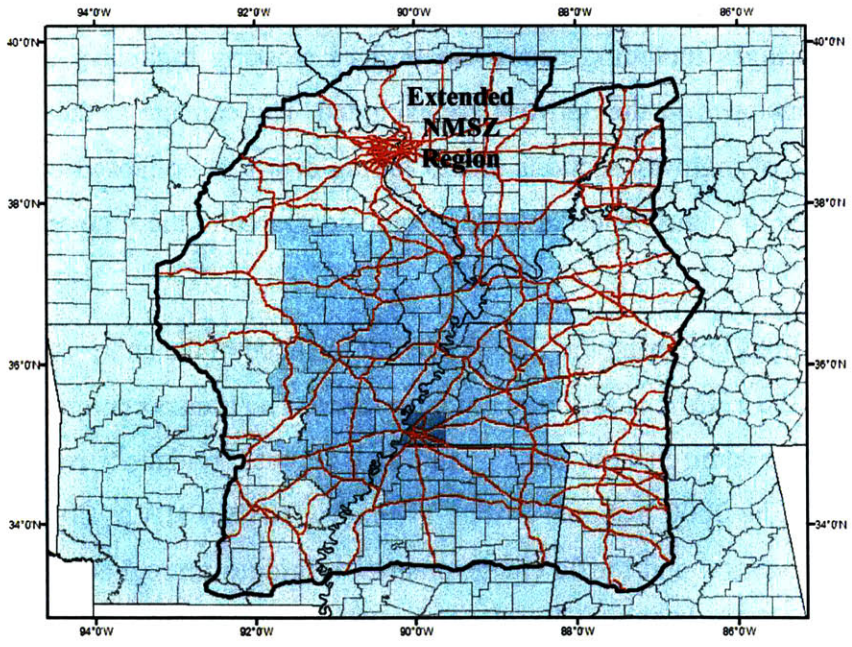

Figure 3-6: Highway Links around NMSZ Included both in Model 1 and Model 2

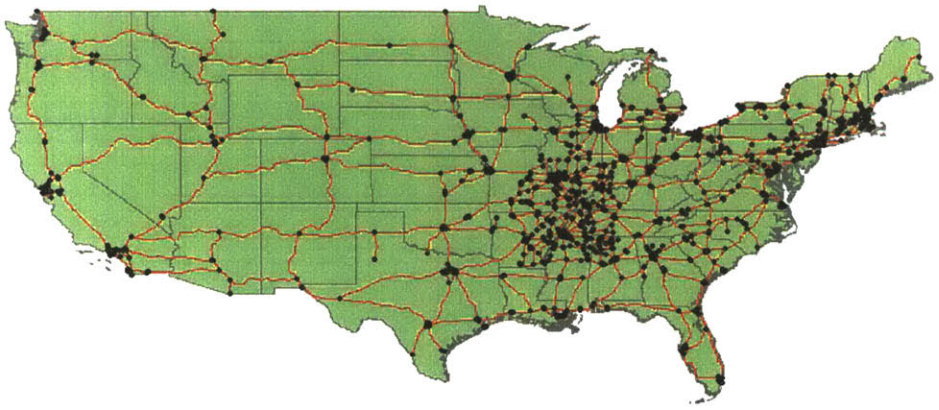

Figure 3-7: Transportation Network Links and Nodes Used in Transportation Network Model 1

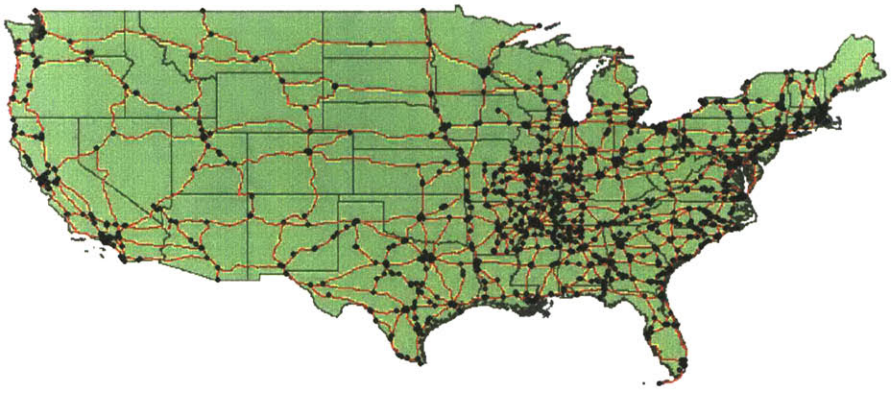

Figure 3-8: Transportation Network Links and Nodes Used in Transportation Network Model 2

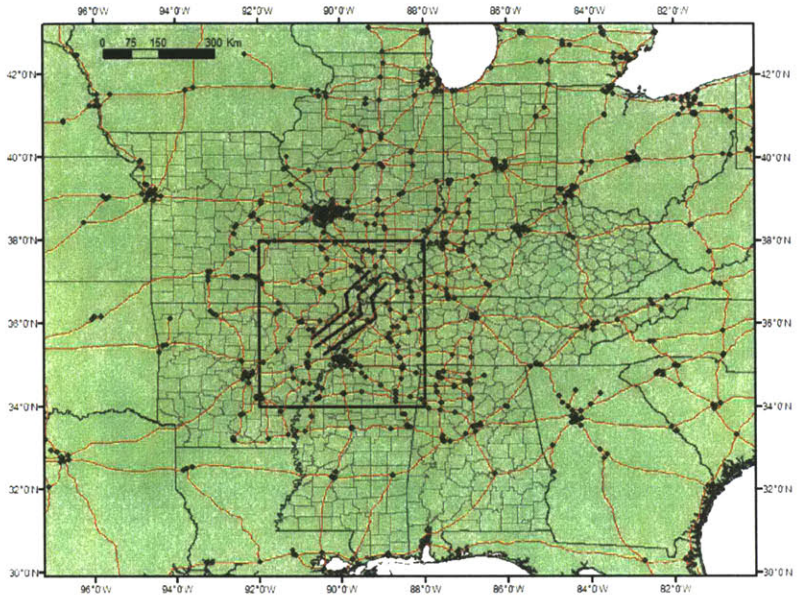

Figure 3-9: Transportation Network Model 1 Links and Nodes around CUS

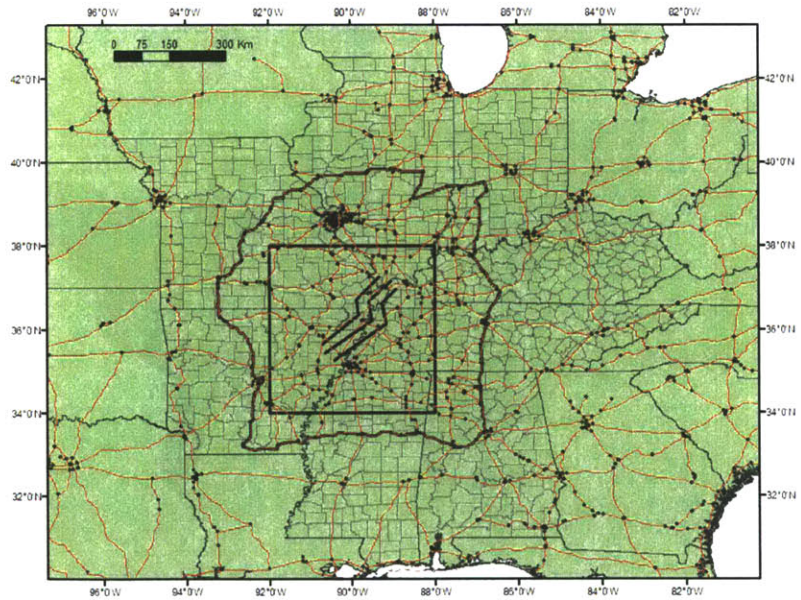

Figure 3-10: Transportation Network Model 2 Links and Nodes around CUS

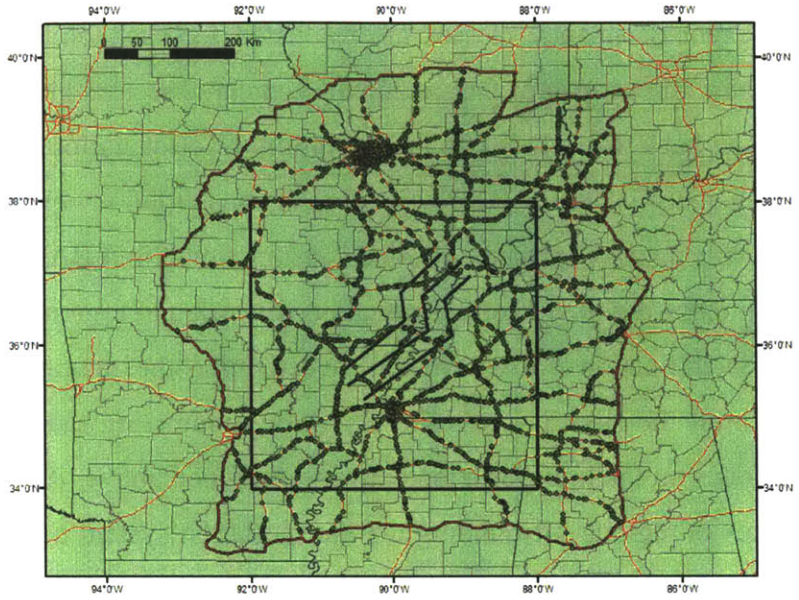

Figure 3-11: Transportation Network Model 1 Highway Bridges

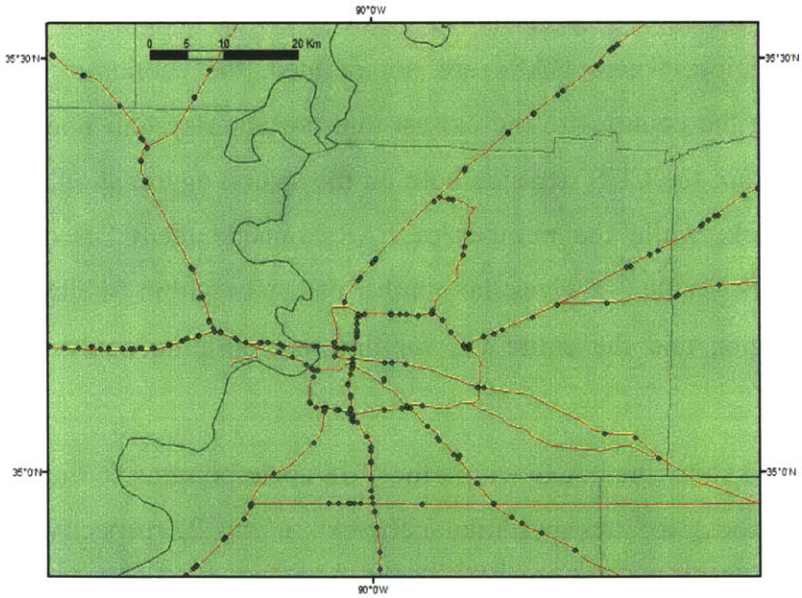

Figure 3-12: Transportation Network Bridges around Shelby County

3.2.3 Economic Analysis Regions

Immediately following the earthquake, the damage for different building types and the functionality for different occupancy classes are evaluated for each building analysis region (BAR). The functionality of occupancy classes and the economic sectors into which such classes are mapped provide the basis for estimating the maximum level of various economic activities achievable within each analysis region. However, through transportation network interactions the actual levels of economic activity (productions and consumptions) in a BAR depend also on the economic activities in other regions. The transportation network and regional economic analysis model explained in later Section 3.4.6 are used to determine the maximum production and consumption levels in all the BARS across the US while minimizing the transportation costs. Since this model operates on the transportation network explained above, it requires estimates of the economic activities in regions surrounding the transportation system nodes as they serve as centers of economic activities and points at which commodities are transported from/to other regions.

In the CUS region, the economic analysis regions (EARs) are obtained by aggregating the BARs (census tracts or counties) around the transportation system nodes closest to their centroids. Outside the CUS region, where BARs are not defined, the economic analysis regions are obtained by mapping the counties to the closest transportation system node. In this regard, the number of EARs within the CUS depends both on the spatial aggregation of the BARs and the transportation network, while the number of EARs outside the CUS depends only on the transportation network. Table 3-2 gives the number of EARs within Shelby County, the NMSZ region, the CUS region and the entire US for different building analysis and transportation network models.

Figures 3-13 and 3-14 show the EARs within the CUS corresponding to building analysis region model 1 (CUS counties) for transportation networks 1 and 2, respectively. The number of resulting EARs is about the same, 283 versus 303. In both cases, the number of EARs within NMSZ is 73 as the transportation network within this region is identical (see Figure 3-15). The difference in the number of EARs results from regions outside NMSZ, where additional transportation links and nodes were included in transportation network 2. When the resolution of

Table 3-2: Number of Economic Analysis Regions

Region	Transportation Network Model 1			Transportation Network Model 2		
	Building Analysis Region			Building Analysis Region		
	Model 1	Model 2	Model 3	Model 1	Model 2	Model 3
Shelby County	1	30	30	1	30	30
NMSZ (excluding Shelby County)	72	72	126	72	72	126
CUS (excluding NMSZ)	210	210	210	230	230	230
US (excluding CUS)	486	486	486	735	735	735
Total	769	798	852	1038	1067	1121

the BARs within NMSZ is increased to the census tract level (building analysis region model 3), this number increases to 156 (see Figure 3-16).

Figures 3-17 and 3-18 show the EARs and the corresponding transportation network nodes located outside CUS for transportation networks 1 and 2, respectively. There are 486 EARs outside CUS for transportation network 1, and 735 for transportation network 2. As can be seen from these figures, there are significantly more EARs in the eastern US compared to the western US, where the highway network is less dense.

3.3 Inventory, Classifications, and Other Data

In this section, we describe the sources of data and classification schemes used in this study, including building inventory, bridge inventory, soil classification maps, economic data, and related classifications.

3.3.1 Building Inventory

In regional earthquake loss estimation studies, it is not possible to structurally analyze all buildings making up the building inventory and evaluate the building performance, damage, and losses on an individual basis as this is a costly process. This can be done only for special buildings such as hospitals, school, etc. It is sometimes difficult to even accurately obtain the exact number, age, or structural system of buildings within a region. For this reason, it is customary in regional loss estimation to extract building inventory information indirectly from more readily available data sources including insurance data, tax records, and local governmental data. These data sources are complemented as much as possible by results from more detailed

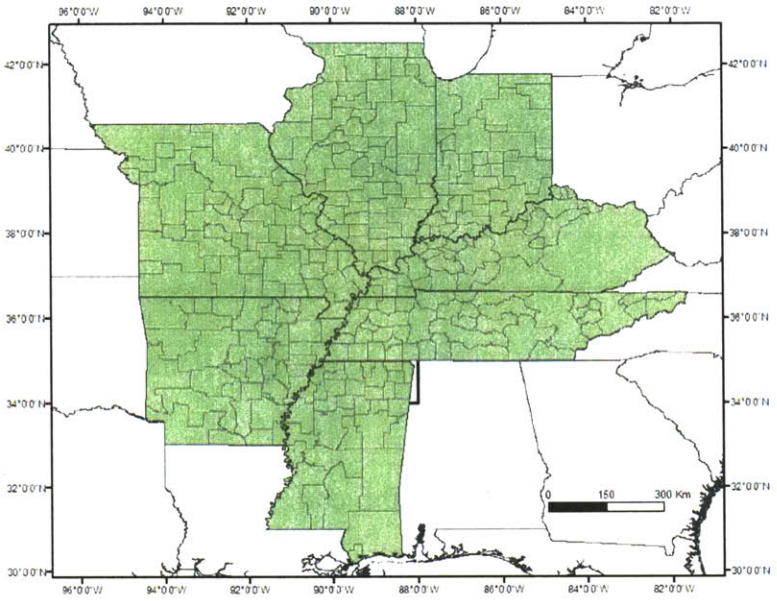

Figure 3-13: Economic Analysis Regions in CUS for Transportation Network 1

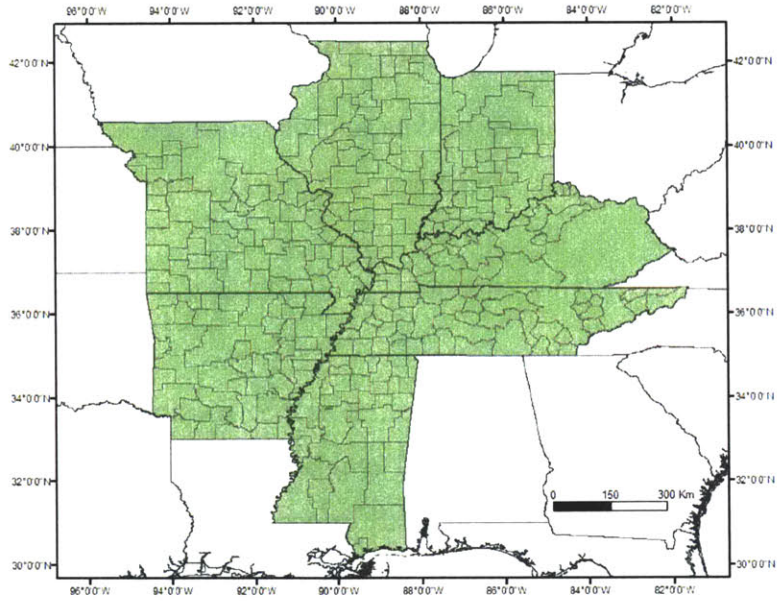

Figure 3-14: Economic Analysis Regions in CUS for Transportation Network 2

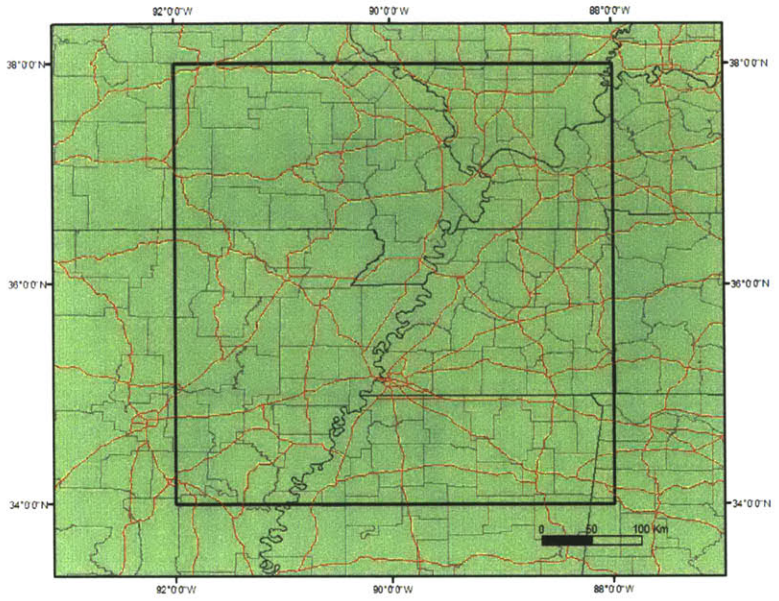

Figure 3-15: Economic Analysis Regions in NMSZ for Building Analysis Region Model 1

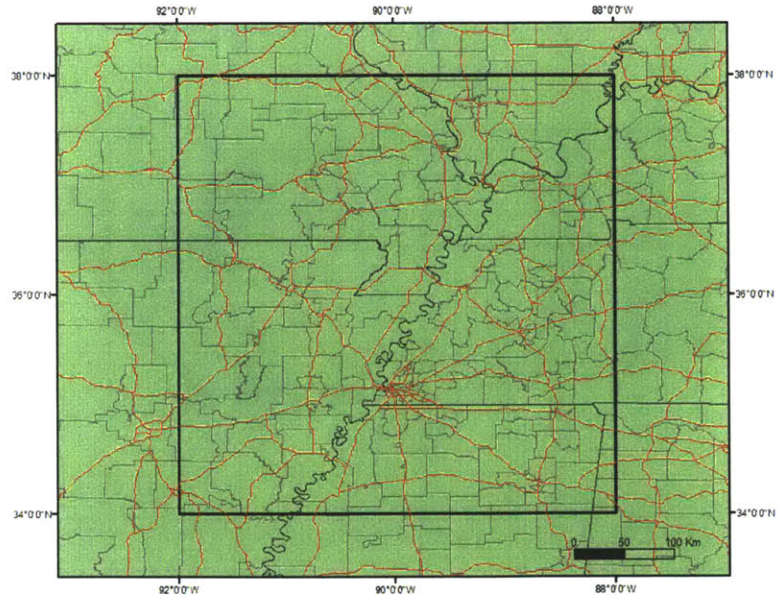

Figure 3-16: Economic Analysis Regions in NMSZ for Building Analysis Region Model 3

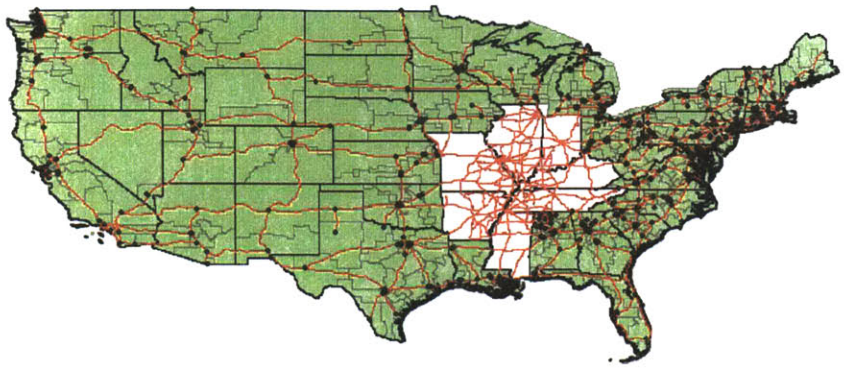

Figure 3-17: Economic Analysis Regions outside CUS for Transportation Network 1

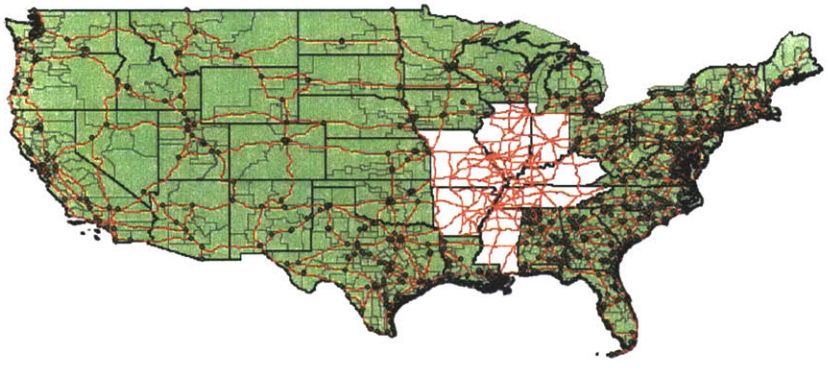

Figure 3-18: Economic Analysis Regions outside CUS for Transportation Network 2

studies on building inventory. During this process, buildings are classified into representative classes according to their use, structural properties, geometry, etc.

For loss estimation studies, generally one needs two sets of data on buildings. One set includes data on the seismic performance of the structure such as the type of structural system, building height, and building age. Another set of data is required to evaluate the value the building and contents for use in estimating losses resulting from seismic damage. Building value is generally more closely related to its use or occupancy type than its structural type.

A possible building classification according to occupancy is residential, commercial, industrial, agricultural, religious, government and educational. The building occupancy inventory provides the floor areas for different building occupancy types in each analysis region. We have obtained this inventory by aggregating the census tract data of HAZUS (NIBS, 2000) in each BAR within the seven CUS states. HAZUS provides the square footage for each of the 33 occupancy classes listed in Table 3-3. The occupancy classification of a building determines the overall value of the structure and its functionality and recovery characteristics following an earthquake.

To determine seismic vulnerability, one needs a different classification of buildings which reflects their structural characteristics. HAZUS uses the 36 building structure types listed in Table 3-4. The building type classification intends to differentiate buildings on the basis of structural capacity and earthquake response. Building height sub-classes reflect the variation of the resonance period and other building characteristics with building height.

Each occupancy class includes buildings of different structural types, hence damage to an occupancy class is calculated as the square foot weighted average of the damages to the structural types making up that class. HAZUS provides default mapping schemes to map the 33 building occupancy classes to the 36 building structural types. Default mappings for low-, mid- and high-rise buildings are different and one needs to specify the proportion of buildings in these three height categories for each occupancy class. However, the building inventory provided in HAZUS is mapped only to low-rise buildings (by default) within the seven CUS states and therefore the results are only affected by the parameters and mappings related to low rise structural types. Table 3-5 provides the default occupancy class-building type mapping for low-rise buildings in Tennessee. For other Midwest or CUS states, the default mapping is the same for all occupancy classes except the RES1 occupancy class (See Table 3-6). For computational

Table 3-3: Building Occupancy Classes (HAZUS)

No.	Label	Occupancy Class	Example Description
		Residential	
1	RES 1	Single Family Dwelling	House
2	RES 2	Mobile Home	Mobile Home
3-8	RES 3	Multi Family Dwelling	Apartment/Condominium
	RES3A	Duplex	
	RES3B	3-4 Units	
	RES3C	5-9 Units	
	RES3D	10-19 Units	
	RES3E	20-49 Units	
	RES3F	50+ Units	
9	RES4	Temporary Lodging	Motel/Hotel
10	RES5	Institutional Dormitory	Group Housing, Jails
11	RES6	Nursing Home	
		Commercial	
12	COM1	Retail Trade	Store
13	COM2	Wholesale Trade	Warehouse
14	COM3	Personal and Repair Services	Service Station/Shop
15	COM4	Professional Technical Services	Offices
16	COM5	Banks	
17	COM6	Hospital	
18	COM7	Medical Office/Clinic	
19	COM8	Entertainment & Recreation	Restaurants/Bars
20	COM9	Theaters	Theaters
21	COM10	Parking	Garages
		Industrial	
22	IND1	Heavy	Factory
23	IND2	Light	Factory
24	IND3	Food/Drugs/Chemicals	Factory
25	IND4	Metals/Mineral Processing	Factory
26	IND5	High Technology	Factory
27	IND6	Construction	Office
		Agriculture	
28	AGR1	Agriculture	
		Religion/Non-Profit	
29	REL1	Church/Non-profit	
		Government	
30	GOV1	General Services	Office
31	GOV2	Emergency Response	Police/Fire station/EOC
		Education	
32	EDU1	Grade Schools	
33	EDU2	Colleges/Universities	Does not include group housing

Table 3-4: Building Structure (Model Building) Types (HAZUS)

No.	Label	Description	Height			
			Range		Typical	
			Name	Stories	Stories	Feet
1	W1	Wood, Light Frame (≤ 5,000 sq. ft.)		1 - 2	1	14
2	W2	Wood, Commercial and Industrial (> 5,000 sq. ft.)		All	2	24
3	S1L	Steel Moment Frame	Low-Rise	1 - 3	2	24
4	S1M		Mid-Rise	4 - 7	5	60
5	S1H		High-Rise	8+	13	156
6	S2L	Steel Braced Frame	Low-Rise	1 - 3	2	24
7	S2M		Mid-Rise	4 - 7	5	60
8	S2H		High-Rise	8+	13	156
9	S3	Steel Light Frame		All	1	15
10	S4L	Steel Frame with Cast-in-Place Concrete Shear Walls	Low-Rise	1 - 3	2	24
11	S4M		Mid-Rise	4 - 7	5	60
12	S4H		High-Rise	8+	13	156
13	S5L	Steel Frame with Unreinforced Masonry Infill Walls	Low-Rise	1 - 3	2	24
14	S5M		Mid-Rise	4 - 7	5	60
15	S5H		High-Rise	8+	13	156
16	C1L	Concrete Moment Frame	Low-Rise	1 - 3	2	20
17	C1M		Mid-Rise	4 - 7	5	50
18	C1H		High-Rise	8+	12	120
19	C2L	Concrete Shear Walls	Low-Rise	1 - 3	2	20
20	C2M		Mid-Rise	4 - 7	5	50
21	C2H		High-Rise	8+	12	120
22	C3L	Concrete Frame with Unreinforced Masonry Infill Walls	Low-Rise	1 - 3	2	20
23	C3M		Mid-Rise	4 - 7	5	50
24	C3H		High-Rise	8+	12	120
25	PC1	Precast Concrete Tilt-Up Walls		All	1	15
26	PC2L	Precast Concrete Frames with Concrete Shear Walls	Low-Rise	1 - 3	2	20
27	PC2M		Mid-Rise	4 - 7	5	50
28	PC2H		High-Rise	8+	12	120
29	RM1L	Reinforced Masonry Bearing Walls with Wood or Metal Deck Diaphragms	Low-Rise	1-3	2	20
30	RM2M		Mid-Rise	4+	5	50
31	RM2L	Reinforced Masonry Bearing Walls with Precast Concrete Diaphragms	Low-Rise	1 - 3	2	20
32	RM2M		Mid-Rise	4 - 7	5	50
33	RM2H		High-Rise	8+	12	120
34	URML	Unreinforced Masonry Bearing Walls	Low-Rise	1 - 2	1	15
35	URMM		Mid-Rise	3+	3	35
36	MH	Mobile Homes		All	1	10

Table 3-5 : Distribution Percentage of Floor Area for Model Building Types within Each Building Occupancy Class, Low-Rise, Tennessee (HAZUS, 2000)

No.	Specific Occup. Class	Model Building Type															
		1	2	3	6	9	10	13	16	19	22	25	26	29	31	34	36
		W1	W2	S1L	S2L	S3	S4L	S5L	C1L	C2L	C3L	PC1	PC2L	RM1L	RM2L	URML	MH
1	RES1	90														10	
2	RES2																100
3	RES3	75												2		23	
4	RES4	50												3	2	45	
5	RES5	20							4	13	2	22	4	2		33	
6	RES6	90														10	
7	COM1		30	2	4	11	6	7		5		5		2		28	
8	COM2		10	2	4	11	6	7	2	10	2	14	2	2		28	
9	COM3		30	2	4	11	6	7		5		5		2		28	
10	COM4		30	2	4	11	6	7		5		5		2		28	
11	COM5		30	2	4	11	6	7		5		5		2		28	
12	COM6				2	4	2	2	6	21	4	33	6	2		18	
13	COM7		30	2	4	11	6	7		5		5		2		28	
14	COM8		30	2	4	11	6	7		5		5		2		28	
15	COM9			2	6	14	8	10	4	13	2	22	4			15	
16	COM10			2	4	11	6	7	6	21	4	33	6				
17	IND1			5	10	25	13	17	2	7	2	12	2			5	
18	IND2		10	2	4	11	6	7	2	10	2	14	2	3		27	
19	IND3		10	2	4	11	6	7	2	10	2	14	2	3		27	
20	IND4			5	10	25	13	17	2	7	2	12	2			5	
21	IND5		10	2	4	11	6	7	2	10	2	14	2	2		28	
22	IND6		30	2	4	11	6	7		5		5		2		28	
23	AGR1		10	2	4	11	6	7	2	10	2	14	2	2		28	
24	REL1	30			3	5	3	4		5		5		2	2	41	
25	GOV1		15	14	21				7	6		4		3		30	
26	GOV2		14	7	17				4	12					3	43	
27	EDU1		10	5	12				5	7				11		50	
28	EDU2		14	6	12			2	8	11					10	37	

Table 3-6: Distribution Percentage of Floor Area for Model Building Types within RES1 Building Occupancy Class for Seven CUS States (HAZUS)

Abbreviation	State	Model Building Type		
		1	19	34
		W1	C2L	URML
AR	Arkansas	87	0	13
IL	Illinois	77	1	22
IN	Indiana	80	0	20
KY	Kentucky	88	0	12
MO	Missouri	76	0	24
MS	Mississippi	94	0	6
TN	Tennessee	90	0	10

purposes, we use for all the CUS the default mapping provided in HAZUS for Shelby County. This may result in a less accurate representation of building structural types in the remaining regions. However, the loss results should be minimally affected since Shelby County includes most of the inventory in the NMSZ region and contributes the most to the final losses.

Following the occupancy class-building type mapping, the inventory of buildings is further mapped into subcategories according to seismic design level. HAZUS considers four seismic design levels, determined mainly from building age and location: pre-code, low-code, moderate-code and high-code. In HAZUS, most of the buildings in Shelby County are considered to be "moderate-code" and the remaining ones are assigned to the pre-code class. The sensitivity of loss estimates to alternative code classifications will be considered in Chapter 4.

3.3.2 Bridge Inventory

As mentioned in Section 3.2.2, the highway bridges in NMSZ are extracted from the 2000 National Bridge Inventory (NBI) (FHWA, 2000). NBI provides data on physical, structural, and traffic related properties of US bridges. Data relevant to transportation analysis (e.g. route to which the bridge belongs and its functionality), and structural classification (e.g. structural type, material, number of spans, age, length, width, and maximum span length) of 4651 bridges are extracted from the 2000 NBI. The structural classification of bridges and corresponding fragility parameters are explained in Section 3.4.4.

In addition to bridges on the highway network, which were extracted from NBI, we have also used HAZUS' bridges inventory in the seven CUS states. These bridges are not included in the network analysis, but are used to assess the regional losses due to bridge damage. The bridge data in HAZUS, which were extracted from the 2001 NBI, are in a form that can be used in HAZUS` loss estimation procedure (see section 3.4.4) without further modification or classification. This dataset is used to estimate damage and repair costs of the bridges in the seven CUS states.

3.3.3 Soil Conditions

Local site conditions describe the deposits/soils that lie between the surface and basement rock. The deposits are usually characterized by the surface or near-surface geology, the shear wave velocity, and the sediment depth. The latter two descriptors are usually preferred since they represent physical quantities that can be related to the dynamic response of the deposits and its effect on buildings and the facilities.

In general, two methods are used to classify a site using shear wave velocity V_s. The first is the average value of V_s in the top 30m of the deposit, referred to as the 30-m velocity, V_{s-30}. The other is the average value of V_s over a depth equal to a quarter-wavelength of a ground motion parameter of specified frequency, referred here to as effective velocity. The former is the most frequently used quantity in engineering practice (Kramer and Stewart, 2004) and it serves as the basis of the site classification used in this study.

In this study, we use NEHRP's Site Classes as defined in the 1997 NEHRP Provisions (FEMA, 1997). This FEMA document uses the 30-m velocity to classify site conditions as shown in Table 3-7. Recent earthquake design codes, including the 1997 UBC and 2000 IBC codes, use the NEHRP site classes and associated amplification factors. Soils classified as NEHRP site class F require site specific analysis. Site amplification factors (discussed in Section 3.4.2) are provided only for NEHRP site classes A to E. As site specific analysis requires detailed knowledge of local site conditions and extensive analysis, in this study we assume that regions classified as site class F are represented by site class E, which is the site class with the closest properties to site class F.

Table 3-7: Site Classes (from the 1997 NEHRP Provisions)

Site Class	Site Class Description	Shear Wave velocity (m/sec)	
		Minimum	Maximum
A	Hard Rock	1500	
B	Rock	760	1500
C	Very Dense Soil and Soft Rock	360	760
D	Stiff Soils	180	360
E	Soft Soils		180
F	Soils Requiring Site Specific Evaluations		

Representative Soil conditions for the analysis regions and at bridge locations are obtained from Bauer (1997), who uses the NEHRP classification. These soil classification maps were developed by State Geologists of the Central US Earthquake Consortium (CUSEC) for use in HAZUS. Base geologic maps of surficial materials or 3-dimensional maps were used in conjunction with shear wave velocity information to classify the soils in the upper 15 to 30 meters. As shown in Figure 3-19, the soil maps cover only parts of the seven CUS states. In the remainder of the CUS states, we have assumed that class D applies. Figure 3-20 shows the site classes in and around the NMSZ area. Site classes D and E are the dominating ones within the immediate vicinity of the NMSZ faults and Shelby County. In other regions, classes B and C are also encountered.

Using soil classification maps, we obtain the soil type at bridge locations and at the centroids of the census tracts. We assume that the soil condition at the centroid of a census tract is representative of the soil conditions in the entire census tract. For analysis regions at the county level, we use the site classes assigned to census tracts and their areas to obtain the percentages of different soil classes within the county, e.g. 80% type D and 20% type E. We assume that the building inventory within a region is uniformly distributed over the whole region and the percentage of buildings located on different soil classes is the same as the percentage of soil classes within the analysis region. In building damage calculations, we analyze the buildings for all 5 site classes and use the percentages of different soil types to obtain average damage and loss in each analysis region. For bridges, we perform the damage and loss calculation for the soil class at each bridge location.

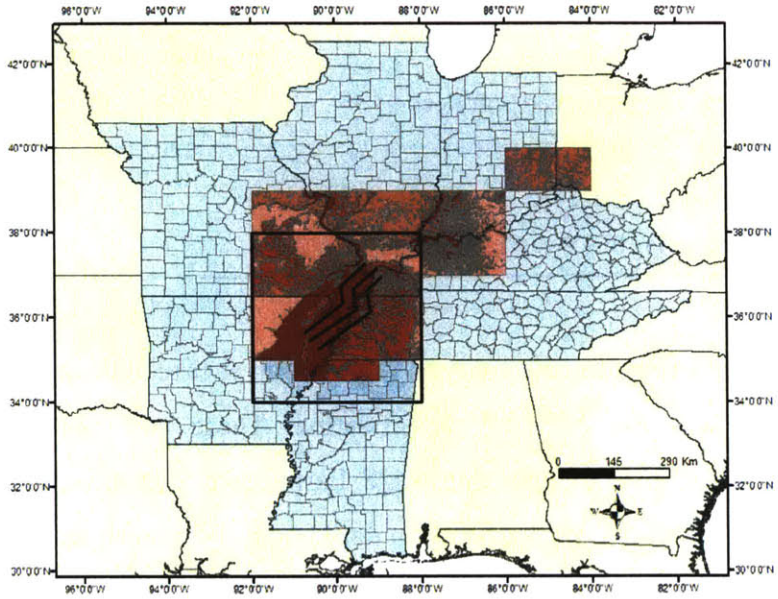

Figure 3-19: CUS Coverage of Soil Classification Maps (Bauer, 1997)

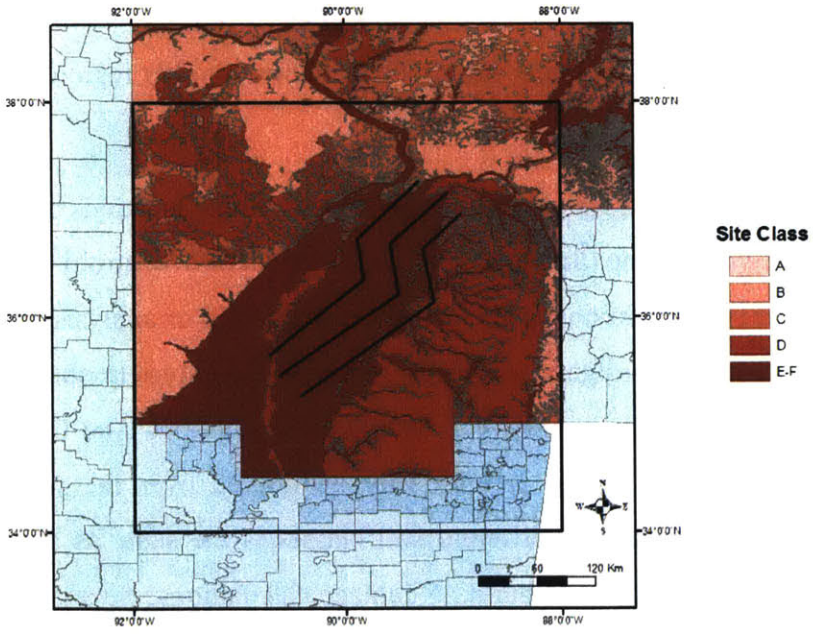

Figure 3-20: NMSZ Coverage of Soil Classification Maps (Bauer, 1997)

3.3.4 Economic Data

The economic data used in the analysis include the production and household consumption for various economic sectors in each analysis region. In addition, we use the value of commodities exported or imported by each state.

Economic sectors

Our analysis uses the 13 economic sectors defined by Okuyama et al (1999) and listed in Table 3-8. This classification system represents the national economy and commodity flows at a reasonable level of detail and is consistent with available economic data. To emphasize the characteristics of the Midwestern economy 7 of the 13 economic sectors correspond to manufacturing industries. The 13^{th} economic sector includes all service sectors and government enterprises and represents more than half of the total industrial output.

Input-output accounts

To obtain the annual output/production levels of the 13 economic sectors in US and the corresponding final demands, we used the data provided by the Bureau of Economic Analysis in the form of national make and use tables. The make and use tables show the value of commodities produced by each industry and the value of commodities used by industries or by final consumers. The online tool at the Bureau of Economic Analysis website (BEA, 2005) has been used to obtain the standard make and use tables for the US for the 13 economic sectors from 1997 Benchmark Input Output Accounts for the US (Lawson et al, 2002). We use the make and use tables to calculate the coefficients of the national input-output matrix for the 13 economic sectors and obtain the regional shares of annual productions and consumptions as explained in the following sections.

The make table (see Table 3-9) is a matrix that shows the value in producer's prices of each commodity produced by each industry. In the matrix, commodities are represented by columns and industries are represented by rows. The entries in a row are the dollar values of various commodities produced by the industry that corresponds to the row. The row total in the make table is the total industry output and the column total is the total commodity output.

Table 3-8: Economic Sectors Used (Okuyama et al, 1999)

	Economic Sector	Annual Output ($B/year)	Annual Final Demand ($B/year)
1	Agriculture, Forestry, and Fisheries	287,324	33,978
2	Mining	229,749	1,062
3	Construction	621,956	483,891
4	Food and Kindred Products	571,335	402,931
5	Chemical and Allied Products	437,051	184,478
6	Primary Metal Industries	177,693	2,124
7	Fabricated Metal Products	175,061	22,564
8	Industrial Machinery and Equipment	249,605	125,553
9	Electronics and Electrical Equipment	426,141	259,858
10	Transportation Equipment	325,496	229,340
11	Other Non-Durable Manufacturing	1,091,142	524,239
12	Other Durable Manufacturing	469,547	263,315
13	Transportation, Communications, Utilities (TCU), Services, and Government Services	5,274,579	3,141,219

The use table (Table 3-10) shows the commodities consumed or used by each industry and by the final consumers. The entries in a row are the dollar values of the use by each industry of the commodity associated with that row and of the sales to the final uses. The industry uses add up to the total intermediate use. The final uses sum up to Gross Domestic Product (GDP). The row total is the total production of the commodity and the column total is the production of the industry. The final uses include government consumption expenditures and investment, personal consumption expenditures, private fixed investments, change in inventories, and exports and imports of services. As it can be seen from the use table the final demands (GDP) for economic sectors 2 and 6 are negative, mainly due to the imports.

In using the US make and use tables to obtain the national consumptions and input-output coefficients, we make the assumption that the US economy is a closed system without exports and imports, i.e. the final demand is free of exports/imports and reflects only personal consumption, government consumption, and investments. In order for the economic data to be consistent with this assumption, we modify the intermediate uses of the commodities by the ratio

Table 3-9: The Make of Commodities by Industries, 1997 ($B/year)

		Commodity													Industry Output
		1	2	3	4	5	6	7	8	9	10	11	12	13	
Industry	1	284511	0	65	312	0	0	0	0	0	0	0	45	1607	286539
	2	0	158239	109	0	1760	0	11	0	0	0	7788	193	553	168653
	3	0	0	670210	0	0	0	0	0	0	0	0	0	0	670210
	4	0	0	65	470805	1592	0	0	0	0	0	256	0	4819	477538
	5	0	0	92	224	393523	0	0	294	358	12	4221	132	9687	408543
	6	0	0	182	0	605	163913	1234	402	582	0	133	786	543	168379
	7	0	0	96	0	59	4258	226588	2379	266	545	700	1237	2987	239115
	8	0	0	28	0	363	74	2556	248839	2246	1396	202	654	4151	260508
	9	0	0	146	0	267	1079	377	984	521029	1398	322	883	9071	535556
	10	0	0	168	0	0	0	1202	3358	2552	556928	31	834	3024	568098
	11	0	194	384	0	15619	451	598	908	690	29	732316	2280	33051	786521
	12	0	533	97	1	531	13	405	73	469	8	2152	327723	8420	340425
	13	556	791	82450	11222	0	0	8	230	207	120	2087	4492	9850629	9952792
Commodity Output		285067	159757	754091	482564	414319	169788	232979	257467	528399	560436	750208	339259	9928543	14862876

Table 3-10: The Use of Commodities by Industries, 1997 ($B/year) (cont. in next page)

		Industry													Intermediate Use
		1	2	3	4	5	6	7	8	9	10	11	12	13	
Commodity	1	74938	15	1121	121984	1319	8	0	0	16	2	12255	14757	16163	242579
	2	370	19461	4281	123	5725	7894	96	63	165	520	92744	5183	58997	195623
	3	1122	29	832	709	1216	439	593	620	920	697	1376	928	62416	71898
	4	18665	0	0	76318	2019	1	0	0	0	32	2249	325	90696	190305
	5	16183	3228	6597	3999	103466	1376	4745	2711	10052	7723	69230	9036	50295	288639
	6	703	2225	4400	15	311	47603	41155	24650	16847	35212	1599	6745	7128	188594
	7	839	2815	38746	10504	5617	3622	22986	22999	15971	32986	6387	8433	38918	210825
	8	2657	4211	13958	502	1663	1858	2555	19480	3084	14545	3556	701	17593	86361
	9	562	245	19326	1249	4767	3672	3850	17566	127803	31688	8901	5845	75880	301353
	10	697	807	3233	180	50	27	505	3135	417	151341	113	536	48660	209700
	11	8386	4615	32754	25796	21500	1625	3712	8883	12377	23739	157290	22966	186515	510156
	12	1116	1130	59899	4281	2436	14803	1646	2553	4901	6824	9606	47624	75119	231936
	13	54653	57140	184191	104483	119928	43209	45644	57257	139624	119940	173852	77515	2611828	3789263
Intermediate Output		180890	95920	369337	350143	270018	126137	127487	159916	332177	425247	539157	200596	3340208	

Table 3-10 (Cont.): The Use of Commodities by Industries, 1997 ($B/year)

		Total Intermediate Use	Final Uses						Sum of Final Uses (GDP)	Total Commodity Output
			Government Expenditures	Personal Consumption	Private Fixed Investment	Change in Inventories	Exports	Imports		
Commodities	1	242579	-956	36132	0	3999	26437	-23123	42488	285067
	2	195623	-205	97	22536	311	5612	-64216	-35866	159757
	3	71898	175843	0	506254	0	96	0	682193	754091
	4	190305	12115	280230	0	2333	25434	-27853	292259	482564
	5	288639	19382	102905	2040	6830	60428	-65906	125680	414319
	6	188594	386	803	0	2462	13342	-35798	-18806	169788
	7	210825	8291	9117	7333	2617	15038	-20242	22154	232979
	8	86361	10143	6526	146490	4273	68608	-64934	171106	257467
	9	301353	38339	67167	168062	6013	139076	-191610	227046	528399
	10	209700	60730	153779	173567	926	110430	-148696	350736	560436
	11	510156	35958	269566	3172	9240	57140	-135023	240052	750208
	12	231936	12980	132296	2886	6307	34044	-81190	107323	339259
	13	3789263	1110144	4512968	287569	16856	342901	-131158	6139280	9928543
Total		6517232	1483149	5571584	1319909	62165.8	898585	-989747	8345646	14862876

of the total intermediate uses plus net exports of a commodity to the total intermediate uses of the commodity

$$U(i,j) = U_{ini}(i,j) \times \left(\frac{\sum_j U_{ini}(i,j) + E(i) - I(i)}{\sum_j U_{ini}(i,j)} \right) \tag{3.1}$$

where $E(i)$ is the value of commodity i exported from the US

$I(i)$ is the value of commodity i imported to the US

$\sum_j U_{ini}(i,j)$ is the total intermediate use of commodity i

Table 3-11 shows the use table for the US after the above modification. This modification does not change the total output of the industrial sectors or commodities. It only changes the fractions of the produced outputs used as intermediate inputs by the industries and used by the consumers. If the net US export of a commodity is positive (export), the total intermediate uses are increased by the net exports. If the net US export of a commodity is negative (import), the total intermediate uses are reduced by such net exports.

This modification slightly changes the inter-industry relations but not the total output of the economic sectors or the total consumptions, which determine the level of economic activities before or after an earthquake. Also, the effects on inter-industry relations are not thought to be large since the net exports/imports are a relatively small fraction of the total output (except for the mining sector).

Input-output matrix

We use the make and use tables to derive the direct requirement or input-output table, $\underline{\underline{A}}$ (see Table 3-12). The values in this table, a_{ij}, referred to as "direct requirement coefficients" or "technical coefficients", show the value of the input commodities needed to make a dollar's worth of the commodity being produced (output). It can be recognized from Table 3-12 that most of the economic sectors depend highly on the 13th economic sector (i.e. TCU, Services, and Government Services), while they depend less on other sectors.

Table 3-11: The Use of Commodities by Industries (after Modification), 1997 ($B/year)

		Industry													Intermediate Use
		1	2	3	4	5	6	7	8	9	10	11	12	13	
Commodity	1	75962	15	1137	123651	1337	8	0	0	17	2	12422	14959	16384	245892
	2	259	13631	2999	86	4010	5529	67	44	116	364	64960	3630	41323	137018
	3	1124	29	833	710	1218	440	594	621	921	698	1378	929	62499	71994
	4	18428	0	0	75348	1993	1	0	0	0	31	2220	321	89543	187887
	5	15876	3166	6471	3923	101503	1350	4655	2659	9861	7576	67916	8865	49340	283162
	6	620	1960	3876	13	274	41935	36255	21715	14841	31019	1409	5942	6279	166138
	7	818	2746	37790	10245	5479	3533	22419	22431	15577	32172	6230	8225	37957	205621
	8	2770	4390	14552	523	1733	1937	2664	20309	3215	15163	3707	731	18342	90035
	9	464	202	15957	1031	3936	3032	3179	14503	105523	26164	7349	4826	62652	248819
	10	569	659	2643	147	41	22	413	2563	341	123725	92	438	39781	171434
	11	7105	3910	27754	21858	18217	1377	3145	7527	10488	20115	133277	19460	158040	432272
	12	889	900	47723	3411	1940	11794	1311	2034	3904	5437	7654	37943	59850	184790
	13	57707	60333	194484	110321	126630	45623	48194	60457	147426	126642	183567	81847	2757776	4001006
Intermediate Output		182590	91942	356217	351267	268313	116580	122896	154863	312230	389108	492180	188116	3399767	

Table 3-11 (Cont.): The Use of Commodities by Industries (after Modification), 1997 ($B/year)

		Total Intermediate Use	Final Uses						Sum of Final Uses (GDP)	Total Commodity Output
			Government Expenditures	Personal Consumption	Private Fixed Investment	Change in Inventories	Exports	Imports		
Commodities	1	245892	-956	36132	0	3999	0	0	39175	285067
	2	137018	-205	97	22536	311	0	0	22739	159757
	3	71994	175843	0	506254	0	0	0	682097	754091
	4	187887	12115	280230	0	2333	0	0	294678	482564
	5	283162	19382	102905	2040	6830	0	0	131157	414319
	6	166138	386	803	0	2462	0	0	3651	169788
	7	205621	8291	9117	7333	2617	0	0	27358	232979
	8	90035	10143	6526	146490	4273	0	0	167432	257467
	9	248819	38339	67167	168062	6013	0	0	279581	528399
	10	171434	60730	153779	173567	926	0	0	389002	560436
	11	432272	35958	269566	3172	9240	0	0	317936	750208
	12	184790	12980	132296	2886	6307	0	0	154469	339259
	13	4001006	1110144	4512968	287569	16856	0	0	5927537	9928543
Total		6426068	1483149	5571584	1319909	62165.8	0	0	8436808	14862876

Table 3-12: The Input-Output Matrix, A

	1	2	3	4	5	6	7	8	9	10	11	12	13
1	0.232	0.000	0.006	0.264	0.003	0.000	0.000	0.000	0.001	0.000	0.010	0.019	0.002
2	0.002	0.166	0.009	0.001	0.028	0.044	0.000	0.000	0.001	0.001	0.102	0.009	0.009
3	0.012	0.017	0.001	0.004	0.008	0.007	0.006	0.006	0.008	0.005	0.007	0.005	0.020
4	0.067	0.000	0.000	0.146	0.006	0.001	0.001	0.001	0.001	0.001	0.003	0.001	0.011
5	0.048	0.013	0.014	0.010	0.224	0.020	0.020	0.005	0.015	0.014	0.068	0.019	0.004
6	0.000	0.011	0.016	0.000	0.002	0.264	0.246	0.087	0.051	0.050	0.002	0.022	0.000
7	0.002	0.006	0.066	0.028	0.009	0.021	0.073	0.042	0.036	0.068	0.003	0.024	0.002
8	0.006	0.022	0.023	0.002	0.005	0.030	0.020	0.132	0.024	0.046	0.005	0.013	0.004
9	0.004	0.002	0.030	0.001	0.001	0.007	0.004	0.081	0.163	0.041	0.001	0.038	0.004
10	0.001	0.001	0.002	0.001	0.000	0.006	0.001	0.003	0.001	0.204	0.001	0.006	0.004
11	0.032	0.017	0.039	0.069	0.072	0.022	0.030	0.031	0.048	0.061	0.212	0.059	0.027
12	0.004	0.004	0.109	0.011	0.006	0.017	0.007	0.009	0.022	0.036	0.015	0.122	0.005
13	0.189	0.237	0.225	0.155	0.209	0.244	0.164	0.157	0.154	0.173	0.183	0.170	0.226

The direct requirements table, $\underline{\underline{A}}$, is obtained by normalizing the make table by commodity output and multiplying it by the use table, normalized by industry output. Algebraically,

$$\underline{\underline{A}} = \underline{\underline{M}}' \times \underline{\underline{U}}' \tag{3.2}$$

$$M'(j,i) = M(j,i) / \sum_{j} U(i,j) \tag{3.3}$$

$$U'(i,j) = U(i,j) / \sum_{i} M(j,i) \tag{3.4}$$

where

$\underline{\underline{A}}$ is the direct requirements or input-output matrix

$\underline{\underline{M}}'$ is the normalized make table

$\underline{\underline{U}}'$ is the normalized use table

$\underline{\underline{M}}$ is the make table

$\underline{\underline{U}}$ is the use table

The direct requirements or input-output matrix, $\underline{\underline{A}}$, shows the linkages among different economic sectors and specifies the value in dollars of different commodities required to produce

one dollar worth of the commodity produced. Commodities produced by industries are either used by other industries as intermediate inputs or to satisfy final demands.

$$\underline{X} = \underline{\underline{A}}\underline{X} + \underline{Y} \tag{3.5}$$

where

$\underline{X}$ is the total industry output

$\underline{Y}$ is the final demand for each commodity

The direct requirement matrix can be used to obtain the total requirements matrix, $(I-A)^{-1}$, which is also called the Leontieff inverse. The total requirements matrix relates final demands to productions. When it is multiplied by the final demand for each commodity, the result is a vector consisting of the required gross outputs

$$\underline{X} = (\underline{\underline{I}} - \underline{\underline{A}})^{-1}\underline{Y} \tag{3.6}$$

where

$\underline{\underline{I}}$ is the identity matrix

Since we assumed that the US is a closed economy without exports and imports, it must be that

$$\underline{X}_{US} = \left(\underline{\underline{I}} - \underline{\underline{A}}\right)^{-1}\underline{C}_{US} \tag{3.7}$$

where

$\underline{X}_{US}$ is the annual national output

$\underline{C}_{US}$ is the annual final demand for each commodity for the US

There are several assumptions inherently associated with this input-output analysis. First, it is assumed that producers are indifferent as to the final destination of their outputs; similarly, consumers are indifferent as to the origin of their inputs. Another assumption is that the technical coefficients are constant with respect to the quantities produced, i.e. no economies of scale. This suggests that inter-industry relations are constant irrespective of the amount of commodities produced. It is further assumed in this study that the industrial structure of individual regions is identical so that the coefficients of the input-output table are the same for all analysis regions.

Disaggregation of national productions and consumptions to analysis regions

The annual outputs/productions, $\underline{X}_{US}$, and consumptions, $\underline{C}_{US}$, for the 13 economic sectors at the national level are obtained from the modified US make and use tables as described in the preceding section. The national productions and consumptions are then disaggregated to the analysis regions, proportionally to each region's share of the national values as described below.

We disaggregate the consumptions $\underline{C}_{US}$ based only on population and distribute the national consumptions proportionally to the population of each analysis region:

$$C_i^k = (P_i / P_{US}) C_{US}^k \qquad \forall i,k \tag{3.8}$$

where

C_i^k consumption of commodity k in region i

C_{US}^k total consumption of commodity k in the US

P_i population of region i

P_{US} total population of US

Equation (3.8) is motivated by the assumption that the consumption patterns does not differ significantly from region to region within the US.

To disaggregate the productions, $\underline{X}_{US}$, we make use of the Gross State Product (GSP) data obtained from the BEA webpage (ref. BEA, webpage). GSP is the value added in production by the labor and property located in a state. In concept, an industry's GSP, referred to as "value added", is equivalent to its gross product (sales or receipts and other operating income, commodity taxes, and inventory change) minus its intermediate inputs (consumption of goods and services purchased from other US industries or imported). In this study, we have mapped the GSP data provided for 81 SIC codes to our 13 economic sectors, using the following procedure.

We first disaggregate national productions/outputs of the 13 economic sectors to state level in proportion to each state's GSP.

$$X_s^k = \frac{GSP_s}{\sum_s GSP_s} X_{US}^k \qquad \forall s,k \tag{3.9}$$

where

X_s^k is the production of commodity k in state s

X_{US}^k is the total production of commodity k in US

GSP_s is the GSP of state s

Then, we disaggregate the state productions to the analysis regions based on the population of the analysis regions:

$$X_i^k = (P_i / P_s) X_s^k \qquad \forall i, s, k \qquad (3.10)$$

where

P_s is the total population of state s.

P_i is the population of analysis region r.

Commodity flow data

Data on flows of commodities between different regions or states are obtained from the 1997 Commodity Flow Survey (CFS) (BTS, 1999). The 1997 CFS data are at the state level and provide information on the value and tonnage of shipments of commodities originating from a state and shipped to other states or to destinations within the state of origin. The 1997 CFS covers businesses in mining, manufacturing, wholesale trade, and selected retail industries. The survey also covers selected auxiliary establishments (e.g. warehouses) of in-scope multiunit and retail complexes. The survey coverage excludes establishments classified as farms, forestry, fisheries, governments, construction, transportation, foreign establishments, services, and most establishments in retail.

The 1997 CFS uses the Standard Classification of Transported Goods (SCTG) for reporting value, tons, and ton-miles of commodities transported from state to state by different modes including truck, rail, water, air, and pipeline. In this research, we assume that all commodities are transported via trucks on highways. According to the 1997 CFS, about 71.7% of all commodities (in terms of value) are transported exclusively by trucks. Compared to percentages of other modes of transportation (4.6% for rail, 1.1% for water, 3.3% for air (includes mixed air and truck

modes), and 1.6% for pipeline), ground transportation by trucks is the dominant mode of transportation for commodities. Their percentage contribution to total value of commodities shipped becomes even higher if mixed modes of transportation (which account for 13.6% of the total value of shipped commodities) are included.

We map the commodity flow data in CFS, which is provided at the two-digit SCTG code level, to the 13 economic sectors considered in our study as shown in Table 3-13. As it can be seen from the table, no commodity is mapped onto economic sectors 3 and 13, as CFS does not provide data on construction and the service sector (government, transportation, etc).

Mapping of Occupancy Classes to Economic Sectors

To reflect the damage caused by earthquakes on industrial facilities, the building occupancy classes are mapped to economic sectors as shown in Table 3-14. This mapping provides the link between the functionality of building occupancy classes and the functionality of the economic sectors. We assume that economic sectors 1 (agriculture) and 3 (construction) do not incur any damage or functionality reduction due to an earthquake. Therefore, no building occupancy classes were mapped onto these two economic sectors.

3.4 Component Models

In this section, we provide a detailed explanation of the component models used in the loss estimation methodology. These component models include:

- Attenuation relationships
- Soil amplification model
- Building vulnerability model
- Bridge vulnerability model
- Loss of functionality and recovery model
- Transportation network and regional economic analysis model

For each component, we first provide a general description of the model and then provide details on the data and parameters selected for application to New Madrid Seismic Zone (NMSZ)

Table 3-13: Mapping of CFS Commodities to Economic Sectors

	Economic Sector	SCTG Code
1	Agriculture, Forestry, and Fisheries	01-03
2	Mining	10-18
3	Construction	-
4	Food and Kindred Products	04-08
5	Chemical and Allied Products	19-23
6	Primary Metal Industries	32
7	Fabricated Metal Products	33
8	Industrial Machinery and Equipment	34
9	Electronics and Electrical Equipment	35
10	Transportation Equipment	36-37
11	Other Non-Durable Manufacturing	09, 24, 27-31
12	Other Durable Manufacturing	31, 38-40
13	TCU, Services, and Government Services	-

Table 3-14: Mapping of Economic Sectors into Building Occupancy Classes

	Economic Sector	Building Occupancy Class	Label
1	Agriculture, Forestry, and Fisheries	-	-
2	Mining	Metals/Mineral Processing	IND4
3	Construction	-	-
4	Food and Kindred Products	Food/Drugs/Chemical	IND3
5	Chemical and Allied Products	Food/Drugs/Chemical	IND3
6	Primary Metal Industries	Heavy Industry	IND1
7	Fabricated Metal Products	Heavy Industry	IND1
8	Industrial Machinery and Equipment	Heavy Industry	IND1
9	Electronics and Electrical Equipment	High Technology	IND5
10	Transportation Equipment	Heavy Industry	IND1
11	Other Non-Durable Manufacturing	Light Industry	IND2
12	Other Durable Manufacturing	Light Industry	IND2
13	TCU, Services, and Government Services	Commercial, Government	COM1-COM10, GOV1-GOV2

earthquakes. When necessary, we provide comparisons between alternative models and parameters.

3.4.1 Ground Motion Attenuation Relationships

Estimates of expected ground motions at a given site resulting from an earthquake are fundamental inputs for many engineering applications including seismic risk analysis and loss estimation. Such estimates are generally provided through attenuation laws, which relate ground motion characteristics to seismological, geologic, and geometric parameters such as earthquake magnitude, distance from the source, type of faulting, and local site conditions (Abrahamson and Shedlock, 1997; Campbell, 2003).

Ground motion attenuation relationships may be derived either empirically or theoretically, depending on the region of interest and the type of information available. In seismically active regions such as California and Japan, ground motion relations are often derived empirically using recorded ground motions. By contrast, in seismically less active regions such as the Central US where there are few strong motion recordings, theoretical models are generally preferred.

The ground motion parameters that are most commonly estimated are peak ground acceleration (PGA), peak ground velocity (PGV), and 5% damped spectral acceleration (SA) at various natural frequencies. For example, the US National Seismic Hazard Maps (NSHM) provide PGA and 0.2, 0.3, and 1.0sec SA with a 10%, 5%, and 2% probability of exceedance in 50 years at firm rock sites (Frankel et al, 1996, 2002).

Key parameters on which ground motion depends are magnitude and distance. Generally, moment magnitude is the preferred magnitude measure as it is related to the seismic moment of the earthquake (a measure of energy release), but other magnitude measures have also been used (McGuire, 2004). There are also different ways to define source to site distance, including the horizontal distance to the vertical projection of rupture (r_{jb}), the distance to the rupture surface (r_{rup}), the distance to the seismogenic rupture surface (r_{seis}), and the hypocentral distance (r_{hypo}). The reader is referred to Abrahamson and Shedlock (1997) for the definition and graphical representation of these distances.

In addition to magnitude and distance, type of faulting is generally considered in attenuation relationships, especially the most recent ones. Reverse and thrust earthquakes tend to generate larger PGA and high-frequency SA than strike-slip and normal earthquakes. Directivity and hanging wall effects have also been considered in some of the derived relations.

Most empirical attenuation relationships have the following form (McGuire, 2004)

$$\ln(y) = C_0 + f(M) + f(R) + f(S) + \varepsilon \tag{3.11}$$

where y is the ground motion amplitude, C_0 is a constant, M is magnitude, R is distance, S is some quantitative description of soil type, and ε is a random variable taking on a specific value for each observation. Some equations involve coupled terms for magnitude M and distance R, i.e. functions $f(M,R)$. It should be noted that attenuation relationships estimate mean log amplitude. If, as it is often assumed, ε has normal distribution, then exponentiation gives the median amplitude. The mean amplitude lies above the median amplitude by the factor $e^{(\sigma^2/2)}$, where σ is the standard deviation of ε. The scatter in ground motion $\ln(y)$ given (M, R, S) is quite large; its coefficient of variation generally varies between 0.6 and 0.8 depending on source characteristics and distance. This is a major uncertainty that contributes to seismic hazard and risk calculations. Uncertainty in ground motion will be discussed in more detail in the following sections.

3.4.1.1 CUS Attenuation Relationships

The CUS is a stable continental region with low seismicity and few ground motion records. One method that can be used to derive attenuation relationships for this region is to formulate a stochastic source model, use the model to generate a synthetic database of strong ground motions, and then use regression analysis to develop simplified equations based on the synthetic data.

Below is a short summary and brief description of the five CUS attenuation relationships that have been used to generate the 2002 USGS National Seismic Hazard Maps (NSHMs). All these relationships were developed from regression analyses of synthetic ground motions. Table 3-15 lists relevant information for the five attenuation relations including the ground motion model used, whether they predict vertical ground motion (V) in addition to the average horizontal

Table 3-15: Ground Motion Relations Used in 2002 USGS National Seismic Hazard Maps (Campbell, 2004)

Ground Motion Relation	Model	Comp	Periods	Model Parameters	Validity
Atkinson and Boore (1995)	Stochastic	H	PGA, 0.10-1.00	M, r_{hypo}	$5.0 \le M_w \le 8.2$, $10 \le r_{hypo} \le 1000$ km
Frankel et al (1996)	Stochastic	H	PGA, 0.10-2.00	M, r_{hypo}	$4.4 \le M_w \le 8.2$, $10 \le r_{hypo} \le 1000$ km
Toro et al. (1997)	Stochastic	H	PGA, 0.03-2.00	M, r_{jb}	$4.5 \le M_w \le 8.0$, $1 \le r_{jb} \le 500$ km
Campbell (2001)	Hybrid Empirical	H	PGA, 0.02-4.00	M_w, r_{rup}	$5.0 \le M_w \le 8.2$, $r_{rup} \le 1000$ km
Somerville et al (2001)	Kinematic	H, V	PGA, 0.04-4.00	M, r_{jb}	$6.0 \le M_w \le 7.5$, $10 \le r_{jb} \le 500$ km

component (H), the range of periods for which they are applicable, the seismological parameters included, and the range of magnitudes and distances within which they are considered valid.

Among these ground motion relations, only those of Somerville et al (2001) and Campbell (2003) explicitly include near-source scaling features. The others require their distance measures to be modified or ground motion estimates capped to give realistic ground motion estimates near the source. In developing the USGS NSHMs, the hypocentral distance r_{hypo} used by Atkinson and Boore (1995) and Frankel et al (1996) was replaced with the distance to the surface projection of faulting, r_{jb}, and a fictitious depth was used to force the relation to asymptotically approach a finite value at short distances. Furthermore, absolute amplitude caps were applied to both the median estimates and the upper tails of the distributions of PGA and selected spectral accelerations. The median PGA was capped at 1.5g, and the median 0.3 and 0.2sec SA values were capped at 3.0g.

Atkinson and Boore (1995, 1997)

Atkinson and Boore (1995) developed empirical stochastic relations for attenuation in Eastern North America (ENA). The relations were developed using an empirical two corner source model and simulating ground motion parameters for different magnitude-distance combinations using the model inputs described below. They used a wide variety of data sources to define the input parameters to the stochastic model and then validated the resulting model against the ENA ground-motion database. Atkinson and Boore (1997) compared their attenuation relation with other models developed for ENA and California.

The data used to specify the model parameters for the earthquake spectrum are all from hard rock sites. The model has the form

$$A(M, r_{hypo}, f) = E(M, f)D(r_{hypo}, f)P(f)I(f) \tag{3.12}$$

where f is frequency, $E(M, f)$ is the earthquake source spectrum (the source spectrum model, which uses two corner frequencies, is empirical; see Atkinson, 1993), $D(r_{hypo}, f)$ is an empirical function that models the geometric and anelastic attenuation of the spectrum as a function of distance (Atkinson and Mereu, 1992), $P(f)$ is a high-cut filter that rapidly reduces amplitudes at very high frequencies ($f >> 10Hz$), and $I(f)$ is a filter used to shape the spectrum to for ground

motion measure of interest. For example, for the computation of response spectra I is the response of an oscillator to ground acceleration. Atkinson and Boore used the $f_{\max}$ model of Hanks (1982) with $f_{\max} = 50Hz$ for hard rock sites. This roughly corresponds to the kappa model with kappa = 0.002.

In addition to the earthquake spectrum, the duration of the ground motion T as the sum of two terms

$$T = T_0 + T_b(r_{ypo}) \tag{3.13}$$

where T_0 is the source duration and T_b is a distance dependent term which accounts for scattering and dispersion. The way the second term is defined differs from the approach used in other studies (e.g. EPRI, 1993) and is a principal factor for discrepancies between alternative relations, particularly at distances between 50 and 150 km.

Using the quantities A and T described above, response spectra for frequencies 0.5Hz to 20Hz as well as PGA and PGV were simulated for 4.00<M<7.25 and 10<r_{hypo}<500km. The median ground motions for the random horizontal component under hard rock conditions are given in tables and approximated by functions of the type

$$\ln(y) = C_1 + C_2(M-6) + C_3(M-6)^2 - \ln R + C_4 R \tag{3.14}$$

The coefficients in equation (3.14) are listed in Table 3-16 for different ground-motion parameters, where SA and PGA are in g, PGV is in cm/s, and R is in km. For small to moderate events (M<5.5), the approximate analytic expressions overpredict the ground motions at distances grater than 30km, compared to the ground motion relations provided in the tables. However, the discrepancies are not large and secondary importance for the present study.

Comparing the ground motion equations derived by Boore and Joyner (1991) for deep soil sites to relations derived by Boore and Atkinson (1987) for rock sites, Atkinson and Boore (1995) provide amplification factors from bedrock conditions to stiff, deep ENA soil sites (depth>60m, shear wave velocity ~500m/s). The latter correspond to NEHRP site class B. The site amplification factors for Sa(0.2sec) and Sa(1.0sec) are 1.7 and 1.9, respectively. For other soil conditions, the amplification factors may be determined analytically or empirically based on

assumed average shear-wave velocity in the top 30 m. The near-surface shear wave velocity for ENA hard rock sites (NEHRP site class A) is about 2800m/s (Silva and Darragh, 1995).

Frankel et al (1996)

Frankel et al (1996) derived an attenuation relation for firm-rock sites in CEUS (NEHRP BC boundary sites) using stochastic simulation and random vibration theory. The relations are based on Brune's source model with a stress drop of 150bars. The simulations contain frequency dependent amplification factors derived from a hypothesized shear-wave velocity profile of a typical CEUS firm rock site. The kappa value, a site attenuation parameter, was set to 0.01, which is much lower than site kappas for typical WUS rock sites. Frankel et al used 0.75, 0.75, 0.75, and 0.80 for the standard deviation of the natural logarithms of PGA, 0.2, 0.3, and 1.0-sec SA, respectively.

Frankel et al also derived ratios between ground motion amplification at firm-rock (NEHRP BC boundary sites) and hard-rock sites (NEHRP site class A), using the near surface velocity and site kappa values of Toro et al (1993). These average ratios were used to adjust Toro et al (1993) hard-rock attenuation values to firm-rock conditions in the development of the USGS Nntional Seismic Hazard Maps. The factors, which are applied independently of magnitude and distance, are 1.52 for PGA, 1.76 for Sa(0.2 sec), 1.72 for Sa(0.3sec), and 1.34 for Sa(1.0sec). The same factors may be used to adjust the attenuation relations of Frankel et al from firm-rock to hard-rock.

The results are presented in tables as a function of moment magnitude and log of hypocentral distance. When using these tables for M8.0 events in New Madrid, Frankel et al specified a source depth of 10km, which is also the default depth in HAZUS. The base 10 logs of PGA, Sa(0.2sec), Sa(0.3sec), and Sa(1.0sec) in g for a moment magnitude of 8.0 are given in Table 3-17, as a function of (base 10) log of hypocentral distance.

Toro et al (1997)

Toro et al (1997) developed attenuation relationships for ground motions in Central and Eastern North America (CENA) based on a stochastic source model and a model of path effects that considers multiple rays in a horizontally layered model of the Earth crust. These models and the values of their parameters were developed from the analysis of ground-motion records and other

relevant data. The study presents the attenuation relationships developed in EPRI (1993) in a functional form to be used in probabilistic hazard analysis and compares the results to other attenuation equations proposed for CENA. In the EPRI (1993) study, best-estimates and uncertainties were obtained for the attenuation parameters and the uncertainties were carried to final results.

The frequency, distance, and magnitude ranges for the proposed relationships are 1 to 35Hz, 1 to 500km (with emphasis on 1 to 100km), and moment magnitude M5.0 to M8.0. Separate attenuation relations were obtained for two crustal regions typical of CENA, namely the Mid-continent and Gulf crustal regions. The results are directly applicable to hard rock (defined as having an average shear velocity of 1830m/s at the surface, i.e. NEHRP site class A).

The functional form of the simplified attenuation relationships is

$$\ln(y) = C_1 + C_2(M-6) + C_3(M-6)^2 - C_4 \ln R_M - (C_5 - C_4)\max\left[\ln(\frac{R_M}{100}), 0\right] - C_6 R_M \qquad (3.15)$$

where

$$R_M = \sqrt{r_{jb}^{\ 2} + C_7^{\ 2}} \qquad (3.16)$$

The coefficients for the mid-continent region are listed in Table 3-18. The quadratic magnitude term in the above equation is required to provide a better fit of the model for low frequency ground motions (f<5Hz). The terms with coefficients C_4 and $(C_5 - C_4)$ represent geometrical spreading with slope (in log-log space) C_4 for R_M<100km and C_5 for R_M>100km.

The model predictions are similar to those of Boore and Atkinson (1987) and Atkinson and Boore (1995). The aleatory uncertainty is decomposed into a magnitude dependent and a distance dependent term, whereas the epistemic uncertainty is magnitude dependent. The aleatory and epistemic uncertainties assessed by Toro et al are similar to those of other studies for high frequencies and moderate distances, but are higher for low frequencies or short distances. These attenuation relations were derived using mainly point-source modeling. As a consequence, the results may overestimate ground motions near the rupture of a large earthquake since other geometric and potential source-scaling effects associated with extended ruptures are not included.

Table 3-16: Coefficients for Atkinson and Boore (1995, 1997) Attenuation Relation

	C_1	C_2	C_3	C_4	$\sigma_{ln(y)}$
PGA	1.841	0.686	-0.123	0.00311	-
Sa(0.2sec)	1.749	0.963	-0.148	0.00105	0.599
Sa(1.0sec)	-0.508	1.428	-0.094	0.00000	0.553

Table 3-17: Log of Ground Motion Parameters in g for M=8.0 as a Function of log Distance (Frankel et al., 1996)

	Log R								
	1.0	1.2	1.5	1.7	2	2.2	2.5	2.7	3
PGA	0.54	0.32	-0.03	-0.29	-0.58	-0.77	-1.21	-1.56	-2.14
Sa(0.2sec)	0.78	0.56	0.24	0.00	-0.24	-0.38	-0.81	-1.21	-2.01
Sa(0.3sec)	0.67	0.46	0.14	-0.09	-0.31	-0.44	-0.81	-1.16	-1.90
Sa(1.0sec)	0.23	0.02	-0.29	-0.51	-0.69	-0.78	-1.05	-1.29	-1.77

Table 3-18: Coefficients for Toro et al (1997) Attenuation Relation

	C_1	C_2	C_3	C_4	C_5	C_6	C_7
PGA	2.20	0.81	0.00	1.27	1.16	0.0021	9.3
Sa(0.2sec)	1.73	0.84	0.00	0.98	0.66	0.0042	7.5
Sa(1.0sec)	0.09	1.42	-0.20	0.90	0.49	0.0023	6.8

HAZUS uses an adjusted distance term R_M to model the saturation effects of extended ruptures on near-fault ground motion. Based on private communication with Toro et al (NIBS, 2000), R_M in equation (3.16) is replaced by

$$R_M = \sqrt{r_{jb}^{\ 2} + C_7^{\ 2}} + 0.089e^{0.6M} \tag{3.17}$$

This adjusted distance R_M is used throughout this study.

Somerville et al (2001)

Somerville et al (2001) developed attenuation relations for CEUS using a finite-fault model. They first developed earthquake scaling relations to generate a suite of ground motion time histories. The slip models of three recent earthquakes in Canada are used to obtain relations between seismic moment and source parameters such as fault dimensions and rise time. Broadband time histories are calculated using a crustal structure model and ranges of source

parameters consistent with source scaling relations. These time histories are used to generate ground motion attenuation relations for hard rock conditions in CEUS. The simulated ground motions have magnitudes $6.0 \le M_w \le 7.5$ and distances $0 \le r_{jb} \le 500$. Ground motion models for both horizontal and vertical components are developed for response spectral acceleration in the 0.0 to 4.0sec period range.

The functional form used for the attenuation relation is

For $r_{jb} < 50km$,

$$\ln(y) = C_1 + C_2(M-6.4) + C_3 \ln R + C_4 \ln(M-6.4) \ln R + C_5 r_{jb} + C_7(8.5-M)^2 \tag{3.18}$$

For $r_{jb} \ge 50km$,

$$\begin{aligned} \ln(y) &= C_1 + C_2(M-6.4) + C_3 \ln R + C_4 \ln(M-6.4) \ln R \\ &+ C_5 r_{jb} + C_6(\ln R - \ln R_1) + C_7(8.5-M)^2 \end{aligned} \tag{3.19}$$

where $R = \sqrt{r_{jb}^2 + 6^2}$ and $R_1 = \sqrt{50^2 + 6^2}$.

Attenuation relations were developed separately for earthquake depth distributions that correspond to rifted and non-rifted domains. In this study, we use the above expressions and regression coefficients for horizontal spectral acceleration in rifted zones; see Table 3-19.

Campbell (2001, 2003)

Campbell (2001, 2003) implemented a hybrid empirical-theoretical procedure that uses ratios of stochastic ground motion estimates to adjust empirical ground motion estimates for one region to be used in another region. Specifically, the method is applied to produce ground motion relations for PGA and spectral acceleration in eastern North America (ENA) using empirical relations for western North America. The method accounts for differences in stress drop, source properties, crustal attenuation, regional crustal structure, and generic versus rock site profiles between the two regions. The resulting hybrid empirical ground motion relations are considered to be most appropriate for ENA hard rock sites with a shear wave velocity of 2800m/sec, for earthquakes with $M_w \ge 5.0$ and at distances $r_{rup} \le 70$. The model has been extended to larger distances using stochastic ground motion estimates.

The attenuation relation of Campbell (2003) has the form

$$\ln(y) = C_1 + C_2 M_w + C_3 (8.5 - M_w)^2 + C_4 \ln\left[f_1(M_w, r_{rup}) \right] + f_2(r_{rup}) + (C_9 + C_{10} M_w) r_{rup} \qquad (3.20)$$

where

$$f_1(M_w, r_{rup}) = \sqrt{{r_{rup}}^2 + \left[C_5 \exp(C_6 M_w) \right]^2} \qquad (3.21)$$

$$f_2(r_{rup}) = \begin{cases} 0 & r_{rup} \le 70km \\ C_7(\ln r_{rup} - \ln 70) & 70 < r_{rup} \le 130km \\ C_7(\ln r_{rup} - \ln 70) + C_8(\ln r_{rup} - \ln 130) & 130km < r_{rup} \end{cases} \qquad (3.22)$$

The standard deviation of $\ln(y)$ depends on magnitude as

$$\sigma_{\ln y} = \begin{cases} C_{11} + C_{12} M_w & M_w < 7.16 \\ C_{13} & M_w \ge 7.16 \end{cases} \qquad (3.23)$$

The C coefficients in the above relationships are given in Table 3-20.

The model is considered valid for $M_w \ge 5.0$ and $r_{rup} \ge 0$ but the empirical database used to develop it is restricted to $M_w \le 7.5$ and distances up to 100km. According to Campbell (2003) the attenuation relation can be used also outside this empirical data range because of its physically based functional form and its seismologically constrained attenuation rate.

3.4.1.2 Comparison of CUS Attenuation Relationships

The above attenuation models for PGA and Sa(1.0sec), an earthquake of moment magnitude M8.0 and NEHRP site class BC conditions are plotted in Figures 3-21 and 3-22. Figures 3-23 and 3-24 show the same relations for distances up to 200km, in semi-log scale. A similar comparison for magnitude M7.0 earthquake is made in Figures 3-25 and 3-26.

If the original attenuation relationship is given for soil conditions other than site class BC, the resulting predictions are adjusted to account for site effects. If soil amplification factors or similar scaling factors for PGA and Sa(1sec) are indicated in the original reference, these factors have been used to obtain ground motions for site class BC. Otherwise, we have used the scaling factors of the USGS NSHMs to convert hard rock ground motions to site class BC.

Table 3-19: Coefficients for Somerville et al (2001) Attenuation Relation

	C_1	C_2	C_3	C_4	C_5	C_6	C_7	$\sigma_{ln(y)}$
PGA	0.239	0.805	-0.679	0.0861	-0.00498	-0.477	0.0000	0.587
Sa(0.2sec)	0.793	0.805	-0.679	0.0861	-0.00498	-0.477	0.0000	0.611
Sa(1.0sec)	-0.307	0.805	-0.696	0.0861	-0.00362	-0.755	-0.1020	0.693

Table 3-20: Coefficients for Campbell (2003) Attenuation Relation

	C_1	C_2	C_3	C_4	C_5	C_6	C_7	C_8	C_9	C_{10}	C_{11}	C_{12}	C_{13}
PGA	0.0305	0.633	-0.0427	-1.591	-0.00428	0.000483	0.683	0.416	1.140	-0.873	1.030	-0.0860	0.414
Sa(0.2sec)	-0.4328	0.617	-0.0586	-1.320	-0.00460	0.000337	0.399	0.493	1.250	-0.928	1.077	-0.0838	0.478
Sa(0.3sec)	-0.6906	0.609	-0.0786	-1.280	-0.00414	0.000263	0.349	0.502	1.241	-0.753	1.081	-0.0838	0.482
Sa(1.0sec	-0.6104	0.451	-0.2090	-1.158	-0.00255	0.000141	0.299	0.503	1.067	-0.482	1.110	-0.0793	0.543

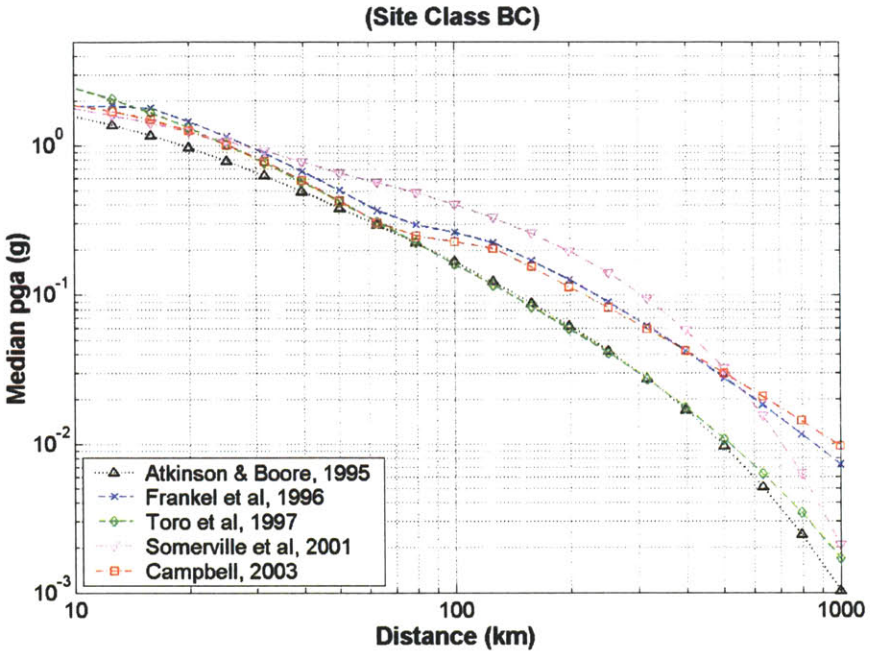

Figure 3-21: Comparison of CEUS Attenuation Relations for PGA, M=8.0

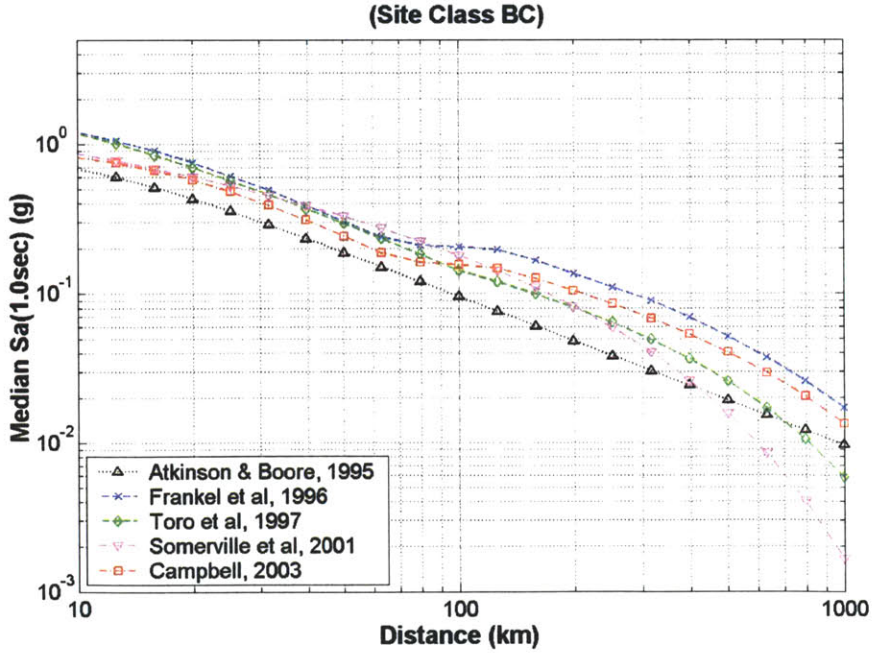

Figure 3-22: Comparison of CEUS Attenuation Relations for Sa(1.0sec), M=8.0

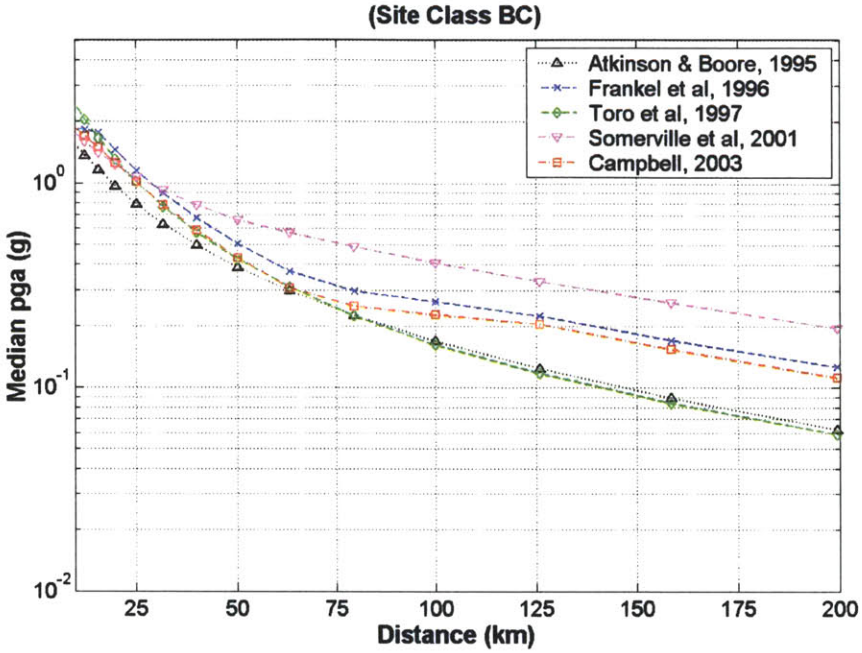

Figure 3-23: Comparison of Attenuation Relations for PGA, M=8.0

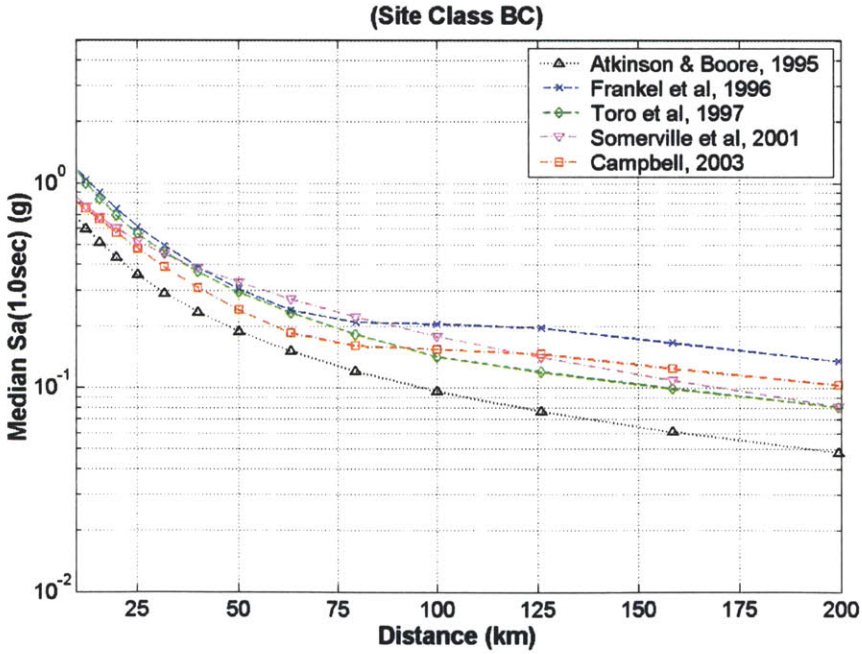

Figure 3-24: Comparison of Attenuation Relations for Sa(1.0sec), M=8.0

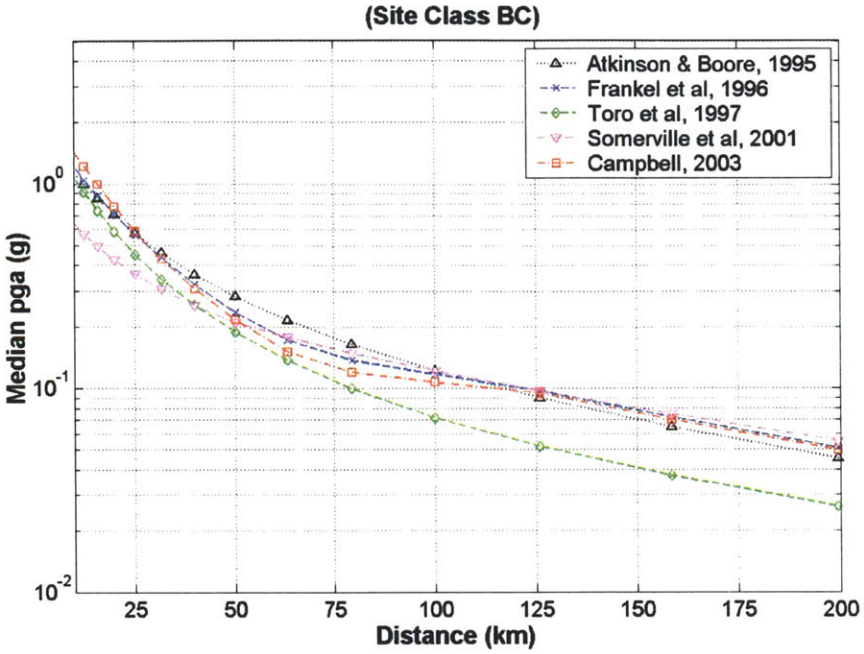

Figure 3-25: Comparison of Attenuation Relations for PGA, M=7.0

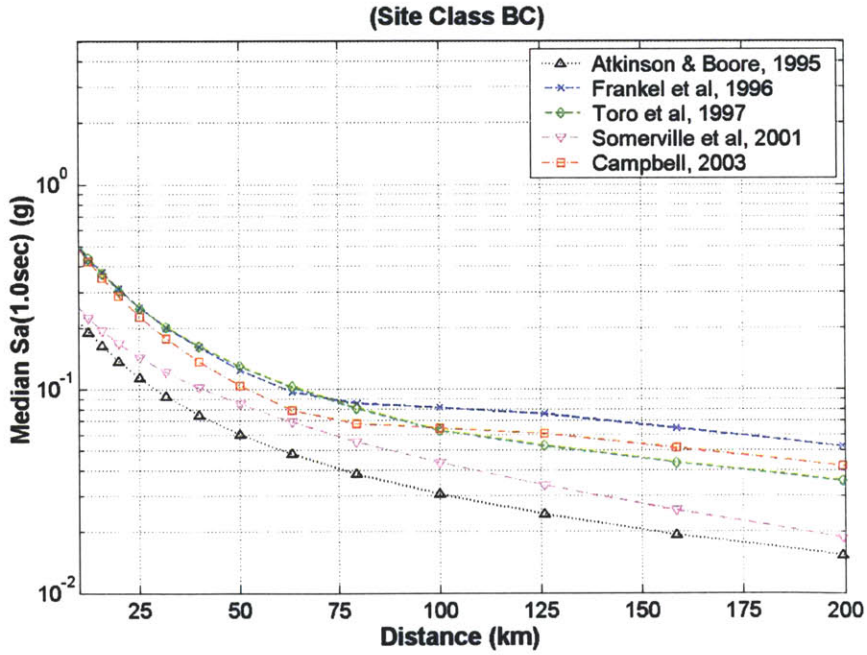

Figure 3-26: Comparison of Attenuation Relations for Sa(1.0sec), M=7.0

As can be seen from Figures 3-21 and 3-23, Atkinson and Boore (1995) and Somerville et al (2001) generally produce the lowest and highest PGA estimates, respectively. Toro et al (1997) predict PGA values similar to Atkinson and Boore at distances greater than 80km, but higher values at closer distances. Frankel et al (1996) and Campbell (2003) give approximately the same PGA at all distances. Figures 3-22 and 3-24 show that also for Sa(1.0sec) the estimates of Atkinson and Boore (1995) are lower than those of the other models, whereas the model of Frankel et al (1996) generally produces the highest estimates.

Figure 3-25 shows the attenuation of PGA for moment magnitude M7.0. Except for the initial 40 km, where Somerville et al (2001) predicts lowest PGA values, the estimates of Toro et al (1997) are lower than the other models. For distances greater than 100km, other four models give very consistent estimates. Note that Atkinson and Boore (1995) was the lowest of all models for M8.0, whereas for M7.0 it is one of the models that provide the highest PGA estimates. In case of Sa(1.0sec), (see Figure 3-26), estimates of Atkinson and Boore (1995) for M=7.0 are much lower compared to estimates of other models in all distance ranges. Again, predictions from Frankel et al are in general the highest.

As will be shown in Chapter 4, the differences among attenuation relations significantly affect the absolute and relative value of earthquake damage in different distance ranges. Further comparison and discussion on the above relations can be found in Campbell (2001) and Bozorgnia and Campbell (2004).

3.4.2 Site Amplification Model

The attenuation relationships described above provide ground motion estimates for specific site conditions. If the conditions are different, the predicted intensities must be modified.

Site conditions that influence the severity of ground motion may include the local geology, basin effects, and surface topography (Kramer and Stewart, 2004). Local geology effects refer to the influence of relatively shallow geologic materials on propagating seismic waves and these effects are usually modeled using one-dimensional wave propagation along the local soil profile. Basin effects refer to the influence of two- or three-dimensional sedimentary basin structures and may include body wave reflections and surface wave generation at basin edges. Finally, topographical effects refer to the influence of surface topography. For example, ground motions are

oftenamplified along ridges or near the tops of slopes and are typically de-amplified in canyons or near the base of a slope.

In this study, we do not consider basin or topographical effects and only account for amplification due to local geologic conditions. In engineering design and analysis, local site response or site amplification can be accounted for by using either site amplification factors or specific ground response analyses. The latter approach requires detailed data on local soils and their dynamic properties, and is more suitable for site specific analysis. The use of site amplification factors is considerably simpler, as it requires a soil classification rather than actual soil data and corresponding amplification factors. This approach is more suitable for regional analyses of the type of interest here.

At any given location, we first determine the site class from CUSEC soil maps as explained in Section 3.3.3. Then, we calculate the ground motion amplification factors corresponding to the ground motion levels estimated using attenuation relationships on reference soil and the site class. The amplified ground motions are used to construct the demand spectra as explained in Section 3.4.3.

The following sections describe the soil classification and soil amplification factors used in this study.

3.4.2.1 Site Amplifications Factors

Site amplification factors give the ratio of a given ground motion intensity parameter (such as PGA) at a given site category to the value of the same parameter at a reference site category. Accordingly, site amplification factors are a convenient (although rather crude) method to account for site effects.

Site amplification factors are obtained either from strong motion records or through wave propagation analysis. The site amplification factors used in modern seismic design codes, such as the 1997 UBC and 2000 IBC, were originally derived for use in the 1994 NEHRP Provisions. Two sets of amplification factors on the spectral acceleration are provided in the NEHRP provisions, one for short periods (T=0.1 to 0.5 sec) and the other for long periods (T= 0.4 to 2.0 sec). The amplified ground motions are simply obtained from

$$SA_{s,i} = SA_{s,r} F_{A,i} \tag{3.24}$$

$$SA_{L,i} = SA_{L,r} F_{V,i} \tag{3.25}$$

where $SA_{s,i}$ is the short period spectral acceleration for Site Class i

$SA_{s,r}$ is the short period spectral acceleration for reference Site Class

$F_{A,i}$ is the short period spectral amplification factor for Site Class i

$SA_{l,i}$ is the long period spectral acceleration for Site Class i

$SA_{l,r}$ is the long period spectral acceleration for reference Site Class

$F_{V,i}$ is the long period amplification factor for Site Class i

The reference condition of the 1997 NEHRP Provisions is Site Class B ($V_{s-30} \approx 1000 m/\sec$), whereas the reference site condition for the USGS NSHMs s is the boundary between NEHRP site classes B and C ($V_{s-30} = 760 m/\sec$) i.e. site class "B/C". Since the ground motions are provided for B/C site conditions, one needs to modify the site amplifications factors to a reference B/C site class. To be conservative in the seismic design codes the value of the ground motion for site class B/C was used by USGS to represent Site B conditions (Campbell and Seligson, 2002, referring to personal communication with Leyendecker, 2002). This is also the procedure used by HAZUS to calculate amplified ground motion intensities. This mismatch in the site conditions of the attenuation relations and the reference site conditions of the site amplification factors results in a positive bias in the loss estimates produced by HAZUS.

Here, we remove this conservative bias by normalizing the soil amplification factors to 1.0 for site class B/C. The factors for B/C are taken as the averages of the amplification factors for classes B and C. The short and long period site amplification factors provided in the NEHRP provisions are given in Tables 3-21 and 3-22. The amplification factors for site class BC, which are used as normalization factors, are also given in these tables. The amplification factors relative to site class B should be divided by these factors to obtain the amplifications relative to site class B/C.

As can be seen from Table 3-21 and Table 3-22, the effect of using site B/C ground motions together with site B site amplification is especially significant for long period ground motions

Table 3-21: NEHRP Short Period Soil Amplification Factors, F_A

	Site Class					
$SA_{S,B}$ (g)	**A**	**B**	**BC**	**C**	**D**	**E**
0.25	0.8	1.0	1.10	1.2	1.6	2.5
0.50	0.8	1.0	1.10	1.2	1.4	1.7
0.75	0.8	1.0	1.05	1.1	1.2	1.2
1.00	0.8	1.0	1.00	1.0	1.1	0.9
1.25	0.8	1.0	1.00	1.0	1.0	0.9

Table 3-22: NEHRP Long Period Soil Amplification Factors, F_V

	Site Class					
$SA_{L,B}$ (g)	**A**	**B**	**BC**	**C**	**D**	**E**
0.1	0.8	1.0	1.35	1.7	2.4	3.5
0.2	0.8	1.0	1.30	1.6	2.0	3.2
0.2	0.8	1.0	1.25	1.5	1.8	2.8
0.4	0.8	1.0	1.20	1.4	1.6	2.4
0.5	0.8	1.0	1.15	1.3	1.5	2.4

since for long periods the site class C amplification factors are larger than those for short periods. The overestimation of ground motion can be as high as a factor 1.35 for long periods and low intensity levels (notice that the long period soil amplification factors for site class C are as high as 1.70 for spectral accelerations less than 0.1g). Due to soil nonlinearity, the long period site amplification factors decrease with increasing ground motion intensity due to soil nonlinearity.

In the following, we review three studies of site amplification, the results of which are used in the present study. All studies use the NEHRP soil classification system and the class B as reference condition. Therefore, the site amplification factors of these studies are modified as explained above to correspond to BC reference conditions.

Dobry et al. (2000)

The site coefficients in Dobry et al. (2000) are the same as those given in the NEHRP provisions and in recent seismic design codes. These are also the site coefficients used by HAZUS (NIBS, 2000). The amplification coefficients are based on empirical studies for motions up to 0.1g and on theoretical and laboratory tests for stronger ground motions. The empirical studies include the records from the Loma Prieta and other earthquakes. The short and long period amplification factors of Dobry et al (2000), modified as explained above are given in Table 3-23.

Hwang et al (1997)

Hwang et al (1997) employ a probabilistic approach to obtain the statistics of amplification factors for the five NEHRP site classes (A to E) by using synthetic acceleration time histories expected to occur in the eastern United States (see Table 3-24). By including uncertainty in seismic source, path attenuation and local site conditions, they perform 250 runs for each site category. Using the simulated records, these authors perform regression analyses to obtain the site coefficients for different site categories.

For site classes A and B, the amplification factors of Hwang et al. (1997) are the same as those of the NEHRP provisions. For site class C, the amplification factors are independent of the ground shaking level, implying linear soil behavior. The amplification factors for site class C are close to those in the NEHRP provisions. However, for site classes D and E, the amplification factors are larger than those of the NEHRP provisions. In Hwang et al. (1997), the long period site coefficients, F_v, increase with increasing ground shaking intensity for site classes D and E.

this trend is opposite to that of the NEHRP provisions, where the amplification factors decrease with increasing ground shaking intensity. According to Hwang et al (1997), the difference could be due to the fact that in their study the site coefficients are derived using synthetic acceleration time histories that are expected to occur in the eastern United States, whereas the site coefficients in the NEHRP provisions are primarily based on ground motion data from the Western United States.

Borcherdt (2002)

Borcherdt (2002) use 1994 Northridge earthquake data and recent geotechnical data to develop empirical estimates of the amplification factors for site classes C and D (see Table 3-25). They derive soil amplification factors only for site classes C and D. When using their estimates, we have assumed that the soil amplification factors for other site classes are the same as those in the NEHRP Provisions.

Borcherdt find that at the 95% confidence level their amplification factor estimates for a ground shaking level of 0.3g or greater are consistent with those in the NEHRP provisions. However, for ground motions of 0.1g and 0.2g the NEHRP values are below their lower confidence bounds by up to 13%. The amplification factors of Borcherdt decrease with increasing ground shaking intensity, which is consistent with the codes. Borcherdt (2002) observe that the short and long period amplification factors given in their study exceed those in the codes for site classes C and D. Hence they suggest that the corresponding factors in the codes may have to be increased.

3.4.2.2 Comparison of Site Amplification Factors

The site amplification factors for site classes A and B are the same in all the above studies (before the modifications due to reference conditions of the ground motion estimates and the site amplification studies). As Borcherdt (2002) only provides estimates of site amplification factors for site classes C and D, here we compare the factors only for those two site classes.

Figure 3-27 and Figure 3-28 compare the short period amplification factors in the above studies for site classes C and D. It can be seen that the estimates of Dobry et al. (2000) are consistently lower than those of the other two studies and that the Borcherdt values are slightly higher than those of Hwang et al. The short period factors decrease with increasing spectral

Table 3-23: Modified Amplification Factors for Dobry et al (2000)

Site Class BC Spectral Acceleration	Site Class					
	A	B	BC	C	D	E
$SA_{S,B}$ (g)	Short Period Amplification Factor, F_A					
0.25	0.727	0.909	1.000	1.091	1.455	2.273
0.50	0.727	0.909	1.000	1.091	1.273	1.545
0.75	0.762	0.952	1.000	1.048	1.143	1.143
1.00	0.800	1.000	1.000	1.000	1.100	0.900
1.25	0.800	1.000	1.000	1.000	1.000	0.900
$SA_{L,B}$ (g)	Long Period Amplification Factor, F_V					
0.1	0.593	0.741	1.000	1.259	1.778	2.593
0.2	0.615	0.769	1.000	1.231	1.538	2.462
0.2	0.640	0.800	1.000	1.200	1.440	2.240
0.4	0.667	0.833	1.000	1.167	1.333	2.000
0.5	0.696	0.870	1.000	1.130	1.304	2.087

Table 3-24: Modified Amplification Factors for Hwang et al (1997)

Site Class BC Spectral Acceleration	Site Class					
	A	B	BC	C	D	E
$SA_{S,B}$ (g)	Short Period Amplification Factor, F_A					
0.25	0.667	0.833	1.000	1.167	1.667	2.167
0.50	0.667	0.833	1.000	1.167	1.417	1.833
0.75	0.667	0.833	1.000	1.167	1.250	1.583
1.00	0.667	0.833	1.000	1.167	1.083	1.417
1.25	0.667	0.833	1.000	1.167	0.917	1.250
$SA_{L,B}$ (g)	Long Period Amplification Factor, F_V					
0.1	0.667	0.833	1.000	1.167	2.167	2.500
0.2	0.667	0.833	1.000	1.167	2.167	2.583
0.2	0.667	0.833	1.000	1.167	2.250	2.750
0.4	0.667	0.833	1.000	1.167	2.333	2.833
0.5	0.696	0.870	1.000	1.130	2.435	3.130

Table 3-25: Modified Amplification Factors for Borcherdt (2002)

Site Class BC Spectral Acceleration	Site Class					
	A	B	BC	C	D	E
$SA_{S,B}$ (g)	Short Period Amplification Factor, F_A					
0.25	0.615	0.769	1.000	1.231	1.585	1.923
0.50	0.640	0.800	1.000	1.200	1.504	1.360
0.75	0.640	0.800	1.000	1.200	1.368	0.960
1.00	0.667	0.833	1.000	1.167	1.283	0.750
1.25	0.696	0.870	1.000	1.130	1.183	0.783
$SA_{L,B}$ (g)	Long Period Amplification Factor, F_V					
0.1	0.533	0.667	1.000	1.333	1.733	2.333
0.2	0.552	0.690	1.000	1.310	1.655	2.207
0.2	0.571	0.714	1.000	1.286	1.571	2.000
0.4	0.593	0.741	1.000	1.259	1.481	1.778
0.5	0.615	0.769	1.000	1.231	1.385	1.846

acceleration, except for the factors of Hwang et al for site class C, which remain constant independent of the ground motion intensity.

Comparison of the long period amplification factors for site class C (Figure 3-29) shows that the site amplification factors of Borcherdt are higher than the other two studies. For this site class, Hwang et al's factors are the lowest ones. On the other hand, the estimates of Hwang et al are the highest for site class D (Figure 3-30). The site amplification factors of Hwang et al for this site class increase with increasing spectral acceleration, whereas those of the other two studies decrease with increasing ground shaking intensity.

Based on the above comparisons, one may expect to obtain less damage and lower losses when the factors in Dobry et al are used since they are smaller than those of the other studies (except the site class C long periods). Comparison of the losses that will be obtained for Borcherdt and Hwang et al amplification factors is more difficult since site class D the long period factors of Hwang et al is much larger than the those of Borcherdt. In regions where class D conditions dominate, higher losses may be expected from using Hwang et al amplification factors.

3.4.3 Building Vulnerability Model

Building vulnerability functions relate a local ground motion intensity measure to the damage or loss induced on a structure or system. The parameter that is typically used to quantify damage is the damage factor (DF), which is the ratio of the dollar loss to the replacement value of the structure. Vulnerability functions thus give the damage factor, in the range from 0 (no damage) to 1 (complete damage), for different structural classes and different levels of ground motion intensity.

The building vulnerability model we use is based on HAZUS (Kircher et al, 1997a; 1997b). HAZUS uses three sets of functions to relate seismic ground motions to building losses: (1) capacity curves, (2) fragility curves, and (3) loss functions. The first two curves are used to estimate damage to specific types of buildings. Capacity curves (together with damping-modified spectra) determine the peak building response given the seismic intensity level, whereas the fragility curves give the probability of reaching or exceeding specific damage states given the peak building response (See Figure 3-31). The loss functions transform building damage into

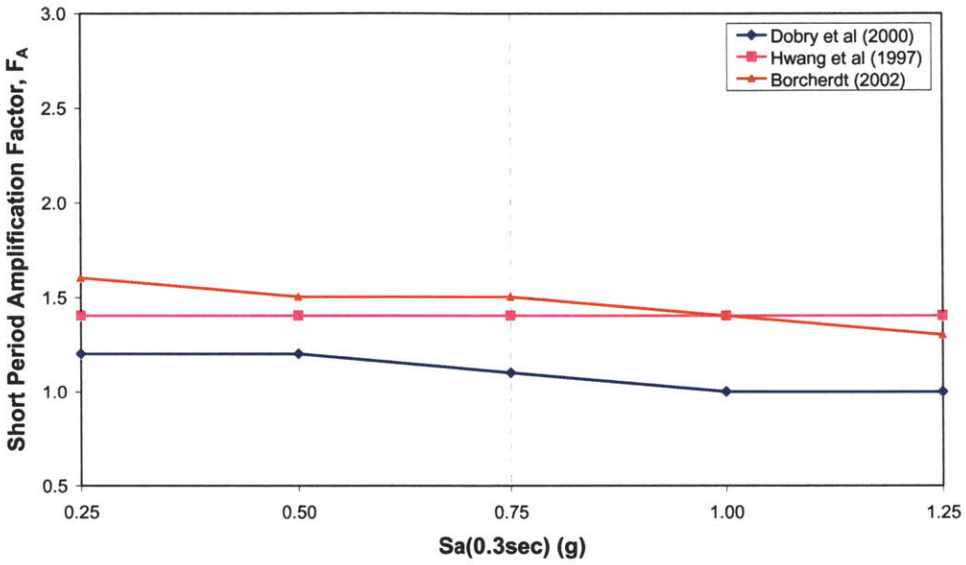

Figure 3-27: Comparison of Short Period Spectral Acceleration Factors for Site Class C

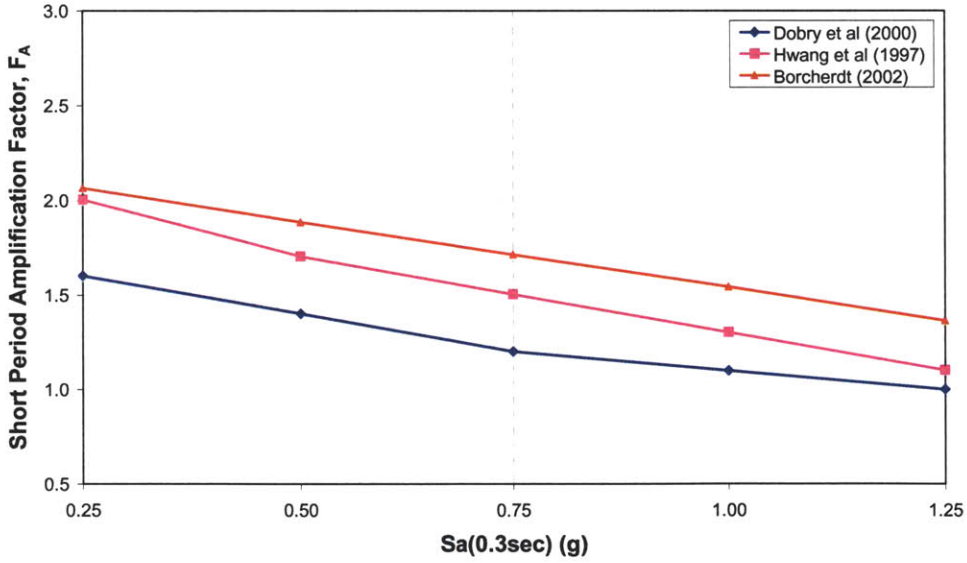

Figure 3-28: Comparison of Short Period Spectral Acceleration Factors for Site Class D

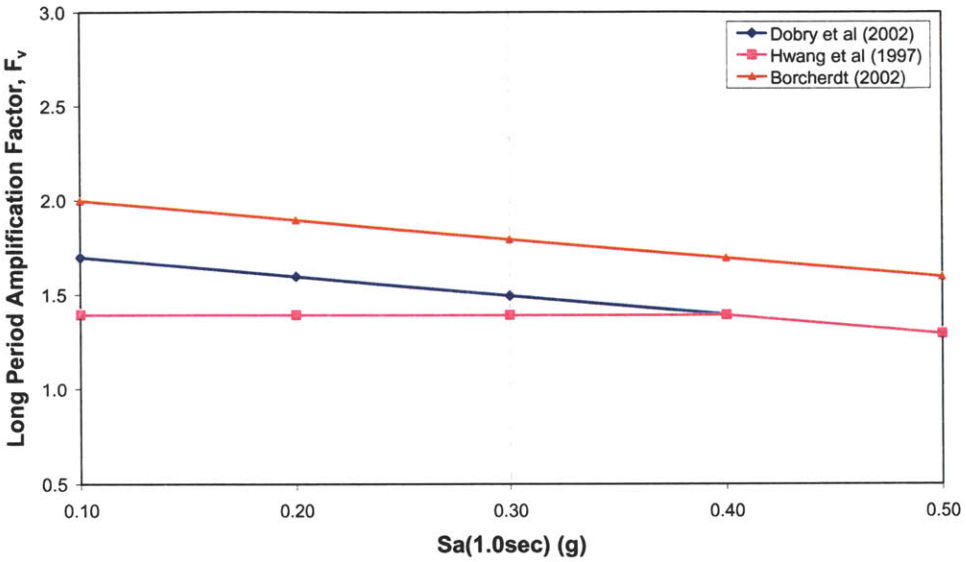

Figure 3-29: Comparison of Long Period Spectral Acceleration Factors for Site Class C

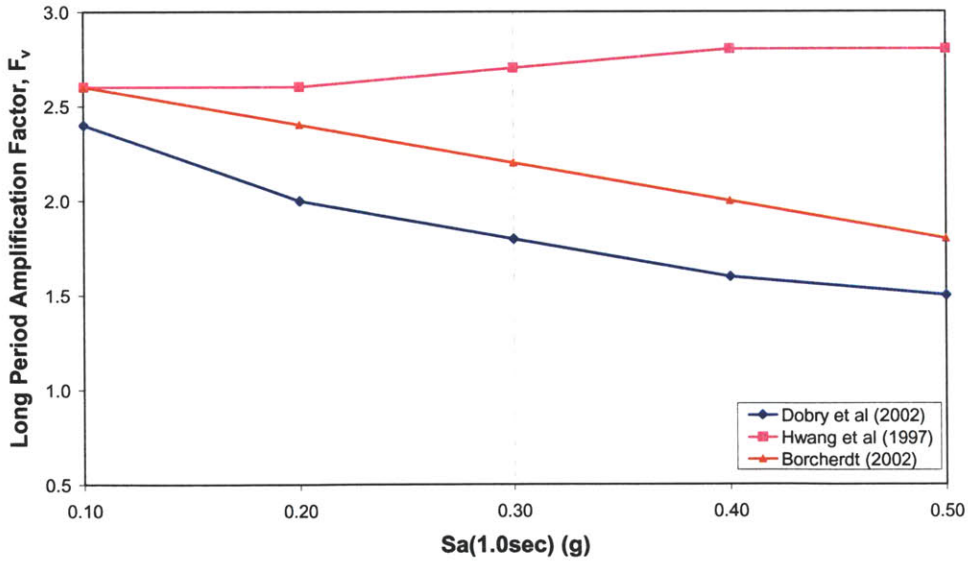

Figure 3-30: Comparison of Long Period Spectral Acceleration Factors for Site Class D

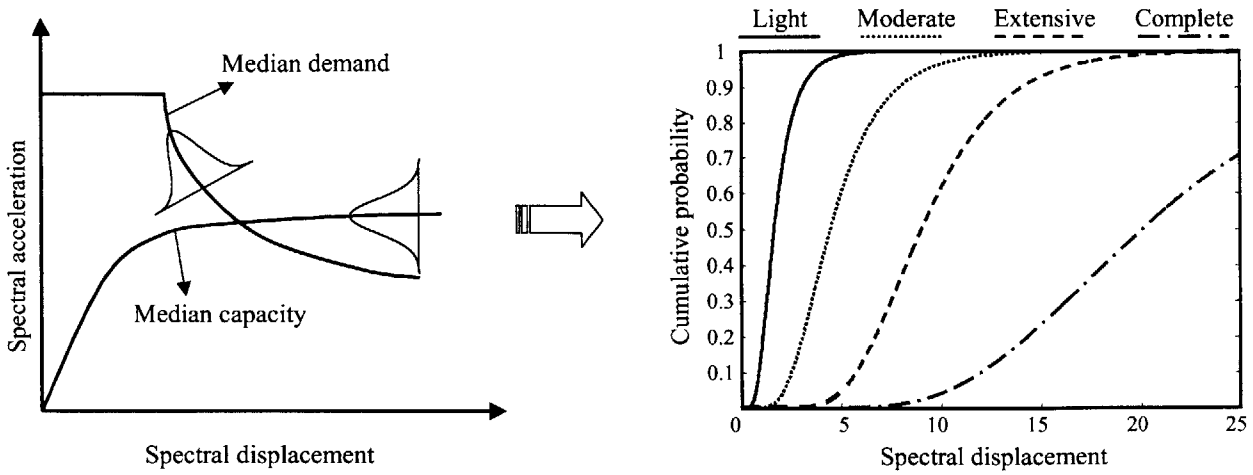

Figure 3-31: Example Building Capacity, Demand, and Fragility Curves

economic losses. These functions will be discussed further in the following sections together with other relevant data and parameters. In this study, we follow the methodology of HAZUS, except that instead of using fragility and loss functions we use vulnerability functions.

In the following sections, we introduce the building capacity functions and the building response estimation procedure of HAZUS, which are also used in this study. Then we discuss the fragility and loss functions in HAZUS, and finally we explain the derivation of the vulnerability functions.

3.4.3.1 Building capacity curves

The building capacity curve is analogous to the pushover curve and represents the lateral load resistance of a building as a function of a characteristic lateral displacement. Capacity curves of model buildings are derived from procedures like those in the NEHRP Guidelines for the Seismic Rehabilitation of Buildings (FEMA, 1997) and Seismic Evaluation and Retrofit of Concrete Buildings (ATC,1996), known as ATC-40. Capacity curves are developed in HAZUS for each of the 36 building structural types and 4 seismic design levels (Kircher et al, 1997a) based on engineering parameters such as the yield and ultimate strengths of the system.

In HAZUS, capacity curves are defined by two control points; the yield capacity and the ultimate capacity (see Figure 3-32). The yield capacity point (D_y, A_y) reflects the lateral strength of the building, accounting for design strength, redundancies, code conservatism, and expected (vs. nominal) material strength. The ultimate capacity point (D_u, A_u) reflects the maximum strength

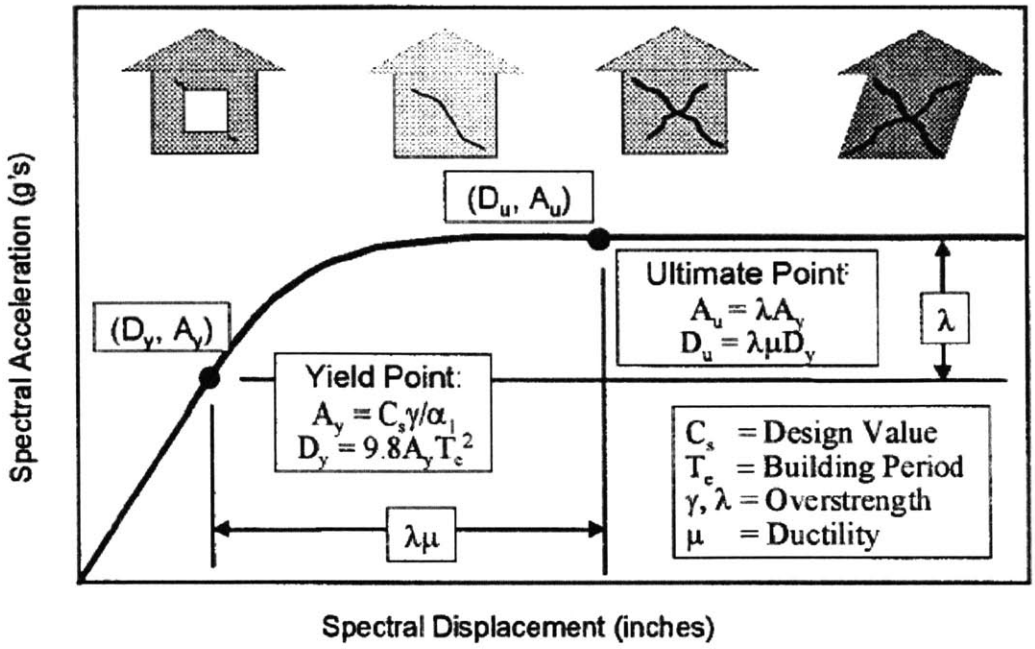

Figure 3-32: Example Building Capacity Curve and Control Points (Kircher et al, 1997a)

of the building as the structural system forms a collapse mechanism. The default values of these control points are provided for each building type and seismic design level.

Up to the yield point, the capacity curve is assumed to be linear with stiffness based on the expected period of the building. Beyond the ultimate point, the capacity curve is flat as it is assumed that the building is capable of deforming beyond its ultimate point without loss of stability but with no additional resistance to lateral loads. The shape of the capacity curve between the two points is not specified. Here we use a power spline to represent this section of the capacity curve. Hence, the capacity curve of a given building type is given by:

$$A = \begin{cases} D\dfrac{A_y}{D_y} & D < D_y \\ A_u - \left(A_u - A_y\right)\left(\dfrac{D_u - D}{D_u - D_y}\right)^{K_e/K_y} & D_y \le D < D_u \\ A_u & D_u \le D \end{cases} \tag{3.26}$$

where

$$K_e = \frac{A_y}{D_y} \tag{3.27}$$

$$K_y = \frac{A_u - A_y}{D_u - D_y} \tag{3.28}$$

The yield and ultimate points are determined by a number of parameters, as indicated in Figure 3-32 and listed below:

C_s design strength coefficient

T_e expected elastic fundamental mode period of building

α_1 fraction of building weight effective in pushover mode

α_2 fraction of building height at the elevation where pushover mode displacement is equal to spectral displacement

γ overstrength factor relating true yield strength to design strength

λ overstrength factor relating ultimate strength to yield strength

μ ductility ratio relating ultimate displacement to λ times the yield displacement

The values of these parameters and the yield and ultimate capacity points for the 36 model building types and 4 seismic design levels are given in HAZUS (NIBS, 2000).

3.4.3.2 Building Response

The building response is determined by the "performance point", which is the point of intersection of the building capacity curve with the "demand spectrum" (See Figure 3-33). The demand spectrum is the 5% damped response spectrum, reduced for effective damping. HAZUS uses a standard response spectrum shape that consists of two parts, a region of constant spectral acceleration at short periods, which is defined by Sa(0.3sec), and a region of constant spectral velocity at long periods, which has spectral acceleration proportional to 1/T and is anchored at Sa(1.0sec). NEHRP short and long period soil amplification factors are used to account for local site conditions. The resulting 5% damped elastic response spectrum is then divided by amplitude

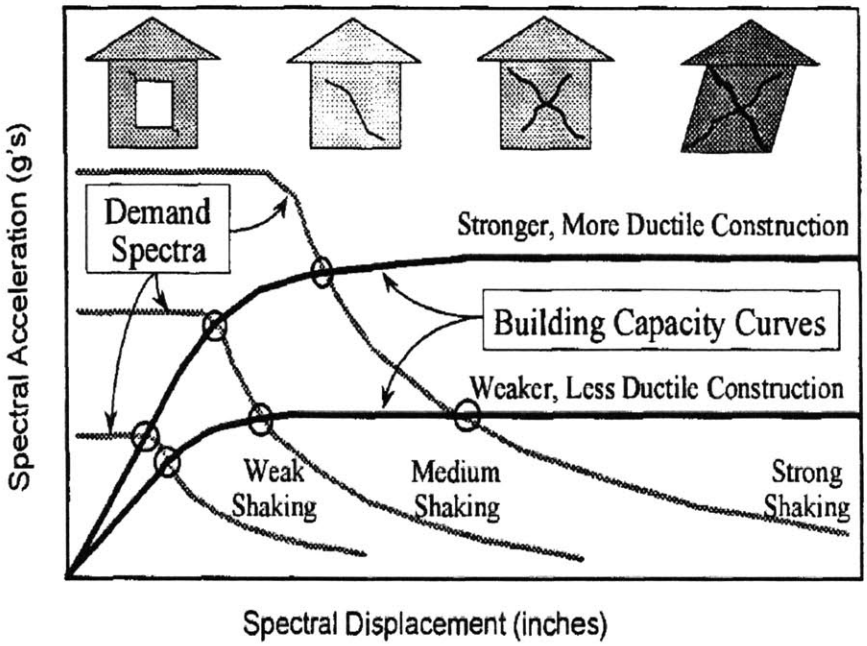

Figure 3-33: Example Intersection of Building Capacity Curves and Demand Spectra (Kircher et al, 1997a)

dependent damping reduction factors to obtain inelastic response (demand) spectrum with a procedure similar to the capacity-spectrum method of ATC-40 (ATC, 1996).

Spectrum reduction factors depends on the effective damping B_{eff}

$$R_A = 2.12/\left(3.21 - 0.68\ln(B_{eff})\right) \tag{3.29}$$

$$R_V = 1.65/\left(2.31 - 0.41\ln(B_{eff})\right) \tag{3.30}$$

The effective damping B_{eff} is the sum of the elastic damping B_E and the hysteretic damping B_H. The elastic damping is assumed to be constant for a building type, whereas the hysteretic damping varies with building type, seismic design level, and shaking duration (to simulate degradation of the hysteresis loop during cyclic response). Specifically, B_{eff} is given by

$$B_{eff} = B_E + \kappa\left(\frac{Area}{2\pi D_p A_p}\right) \tag{3.31}$$

where

B_E is the elastic damping expressed as a percentage of critical damping

$Area$ is the area enclosed by the hysteresis loop, as defined by the symmetrical push-pull of the building capacity curve up to peak positive and negative displacements

D_p is the peak displacement response

A_p is the peak acceleration response at peak displacement D_p

κ is a degradation factor expressed as a fraction of non-degraded hysteretic behavior for given earthquake duration.

The elastic dampings and degradation factors used in HAZUS generally follow the recommendations of Newmark and Hall (1982). Values of these two parameters for the 36 model building types and 4 code design levels are given in the HAZUS manual (NIBS, 2000). Since the degradation factor κ depends also on the duration of earthquake shaking, the elastic damping and the degradation factors are provided for three shaking durations: short, medium, and long. Shaking duration is assumed to be a function of earthquake magnitude, with magnitudes $M \leq 5.5$ producing short durations and magnitudes $M \geq 7.5$ producing long durations. For all other earthquake magnitudes, $5.5 < M < 7.5$, κ values are based on the assumption of moderate duration.

Determination of the intersection of the building capacity curve and the demand spectrum requires an iterative procedure, as the reduction factors used to construct demand spectra depend on the peak building response (D_p, A_p) through the effective damping determined by equation (3.31). One starts with finding the intersection point of the elastic demand spectra with the capacity curve and then one iteratively updates the reduction factors and uses them to construct new demand spectra. This gives a new intersection point. The procedure is repeated until convergence. For each analysis region, we perform these calculations for each building class, code level, and soil condition. The calculated peak building responses ($S_d = D$, $S_a = A$) are used with the structural and nonstructural vulnerability functions to obtain building damage ratios ad losses, as explained next.

3.4.3.3 Fragility relations and damage calculation in HAZUS (NIBS, 2000)

HAZUS uses fragility relations to calculate probabilities of being in different damage states and loss functions to estimate losses for a given damage state. In this section, we explain these two sets of functions and the procedure to calculate building losses in HAZUS.

Building Fragility Relations

Structural fragility curves give the probability of reaching or exceeding a given structural damage state as a function of spectral displacement. In HAZUS (NIBS, 2000), these curves have the shape of cumulative lognormal distribution functions, whose mean value and variance depend on the seismic vulnerability class and the damage level. These fragility curves have been developed considering the variability and uncertainty of the capacity curve, damage state thresholds, and the ground shaking intensity for a given magnitude and distance.

HAZUS provides fragility curves for 36 model building types, 4 seismic code levels, and 4 damage states. Moreover, separate fragility curves are provided for structural, non-structural drift sensitive and non-structural acceleration sensitive components. The building response parameter used in the fragility curves of structural and nonstructural drift sensitive components is the spectral displacement S_d. For nonstructural acceleration sensitive components, spectral acceleration S_a is the selected building response parameter.

Each fragility curve is defined by the median value of the demand parameter (spectral displacement or spectral acceleration) that corresponds to the threshold of a given damage state and the variability associated with that demand parameter. For example, the spectral displacement, S_d, that produces a particular damage state, ds, is expressed as

$$S_d = \overline{S}_{d,ds}\varepsilon_{ds} \tag{3.32}$$

where

$\overline{S}_{d,ds}$ is the median value of spectral displacement for damage state, ds

and ε_{ds} is a lognormal random variable with a unit median and logarithmic standard deviation β_{ds}.

Given the median spectral displacement S_d, the conditional probability of being in or exceeding a damage state ds or the probability that the damage factor DF exceeds the value DF_{ds} associated with damage state ds can be obtained from

$$P(DS \geq ds \mid S_d) = P(DF \geq DF_{ds} \mid S_d) = \Phi\left(\frac{\ln(S_d) - \ln(\bar{S}_{d,ds})}{\beta_{ds}}\right) \tag{3.33}$$

where

Φ is the standard normal cumulative distribution function.

The discrete damage state probabilities(the probability mass function of damage state) can be calculated as the difference between the cumulative probabilities obtained from equation (3.33) for consecutive damage states.

$$\begin{aligned}
&P(DS = none \mid S_d) = 1 - P(DS \geq slight \mid S_d) \\
&P(DS = slight \mid S_d) = P(DS \geq slight \mid S_d) - P(DS \geq moderate \mid S_d) \\
&P(DS = moderate \mid S_d) = P(DS \geq moderate \mid S_d) - P(DS \geq extensive \mid S_d) \\
&P(DS = extensive \mid S_d) = P(DS \geq extensive \mid S_d) - P(DS \geq complete \mid S_d) \\
&P(DS = complete \mid S_d) = P(DS \geq complete \mid S_d)
\end{aligned} \tag{3.34}$$

The above damage state probabilities can be used with the expected value of DF given DS, $DF_{ds} = E[DF \mid DS = ds]$,to obtain the mean damage factor $\overline{DF}$ given S_d, as

$$\overline{DF} = \sum_{ds=1}^{4} E[DF \mid DS = ds] P[DS = ds \mid S_d] \tag{3.35}$$

The mean damage factor for damage state ds, DF_{ds}, (the mean cost to repair a component in damage state ds, expressed as a fraction of the total component replacement cost) is assumed to be the same for structural, non-structural drift sensitive, and non-structural acceleration sensitive components. The mean damage factors used in HAZUS are listed in Table 3-26.

Variability of the spectral displacement S_d that produces a given damage state ds is contributed by three sources: (1) variability of the building capacity curve, (2) variability of the seismic demand (with the ground motion attenuation), and (3) variability of the response threshold for

Table 3-26: Mean Damage/Loss Factors (HAZUS, 2000)

Damage State	Mean Damage Factor
Slight	0.02
Moderate	0.10
Extensive	0.50
Complete	1.00

each damage state. Each of these three contributors to the damage uncertainty is assumed to be a log-normally distributed random variable and β_{ds} is obtained as

$$\beta_{ds} = \sqrt{(CONV[\beta_C, \beta_D])^2 + (\beta_{M(ds)})^2} \tag{3.36}$$

where

β_C is the logarithmic standard deviation of the building capacity curve

β_D is the logarithmic standard deviation of the variability of the demand spectrum. This parameter includes uncertainty on the ground motion given a median attenuation relation and the building damping parameters.

$\beta_{M(ds)}$ is the logarithmic standard deviation of the median value of the threshold of the spectral displacement that produces damage state *ds*. For example, in HAZUS (2000) the spectral displacement at which the slight damage state (corresponding to a damage factor of 0.02) in structural class W1 is exceeded is 0.5 inches. However, a 2% structural loss could be incurred at spectral displacements smaller or greater than 0.5 inches.

The function "*CONV*" in equation (3.36) denotes a convolution of the probability distributions of building capacity and demand. This convolution process involves the following steps:

(1) A suite of capacity curves, which represent the capacity curve variability, are drawn in the spectral acceleration-spectral displacement domain.

(2) A suite of demand curves, which represent the variability in the demand spectrum are overlaid on the curves representing the capacity curve variability. Let D_i be the spectral

displacement corresponding to the intersection of the median demand spectrum and the median capacity curve.

(3) The probabilities of the points of intersection of the suite of demand and capacity curves are ascertained. Using these probabilities, the conditional probability of being in or exceeding a given damage state, given $\beta_{M(ds)} = 0$, is obtained for the median peak spectral displacement of D_i.

(4) Steps 2 and 3 are repeated for different levels of ground shaking (i.e., different values of D_i), to obtain a set of values describing the probability of being in or exceeding a particular damage state, given $\beta_{M(ds)} = 0$.

(5) A lognormal distribution is fit to these data points, to obtain an estimate of the lognormal standard deviation of the combined effect of capacity and demand variability on structural fragility.

Figure 3-34 illustrates the convolution process for the probability distributions of building capacity and demand. The lognormal standard deviation parameter $CONV[\beta_C, \beta_D]$, which represents the combined effects of the demand and capacity variability is combined with $\beta_{M(ds)}$, which is assumed to be independent of the capacity and demand, using the square-root-of-sum-of-squares (SRSS) rule to obtain the total variability of the damage state ds, β_{ds} . For further details of the theory behind equation (3.36), see Kircher et al (1997a).

Calculation of Building Repair Costs

In HAZUS, restoration costs are calculated based on occupancy class of the building not the structural type of a building. Hence, damage state probabilities for model building types are combined to yield the damage state probabilities of occupancy classes. The probability of a building occupancy class being in a damage state is calculated as the sum of the damage state probabilities of the model building classes making up that occupancy class weighted according to their respective floor areas.

$$P_{oc}[DS = ds] = \sum_{sc=1}^{36} P_{sc}[DS = ds] \frac{FA_{oc,sc}}{FA_{oc}} \tag{3.37}$$

where

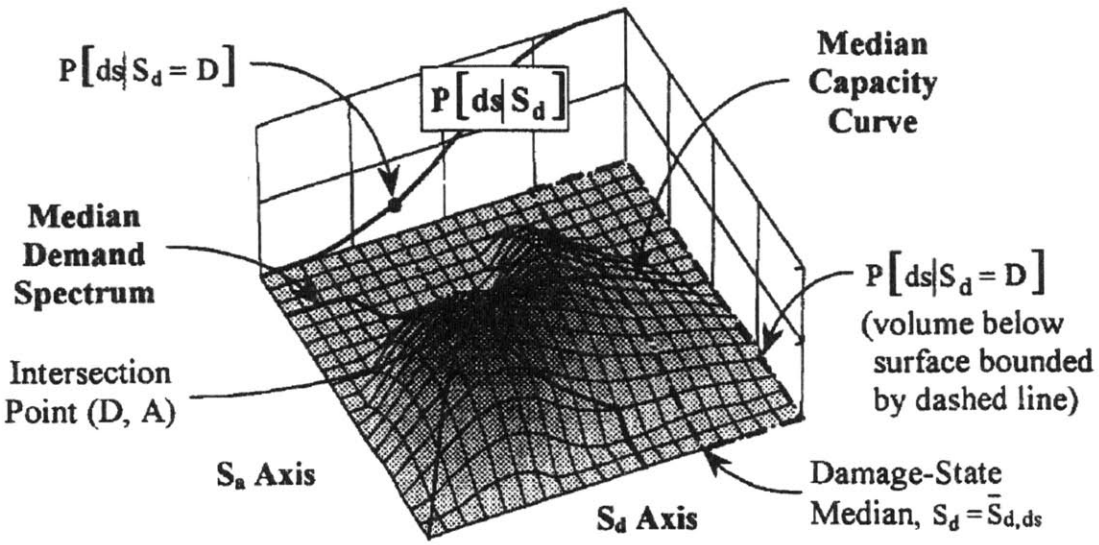

Figure 3-34: Joint Probability Surface of Demand and Capacity Intersection Points (Kircher et al, 1997a)

$P_{oc}[DS = ds]$ is the probability of building occupancy class oc being in damage state ds

$P_{sc}[DS = ds]$ is the probability of model building type sc being in damage state ds

$FA_{oc,sc}$ is the floor area of model building type sc within building occupancy class oc

FA_{oc} is the floor area of building occupancy class oc

The damage state probabilities of structural and nonstructural components calculated using equation (3.37) are further combined with the repair costs of the building type per square area for the given damage state. For example, the structural repair costs for a building occupancy class oc in a given analysis region is calculated as

$$BRC_{oc}^{str} = FA_{oc} \times UBRC_{oc} \times \sum_{ds=1}^{4} \left(PRC_{oc,ds}^{str} \times P_{oc}^{str}[DS = ds] \right) \tag{3.38}$$

where

BRC_{oc}^{str} is the cost of structural damage for building occupancy class oc

$UBRC_{oc}$ is the unit building replacement cost for occupancy class oc

$PRC_{oc,ds}^{str}$ is the percent replacement cost of structural components for damage state ds and for occupancy class oc

Default values of percent replacement costs of structural and non structural building components for different damage states ($PRC^{str}_{oc,ds}$, $PRC^{drift}_{oc,ds}$, and $PRC^{acc}_{oc,ds}$) are provided in HAZUS for each of the 33 building occupancy classes. For a given building component, the replacement cost ratios for different damage states are almost identical to the mean damage factors in Table 3-26. Therefore, rather than using the percent replacement values of individual damage states, we use mean damage factors and the relative percentages of building replacement value allocated to structural, nonstructural drift sensitive, nonstructural acceleration sensitive components to obtain the percent replacement cost for different damage states.

Table 3-27 lists the unit building replacement costs obtained from HAZUS based on 2003 estimates. The relative percentages of building components and components with respect to the total building replacement value are provided in Table 3-28. For most of the building occupancy types, the non-structural components make up for the bulk of the building replacement value.

The total cost of building damage for building occupancy class oc is simply the sum of structural and non-structural repair costs

$$BRC_{oc} = BRC^{str}_{oc} + BRC^{acc}_{oc} + BRC^{drift}_{oc} \tag{3.39}$$

where

BRC_{oc} is the total building replacement cost for building occupancy class oc

BRC^{acc}_{oc} is the cost of acceleration sensitive nonstructural damage for building occupancy class oc

BRC^{drift}_{oc} is the cost of drift sensitive nonstructural damage for building occupancy class oc

Next we describe the building vulnerability model that we derived and used in this study. Although, the parameters of the vulnerability model are based on HAZUS data, the model itself is different from the one used in HAZUS.

3.4.3.4 Vulnerability Model and Damage Calculation

As stated earlier, fragility curves define the probability of reaching or exceeding a damage state for a given seismic demand parameter. Using these exceedance probabilities, discrete

Table 3-27 : Unit Building Replacement Costs (NIBS, 2000)

No.	Building Occupancy Class	Building Replacement Cost ($/sqft)
1	RES1	90.0
2	RES2	31.0
3	RES3a	67.2
4	RES3b	73.1
5	RES3c	125.6
6	RES3d	112.8
7	RES3e	108.8
8	RES3f	106.2
9	RES4	104.6
10	RES5	118.8
11	RES6	104.6
12	COM1	71.5
13	COM2	61.9
14	COM3	86.8
15	COM4	99.0
16	COM5	154.0
17	COM6	144.6
18	COM7	129.8
19	COM8	147.0
20	COM9	102.4
21	COM10	100.0
22	IND1	73.8
23	IND2	61.9
24	IND3	119.5
25	IND4	119.5
26	IND5	119.5
27	IND6	62.0
28	AGR1	61.9
29	REL1	114.0
30	GOV1	90.3
31	GOV2	136.1
32	EDU1	92.8
33	EDU2	114.7

Table 3-28 : Relative Percentages of Building Replacement Costs (HAZUS, 2000)

No.	Occupancy Class	Building Component			Contents
		Structural	Non-structural Acceleration Sensitive	Non-structural Drift Sensitive	
1	RES1	23.4	26.6	50.0	50.0
2	RES2	24.4	37.8	37.8	50.0
3	RES3a	13.8	43.7	42.5	50.0
4	RES3b	13.8	43.7	42.5	50.0
5	RES3c	13.8	43.7	42.5	50.0
6	RES3d	13.8	43.7	42.5	50.0
7	RES3e	13.8	43.7	42.5	50.0
8	RES3f	13.8	43.7	42.5	50.0
9	RES4	13.6	43.2	43.2	50.0
10	RES5	18.8	41.2	40.0	50.0
11	RES6	18.4	40.8	40.8	50.0
12	COM1	29.4	43.1	27.5	50.0
13	COM2	32.4	41.1	26.5	50.0
14	COM3	16.2	50.0	33.8	50.0
15	COM4	19.2	47.9	32.9	50.0
16	COM5	13.8	51.7	34.5	50.0
17	COM6	14.0	51.3	34.7	50.0
18	COM7	14.4	51.2	34.4	50.0
19	COM8	10.0	54.4	35.6	50.0
20	COM9	12.2	52.7	35.1	50.0
21	COM10	60.9	21.7	17.4	50.0
22	IND1	15.7	72.5	11.8	50.0
23	IND2	15.7	72.5	11.8	50.0
24	IND3	15.7	72.5	11.8	50.0
25	IND4	15.7	72.5	11.8	50.0
26	IND5	15.7	72.5	11.8	50.0
27	IND6	15.7	72.5	11.8	50.0
28	AGR1	46.2	46.1	7.7	50.0
29	REL1	19.8	47.6	32.6	50.0
30	GOV1	17.9	49.3	32.8	50.0
31	GOV2	15.3	50.5	34.2	50.0
32	EDU1	18.9	32.4	48.7	50.0
33	EDU2	11.0	29.0	60.0	50.0

probabilities of being in different damage states can be calculated. In HAZUS, building losses are calculated by combining the discrete damage state probabilities with the repair costs for those states. In addition, building repair and recovery time are calculated based on damage state. Repair and recovery times are defined not as continuous functions of damage. Rather, values are given for each discrete damage state.

In our methodology, we use vulnerability functions, which give loss as a continuous function of a given seismic demand parameter. For example, a vulnerability function can provide the damage factor for a building (repair cost divided by replacement cost), whereas HAZUS fragility functions provide the probability that a building is in various discrete damage states (Porter, 2003).

Vulnerability Model

Here, we use vulnerability functions to calculate building damage levels and corresponding losses. We use the seismic vulnerability classes of HAZUS and derive the parameters of the vulnerability model from the fragility functions of HAZUS. The procedure for calculating building response is identical. However, rather than representing uncertainty in damage and loss levels for a given seismic demand through fragility curves, we use vulnerability functions as described below.

The vulnerability curve gives the damage factor of a building component as a function of an appropriate seismic demand parameter. The seismic demand parameters used for different building components are the same as in HAZUS, i.e. they are logs of spectral displacement for structural and drift sensitive nonstructural components and logs of spectral acceleration for acceleration sensitive nonstructural components.

Our vulnerability model is based on the assumption that the vulnerability curve of the generic building in a seismic vulnerability class has a fixed functional form with one uncertain parameter. Specifically, we assume that the vulnerability curve has the form of a normal cumulative distribution function (CDF) whose mean M is uncertain. Uncertainty in the mean models the variability in damage from building to building within a given vulnerability class. The mean of the fragility curve, M, is assumed to be a Gaussian random variable with

parameters that depend on the vulnerability class. Figure 3-35 illustrates the components of the vulnerability model used in this study.

Damage calculation

As just explained, we express the variability in damage from building to building in a given vulnerability class i with standard deviation σ_{M^i}, and the vulnerability of a generic building in vulnerability class i with the CDF of $(R^i \mid M^i)$, which is also Gaussian with mean M^i and standard deviation σ_{ε^i}.

The mean damage factor for a building with mean parameter M^i subjected to spectral displacement S_d, $D^i(S_d, M^i)$, is then

$$D^i(S_d, M^i) = \Phi\left(\frac{\ln(S_d) - M^i}{\sigma_{\varepsilon^i}}\right) \tag{3.40}$$

Again, given S_d, the mean damage factor for the overall building class i, $\overline{D^i(S_d)}$, including the building to building variability is obtained by

$$\overline{D^i(S_d)} = \int_{m=-\infty}^{\infty} D^i(S_d, m) f_{M^i}(m) dm = \Phi\left(\frac{\ln(S_d) - E[M^i]}{\sigma_{R^i}}\right) \tag{3.41}$$

where

$f_{M^i}(m)$ is the probability density function of M^i and

$$\sigma_{R^i}^2 = \sigma_{M^i}^2 + \sigma_{\varepsilon^i}^2 \tag{3.42}$$

The next section estimates the parameters $E[M^i]$ and σ_{R^i} from HAZUS fragility curve information.

Parameter estimation

Let $P(DF \geq D_{ds} \mid S_d)^i_{HAZUS}$ be a damage probability function given in HAZUS for seismic vulnerability class i. Specifically, this is the probability of being in or exceeding the damage factor DF_{ds} that corresponds to damage state ds, as a function of spectral displacement S_d. The

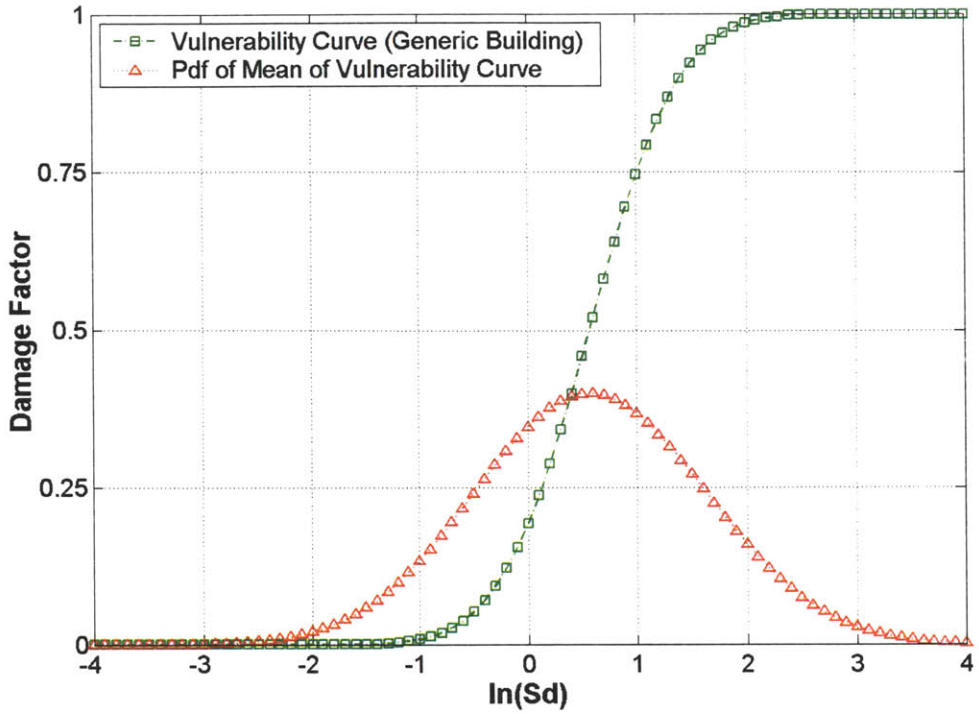

Figure 3-35: Representation of the Vulnerability Model Used

unknown parameters of our vulnerability model, $E[M^i]$, σ_{M^i}, and σ_{ε^i} are estimated by matching the values of $P(DF \geq DF_{ds} \mid S_d)^i_{HAZUS}$ given in HAZUS for different damage states ds with those given by our model, say $P(DF \geq DF_{ds} \mid S_d)^i_{Derived}$

$$P(DF \geq DF_{ds} \mid S_d)^i_{Derived} = P(DF \geq DF_{ds} \mid S_d)^i_{HAZUS} \tag{3.43}$$

Denote by $m(D_{ds}, S_d, \sigma_{\varepsilon^i})$ the mean parameter of the vulnerability curve of a building of type i that suffers damage factor DF_{ds} under spectral displacement S_d and standard deviation σ_{ε^i}. Using equation (3.40), we write m as

$$m(DF_{ds}, S_d, \sigma_{\varepsilon^i}) = \ln(S_d) - \sigma_{\varepsilon^i}\Phi^{-1}(DF_{ds}) \tag{3.44}$$

If the mean parameter is less than the value in (3.44), the damage factor is greater than D_{ds}. Therefore,

$$P(DF \geq DF_{ds} \mid S_d)^i_{Derived} = P(M^i \leq m(DF_{ds}, S_d, \sigma_{\varepsilon^i})) = \Phi\left(\frac{m(DF_{ds}, S_d, \sigma_{\varepsilon^i}) - E[M^i]}{\sigma_{M^i}}\right) \tag{3.45}$$

Substituting equation (3.44) into (3.45),

$$P(DF \geq DF_{ds} \mid S_d)^i_{Derived} = \Phi\left(\frac{\ln(S_d) - \sigma_{\varepsilon^i}\Phi^{-1}(DF_{ds}) - E[M^i]}{\sigma_{M^i}}\right) \tag{3.46}$$

As we aim to match the predictions from our model with those of HAZUS, we substitute equations (3.46) and (3.33), into equation (3.43) to get

$$\Phi\left(\frac{\ln(S_d) - \sigma_{\varepsilon^i}\Phi^{-1}(DF_{ds}) - E[M^i]}{\sigma_{M^i}}\right) = \Phi\left(\frac{\ln(S_d) - \ln(\overline{S}_{d,ds})}{\beta^i_{ds}}\right) \tag{3.47}$$

Since Φ is a monotonically increasing function, we equate the arguments on both sides. This gives

$$\frac{\ln(S_d) - \sigma_{\varepsilon^i}\Phi^{-1}(DF_{ds}) - E[M^i]}{\sigma_{M^i}} = \frac{\ln(S_d) - \ln(\overline{S}_{d,ds})}{\beta^i_{ds}} \tag{3.48}$$

For $S_d = \overline{S}_{d,ds}$, equation (3.48) simplifies to

$$\sigma_{\varepsilon^i}\Phi^{-1}(DF_{ds}) + E[M^i] = \ln(\overline{S}_{d,ds}) \tag{3.49}$$

By substituting the expression for $\overline{S}_{d,ds}$ in (3.48), we get

$$\sigma_{M^i} = \beta^i_{ds} \tag{3.50}$$

This means that, in order for the predictions of our model to match those from HAZUS (NIBS, 2000) for damage state ds, the standard deviation of the mean of the vulnerability curve in our model must equal the logarithmic standard deviation of the fragility curve for damage state ds in HAZUS. However, the β's given in HAZUS (NIBS, 2000) for different damage states ds are not always the same. In such cases, we estimate σ_{M^i} as the average of the β values for the various (slight, moderate, extensive and complete) damage states.

To obtain $E[M^i]$ and σ_{ε^i}, we write equation (3.49) for the four damage states used in HAZUS. By simultaneously solving the equations, we obtain the average values of the parameters $E[M^i]$ and σ_{ε^i}. In estimating these parameters, we used the mean damage factors given in Table 3-26 except for the case of complete damage state. As the damage factor of the complete damage state

is 1.0, which causes divergence of the term $\Phi^{-1}(DF_{Complete})$, for complete damage state we use a damage factor of 0.95. Using mean damage factors rather than the damage factors that define the lower bounds of the corresponding damage states results in conservative estimates of the mean damage factors as discussed in the next section.

Parameter validation and comparison

The above procedure can be validated by comparing the fragility functions given in HAZUS, $P(DF \geq DF_{ds} \mid S_d)^i_{HAZUS}$, with those derived from our fitted vulnerability model, $P(DF \geq DF_{ds} \mid S_d)^i_{Derived}$. Figure 3-36 shows a comparison of these functions for low code URM buildings. The slight differences are mainly due to averaging the logarithmic standard deviations of the fragility curves for different damage states in HAZUS.

In Figure 3-37, we compare the mean damage factors calculated by different approaches. There are three curves in the figure. The first curve is obtained by using the HAZUS fragility curves plotted in Figure 3-36 for the four damage states, using equation (3.35). The green line plotted shows the vulnerability function for a generic building obtained from equation (3.40). The vulnerability of the overall building class, including building to building variability, is plotted in black in Figure 3-37.

The mean damage functions obtained from our vulnerability model are higher than those calculated from HAZUS, up to 0.15 for this building class. The difference is a result of the discretization of the damage states in the two models and the use of mean damage factors rather than the lower bound values for the four damage states considered. In HAZUS, only four damage states are considered and the discrete damage state probabilities calculated using fragility curves are assigned to the corresponding mean damage factor to calculate mean damage factors using equation (3.35). In our case, the vulnerability model involves continuous curves or, in a sense, infinite number of similar fragility curves to represent building vulnerability. Using an increased number of fragility curves or increasing the discretization during the convolution of damage state probabilities and corresponding damage factors in equation (3.35) results in increased mean damage factors.

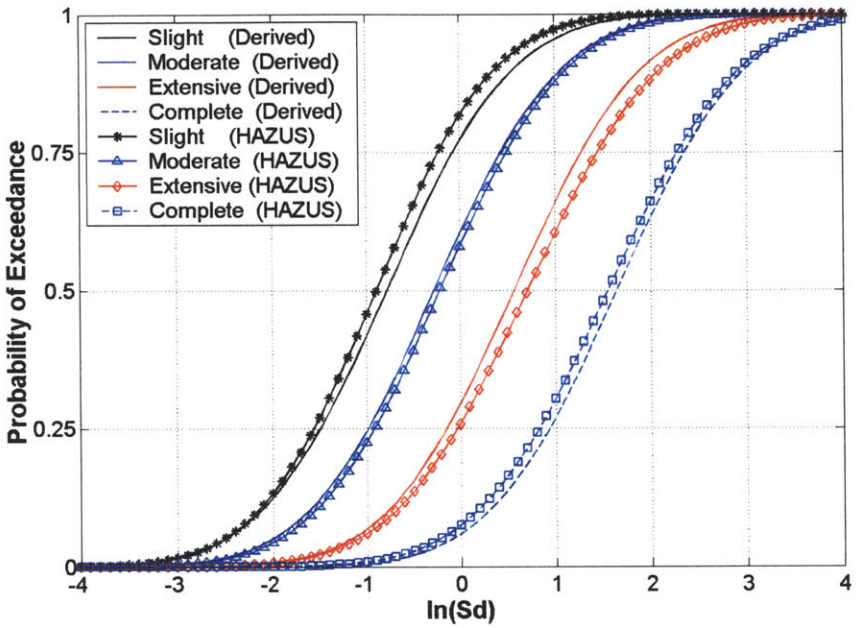

Figure 3-36: Comparison of HAZUS and Derived Fragility Curves (Low Code URML)

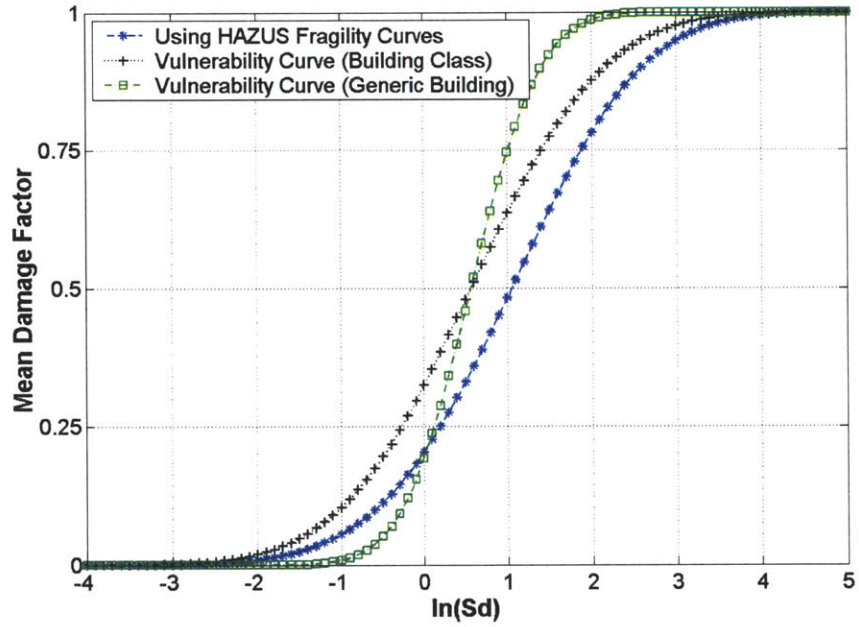

Figure 3-37: Comparison of Mean Damage Factors (Low Code URML)

3.4.4 Bridge Vulnerability Model

Bridge fragility models are used to estimate the damage factor for bridges. The first part of this section reviews the fragility models proposed in three previous studies and the second part compares the damage factors predicted by these models.

3.4.4.1 HAZUS (NIBS, 2000)

HAZUS (NIBS, 2000) provides fragility information for 28 bridge types, classified by National Bridge Inventory (NBI) category, location (California or outside California), year built, and maximum span. HAZUS provides damage functions separately for ground shaking and ground failure. The fragility curves for ground shaking are based on the probability of exceedance of four damage states: slight, moderate, extensive and complete. These are given as functions of Sa(1.0sec). Table 3-29 shows the nomenclature used in HAZUS and the corresponding NBI categories for non-California bridges.

3.4.4.2 Hwang et al (2000)

Hwang et al (2000) provide fragility information for highway bridges in Shelby County, Tennessee. They use a bridge classification that is primarily based on the NBI classification. They also include the pier (bent) information of each bridge in their classification. The NBI/FHWA recording and coding guide (FHWA, 1995) classifies the superstructure type and material using a three digit code. For example, "202" refers to a multiple span continuous concrete girders. In addition, Hwang et al (2000), use a two digit code to identify the bent material. For example, bridge type 202-11 corresponds to a bridge with multiple span continuous concrete girders (202) supported by concrete multi column bents (11). Table 3-30 lists the bridge types assigned to each of the 6 bridge classes used by Hwang et al (2000). They use PGA as input parameter for the fragility curves to determine probabilities of being in three damage states defined: no/minor damage, repairable damage, and significant damage.

3.4.4.3 DesRoches (2002)

DesRoches (2002) developed fragility curves for 6 bridge classes that are representative of bridges in the CUS region. Probabilities of exceedance of four damage states (slight, moderate, extensive and complete) are given as a function of PGA. Six bridge classes are considered based

on the number of spans, continuity at the supports and superstructure type material. Table 3-31 shows the different classes for which bridge fragility information is given by DesRoches (2002).

3.4.4.4 Comparison of bridge fragility models

In order to compare the bridge damages predicted by different models, a mapping needs to be made between the classifications used in the studies. This is done by using the NBI classification as a reference. Table 3-32 shows our mapping of the NBI material class to the classes used in different studies. In some cases, there are multiple bridge classes corresponding to a given NBI class as the bridge classification uses different parameters and data.

Since the fragility information in DesRoches (2002) and Hwang et al (2000) is in terms of PGA and that in HAZUS (2000) is in terms of Sa(1.0sec), comparisons between the bridge fragilities given in the different data sources is done as follows. Bridges of a certain class (based on the NBI material classification) are assumed to be located at certain distances from the epicenter at a location with NEHRP site class C. By using the PGA and Sa(1.0sec) values predicted by the attenuation relationships, damage to each bridge is estimated as a function of epicentral distance, for an earthquake of magnitude M8.0. Figure 3-38 compares the estimated damage as a function of distance for NBI bridge material class 2 and Figure 3-39 shows similar comparisons for a NBI bridge material class 1. It can be seen that there are large differences in the damage estimates given by different studies. In such cases, damage estimates from HAZUS (2000) are much below the estimates by Hwang et al (2000) and DesRoches (2002) in both cases. The comparisons for other bridge classes are similar with HAZUS and damage estimates of HAZUS are much lower than those of the other two models. It is important to note that the fragility models of Hwang et al (2000) and DesRoches (2002) were developed considering properties of typical bridges in CUS, whereas the fragility relations used in HAZUS are mainly derived for bridges in California, although modifications are made for non-California bridges.

3.4.5 Loss of Functionality and Recovery Model

As a result earthquake damage, a facility or structure may lose all or part of its functionality for a period of time. The duration of this functionality loss depends on the amount of structural, non-structural, and contents damage incurred by the facility itself, as well as on the functionality of

Table 3-29: Bridge Classification Used in HAZUS for Non-California Bridges

Bridge Class	NBI Class	Year Built	No of Spans	Length of Max Span (m)	Length less than 20m	Design	Description
1	All	<1990		>150	N/A	Conv.	Major Bridge, Length > 150m
2	All	>=1990		>150	N/A	Seismic	Major Bridge, Length > 150m
3	All	<1990	1		N/A	Conv.	Single Span
4	All	>=1990	1		N/A	Seismic	Single Span
5	101-106	<1990			N/A	Conv.	Multi-Col. Bent, Simple Support, Concrete
7	101-106	>=1990			N/A	Seismic	Multi-Col. Bent, Simple Support, Concrete
10	201-206	<1990			N/A	Conv.	Continuous Concrete
11	201-206	>=1990			N/A	Seismic	Continuous Concrete
12	301-306	<1990			No	Conv.	Multi-Col. Bent, Simple Support, Steel
14	301-306	>=1990			N/A	Seismic	Multi-Col. Bent, Simple Support, Steel
15	402-410	<1990			No	Conv.	Continuous Steel
16	402-410	>=1990			N/A	Seismic	Continuous Steel
17	501-506	<1990			N/A	Conv.	Multi-Col. Bent, Simple Support, Prestressed Concrete
19	501-506	>=1990			N/A	Seismic	Multi-Col. Bent, Simple Support, Prestressed Concrete
22	601-607	<1990			N/A	Conv.	Continuous Concrete
23	601-607	>=1990			N/A	Seismic	Continuous Concrete
24	301-306	<1990			Yes	Conv.	Multi-Col. Bent, Simple Support, Steel
26	402-410	<1990			Yes	Conv.	Continuous Steel
28							All other bridges that are not classified

Table 3-30: Bridge Classification Used in Hwang et al (2000)

Bridge Class	NBI Bridge Type – Bridge Bent Type
1	302-11
2	302-31, 101-31, 102-31, 105-31, 201-31, 202-31, 402-31, 502-31, 505-31, 506-31, 602-31
3	402-11, 407-11, 407-52
4	502-11, 505-11, 506-11, 506-51, 101-11, 102-11, 105-11, 207-51
5	602-11, 605-11, 605-41, 606-11, 201-11, 202-11, 205-11, 207-11
6	Single span bridges, 101-21, 402-21, 502-21, 602-21, 605-21, 606-21

Table 3-31: Bridge Classification Used in Desroches (2002)

Bridge Class	Description
MSSS-C	Multi-span simply supported, Concrete
MSC-C	Multi-span continuous, Concrete
MSSS-S	Multi-span simply supported, Steel
MSC-S	Multi-span continuous, Steel
SS-C	Single Span, Concrete
SS-S	Single Span, Steel

Table 3-32: Mapping of NBI Material Classes to Classifications in Different Bridge Fragility Evaluation Studies

NBI Material Class	Description	HAZUS (2000)	Hwang et al (2000)	DesRoches (2002)
1	Multi-span simply supported, Concrete	HWB5, HWB7	4	MSSS-C
2	Multi-span continuous, Concrete	HWB10, HWB11	5	MSC-C
3	Multi-span simply supported, Steel	HWB12, HWB14	1	MSSS-S
4	Multi-span continuous, Steel	HWB15, HWB16, HWB26	3	MSC-S
5	Multi-span simply supported, Prestressed Concrete	HWB17, HWB19	4	MSSS-C
6	Multi-span continuous, Prestressed Concrete	HWB22, HWB23	5	MSC-C

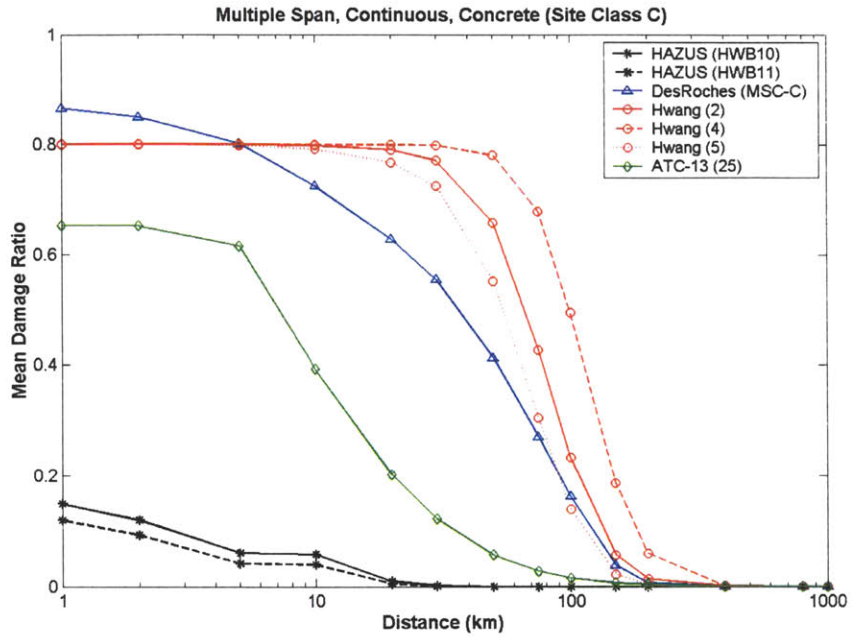

Figure 3-38: Comparison of Attenuation of Damage for an NBI Material Class 2 Bridge

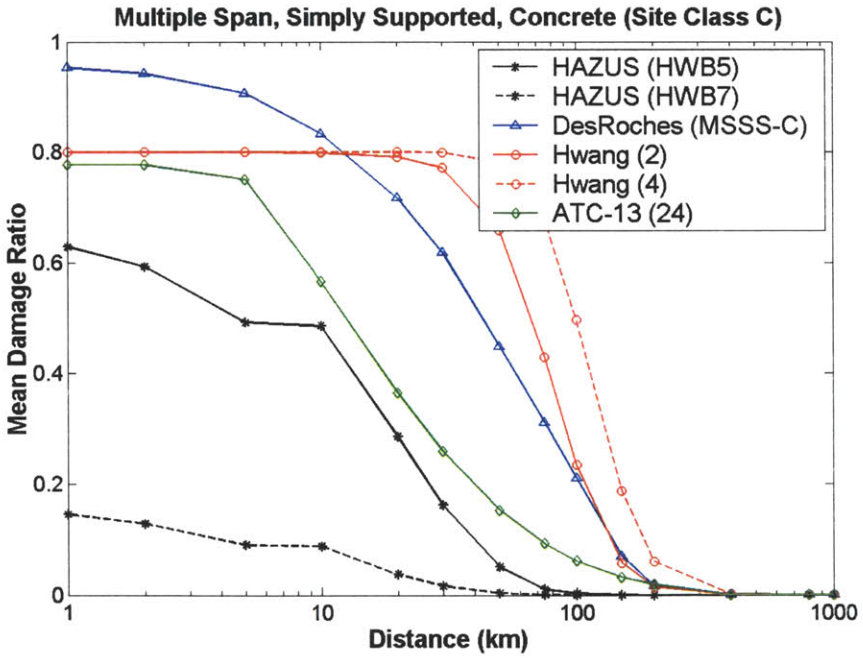

Figure 3-39: Comparison of Attenuation of Damage for an NBI Material Class 1 Bridge

the lifelines serving the facility and other facilities it interacts with. Functionality is recovered as the facility and lifeline systems are repaired over time. The rate at which functionality is restored may itself depend on the rate of recovery of the lifelines and the availability of human resources on which the operation of the facility depends.

Hence, to estimate business interruption losses and increased transportation costs, one needs to model the functionality over time of buildings, bridges, and lifeline systems. There is much uncertainty on these processes, due to a number of reasons including lack of statistical data from past earthquakes, political and economic decisions made during the recovery process, and the overall dynamic nature of the processes. Next we describe the recovery model used in this study.

3.4.5.1 Functionality and Recovery of Infrastructure Components

We have extracted functionality and recovery parameters from ATC-13 (ATC, 1985). ATC- 13 gives the times ($\overline{T}_{30}$, $\overline{T}_{60}$, $\overline{T}_{100}$) to 30%, 60%, and 100% recovery of functionality for different social classes (building occupancy classes, bridges, lifeline components, etc) as a function of 7 damage states. These estimates were obtained from expert opinion assuming that the restoration times refer to long–term restoration rather than restoration immediately following an earthquake where resources or access to some of the facilities may be limited. We fit exponential or power functions to the restoration time estimates in ATC-13. The fitted curves are first used to obtain the time to 30%, 60%, and 100% recovery of functionality as a continuous function of the damage factor.

We extract restoration time data from ATC-13 for building occupancy classes, bridges, roadways, and electrical substations. As the building occupancy classification in ATC-13 is coarser than that of HAZUS (the latter is the one used in this study), the restoration parameters for some of the building occupancy classes are the same. For bridges, we consider two bridge functionality classes, depending on whether the bridge is "major" or "conventional". Major bridges have a span length above 500ft, while all other bridges are classified as conventional. As we do not model the lifeline networks explicitly, we assume that electrical substations give an indication of the level of lifeline damage in each analysis region, hence we have used restoration data for electrical substations to represent the recovery of utility lifelines. For infrastructure components other than bridges, we impose a minimum initial functionality of 10%, assuming

that there is such minimum level of functionality independent of the damage level. For bridges, we assume there is no functionality up to time $\bar{T}_{30}/3$. To calculate the recovery rate of infrastructure components, we use linear interpolation through the times $\bar{T}_{30}(D)$, $\bar{T}_{60}(D)$, and $\bar{T}_{100}(D)$ for a given initial damage level D. For example, the recovery rate of a component with a damage factor D between 30% and 60% functionality is

$$RR_{30,60}(D) = \frac{0.30}{\left(\bar{T}_{60}(D) - \bar{T}_{30}(D)\right)} \tag{3.51}$$

The functionality of the infrastructure component at time $t + \Delta t$, $F(t + \Delta t, D)$, is simply

$$F(t + \Delta t, D) = F(t, D) + \Delta t\left(RR(D)\right) \tag{3.52}$$

In calculating the functionalities (except for bridges), we do not use the mean damage factors but consider the variability in the damage levels. For example, in the case of buildings we calculate the functionality as the average of the functionalities of buildings suffering different levels of damage.

$$\bar{F}(t) = \int_{m=-\infty}^{\infty} F\left(t, D(S_d, m)\right) f_M(m) dm \tag{3.53}$$

where

$\bar{F}(t)$ is the average functionality of building occupancy class at time t

$F\left(t, D(S_d, m)\right)$ is the functionality of a generic building at time t with initial damage $D(S_d, m)$

$D(S_d, m)$ is the damage factor of a generic building as given in equation (3.40)

$f_M(m)$ is the variability in damage from building to building (see equation (3.41))

In case of bridges, we use the damage factor corresponding to a simulated damage state. This is done by calculating the probability of the bridge being in different damage states and then assigning a simulated damage state to the bridge based on these probabilities. This results in bridges with similar properties having different damage levels. In general there are multiple bridges on a link and the functionality of the link over time is determined by the bridge with the

highest damage level, or the one recovering slowest. Therefore, there is greater loss of functionality over time when the bridge damage level is determined stochastically compared to using the average damage level for all bridges.

3.4.5.2 Functionality and Recovery Interactions

The functionalities and recovery rates of infrastructure components calculated above are based on the level of damage of the component itself. We refer to these quantities as "physical" functionalities and "physical" recovery rates. They are the maximum possible functionalities and recovery rates. The "actual" functionality of a component depends also on the functionality of other components and due to these effects may be lower than the maximum possible value. For example, the actual functionality of an industrial facility might be reduced by disruptions of the electric power network. Interactions also affect the rate of recovery. For example, limitations on access to industrial facilities due to damage in the roadways may slow its recovery rate.

For an infrastructure class i, we represent the effect of interactions y expressing the actual functionality and recovery rate as

$$F^i_{Act}(t) = F^i_{Phy}(t) * RF^i_{Func}(t) \tag{3.54}$$

$$RR^i_{Act}(t) = RR^i_{Phy}(t) * RF^i_{\mathrm{Rec}Rate}(t) \tag{3.55}$$

where

$F^i_{Phy}(t)$ is the maximum physical functionality as given in (3.52)

$RR^i_{Phy}(t)$ is the maximum recovery rate when the physical functionality is $F^i_{Phy}(t)$

$F^i_{Act}(t)$ is the functionality accounting for interaction effects

$RR^i_{Act}(t)$ is the recovery rate accounting for interaction effects

$RF^i_{Func}(t)$ is the functionality reduction factor due to interaction effects

$RF^i_{\mathrm{Rec}Rate}(t)$ is the recovery rate reduction factor due to interaction effects

We express the functionality and recovery reduction factors using a multiplicative interaction model. In this model, the reduction factors are calculated as products of the actual functionalities of the components on which a facility depends raised to certain powers, i.e.,

$$RF^{i}_{Func}(t) = \prod_{j} \left(F^{j}_{Act}(t) \right)^{\gamma_{j,i}} \tag{3.56}$$

$$RF^{i}_{RecRate}(t) = \prod_{j} \left(F^{j}_{Act}(t) \right)^{\beta_{j,i}} \tag{3.57}$$

where

γ_{ji} is the interaction coefficient that controls the effect of functionality of component j on the functionality of component i

β_{ji} is the interaction coefficient that controls the effect of functionality of component j on the recovery rate of component i

The multiplicative model implies a series system, such that if any of the components on which a facility depends has no functionality, the functionality and recovery rate of the facility goes to zero as well. This may be an extreme assumption, which at least for small functionalities may give an upper bound on the effect of interactions. This also poses numerical problem, as components that depend on each other may never recover if one of them has zero functionality. This situation is avoided by allowing only "one way" interactions, i.e. if i depends on j, then dependence of j on i is not allowed. In addition, we set minimum functionality levels for all infrastructure components.

Specifically, we assume that all building occupancy classes depend on the electric power and intra-nodal transportation lifelines. We also assume that building occupancy classes other than residential depend on the residential class, which coarsely models the labor requirements for these sectors. The inter-industry interactions are quantified separately in the economic input-output model described in the next section.

The functionality and recovery interaction coefficients γ_{ji} and β_{ji} listed in Tables 3-33 and 3-34. These coefficients are judgmentally assigned values based on Kunnumkal (2002) and (Jammalamadaka, 2003) as literature lacks data on functionality interaction coefficients. The

basis for assigning these values is that the functionality of utilities should have a greater effect on the functionalities of building classes than on their recovery rates. The sensitivity of the losses to the functionality and recovery interactions is examined in Chapter 4.

3.4.6 Transportation Network and Regional Economic Analysis Model

Following an earthquake, the production capacity of different economic sectors decreases due to damage to production facilities and inventories and unavailability of utilities required for production. However, since each economic sector directly or indirectly requires inputs from or provides inputs to other economic sectors, business interruption losses depend not only on direct damage to individual economic sectors but also on the production capacities of other sectors in the region. Moreover, by importing/exporting commodities, an individual economic sector interacts not only with other economic sectors in the same region but also with economic sectors in other regions. The conduit for these interactions is the transportation system. Hence, any reduction in transportation capacity may result in further reductions in economic output.

Considering the above, a linear programming model has been developed to optimize regional economic activities and transportation flows under various constraints. The model uses an input-output analysis for inter-industry relations within and among regions. Additional constraints/equations are included to represent the transportation system. At any given time, the aim is to obtain the maximum regional productions and consumptions possible given the damaged state of the system by optimizing capacity utilization and commodity flows and considering inter-industry relations while minimizing the total transportation cost. In this regard, the problem is modeled as system optimum rather than user optimum. In reality the system response would be a combination of the system and user optimum models. Therefore, the solution to the formulated problem can be considered as a lower bound on the system cost.

The objective of the formulation given below is to maximize productions and consumptions of economic sectors over all regions while minimizing transportation costs in the system. The model includes constraints on productions and consumptions, inter-industry relations, link capacity limitations, material balance, flow conservation, and established regional export and import. We first introduce the model formulation and then provide details on its various components.

Table 3-33 : Functionality Interaction Coefficients

		Infrastructure Class										
Infrastructure Class		1	2	3	4	5	...	21	22	23	24	25
RES	1	0.00	0.30	0.30	0.30	0.30		0.30	0.30	0.30	0.00	0.00
COM1	2	0.00	0.00	0.00	0.00	0.00		0.00	0.00	0.00	0.00	0.00
COM2	3	0.00	0.00	0.00	0.00	0.00		0.00	0.00	0.00	0.00	0.00
COM3	4	0.00	0.00	0.00	0.00	0.00		0.00	0.00	0.00	0.00	0.00
COM4	5	0.00	0.00	0.00	0.00	0.00		0.00	0.00	0.00	0.00	0.00
COM5	6	0.00	0.00	0.00	0.00	0.00		0.00	0.00	0.00	0.00	0.00
COM6	7	0.00	0.00	0.00	0.00	0.00		0.00	0.00	0.00	0.00	0.00
COM7	8	0.00	0.00	0.00	0.00	0.00		0.00	0.00	0.00	0.00	0.00
COM8	9	0.00	0.00	0.00	0.00	0.00		0.00	0.00	0.00	0.00	0.00
COM9	10	0.00	0.00	0.00	0.00	0.00		0.00	0.00	0.00	0.00	0.00
COM10	11	0.00	0.00	0.00	0.00	0.00		0.00	0.00	0.00	0.00	0.00
IND1	12	0.00	0.00	0.00	0.00	0.00		0.00	0.00	0.00	0.00	0.00
IND2	13	0.00	0.00	0.00	0.00	0.00		0.00	0.00	0.00	0.00	0.00
IND3	14	0.00	0.00	0.00	0.00	0.00		0.00	0.00	0.00	0.00	0.00
IND4	15	0.00	0.00	0.00	0.00	0.00		0.00	0.00	0.00	0.00	0.00
IND5	16	0.00	0.00	0.00	0.00	0.00		0.00	0.00	0.00	0.00	0.00
IND6	17	0.00	0.00	0.00	0.00	0.00		0.00	0.00	0.00	0.00	0.00
AGR1	18	0.00	0.00	0.00	0.00	0.00		0.00	0.00	0.00	0.00	0.00
REL1	19	0.00	0.00	0.00	0.00	0.00		0.00	0.00	0.00	0.00	0.00
GOV1	20	0.00	0.00	0.00	0.00	0.00		0.00	0.00	0.00	0.00	0.00
GOV2	21	0.00	0.00	0.00	0.00	0.00		0.00	0.00	0.00	0.00	0.00
EDU1	22	0.00	0.00	0.00	0.00	0.00		0.00	0.00	0.00	0.00	0.00
EDU2	23	0.00	0.00	0.00	0.00	0.00		0.00	0.00	0.00	0.00	0.00
Trans	24	0.45	0.45	0.90	0.90	0.90		0.90	0.90	0.90	0.00	0.00
Util	25	0.15	0.15	0.30	0.30	0.30		0.30	0.30	0.30	0.00	0.00

Table 3-34 : Recovery Interaction Coefficients

		Infrastructure Class										
Infrastructure Class		1	2	3	4	5	...	21	22	23	24	25
RES	1	0.00	0.45	0.45	0.45	0.45		0.45	0.45	0.45	0.00	0.00
COM1	2	0.00	0.00	0.00	0.00	0.00		0.00	0.00	0.00	0.00	0.00
COM2	3	0.00	0.00	0.00	0.00	0.00		0.00	0.00	0.00	0.00	0.00
COM3	4	0.00	0.00	0.00	0.00	0.00		0.00	0.00	0.00	0.00	0.00
COM4	5	0.00	0.00	0.00	0.00	0.00		0.00	0.00	0.00	0.00	0.00
COM5	6	0.00	0.00	0.00	0.00	0.00		0.00	0.00	0.00	0.00	0.00
COM6	7	0.00	0.00	0.00	0.00	0.00		0.00	0.00	0.00	0.00	0.00
COM7	8	0.00	0.00	0.00	0.00	0.00		0.00	0.00	0.00	0.00	0.00
COM8	9	0.00	0.00	0.00	0.00	0.00		0.00	0.00	0.00	0.00	0.00
COM9	10	0.00	0.00	0.00	0.00	0.00		0.00	0.00	0.00	0.00	0.00
COM10	11	0.00	0.00	0.00	0.00	0.00		0.00	0.00	0.00	0.00	0.00
IND1	12	0.00	0.00	0.00	0.00	0.00		0.00	0.00	0.00	0.00	0.00
IND2	13	0.00	0.00	0.00	0.00	0.00		0.00	0.00	0.00	0.00	0.00
IND3	14	0.00	0.00	0.00	0.00	0.00		0.00	0.00	0.00	0.00	0.00
IND4	15	0.00	0.00	0.00	0.00	0.00		0.00	0.00	0.00	0.00	0.00
IND5	16	0.00	0.00	0.00	0.00	0.00		0.00	0.00	0.00	0.00	0.00
IND6	17	0.00	0.00	0.00	0.00	0.00		0.00	0.00	0.00	0.00	0.00
AGR1	18	0.00	0.00	0.00	0.00	0.00		0.00	0.00	0.00	0.00	0.00
REL1	19	0.00	0.00	0.00	0.00	0.00		0.00	0.00	0.00	0.00	0.00
GOV1	20	0.00	0.00	0.00	0.00	0.00		0.00	0.00	0.00	0.00	0.00
GOV2	21	0.00	0.00	0.00	0.00	0.00		0.00	0.00	0.00	0.00	0.00
EDU1	22	0.00	0.00	0.00	0.00	0.00		0.00	0.00	0.00	0.00	0.00
EDU2	23	0.00	0.00	0.00	0.00	0.00		0.00	0.00	0.00	0.00	0.00
Trans	24	0.150	0.15	0.30	0.30	0.30		0.30	0.30	0.30	0.00	0.00
Util	25	0.150	0.15	0.30	0.30	0.30		0.30	0.30	0.30	0.00	0.00

The optimization model for transportation network and economic analysis is formulated as follows.

$$Max\left\{\sum_{k=1}^{K}\sum_{r=1}^{R}X_r^{k,t}+\sum_{k=1}^{K}\sum_{r=1}^{R}C_r^{k,t}-\sum_{k=1}^{K}\sum_{(i,j)}c_{ij}^{k}x_{ij}^{k,t}-\sum_{k=1}^{K}\sum_{(j,i)}c_{ji}^{k}x_{ji}^{k,t}\right\} \tag{3.58}$$

s.t.

$$X_r^{k,t}\le X_r^{k,t,\max} \qquad \forall k,r \tag{3.59}$$

$$C_r^{k,t}\le C_r^{k,t,\max} \qquad \forall k,r \tag{3.60}$$

$$\left(\underline{\underline{I}}-\underline{\underline{A}}\right)\underline{X}_r^t-\underline{C}_r^t=\underline{b}_r^t \qquad \forall r \tag{3.61}$$

$$\sum_{j:(i,j)\in LN_i}x_{ij}^{k,t}-\sum_{j:(j,i)\in LN_i}x_{ji}^{k,t}=\frac{b_i^{k,t}}{\lambda^k} \qquad \forall k,i \tag{3.62}$$

$$\sum_{k=1}^{K}x_{ij}^{k,t}\le u_{ij}^{t,\max} \qquad \forall(i,j) \tag{3.63}$$

$$\sum_{k=1}^{K}x_{ji}^{k,t}\le u_{ji}^{t,\max} \qquad \forall(i,j) \tag{3.64}$$

$$\sum_{i\in NS_s,\,j\notin NS_s}x_{ij}^{k,t}\ge E_s^{k,CFS} \qquad \forall k,s \tag{3.65}$$

$$\sum_{i\in NS_s,\,j\notin NS_s}x_{ji}^{k,t}\ge I_s^{k,CFS} \qquad \forall k,s \tag{3.66}$$

$$X_r^{k,t}\ge 0 \qquad \forall k,r \tag{3.67}$$

$$C_r^{k,t}\ge 0 \qquad \forall k,r \tag{3.68}$$

$$x_{ij}^{k,t}\ge 0 \qquad \forall(i,j) \tag{3.69}$$

where

$X_r^{k,t}$ is the production of commodity k in region r at time t

$C_r^{k,t}$ is the domestic consumption of commodity k in region r at time t

$X_r^{k,t,\max}$ is the production capacity of economic sector k in region r at time t

$C_r^{k,t,\max}$ is the maximum domestic consumption of commodity k in region r at time t

$b_r^{k,t}$ is the net export/import of commodity k in region r at time t

$b_i^{k,t}$ is the net export/import of commodity k at node i at time t

(i, j) is the link connecting node i to node j

$x_{ij}^{k,t}$ is the flow of commodity k on link (i, j) at time t

$u_{ij}^{t,\max}$ is the capacity of link (i, j) at time t in truck units

c_{ij}^k is the cost per unit flow of commodity k on link (i, j)

λ^k is a factor for converting $ value of commodity k to vehicle units

K is the number of economic sectors

R is the number of analysis regions

S is the number of states in continental US plus D.C. (=49)

$E_s^{k,CFS}$ is the total export of commodity k from state s obtained from CFS

$I_s^{k,CFS}$ is the total import of commodity k to state s obtained from CFS

RN_i is the set of analysis regions attached to node i

RS_s is the set of analysis regions in state s

NS_s is the set of nodes in state s

LN_i is the set of links associated with node i

$\underline{\underline{A}}$ is the input-output matrix $(K \times K)$

$\underline{\underline{I}}$ is the identity matrix $(K \times K)$

The objective of the formulation, given in equation (3.58), is to maximize productions and consumptions in various economic sectors over all regions while minimizing transportation costs over the entire system. Although the objective function includes maximization of both productions and consumptions, including only one of them produces the same results since these variables are linked through the inter-industry relationships and no foreign export/import is considered.

Equations (3.59) and (3.60) impose limits on productions and consumptions, respectively, for each economic sector in each analysis region. The maximum production capacity of economic sector k in region r is calculated as

$$X_r^{k,t,\max} = \overline{X}_r^{k,preEQ} slack_r^{k,t} F_r^{k,t} \qquad \forall k,r \tag{3.70}$$

where,

$\overline{X}_r^{k,preEQ}$ is the nominal pre-earthquake production of commodity k in region r

$F_r^{k,t}$ is the functionality of economic sector k in region r at time t

$slack_r^{k,t}$ is the slack factor for production of commodity k in region r at time t

In this equation, the factor $slack_r^{k,t}$ is introduced to account for unused capacity and for the buffering effect of inventories. This factor is generally assigned a value between 1.0 and 1.05, for no slack and 5% slack in production, respectively. Economic sectors are allowed to increase their production levels up to the selected factor. The value of the slack factor depends not only on pre-earthquake economic and social conditions but also on the responses of different economic sectors in the various regions to the economic environment after the earthquake. Assigning the slack factor more objectively is a difficult task and is beyond the scope of this study. In the application to New Madrid earthquakes, the same factor is applied to all economic sectors regardless of damage level and location.

Contrary to productions, maximum regional consumptions (final demands) are assumed to be insensitive to earthquake damage or the functionality of the economic sectors. Hence, their upper limit is set to the consumption demand in the pre-earthquake state:

$$C_r^{k,t,\max} = C_r^{k,preEQ} \qquad \forall k,r \tag{3.71}$$

where

$C_r^{k,preEQ}$ is the pre-earthquake domestic consumption of commodity k in region r.

Equation (3.61) uses a linear input-output model to represent inter-industry relations. Economic activity in each analysis region is characterized by the productions in the various economic sectors in that region. Each economic sector uses commodities/services from other sectors, which constitute the inter-industry demands. These inter-industry relations are modeled by the input-output coefficient matrix, $\underline{\underline{A}}$. The generic coefficient a_{ij} of $\underline{\underline{A}}$ is the total input (in \$) from economic sector i required to produce \$1 of output in economic sector j. In application, the input-output coefficient matrix is assumed to be the same for all analysis regions. The sum of inter-industry demand and domestic consumption constitutes the final demand. Depending on the productions of different economic sectors in a region and the final local demands for commodities, an analysis region either exports or imports commodities from or to other regions. Net exports from a region can be obtained by applying Equation (3.61) to that region.

Equation (3.62) represents conservation of commodity flow at each node. The difference between the amount of a commodity transported from other nodes and the amount of a commodity transported from and to other nodes is the net export of that commodity for that node. Rather than performing this analysis in monetary units, net exports are expressed in vehicle units using conversion factors λ^k for different economic sectors k and flow conservation is stated in terms of number of vehicles.

Equation (3.63) introduces a capacity limitation for each transportation link. The total number of vehicles transporting different commodities on a link cannot exceed the capacity of that link. The capacity of link (i, j) at time t is calculated by multiplying its pre-earthquake capacity by its functionality

$$u_{ij}^{t,\max} = u_{ij}^{preEQ} F_{ij}^t \qquad \forall k, r \qquad (3.72)$$

where,

u_{ij}^{preEQ} is the pre-earthquake capacity of link (i, j)

F_{ij}^t is the functionality of link (i, j) at time t

Equations (3.65) and (3.66) are lower limits on the value of exports from and imports to a state based on 1997 Commodity Flow Survey (CFS) data, in the pre- and post-earthquake states. These constraints are used mainly to account for established trade patterns at the state level. The limits are the exports originating from a state or imports for a destination state and do not include the commodities passing through the state, which would contribute to both exports and imports at the state level. For most of the states, especially those in the CUS region which are on major transportation routes, the total value of exports and imports are much higher than the lower limits set by these equations. These constraints also create some cross-hauling of commodities in the transportation links crossing state borders.

Finally, equations (3.67), (3.68), and (3.69) impose non-negativity constraints on regional productions, regional consumptions, and transportation link flows, respectively.

At each time step, the above linear programming problem is solved using a solver called PCX (Czyzyk et al, 1997) and the resulting regional productions, consumptions, and link flows are stored. After each analysis, the functionalities of infrastructure components and different economic sectors are updated and the LP problem is solved again at the next time step. The same LP formulation is used to obtain the link flows and other parameters of interest in the pre-earthquake state with functionalities of economic sectors and transportation links set to unity. When applying the model to pre-earthquake conditions, the slack in the production capacities is allowed to be utilized. This results in a (small) reallocation of productions among regions to reduce the transportation costs. However, regional domestic consumptions remain the same since they are based on regional populations. The pre-earthquake productions and consumptions are compared with productions and consumptions at different times following the earthquake and economic losses are calculated as explained in the next section.

3.4.7 Economic losses

The economic consequences evaluated by the present model include direct losses due to physical damage, direct losses due to business interruption, and indirect losses due to business interruption. These loss components are defined and obtained as follows.

Direct losses due to physical damage

Direct losses due to physical damage include the costs of repair/replacement of damaged buildings, contents, and bridges. These losses are obtained by multiplying the damage ratio of each infrastructure component by its replacement value. The replacements costs for different building occupancy classes and bridges are taken from HAZUS. Building replacement costs are obtained by summing the repair costs for structural, non-structural acceleration sensitive and non-structural drift sensitive components as explained in section 3.4.3. Bridge repair costs are calculated as described in section 3.4.4.

Direct losses due to business interruption

Direct business interruption losses include losses due to reduced functionality of the facilities used by different economic sectors and the lifelines on which they depend. Losses resulting from unavailability of commodities produced by other economic sectors that are used as input for production are assessed separately as indirect losses (see below).

Direct production losses up to time T, $DPL(T)$, can be calculated by integrating the decrease in production capacity over all economic sectors, all analysis regions, and time:

$$DPL(T) = \sum_{t=0}^{T} \sum_{r=1}^{R} \sum_{k=1}^{K} (X_r^{k,preEQ} - X_r^{k,t,\max}) \Delta t \tag{3.73}$$

where

$X_r^{k,preEQ}$ is the pre-earthquake production of commodity k in region r obtained from analysis of the system in the pre-earthquake state considering the available slack

$X_r^{k,t,\max}$ is the physical post-earthquake production capacity for commodity k in region r at time t

In addition to the direct production losses, we also calculate and report the loss in added value $DVAL(T)$ due to reduced productions by multiplying the direct production losses by the corresponding value-added factors.

Indirect losses due to business interruption

Business interruption losses other than those directly caused by physical damage are considered "indirect" business interruption losses. These losses are due to the interdependence among economic sectors and may arise from non-uniform functionality reductions of different economic sectors or from disruptions in commodity flows due to transportation capacity reductions. Unfortunately, indirect business losses depend in a complicated way on the functionality reductions of different sectors in different regions and the above mentioned integrated transportation and economic analysis has to be used to assess them. The linear programming model in equations (3.58)-(3.69) provides regional productions of different economic sectors at different times, $X_r^{k,t}$. Comparing these productions with the maximum possible productions, indirect economic losses at time T, $IPL(T)$ are obtained from

$$IPL(T) = \sum_{t=0}^{T} \sum_{r=1}^{R} \sum_{k=1}^{K} (X_r^{k,t,\max} - X_r^{k,t}) \Delta t \tag{3.74}$$

Similarly, total business interruption losses at time T, $TPL(T)$, can be obtained from

$$TPL(T) = \sum_{t=0}^{T} \sum_{r=1}^{R} \sum_{k=1}^{K} (X_r^{k,preEQ} - X_r^{k,t}) \Delta t \tag{3.75}$$

As in the case of direct production losses, we again calculate the corresponding indirect and total value added losses for each of the analysis regions.

3.5 Concluding Remarks

In this chapter, we have presented the general framework of the loss estimation methodology and provided details on its various component models. The methodology is comprehensive in that it involves relatively detailed calculation of building damages and losses, models for loss of functionality and recovery of infrastructure components over time, and integrated analysis of the transportation network and the regional economies. The calculated quantities include building repair restoration costs, production losses, value added losses, and increased transportation costs.

The loss estimation model is implemented in a flexible and modular way that allows sensitivity and uncertainty analysis. In many cases, alternative representations of data or sets of parameters may be used in the component models of the methodology. Also, the methodology, especially calculation of building damage and losses, requires much less computational time compared to

similar tools such as HAZUS. This makes the implemented methodology attractive for purposes of sensitivity and uncertainty analysis. In Chapters 4 and 5, we make use of these advantages of the methodology to perform first a detailed sensitivity analysis of earthquake losses and then to develop loss risk curves for selected regions of interest.

4 Scenario Earthquake Losses and Sensitivity Analysis

In this chapter, we apply the loss estimation methodology described in Chapter 3 to scenario earthquakes and assess the sensitivity of the losses to various components or parameters in the methodology. Section 4.1 discusses in detail the results for a selected earthquake in NMSZ. Section 4.2 investigates the sensitivity of the losses to component models and parameters. Section 4.3 summarizes our main conclusions.

4.1 Scenario Earthquake Loss

Here, we present and discuss the results for a moment magnitude M7.5 earthquake using best estimate values or default parameters/models as discussed in Section 4.2. The epicenter of the earthquake at (35.50°N, 90.00°W) is located about 35km to the population centroid of Shelby County; see Figure 4-1. The earthquake is modeled as a point not line source, close to the eastern NMSZ fault used by USGS. The location corresponds to the closest section of the eastern NMSZ fault to the centroid of Shelby County; hence this is one of the most damaging earthquakes threatening Shelby County.

We first present the spatial distribution and intensity of ground motions generated by the scenario event. Next, we discuss and compare building losses in Shelby County, the NMSZ region, and the CUS region. This is followed by discussions on bridge damage and losses and the effects of bridge damage on transportation link functionality and recovery. Finally, we discuss the business losses calculated for different regions and the entire US.

4.1.1 Ground Motion Intensity

The spatial distributions of Sa(0.3sec) and Sa(1.0sec) for the magnitude M7.5 scenario earthquake are shown in Figure 4-2 for the CUS region and in Figure 4-3 for the NMSZ region. These spectral accelerations are for site class B-C. The scale and colors used to represent ground motion intensities are the same in all figures.

For this M7.5 earthquake, Sa(0.3sec) reaches values as high as 2.6g in the epicentral region, whereas the maximum Sa(1.0sec) value is approximately 1.0g. In the entire NMSZ region Sa(0.3sec) is greater than 0.1g. The region with Sa(0.3sec) $\geq 0.05g$ extends as far as 400km. On the other hand, Sa(1.0sec) $\geq 0.05g$ only as far as 250km from the epicenter. In Shelby County, Sa(0.3sec) is as high as 1.2g at the northwest corner with a minimum value of 0.4g at the southeast corner, which is farthest from the epicenter; see Figure 4-4. The Sa(1.0sec) values at the same locations are approximately 0.4g and 0.15g. In the epicentral region, Sa(1.0sec) is less than half the Sa(0.3sec) value; see Figure 4-5. However, with increasing distance, the ratio of Sa(1.0sec)/Sa(0.3sec) increases due to differences in the attenuation characteristics of long and short period waves.

As mentioned above, these ground motion intensities apply to B-C soil conditions. As most of the sites in the region are actually in class D or E, the ground motion intensities are amplified up to a factor of 2. This enlarges the area with damaging ground motion intensities.

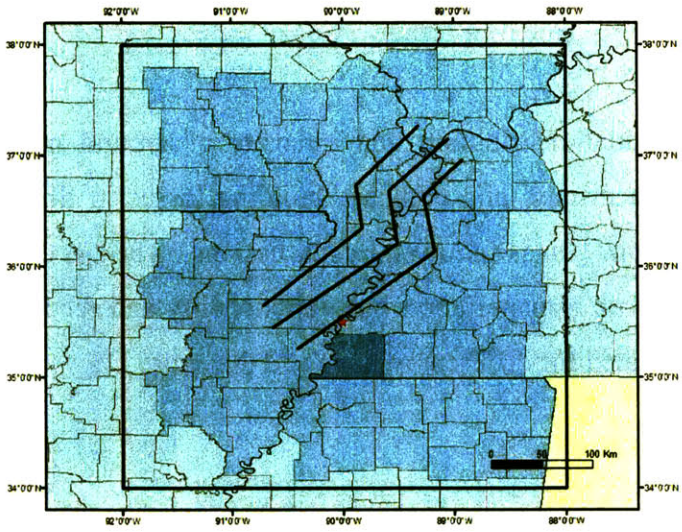

Figure 4-1: Location of Scenario Earthquake

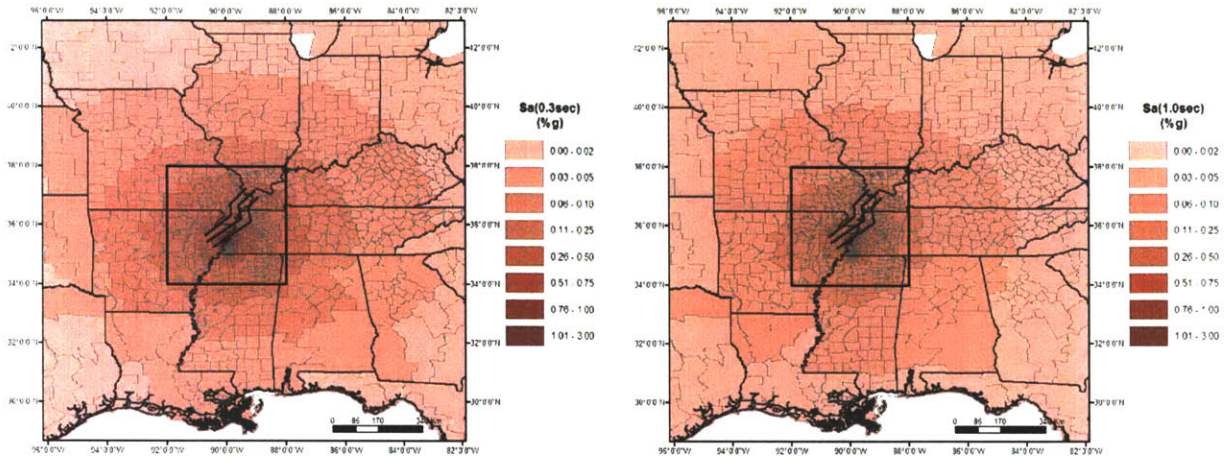

Figure 4-2: Estimated (a) Sa(0.3sec) and (b) Sa(1.0sec) in CUS for Scenario Earthquake

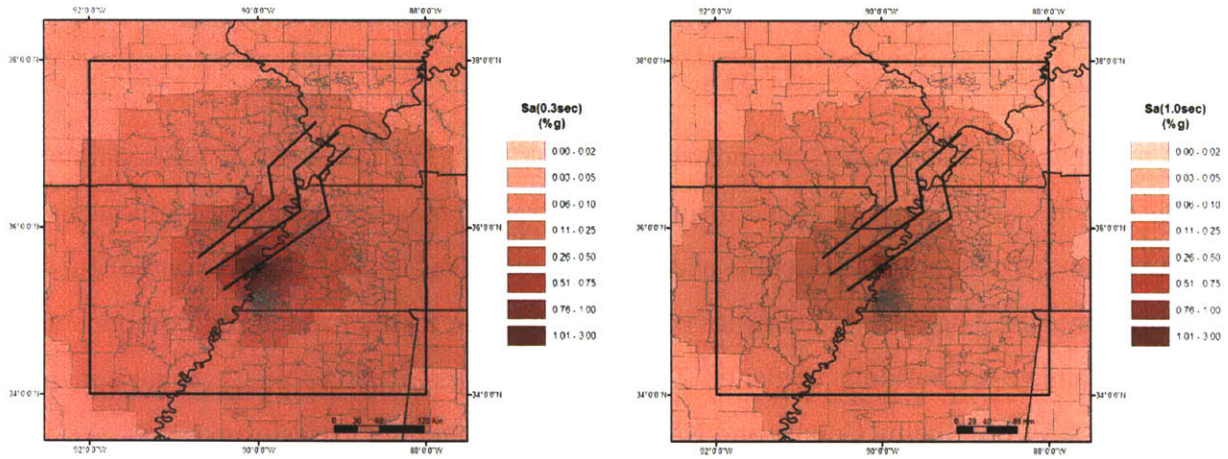

Figure 4-3: Estimated (a) Sa(0.3sec) and (b) Sa(1.0sec) in NMSZ for Scenario Earthquake

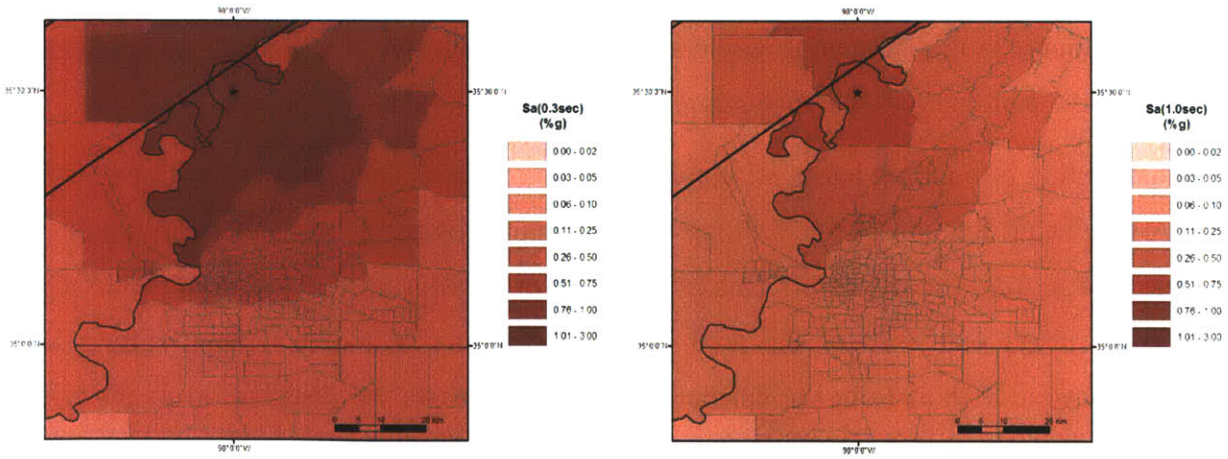

Figure 4-4: Estimated (a) Sa(0.3sec) and (b) Sa(1.0sec) in Shelby County for Scenario Earthquake

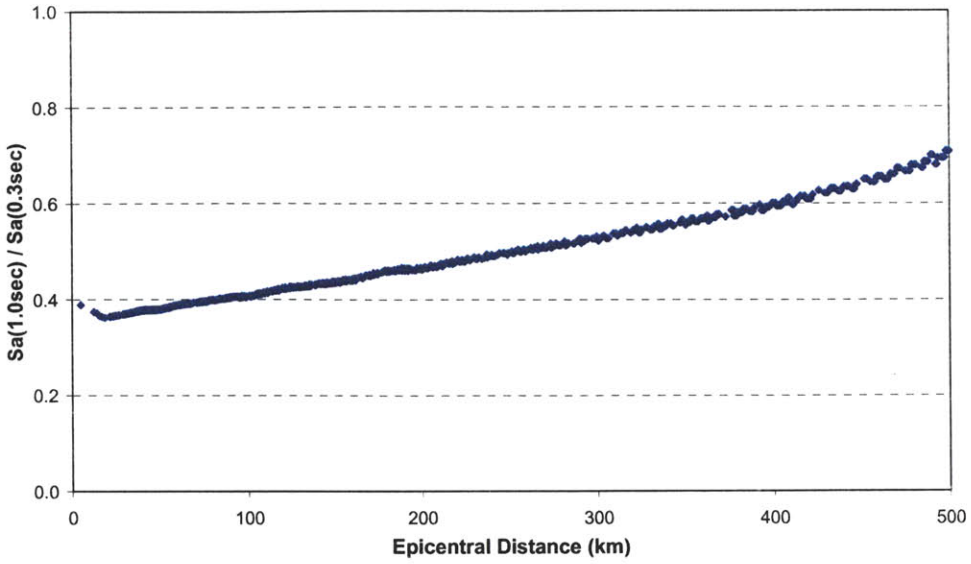

Figure 4-5: Ratio of Sa(1.0sec) to Sa(0.3sec) for Scenario Earthquake

4.1.2 Building Damage and Loss

Building repair/restoration costs are provided in Table 4-1. The losses are listed separately for Shelby County, NMSZ, and CUS and include losses from damage to structural components, drift sensitive non-structural components, acceleration sensitive non-structural components, and building contents. The total building loss is the sum of the losses to building components and excludes damage to building contents. Table 4-2 provides a percentage comparison of the building losses from Shelby County and NMSZ relative to building losses from CUS.

For the M7.5 scenario earthquake, the total building loss is estimated to be $24.2B. Of these, $21.7B is contributed by the NMSZ region. About 50% of the losses ($11.7B) come from Shelby County. Damage to non-structural acceleration and drift sensitive components each account for 35-45% of the building losses and structural components contribute about 20%.

The distribution of building losses within different epicentral distance ranges is shown in Figure 4-6. A significant fraction of the building losses originate from regions located in the 20-50km distance range from the epicenter. This range includes most of Shelby County (Shelby County contributes about one third of the total building inventory in NMSZ). No building loss is observed beyond 350km from the epicenter. Figure 4-7 shows the distribution of the building losses by distance range, normalized by the building inventory value in that range. The

normalized building loss ratio is about 0.6 in the epicentral region and less than 10% in the 100-150km distance range. Figures 4-8 and 4-9 show the spatial distribution of the total and normalized building losses around NMSZ, respectively. Figures 4-10 and 4-11 are Shelby County close-ups. As building loss depends on both building damage and building inventory in a region, the regions with higher building losses in Figure 4-8 represent regions with higher building inventory, higher damage level, or both. That is why some of the regions farther away from the epicenter have higher losses compared to regions closer to the epicenter. In general, these regions are either large and/or include a higher concentration of buildings. In this regard, Figure 4-9 provides a better picture of the relative distribution of building loss levels as the losses are normalized by building inventory value. The normalized building loss in the analysis region closest to the epicenter is 80%. As expected, the normalized losses decrease with increasing epicentral distance. The normalized losses within Shelby County range between 8% and 35%.

Although Figures 4-9 and 4-11 show losses normalized by building inventory, one still observes regions at similar epicentral distances having different normalized losses. This is due in part to variable soil conditions and in part to variation in the composition of the building inventory. Specifically, analysis regions with softer soil conditions incur more loss due to higher amplification of the ground motion and the building inventory mixture in urban and rural regions may be quite different.

To compare the building loss estimates with those from HAZUS, we used HAZUS software with the default parameters for evaluating building losses in Shelby County for the same earthquake. The loss from structural components is $1,954M compared to $2.238 obtained from our methodology. The loss from non-structural components is $6,841M, which is much lower than our estimate, $9,503M. The differences arise from differences in soil amplification, soil type, and the vulnerability model used. If we calculate building losses with our methodology but using HAZUS fragility curves rather than the derived vulnerability curves, we estimate much lower building losses, $1,364M and $4,973M for structural and nonstructural losses. The difference is mainly due to the use of higher damage factors for the four damage states (in HAZUS) in vulnerability curve parameter estimation. These differences will be investigated in further detail and addressed more thoroughly in future studies as they result in overestimation of losses.

Table 4-1: Building Losses for Scenario Earthquake

Building Loss ($M)	Shelby County	NMSZ	CUS
Building Losses	11,740	21,656	24,206
Structural	2,238	4,307	5,045
Non-Str. Drift Sensitive	4,394	8,290	9,458
Non-Str. Acceleration Sensitive	5,109	9,060	9,703
Contents	4,480	7,982	8,553
Building Losses + Contents	27,961	51,295	56,965

Table 4-2: Percent Building Losses for Scenario Earthquake

Building Loss (%)	% Shelby/NMSZ	% Shelby/CUS	% NMSZ /CUS
Building Losses	55.3	50.8	91.8
Structural	52.0	44.4	85.4
Non-Str. Drift Sensitive	53.0	46.5	87.7
Non-Str. Acceleration Sensitive	56.4	52.7	93.4
Contents	56.1	52.4	93.3
Building Losses + Contents	54.5	49.1	90.0

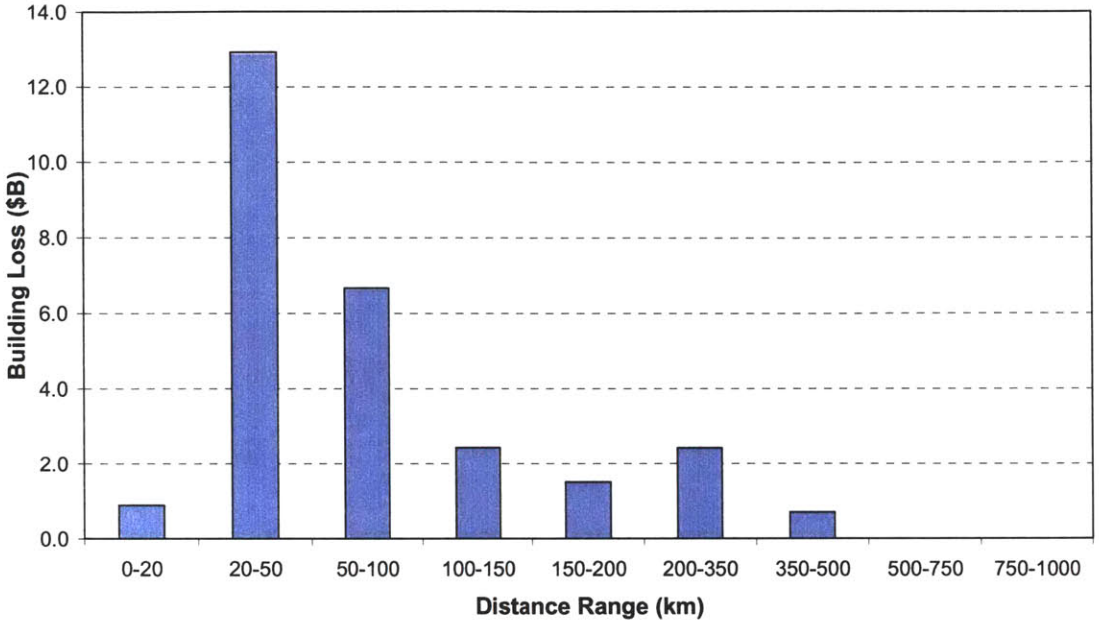

Figure 4-6: Distribution of Building Losses with Distance for Scenario Earthquake

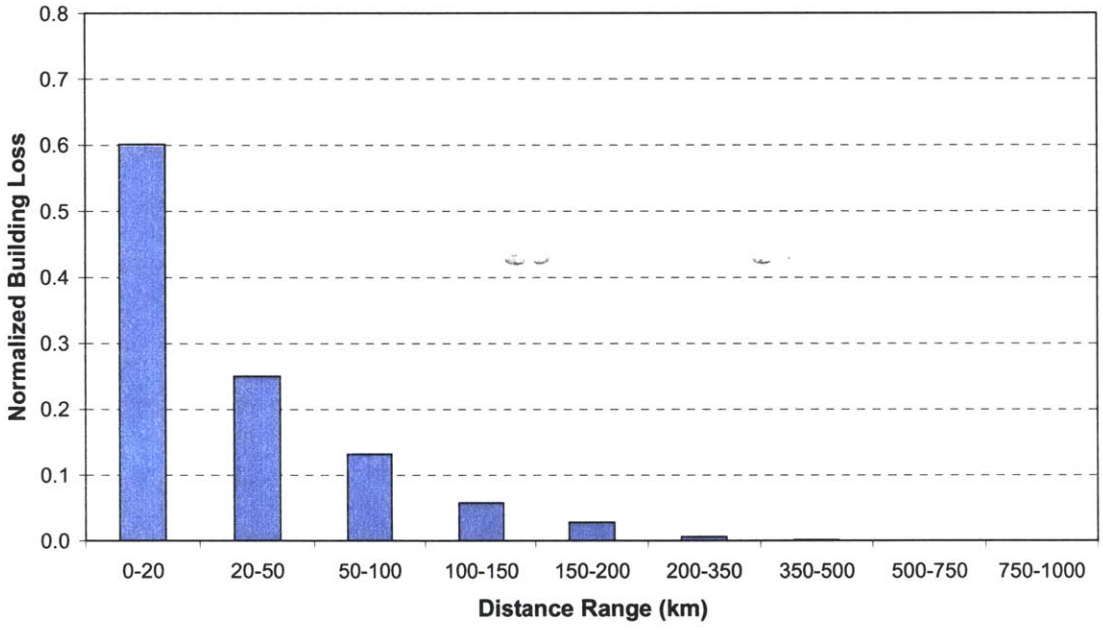

Figure 4-7: Distribution of Normalized Building Losses with Distance for Scenario Earthquake

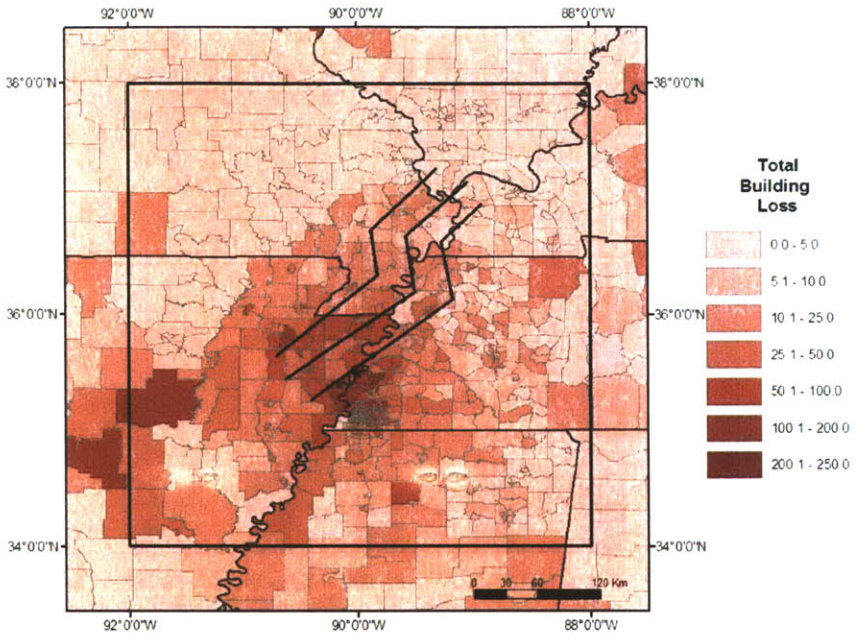

Figure 4-8: Spatial Distribution of Building Losses in NMSZ

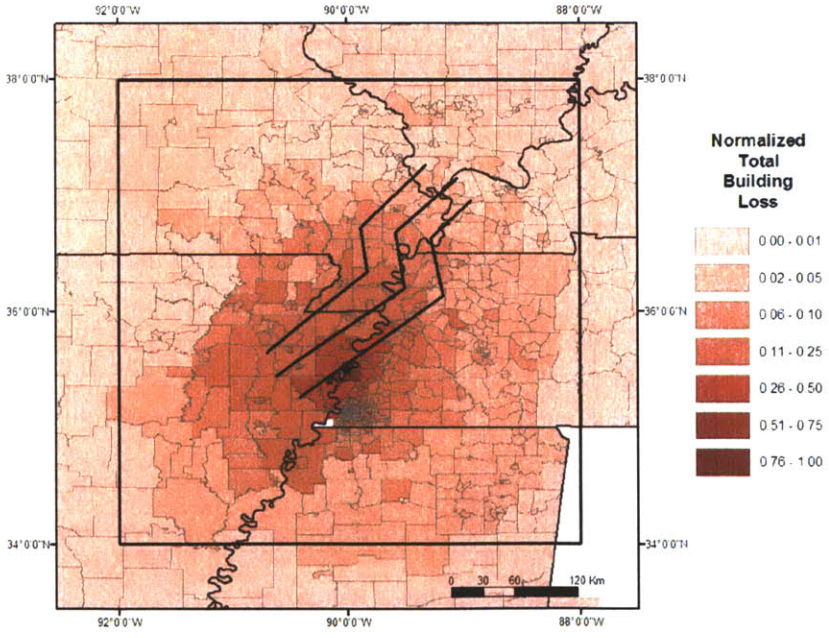

Figure 4-9: Spatial Distribution of Normalized Building Losses in NMSZ

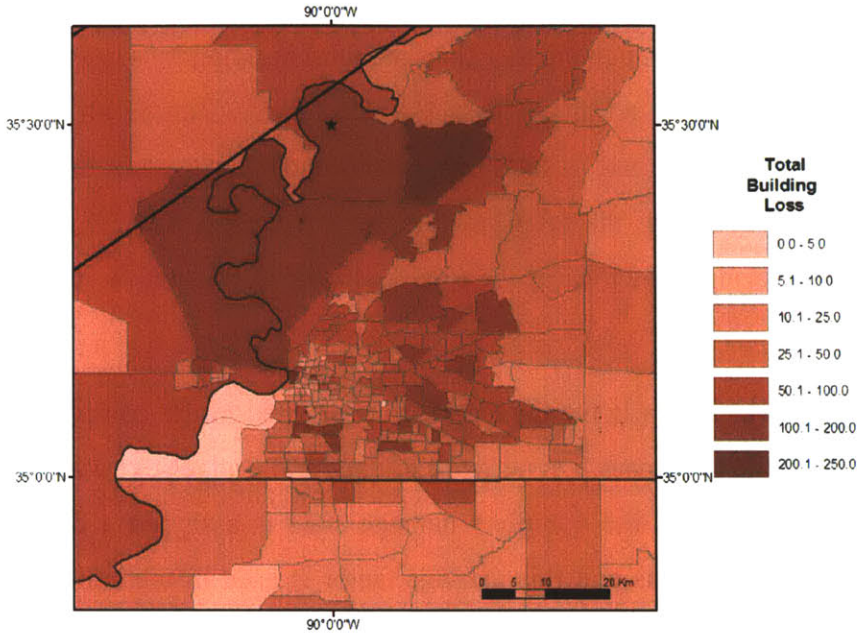

Figure 4-10: Spatial Distribution of Building Losses in Shelby County

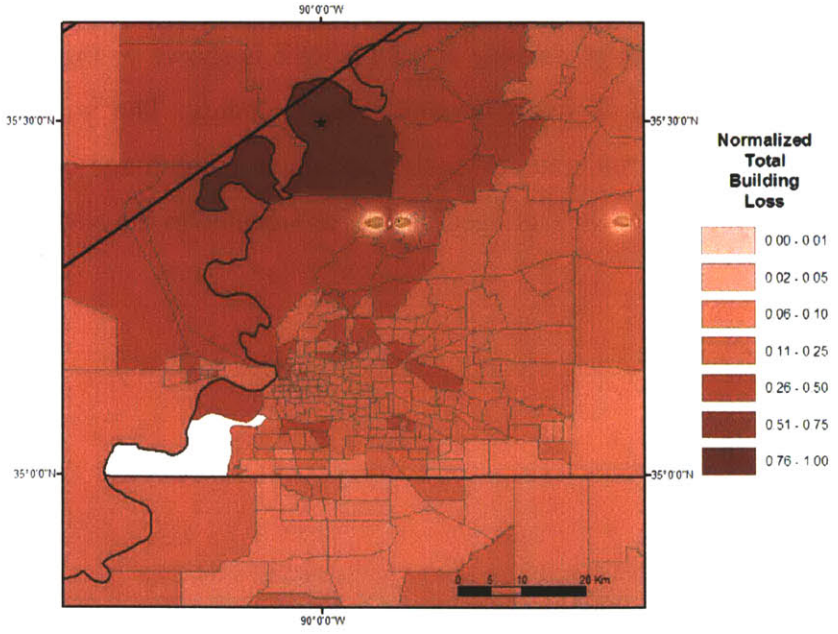

Figure 4-11: Spatial Distribution of Normalized Building Losses in Shelby County

4.1.3 Bridge Damage and Loss

The repair/restoration costs of the 4651 bridges in the transportation network are given in Table 4-3. The total loss, $269M, is much smaller than the total building loss. Also listed in Table 4-3 are the losses for the bridges extracted from HAZUS. These include all bridges in the CUS region whether or not they are part of the transportation network used in the analysis. Although the number of bridges is larger, the total loss for these bridges is $222M that is slightly lower than that for network bridges. $215M of the total loss originates from the bridges located in the NMSZ region.

The reason for the lower losses is the damage factor assigned to the complete damage state for multi-span bridges in the two cases, i.e. network bridges and bridges extracted from the HAZUS inventory. In the former case, the complete damage state is assigned a damage factor of 1.0 independent of number of spans and this damage factor is used in the subsequent functionality calculations. By contract, in the HAZUS bridge analysis case, the loss factor for bridges with 3 or more spans is calculated by normalizing the damage factor by the number of spans. This normalization reduces the losses from the bridges in complete damage state.

The distribution of network bridge damage around NMSZ is shown in Figure 4-12. Figure 4-13 provides a close up of the same figure around Shelby County. The number of bridges with damage factors in the slight, moderate, extensive and complete damage categories are 120, 82, 98 and 59, respectively. Most of the damaged bridges are located in the NMSZ region.

Table 4-3: Bridge Losses for Scenario Earthquake

Bridge Loss	Loss ($M)
Network Bridges - All	269
HAZUS Bridges - All	222
HAZUS Bridges - NMSZ	215

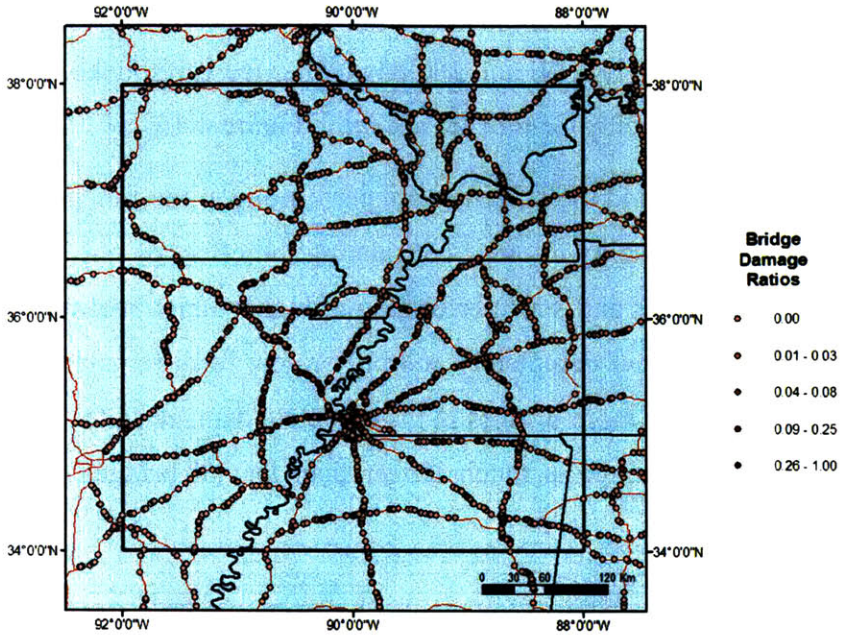

Figure 4-12: Bridge Damage around NMSZ

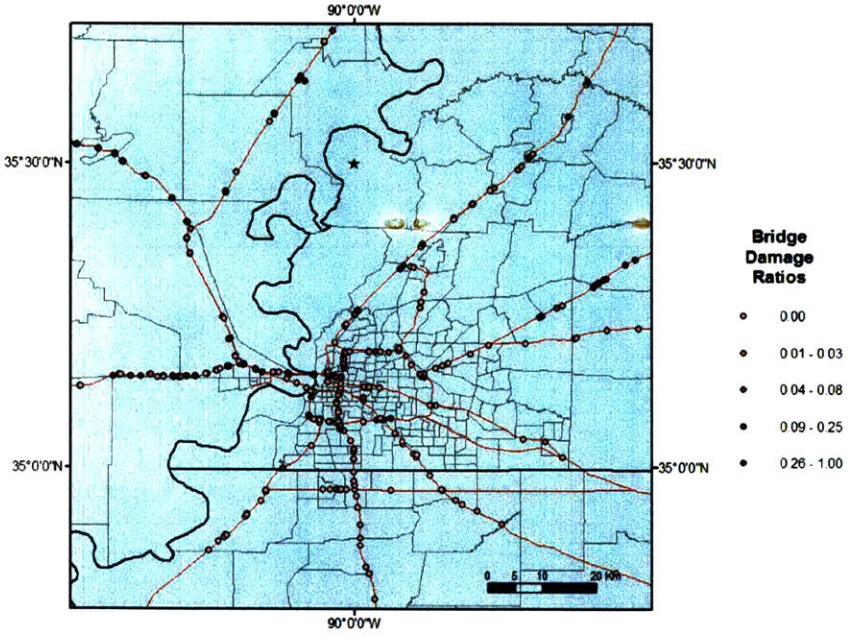

Figure 4-13: Bridge Damage around Shelby County

4.1.4 Transportation Link Functionality and Flows

The functionality of the transportation links depends primarily on the damage and functionality of the bridges located on the links. Figure 4-14 shows the functionality of the links around the NMSZ region at various times (1, 7, 30 and 180 days) after the earthquake. The functionality of the links and bridges around Shelby County are shown in Figure 4-15.

At day 1 most of the links around the epicenter are performing at the functionality level of 0.10, which is the minimum functionality allowed considering the effect of rerouting. After 7 and 30 days, some of the links recover and start performing at higher functionality levels. At day 180, most of the links have recovered completely and only a few links remain at low functionality. These are the links with one or more bridges in the complete damage state. The recovery time of the bridges with complete damage is much longer than that of bridges with more moderate

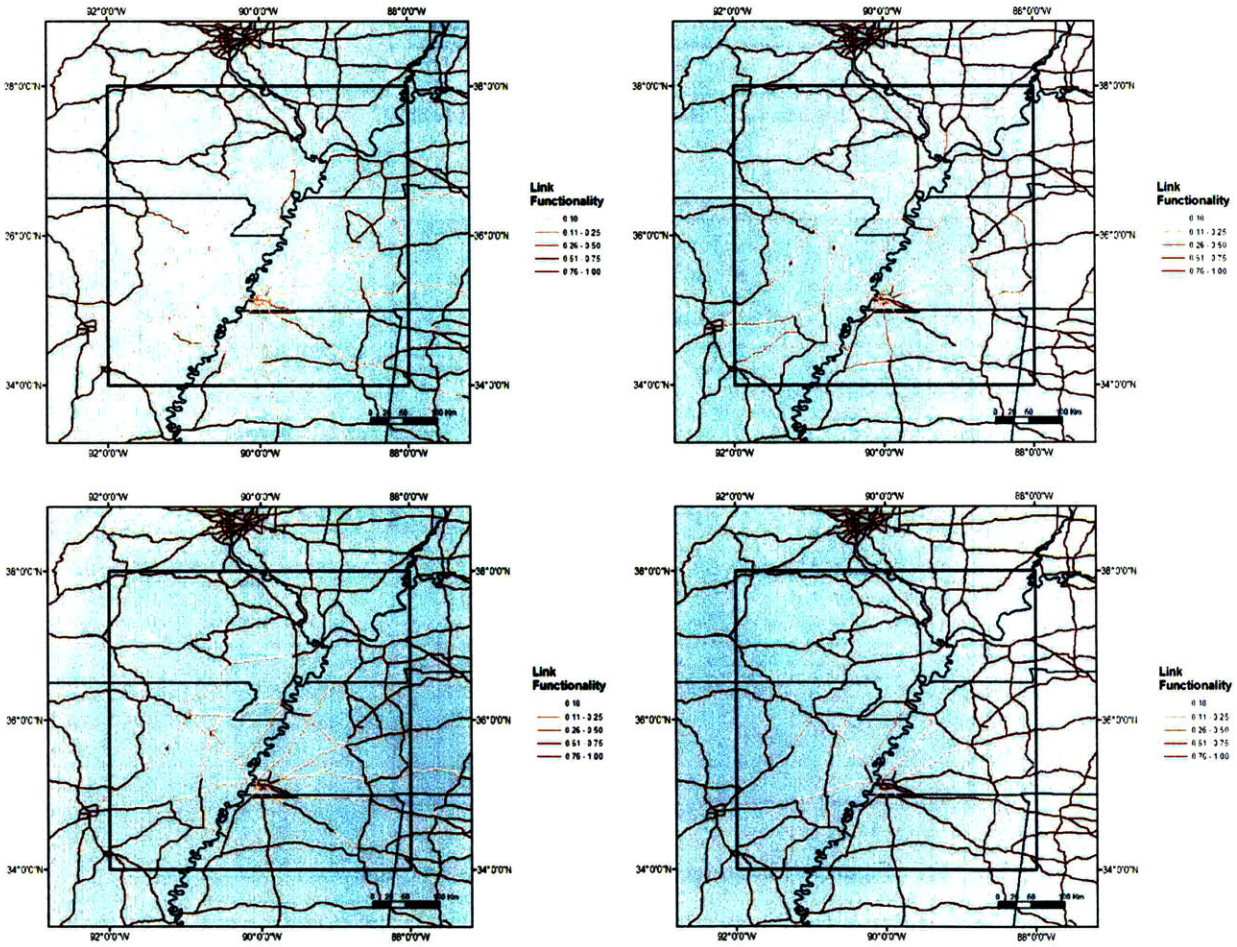

Figure 4-14: Functionality of Links around NMSZ at (a) Day 1, (b) Day 7, (c) Day 30, and (d) Day 180

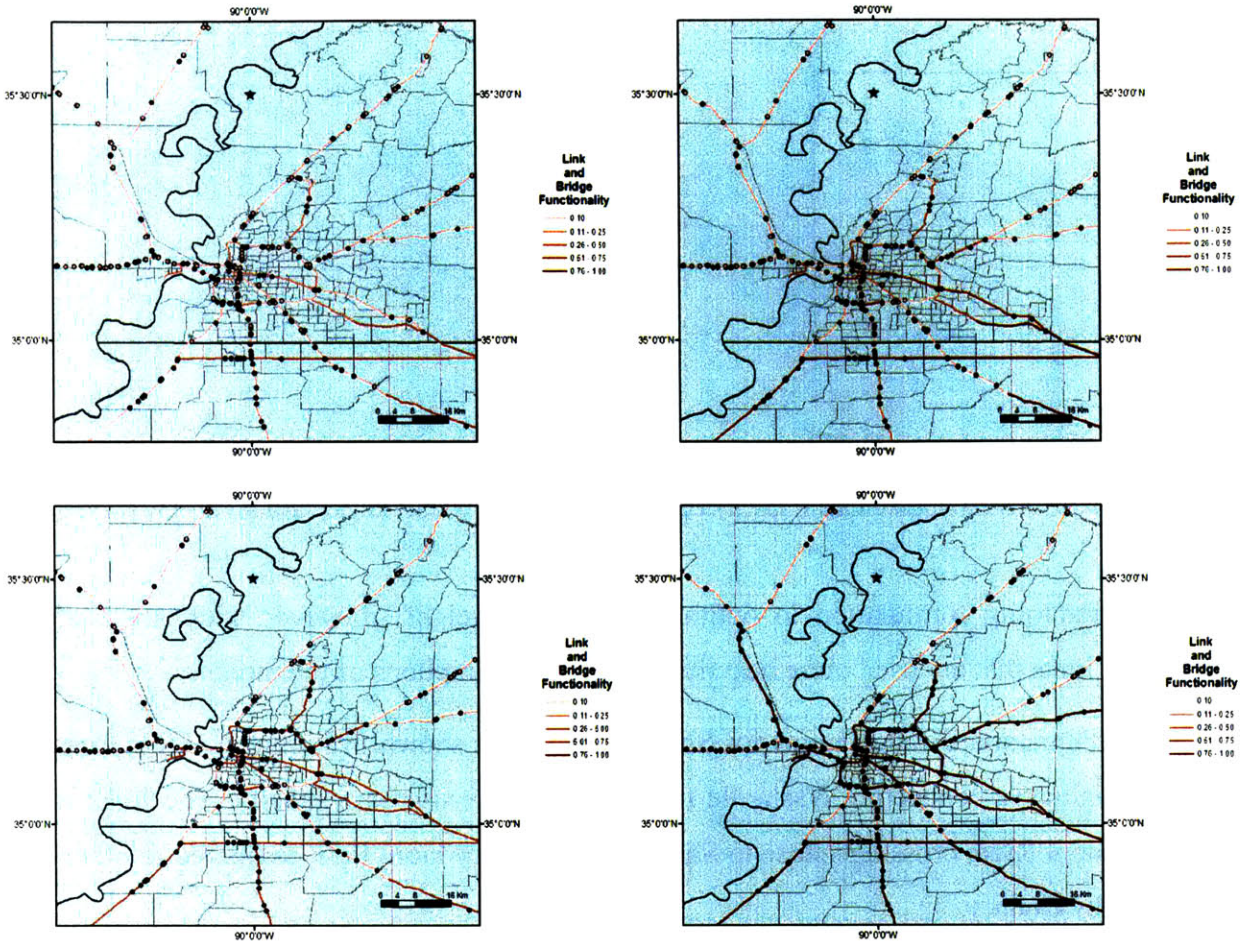

Figure 4-15: Functionality of Links around Shelby County at (a) Day 1, (b) Day 7, (c) Day 30, and (d) Day 180

damage. Therefore, links that have bridges in the complete damage state take longer to recover. For example, Figure 4-15(d) shows the functionality of bridges and links around Shelby County at day 180. One can observe that there are only a few bridges that control the functionality of the links on which they are located. These are the bridges with complete damage. The remaining bridges have already recovered and performing at full functionality at this time.

The capacity utilization ratios of the links around NMSZ, obtained from the transportation network-regional economic analysis for the pre-earthquake state, are shown in Figure 4-16. The links connecting Memphis, TN to Little Rock, AR and Nashville, TN are used up to capacity. These routes are the shortest ones between these densely populated regions and are used to carry most of the commodity flow between these cities. The capacity utilization ratios for other links in the region are generally less than 0.25. These flow ratios might not represent the actual flow ratios within the region since we do not include passenger flows in the analysis and we use a

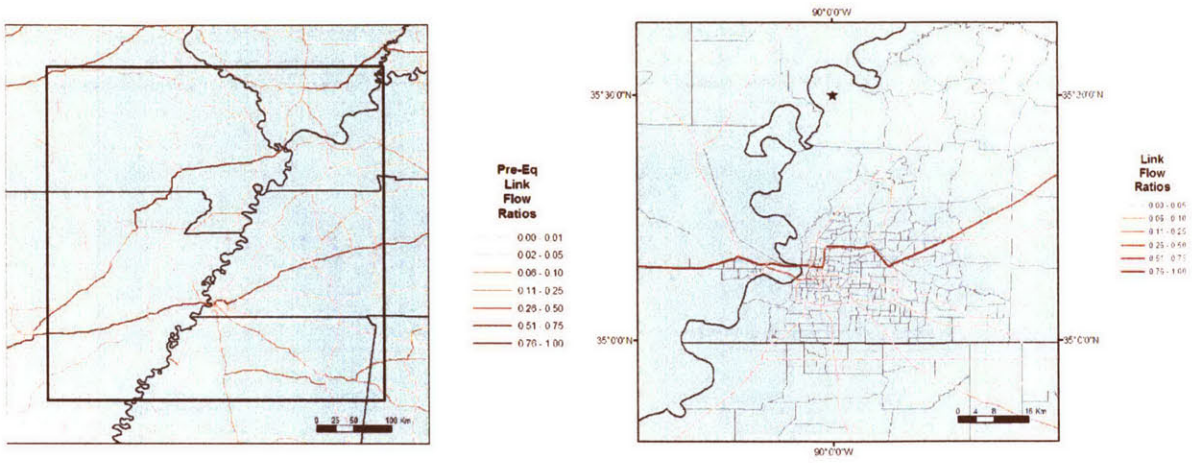

Figure 4-16: Pre-Earthquake Link Capacity Utilization around (a) NMSZ Region and (b) Shelby County

linear programming formulation to optimally transport freight. However, they are useful to identify the links that are used more heavily, within the assumptions of the model.

The pre-earthquake utilization ratios for Shelby County are shown in Figure 4-16(b). Again the interstate highways connecting Nashville to Little Rock are used at capacity. The links on the two Mississippi River crossings close to Shelby County carry more flow compared to other links within Shelby County.

The capacity utilization ratios for the links after the earthquake are shown in Figure 4-17. The capacity utilization ratios of links close to the epicenter increase, since their capacity is reduced due to heavier damage. Also, notice that the interstate highways within Shelby County, which were utilized up to capacity in the pre-earthquake state, are not fully utilized after the earthquake. This is mainly due to the damage to the Mississippi River Crossings and the links connecting Shelby County to Nashville and Little Rock. These links are damaged more than most links within Shelby County and recover slower (e.g. see Figure 4-14). The commodities that were transported through these routes are now transported through other routes. Therefore, the capacity utilization ratios for some of the links within Shelby County decrease. Another contributing factor is that the production of the economic sectors located around Shelby County decrease due to damage and fewer commodities are transported to and from the region. This reduced economic activity also results in a decrease in the link flows within Shelby County.

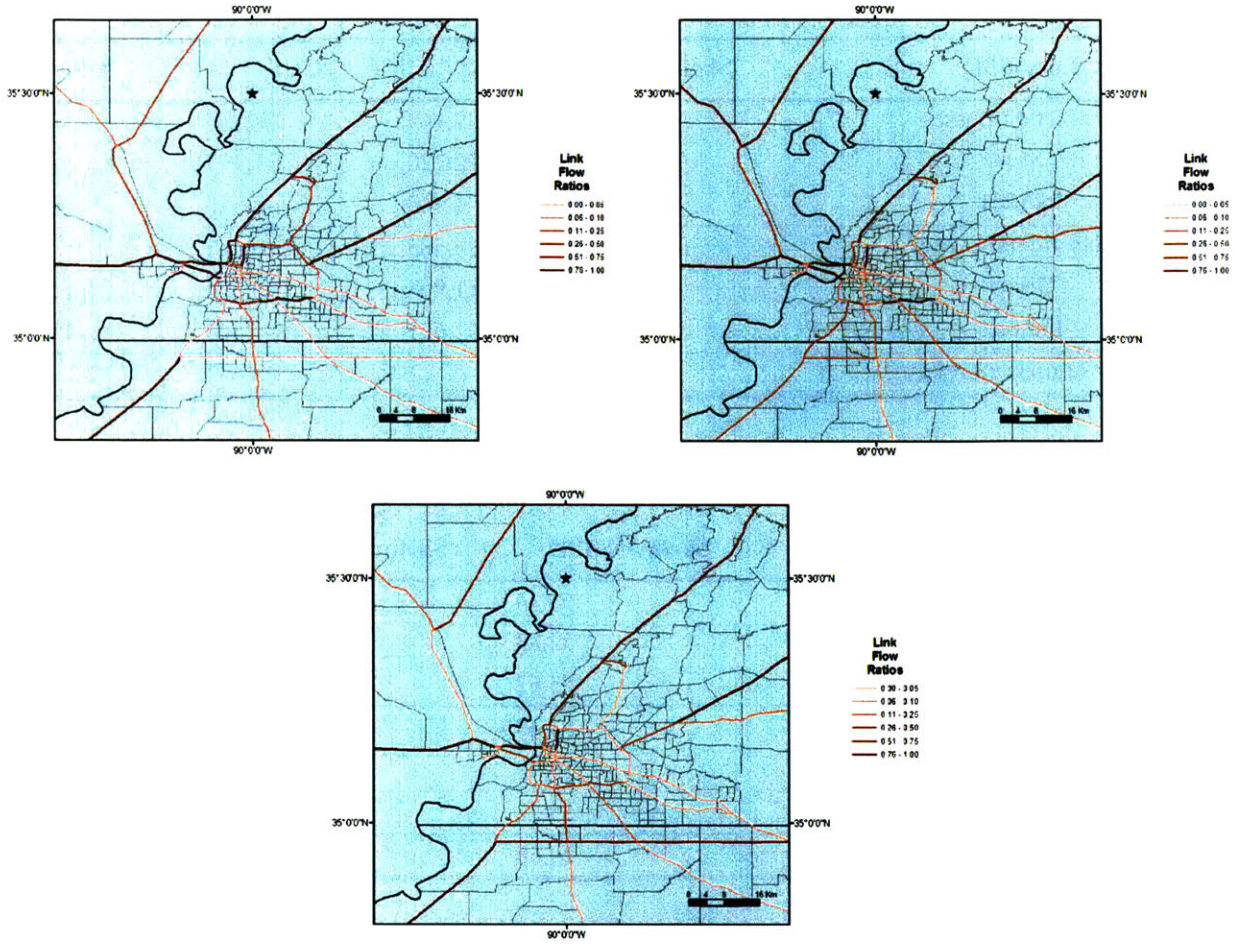

Figure 4-17: Link Capacity Utilization around Shelby County at (a) Day 1, (b) Day 7, and (c) Day 180

4.1.5 Economic Losses

The business losses for the chose scenario earthquake are listed in Table 4-4. The table includes losses resulting from decrease in production, value added, and consumption levels after the earthquake until full recovery. We report production losses as an indicator of reduced or increased economic activity in different regions after the earthquake. However, our main business loss indicator is the value added and the total loss from a scenario earthquake is the sum of value added losses and structure repair/restoration costs. The consumption losses indicate the amount of unsatisfied demand from households.

The total value added losses for Shelby County and NMSZ are $7.8B and $14.6B, respectively. Most of these losses are direct value added losses caused by damage to the facilities themselves. The indirect value added losses, which result from interactions among various economic sectors,

Table 4-4: Economic Losses for Scenario Earthquake

Loss ($M)	Shelby	NMSZ	CUS	US
Production Losses	14,490	27,164	26,867	-8,827
Direct	11,740	22,220	31,177	31,177
Indirect	2,750	4,944	-4,310	-40,004
Value Added Losses	7,789	14,585	15,447	-339
Direct	6,309	11,908	16,891	16,891
Indirect	1,480	2,677	-1,443	-17,230
Consumption Losses	3	13	33	80

Table 4-5: Percent Economic Losses for Scenario Earthquake

Loss ($M)	% Shelby/NMSZ	% Shelby/CUS	% NMSZ /CUS
Production Losses	53.34	53.93	101.10
Direct	52.83	37.65	71.27
Indirect	55.62	-63.80	-114.70
Value Added Losses	53.40	50.42	94.42
Direct	52.98	37.35	70.50
Indirect	55.28	-102.52	-185.46
Consumption Losses	19.68	7.97	40.51

account for about 20% of total value added losses. As in the case of building losses, about half of the value added losses in NMSZ are from Shelby County (see Table 4-5).

The total value added loss for the CUS region, $15.4B, is only slightly higher than that in the NMSZ region. For the CUS region, the indirect business losses are negative, indicating gains within this region. This is a result of the slack in the production capacities of the economic sectors. Specifically, after the earthquake, some regions within the CUS increase their production levels to make up for lost production in the heavily damaged regions resulting in economic gains. At the national level, the increased productions offset the direct value added losses, resulting in a gain of $-0.34B in total value added loss. The direct value added loss at the national level is $16.9B and the indirect value added loss is $-17.2B.

The overall gain in value added at the national level is a result of the slack in production, as mentioned above, and the reconstruction spending following the earthquake. In the absence of slack in production or in a fully constrained economy, the production losses in the damaged regions cannot be replaced by increasing production in other regions. In that case, the indirect

value added losses are positive, resulting in much higher total value added losses in the CUS and the US (see Section 4.2.14). For example, in the absence of slack in production, the indirect total value added loss in the US is $19.6B, resulting in a total value added loss of $35.7B. The actual loss from a scenario earthquake can be expected to be the losses obtained from these cases. In the present analysis, we have assumed a constant slack value of 5%, which can be used immediately following the earthquake. However, in reality, slack values for different sectors and regions differ. In addition, the extra production capacity may not be utilized immediately after the earthquake but it might come into effect gradually over time.

Finally, in the absence of reconstruction spending or when borrowing costs for reconstruction are introduced, the value added losses increase both locally and nationally. The total value added loss may become positive at the national level as opposed to the present analysis results, where a negative total value added loss indicating economic gains, is observed. (see Sections 4.2.12 and 4.2.13). For example, in the absence of reconstruction spending, the total value added loss in the US is $77M. Again slack in production results in economic gains for some regions but the gains are not large enough to offset the direct business losses.

4.2 Sensitivity analysis

Next, we investigate the sensitivity of the losses to alternative models and parameters in various parts of the loss estimation methodology. The main objective is to identify the models/variables that most significantly affect the results or contribute to the overall uncertainty in the loss. There are several reasons for doing this. First, the models/parameters that do not contribute much to the overall uncertainty can be excluded from more detailed uncertainty analysis, thus saving computational effort. Second, the important models/parameters may be studied or modeled in greater detail to obtain more accurate loss estimates.

To achieve these objectives, we perform a sensitivity analysis in which the losses are found under different assumptions. First, we analyze the system for a baseline scenario in which best estimate values of the models and parameters are used. Then, we re-analyze the system under various perturbed conditions. Comparison with the base case produces the desired sensitivities.

The baseline scenario selected is the moment magnitude M7.5 earthquake at (35.50°N, 90.00°W), which was used in the previous section. Table 4-6 lists the component models and

parameters used in the sensitivity analysis. In the table, the default models/parameters are indicated in bold. In the sensitivity analysis, we perturb, one at a time, the following parameters:

- Earthquake location
- Earthquake magnitude
- Attenuation relations
- Soil amplification
- Soil conditions
- Building code levels
- Expected mean building vulnerability
- Variation in expected mean building vulnerability
- Weights assigned to functionality of structural and nonstructural building components
- Functionality and recovery interactions
- Rerouting Parameter
- Total borrowing costs
- Slack in production capacity

4.2.1 Sensitivity to Earthquake Location

First, we present results on the sensitivity of the losses to earthquake location. We do so by comparing results from four M7.50 earthquakes, one at (36.00N, 90.00W) which is modeled as a point source as the baseline earthquake (Eq. B), and three others at the south ends of the three USGS faults, modeled as line sources with a rupture length of 97km (Eqs. C-E). The latter three earthquakes are the M7.5 events on each NMSZ fault that are most damaging to Shelby County. As previously mentioned, the baseline scenario earthquake is about 35km from the population centroid of Shelby County. The closest distance from the epicenter/fault rupture of the four additional scenario earthquakes to the population centroid of Shelby County is about 90km, 30km, 60km, and 85km, respectively. The losses obtained for these four scenario earthquakes are given in Tables 4-7 and 4-9.

Table 4-6: Component Models and Parameters Considered in Sensitivity Analysis

Model/Parameter	Alternative Models/Parameters Used
Earthquake Location	**35.50, 90.00**
	36.00, 90.00
	NMSZ, East Fault
	NMSZ, Center Fault
	NMSZ, West Fault
Earthquake Magnitude	**7.5**
	8.0
	7.0
	6.5
	6.0
Attenuation Relations	**Default weights used in 2002 USGS Maps**
	Atkinson and Boore, 1995
	Frankel et al, 1996
	Toro et al, 1997
	Somerville et al, 2001
	Campbell, 2003
Site Amplification Factors	**Dobry et al (2000)**
	Hwang et al (1997)
	Borcherdt et al (2002)
Soil Class	**CUSEC Maps**
	Class C
	Class D
	Class E
Building Code Level	**Default Mapping for Shelby County**
	100% Pre-Code Construction
	100% Low-Code Construction
	100% Moderate-Code Construction
Expected Value of Mean of Building Vulnerability Curves	**Nominal (Derived from HAZUS)**
	Nominal + 0.25 Standard Deviation
	Nominal - 0.25 Standard Deviation

Table 4-6 (Cont.): Component Models and Parameters Considered in Sensitivity Analysis

Model/Parameter	Alternative Models/Parameters Used
Standard Deviation of Mean Of Building Vulnerability Curves	**Nominal (Derived from HAZUS)** Nominal + 25% Nominal Nominal + 25% Nominal
Weights Assigned to Structural And Nonstructural Components In Calculation of Functionality	**(100.0, 0.0, 0.0, 0.0)** (70.0, 10.0, 10.0, 10.0) (70.0, 30.0, 0.0, 0.0) (70.0, 0.0, 30.0, 0.0) (70.0, 0.0, 0.0, 30.0)
Functionality and Recovery Interaction (All sectors)	**Both Functionality And Recovery Interactions** No interaction Only Functionality Interactions Only Recovery Interactions
Functionality and Recovery Interaction (Individual sectors)	**Functionality And Recovery Interactions All Sectors** Only residential sector Only intra-nodal transportation Only utilities No dependence on residential sector No dependence on intra-nodal transportation No dependence on utilities
Highway Network Rerouting Parameter	**0.10** 0.05 0.01
Reconstruction Spending	Yes No
Total Borrowing Cost	**0.00** 0.01 0.03 0.05 0.10
Available Slack	**0.05** 0.02 0.01 0.00

Table 4-7: Sensitivity of Building Losses to Earthquake Location

Building Loss ($M)	Earthquake Location				
	35.50N* -90.00W	36.00N -90.00W	NMF-E 0.0-97.0	NMF-C 0.0-97.0	NMF-W 0.0-97.0
Shelby County					
Building Losses	11,740	4,109	12,649	6,929	4,804
Structural	2,238	809	2,409	1,305	918
Non-Str. Drift Sensitive	4,394	1,521	4,782	2,501	1,751
Non-Str. Acceleration Sensitive	5,109	1,780	5,458	3,123	2,134
Contents	4,480	1,570	4,775	2,741	1,877
NMSZ					
Building Losses	21,656	14,271	28,048	22,195	20,758
Structural	4,307	2,968	5,620	4,556	4,356
Non-Str. Drift Sensitive	8,290	5,601	11,021	8,821	8,542
Non-Str. Acceleration Sensitive	9,060	5,702	11,407	8,818	7,861
Contents	7,982	5,050	10,048	7,791	6,961
CUS					
Building Losses	24,206	17,026	32,480	26,820	25,557
Structural	5,045	3,775	6,779	5,759	5,606
Non-Str. Drift Sensitive	9,458	6,863	12,951	10,826	10,621
Non-Str. Acceleration Sensitive	9,703	6,388	12,750	10,235	9,330
Contents	8,553	5,656	11,240	9,048	8,262

Table 4-8: Sensitivity of Bridge Losses to Earthquake Location

Bridge Loss ($M)	Earthquake Location				
	35.50N* -90.00W	36.00N -90.00W	NMF-E 0.0-97.0	NMF-C 0.0-97.0	NMF-W 0.0-97.0
Bridge Losses (Network)	269	108	428	253	178
Bridge Losses (HAZUS)	222	180	358	322	304

Table 4-9: Sensitivity of Economic Losses to Earthquake Location

Business Loss ($M)	Earthquake Location				
	35.50N -90.00W	36.00N -90.00W	NMF-E 0.0-97.0	NMF-C 0.0-97.0	NMF-W 0.0-97.0
Shelby					
Production Losses	14,490	4,909	15,732	7,572	5,287
Direct	11,740	4,029	12,734	6,188	4,337
Indirect	2,750	880	2,997	1,384	951
Value Added Losses	7,789	2,662	8,454	4,076	2,858
Direct	6,309	2,180	6,845	3,328	2,341
Indirect	1,480	482	1,609	747	518
Consumption Losses	3	3	2	3	3
NMSZ					
Production Losses	27,164	18,404	35,626	27,193	25,479
Direct	22,220	15,005	28,751	21,789	20,386
Indirect	4,944	3,399	6,875	5,404	5,093
Value Added Losses	14,585	9,860	19,067	14,476	13,565
Direct	11,908	8,030	15,390	11,621	10,868
Indirect	2,677	1,830	3,678	2,855	2,697
Consumption Losses	13	14	12	14	13
CUS					
Production Losses	26,867	23,150	37,485	30,872	30,549
Direct	31,177	25,597	40,580	34,013	33,769
Indirect	-4,310	-2,448	-3,094	-3,141	-3,220
Value Added Losses	15,447	13,280	21,207	17,478	17,361
Direct	16,891	13,951	21,946	18,398	18,291
Indirect	-1,443	-671	-739	-920	-930
Consumption Losses	33	34	29	34	31
US					
Production Losses	-8,827	-5,886	-12,107	-9,724	-9,291
Direct	31,177	25,597	40,580	34,013	33,769
Indirect	-40,004	-31,483	-52,686	-43,736	-43,060
Value Added Losses	-339	-190	-512	-364	-349
Direct	16,891	13,951	21,946	18,398	18,291
Indirect	-17,230	-14,141	-22,458	-18,763	-18,640
Consumption Losses	80	82	68	81	76

Table 4-7 lists the building losses for Shelby County, and the NMSZ and CUS regions. Two main factors determine the relative values of these losses. One is the epicentral/fault rupture distance to Shelby County, where most of the building inventory in the near-field region is located. The other is whether the scenario earthquake is modeled as a point or line source. Losses are higher for line sources as there is a greater amount of inventory close to the fault rupture compared to a point source.

The CUS building losses for the three NMSZ fault earthquakes are higher than those for the baseline scenario earthquake B, which is treated as a point source. The highest losses are obtained for Eq. C, whose fault rupture is closest to Shelby County. The lowest losses are caused by Eq. B. The results building losses in NMSZ are similar, except that the baseline scenario causes more damage than earthquakes D and E as it is closer to Shelby County. The building losses for Shelby County are again highest for Eq. C and the baseline scenario. The lowest losses are again obtained for scenario Eq. B.

The distribution of total building loss with epicentral distance is shown in Figure 4-18. The maximum occurs in the distance range that includes Shelby County, i.e. 20-50 km for the baseline scenario and Eq. C, 50-100km for scenario D, and 50-150km for Eqs. B and E. The building losses normalized by the total inventory value are shown in Figure 4-19. These normalized losses are approximately the same for all scenario earthquakes, the differences being due to varying soil conditions and building inventory composition in the vicinity of each earthquake.

The economic losses for the four scenario earthquakes for Shelby County, NMSZ, CUS, and US are summarized in Table 4-9. The distribution of value-added losses and normalized value-added losses for different distance ranges are shown in Figures 4-26 and 4-27. The observations made about the relative building losses caused by different scenario earthquakes are generally valid also for production (especially direct production) and value added losses, since they are mainly determined by the recovery time of the economic sectors, which in turn depends mostly on the level of building damage. The highest economic losses for Shelby County, NMSZ and CUS are obtained for scenario Eq. C and the lowest for Eq. B. Exceptions to these general observations are the indirect losses in the CUS and US, as productions in these regions increase by utilizing the available slack to make up for lost production in the immediate vicinity of the earthquakes,

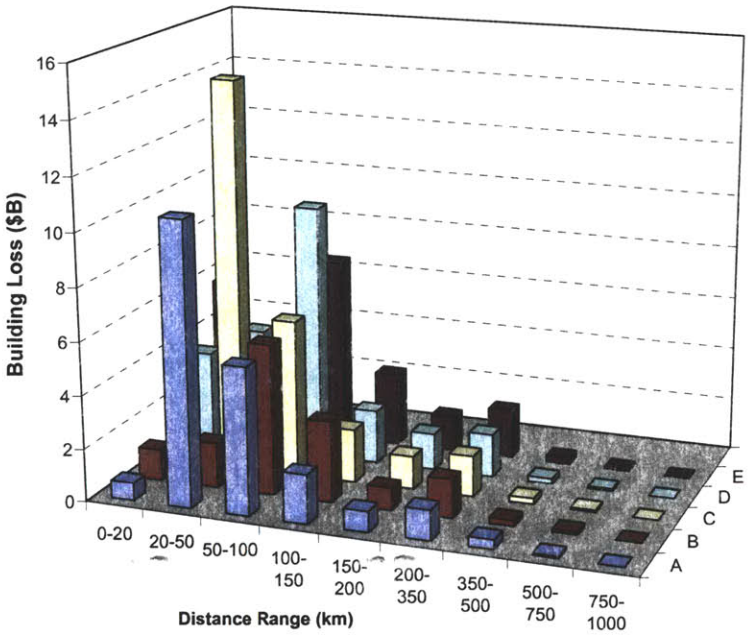

Figure 4-18: Distribution of Building Losses with Distance for Different Scenario Earthquakes

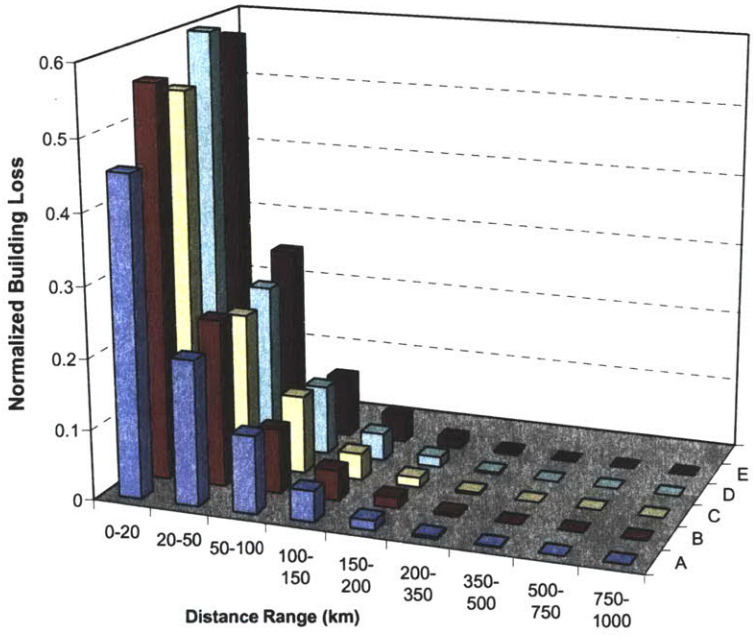

Figure 4-19: Distribution of Normalized Building Losses with Distance for Different Scenario Earthquakes

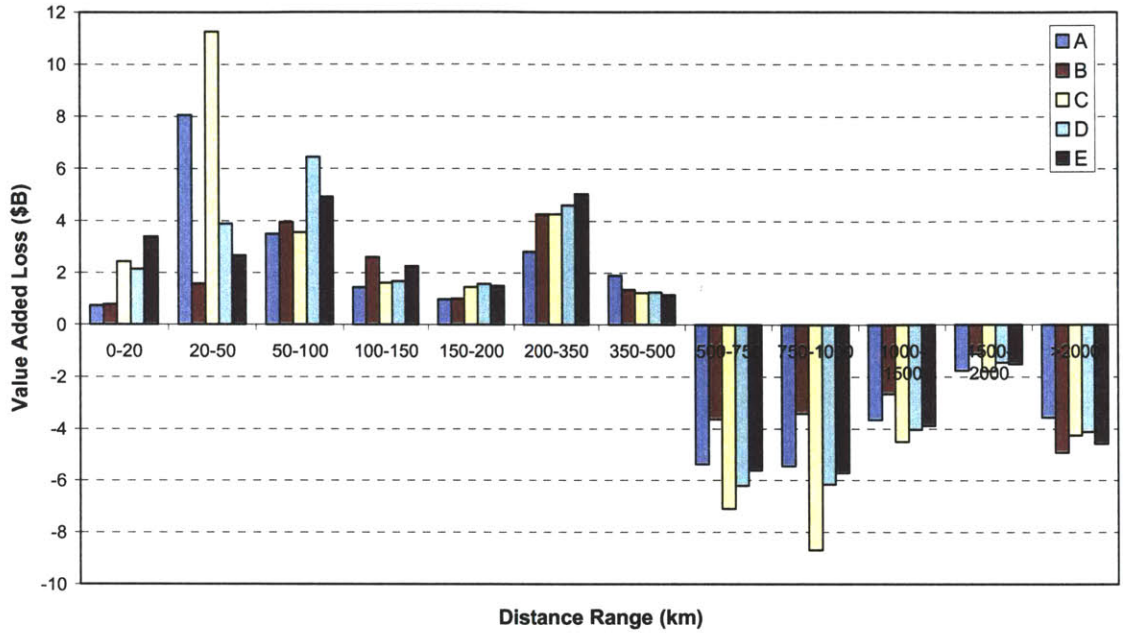

Figure 4-20: Distribution of Value Added Losses with Distance for Different Scenario Earthquakes

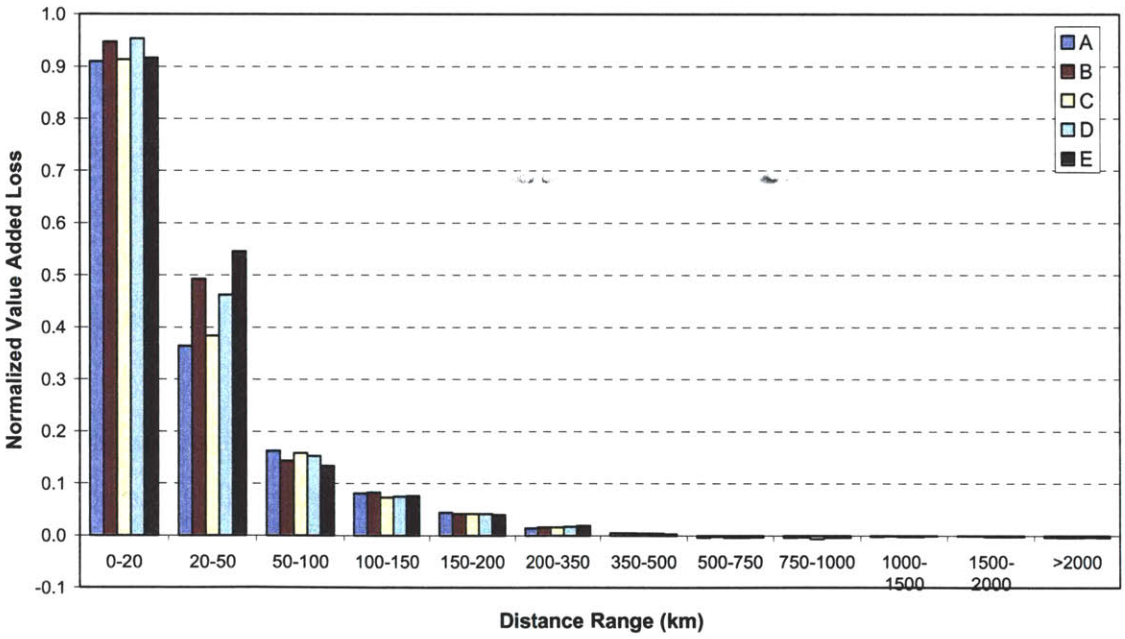

Figure 4-21: Distribution of Normalized Value Added Losses with Distance for Different Scenario Earthquakes

i.e. in Shelby County, NMSZ, and in parts of the CUS closer to the earthquake epicenter. From Figures 4-20 and 4-21 one can see that the value added losses are negative for regions farther than 500km from the epicenter. These negative losses correspond to gains. The economic gains in these regions offset some of the economic losses in the epicentral region. The net effect is a reduction in the losses relative to those of NMSZ and CUS and even increases in value added for the entire US.

4.2.2 Sensitivity to Earthquake Magnitude

To analyze the sensitivity to earthquake magnitude, we consider five earthquakes with moment magnitudes ranging from M6.0 to M8.0, including the baseline scenario with M7.5. All earthquakes have the same epicenter and are modeled as point sources. The resulting building and economic losses in different regions are listed in Tables 4-10 to 4-12.

The building losses for the CUS region range from $2.2B to $32.5B. For magnitude M6.0, 65% of the building losses originate from Shelby County, with the NMSZ region accounting for 99% of all the building losses originated from CUS. The percentage contribution of Shelby county and NMSZ for the M8.0 event drops to 45% and 87%, respectively, due to additional damage outside the NMSZ region from this larger event. For all magnitudes, losses from acceleration sensitive non-structural components are higher than those from structural and drift sensitive non-structural components. However, the relative contribution of acceleration sensitive nonstructural components to the overall building loss is much larger for smaller magnitude events. For example, these components account for approximately 70% of the total building losses for a M6.0 event and only 42% of the total building losses for the M8.0 event.

Figures 4-22 and 4-23 show the distribution of building losses and normalized building losses for different distance ranges. For the M6.0 event, buildings farther than 150km from the epicenter sustain no damage, whereas the damaged region extends as far as 750 km for the M8.0 event. The normalized building losses in the immediate vicinity of the earthquake epicenter range from 0.15 to 0.65 for different earthquake magnitudes. In the 20-50km range in which Shelby County is located, the mean loss ratio changes from 0.03 to 0.27.

The economic losses for different regions are provided in Table 4-12. The value added losses for Shelby county range between $1.0Billion and $11.4Billion for different magnitudes. The value

Table 4-10: Sensitivity of Building Losses to Earthquake Magnitude

Building Loss ($M)	Earthquake Magnitude				
	6.00	6.50	7.00	7.50	8.00
Shelby County					
Building Losses	1,545	4,202	7,132	11,740	15,698
Structural	202	629	1,176	2,238	3,129
Non-Str. Drift Sensitive	398	1,283	2,342	4,394	6,306
Non-Str. Acceleration Sensitive	945	2,290	3,613	5,109	6,263
Contents	833	2,013	3,173	4,480	5,486
NMSZ					
Building Losses	2,583	6,948	12,259	21,656	30,908
Structural	368	1,121	2,142	4,307	6,461
Non-Str. Drift Sensitive	715	2,239	4,209	8,290	12,572
Non-Str. Acceleration Sensitive	1,500	3,589	5,908	9,060	11,875
Contents	1,326	3,164	5,206	7,982	10,463
CUS					
Building Losses	2,627	7,185	13,038	24,206	36,843
Structural	388	1,211	2,402	5,045	8,037
Non-Str. Drift Sensitive	737	2,354	4,581	9,458	15,205
Non-Str. Acceleration Sensitive	1,502	3,620	6,055	9,703	13,600
Contents	1,329	3,192	5,337	8,553	11,995

Table 4-11: Sensitivity of Bridge Losses to Earthquake Magnitude

Bridge Loss ($M)	Earthquake Magnitude				
	6.00	6.50	7.00	7.50	8.00
Bridge Losses (Network)	2	17	69	269	443
Bridge Losses (HAZUS)	3	21	77	222	435

Table 4-12: Sensitivity of Economic Losses to Earthquake Magnitude

Loss ($M)	Earthquake Magnitude				
	6.00	6.50	7.00	7.50	8.00
Shelby					
Production Losses	1,791	4,325	7,676	14,490	21,248
Direct	1,470	3,500	6,269	11,740	16,962
Indirect	321	826	1,407	2,750	4,287
Value Added Losses	995	2,363	4,154	7,789	11,409
Direct	814	1,912	3,391	6,309	9,120
Indirect	181	451	763	1,480	2,289
Consumption Losses	2	3	3	3	2
NMSZ					
Production Losses	3,322	8,266	14,318	27,164	40,530
Direct	2,929	6,683	11,738	22,220	32,682
Indirect	393	1,583	2,580	4,944	7,848
Value Added Losses	1,854	4,507	7,738	14,585	21,668
Direct	1,619	3,647	6,345	11,908	17,476
Indirect	234	860	1,394	2,677	4,192
Consumption Losses	12	16	13	13	11
CUS					
Production Losses	1,714	7,832	13,488	26,867	47,015
Direct	3,465	8,569	15,977	31,177	48,670
Indirect	-1,751	-737	-2,489	-4,310	-1,656
Value Added Losses	1,159	4,516	7,809	15,447	26,383
Direct	1,924	4,707	8,717	16,891	26,314
Indirect	-765	-191	-908	-1,443	69
Consumption Losses	30	40	32	33	28
US					
Production Losses	-771	-2,348	-4,551	-8,827	-13,795
Direct	3,465	8,569	15,977	31,177	48,670
Indirect	-4,236	-10,916	-20,527	-40,004	-62,465
Value Added Losses	31	-18	-136	-339	-625
Direct	1,924	4,707	8,717	16,891	26,314
Indirect	-1,894	-4,726	-8,852	-17,230	-26,939
Consumption Losses	72	97	78	80	69

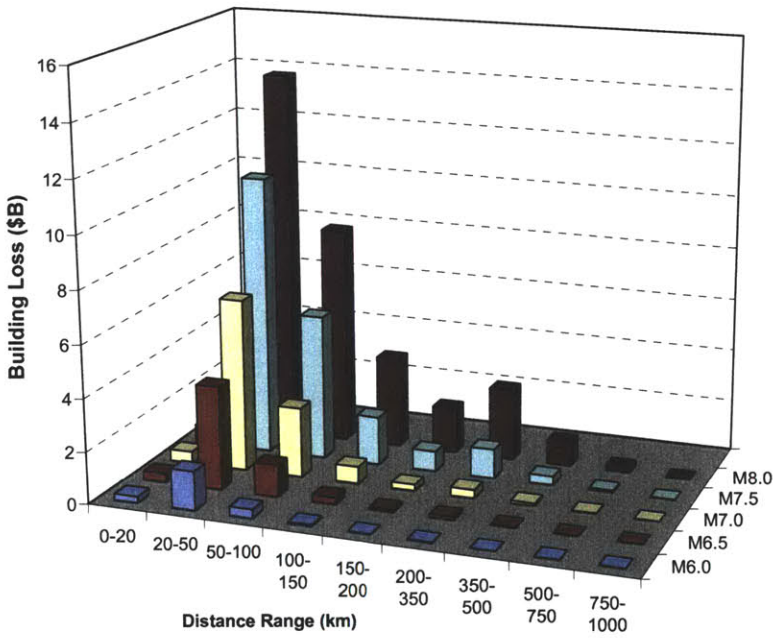

Figure 4-22: Distribution of Building Losses with Distance for Different Earthquake Magnitudes

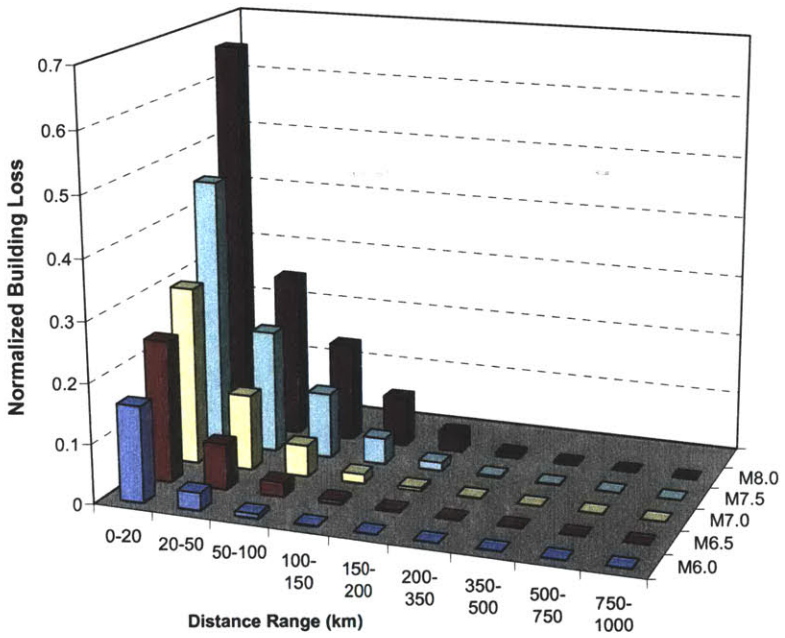

Figure 4-23: Distribution of Normalized Building Losses with Distance for Different Earthquake Magnitudes

added losses for NMSZ are about twice the losses from Shelby County. The value added losses for CUS depend on the extent of damage and the resulting reduction in functionality. For example, for the M6.0 event the value added loss in CUS is less than that in NMSZ as CUS regions surrounding NMSZ make up for the productions in the locally damaged region. For magnitudes M6.0 to M7.5, we observe a gain in indirect value added in CUS. But for M8.0, we continue to observe a loss in indirect value added loss due to greater extent of damage and loss of functionality. These can also be observed from the direct and total value added losses provided in Figure 4-24 and Figure 4-25. The direct value added losses extend only up to 500km for a M6.0 scenario, whereas for the M8.0 scenario these losses extend to 1000km. The normalized value added loss in Figure 4-26 shows that in the immediate vicinity of the earthquake this quantity ranges between 30% and 105% of the annual value added. In the 20-50 km distance range in which Shelby County is located, the normalized value added loss decreases to 5% to 50% of the annual value added for events of magnitude M6.0 and M8.0. For other magnitudes, the normalized value added losses are intermediate between these values.

4.2.3 Sensitivity to Ground Motion Attenuation

The sensitivity of earthquake losses to ground motion attention is studied by considering the five attenuation relations used in the 2002 USGS National Seismic Hazard Maps; see Section 3-4. Economic losses from the base-case earthquake using these attenuation relations are given in Tables 4-13 to 4-15.

Figures 4-27 and 4-28 show the distribution of building and normalized building losses for the different attenuation relationships. At almost all distance ranges, the highest building losses are obtained from the Frankel et al (1996) relationship followed by Somerville et al (2001). In the 50-100km distance range, the losses from Somerville et al (2001) slightly exceed those from Frankel et al (1996). The lowest building losses are obtained from the Atkinson and Boore (1995) and Toro et al (1997) relations. The losses from Campbell (2003) are intermediate between these two sets of relationships. The normalized losses in the 0-20km range vary between 35% and 63%. The same percentages for the 20-50km distance range in which Shelby County is located are 17% and 25%. The normalized losses decrease to less than about 1% in the 200-350 km range. However, the difference in building losses in this distance range is still significant, due

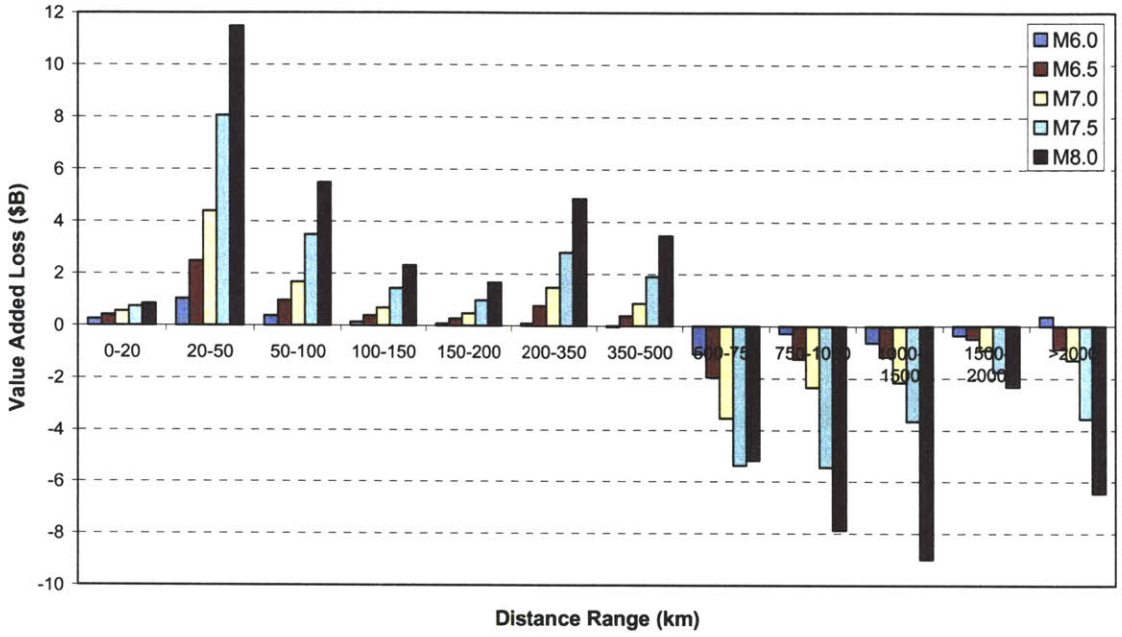

Figure 4-24: Distribution of Value Added Losses with Distance for Different Earthquake Magnitudes

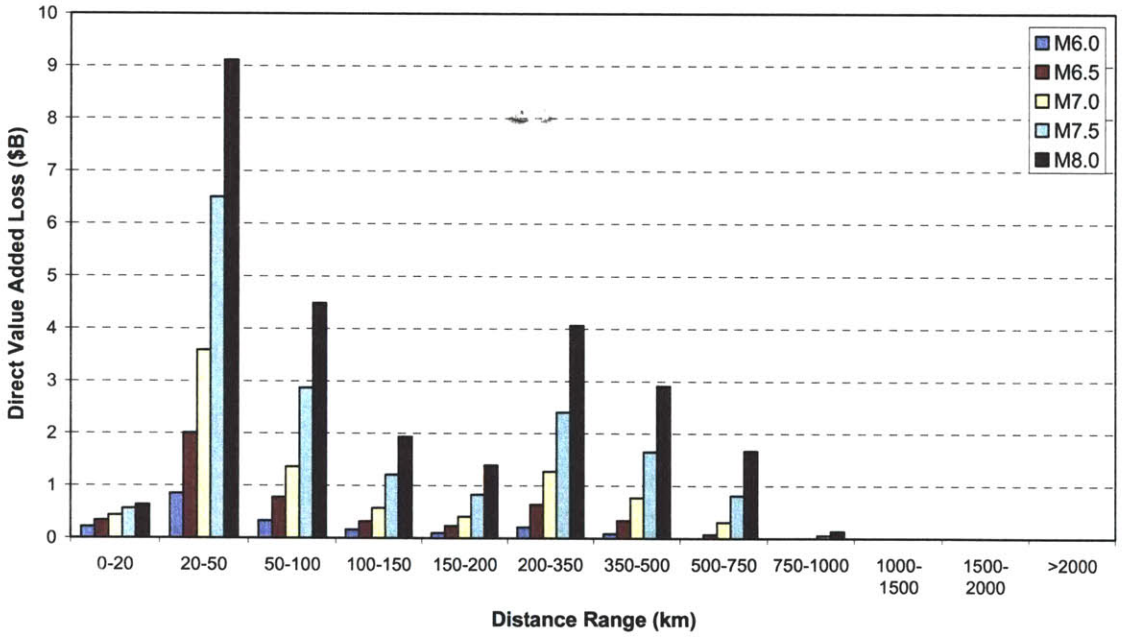

Figure 4-25: Distribution of Direct Value Added Losses with Distance for Different Earthquake Magnitudes

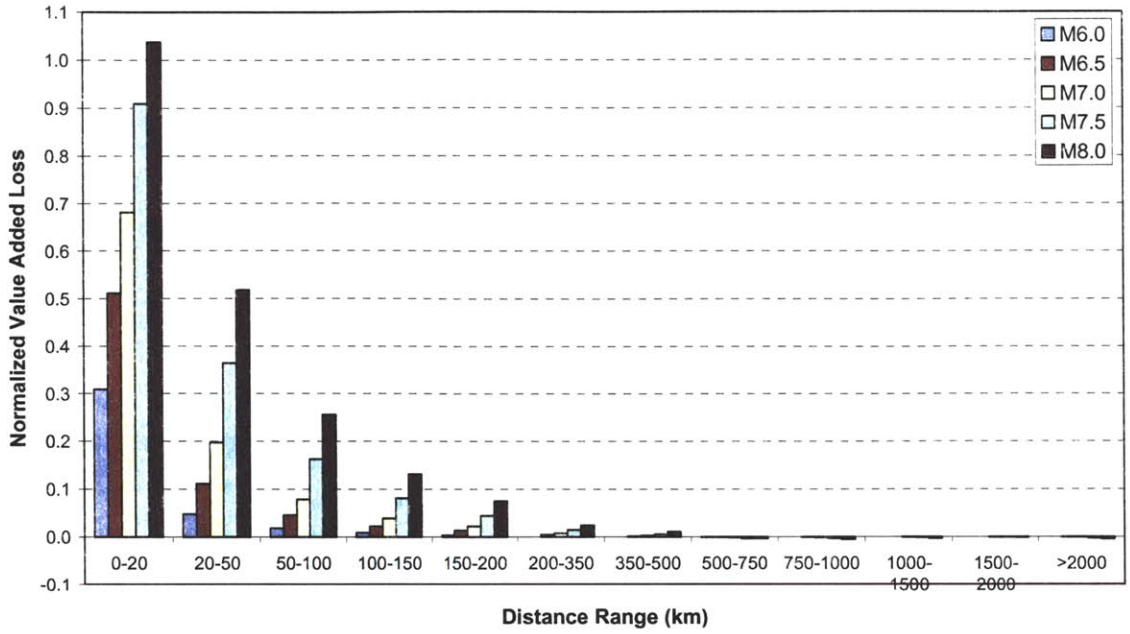

Figure 4-26: Distribution of Normalized Value Added Losses with Distance for Different Earthquake Magnitudes

to the large inventory. For example, the building losses from Frankel et al (1996) in this distance range ($2.7B) are about 7 times those from the Toro et al (1997) relation ($0.4B).

There are significant differences in the total losses in CUS, NMSZ, and Shelby County when using different attenuation relations (see Table 4-13). The building losses in CUS obtained using Somerville et al (2001) and Frankel et al (1996) are about 55% to 75% higher than those from Atkinson and Boore (1995) and Toro et al (1997). In Shelby County, the percent differences in losses from these two sets of attenuation relations decrease to 35% to 40%. The losses in CUS for Campbell (2003) are about 35% higher than those from the latter two attenuation relations.

The business losses for different attenuation relations generally follow the trends observed for building losses (see Table 4-15). The total value added losses for Shelby County range between $6.2B and $9.8B. The lowest value added losses are obtained from Atkinson and Boore (1995), except for CUS. Toro et al (1997) results in the lowest value added loss for CUS. The highest business losses are obtained from Frankel et al (1996) for all regions. The distribution of value added and normalized value added losses for different attenuation relationships are shown in

Table 4-13: Sensitivity of Building Losses to Attenuation Relations

Building Loss ($M)	Attenuation Relation				
	AB'95	F'96	T'97	S'01	C'03
Shelby County					
Building Losses	10,160	13,972	10,576	13,907	11,862
Structural	1,641	2,749	2,195	2,599	2,267
Non-Str. Drift Sensitive	3,336	5,480	4,222	5,376	4,428
Non-Str. Acceleration Sensitive	5,182	5,743	4,159	5,933	5,166
Contents	4,544	5,033	3,649	5,195	4,531
NMSZ					
Building Losses	17,798	28,121	18,119	27,095	22,666
Structural	2,987	5,833	3,883	5,058	4,534
Non-Str. Drift Sensitive	6,021	11,266	7,347	10,297	8,665
Non-Str. Acceleration Sensitive	8,790	11,022	6,889	11,740	9,467
Contents	7,740	9,714	6,068	10,343	8,342
CUS					
Building Losses	19,722	33,793	18,947	30,125	26,264
Structural	3,595	7,327	4,148	5,768	5,515
Non-Str. Drift Sensitive	6,939	13,773	7,744	11,516	10,258
Non-Str. Acceleration Sensitive	9,188	12,693	7,054	12,841	10,492
Contents	8,092	11,199	6,215	11,320	9,252

Table 4-14: Sensitivity of Bridge Losses to Attenuation Relations

Bridge Loss ($M)	Attenuation Relation				
	AB'95	F'96	T'97	S'01	C'03
Bridge Losses (Network)	85	372	277	260	288
Bridge Losses (HAZUS)	91	378	229	204	262

Table 4-15: Sensitivity of Economic Losses to Attenuation Relations

Loss ($M)	Attenuation Relation				
	AB'95	F'96	T'97	S'01	C'03
Shelby					
Production Losses	11,556	18,207	13,035	15,393	15,417
Direct	9,414	14,601	10,548	12,478	12,422
Indirect	2,142	3,606	2,486	2,915	2,995
Value Added Losses	6,244	9,776	6,979	8,275	8,282
Direct	5,090	7,847	5,646	6,711	6,678
Indirect	1,155	1,929	1,333	1,564	1,604
NMSZ					
Production Losses	20,598	35,944	23,695	29,380	29,547
Direct	16,674	29,045	19,281	23,882	23,919
Indirect	3,924	6,899	4,413	5,498	5,629
Value Added Losses	11,103	19,216	12,667	15,749	15,828
Direct	8,997	15,530	10,305	12,804	12,816
Indirect	2,106	3,686	2,361	2,945	3,012
CUS					
Production Losses	22,604	41,398	19,040	25,760	31,544
Direct	25,564	43,692	23,171	30,954	34,994
Indirect	-2,960	-2,294	-4,131	-5,194	-3,450
Value Added Losses	13,067	23,295	10,917	14,857	17,966
Direct	13,997	23,618	12,484	16,767	18,982
Indirect	-930	-323	-1,567	-1,910	-1,016
US					
Production Losses	-7,020	-12,460	-6,959	-11,184	-9,577
Direct	25,564	43,692	23,171	30,954	34,994
Indirect	-32,584	-56,152	-30,131	-42,138	-44,570
Value Added Losses	-234	-523	-253	-460	-378
Direct	13,997	23,618	12,484	16,767	18,982
Indirect	-14,231	-24,141	-12,737	-17,227	-19,360

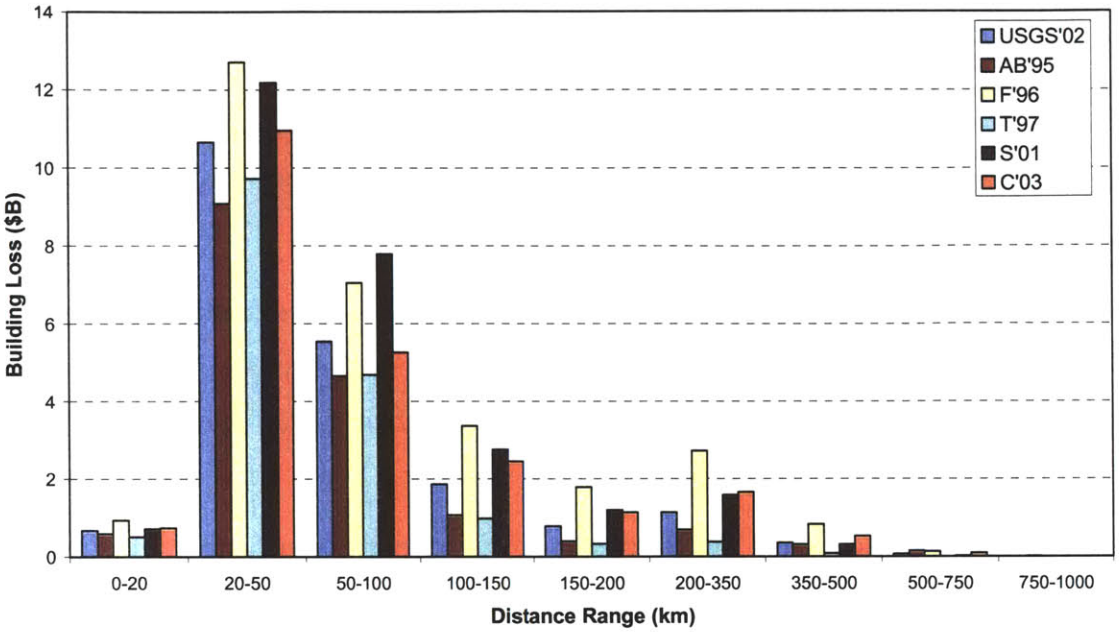

Figure 4-27: Distribution of Building Losses with Distance for Different Attenuation Relations

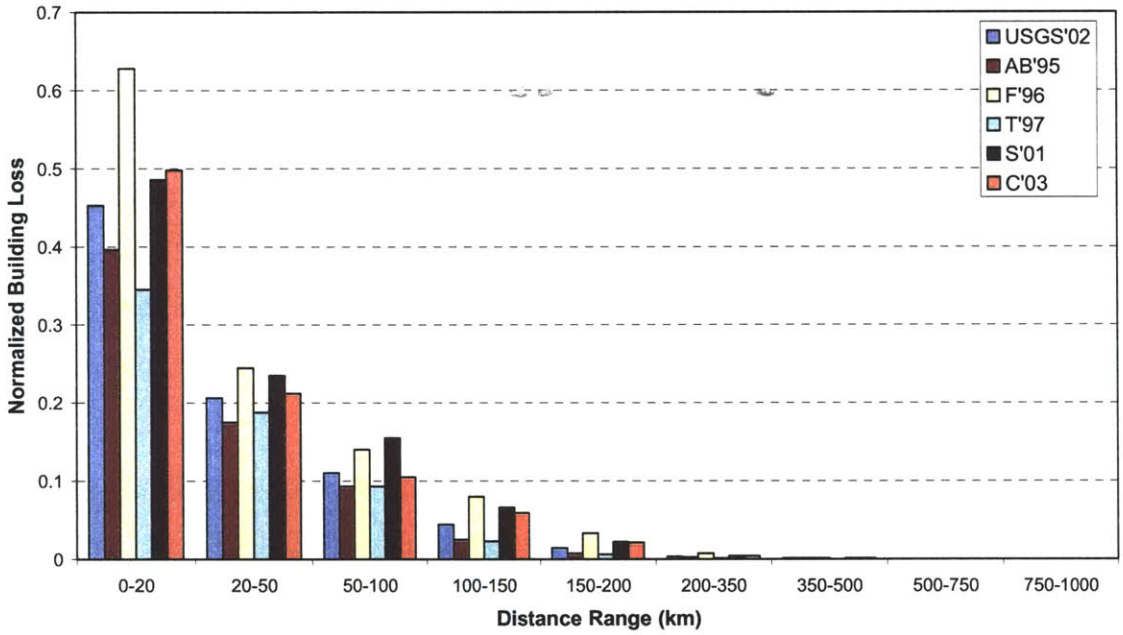

Figure 4-28: Distribution of Normalized Building Losses with Distance for Different Attenuation Relations

Figures 4-29 and 4-30. Again, the general trends are similar to those of building losses at distances where building damage is observed.

4.2.4 Sensitivity to Site Amplification

In this section, we study the sensitivity of the building and business losses to the soil amplification factors using the Borcherdt (2002), Hwang et al (1997), and Dobry et al (2000) models. Tables 4-16 and 4-18 summarize the calculated losses.

The Hwang et al (1997) soil amplification factors produce the highest building losses; see Table 4-16. These losses are about 25-30% higher than those from Dobry et al (2000). In fact, at all intensity levels the soil amplification factors of Hwang et al are higher than those of Dobry et al for site classes C, D, and E (see Chapter 3).

The building losses when using the Borcherdt (2002) amplification factors are slightly higher than those from Dobry et al (2000), by about 2-3% in NMSZ and CUS and about 10% in Shelby County. The amplification factors of Borcherdt (2002) are higher than those of Dobry et al (2000) for site classes C and D but they are lower for site class E. Hence, the dominant soil condition in the analysis region significantly affects the comparison of these two amplification models.

In the case of Hwang et al (1997), about half of the difference in building loss comes from drift sensitive nonstructural components as these losses are about 40-50% higher than in the baseline scenario. Structural and acceleration sensitive nonstructural components are 28-34% and 14-16% higher, respectively, and each constitutes about 25% of the difference in building losses. In the case of Borcherdt (2002), the percent increases in different building loss components are about the same, 8-12% in Shelby County and 2-3% in NMSZ and CUS.

Figures 4-31 and 4-32 show the distribution of building and normalized building losses for the soil amplification models considered. Most of the differences in building losses among the soil amplification models arise from Shelby County, which is located in 20-50km epicentral distance range. The normalized losses in this distance range are between 20% and 27%. In the 0-20km distance range the differences in the normalized losses are much higher, ranging from 40% to 75%, but the contribution to the overall loss is not large due to the small inventory.

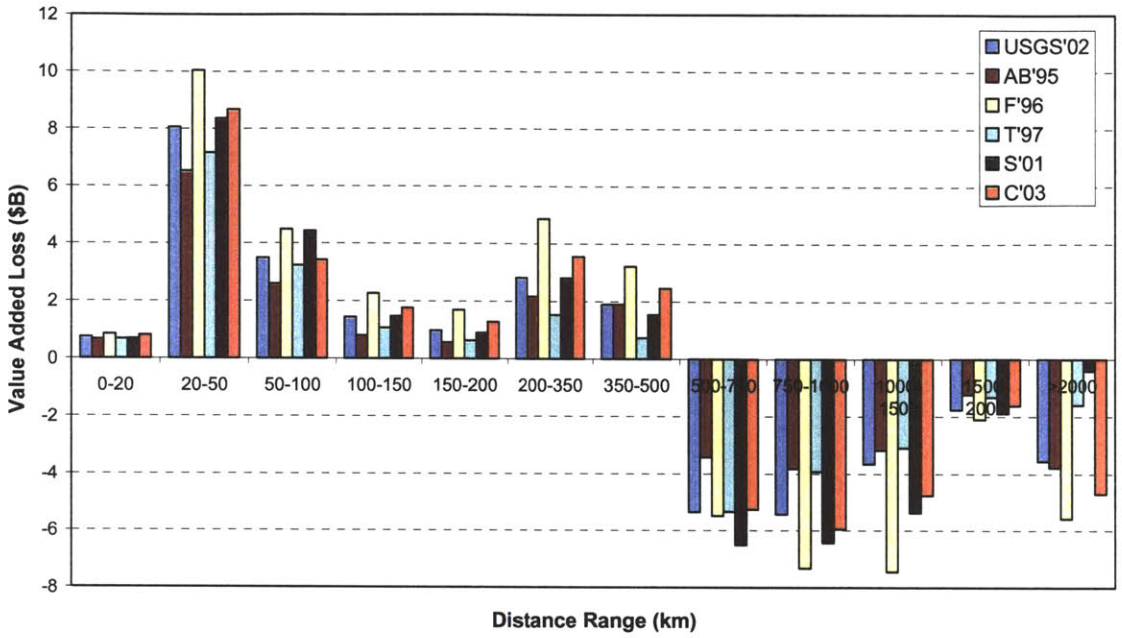

Figure 4-29: Distribution of Value Added Losses with Distance for Different Attenuation Relations

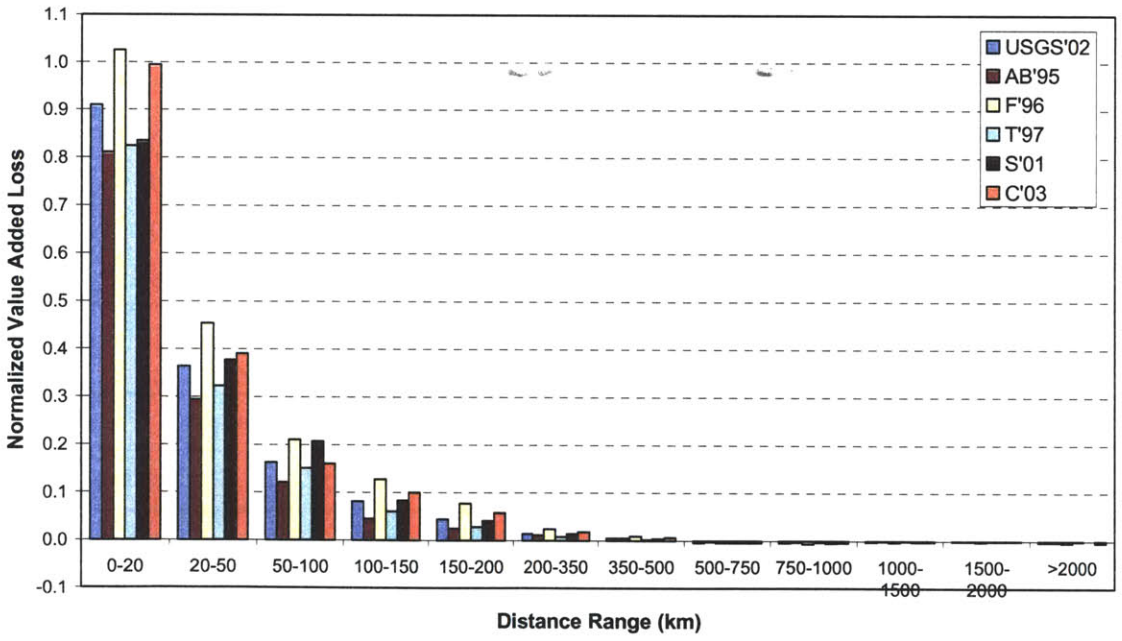

Figure 4-30: Distribution of Normalized Value Added Losses with Distance for Different Attenuation Relations

Table 4-16: Sensitivity of Building Losses to Soil Amplification

Building Loss ($M)	Soil Amplification Model		
	Hwang	Dobry*	Borcherdt
Shelby County			
Building Losses	14,928	11,740	12,836
Structural	3,009	2,238	2,413
Non-Str. Drift Sensitive	6,024	4,394	4,848
Non-Str. Acceleration Sensitive	5,895	5,109	5,575
Contents	5,167	4,480	4,882
NMSZ			
Building Losses	26,728	21,656	22,169
Structural	5,534	4,307	4,344
Non-Str. Drift Sensitive	10,849	8,290	8,476
Non-Str. Acceleration Sensitive	10,345	9,060	9,350
Contents	9,112	7,982	8,227
CUS			
Building Losses	30,037	24,206	25,059
Structural	6,464	5,045	5,171
Non-Str. Drift Sensitive	12,349	9,458	9,796
Non-Str. Acceleration Sensitive	11,224	9,703	10,093
Contents	9,893	8,553	8,888

Table 4-17: Sensitivity of Bridge Losses to Soil Amplification

Bridge Loss ($M)	Soil Amplification Model		
	Hwang	Dobry*	Borcherdt
Bridge Losses (Network)	296	269	163
Bridge Losses (HAZUS)	282	222	193

Table 4-18: Sensitivity of Economic Losses to Soil Amplification

Business Loss ($M)	Soil Amplification Model		
	Hwang	Dobry*	Borcherdt
Shelby			
Production Losses	19,984	14,490	15,115
Direct	15,941	11,740	12,303
Indirect	4,043	2,750	2,811
Value Added Losses	10,725	7,789	8,118
Direct	8,566	6,309	6,610
Indirect	2,159	1,480	1,508
NMSZ			
Production Losses	34,709	27,164	26,778
Direct	27,856	22,220	21,827
Indirect	6,854	4,944	4,951
Value Added Losses	18,603	14,585	14,358
Direct	14,937	11,908	11,705
Indirect	3,666	2,677	2,653
CUS			
Production Losses	35,612	26,867	27,591
Direct	38,518	31,177	31,561
Indirect	-2,906	-4,310	-3,970
Value Added Losses	20,190	15,447	15,801
Direct	20,865	16,891	17,129
Indirect	-675	-1,443	-1,328
US			
Production Losses	-11,254	-8,827	-9,119
Direct	38,518	31,177	31,561
Indirect	-49,772	-40,004	-40,679
Value Added Losses	-473	-339	-357
Direct	20,865	16,891	17,129
Indirect	-21,338	-17,230	-17,486

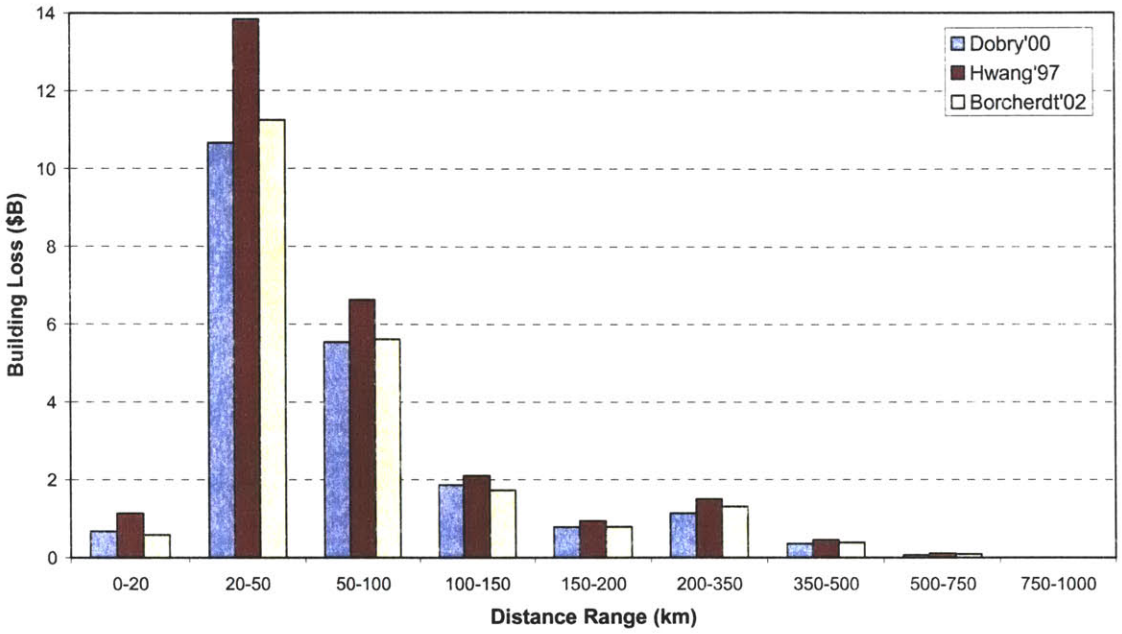

Figure 4-31: Distribution of Building Losses with Distance for Different Soil Amplification Models

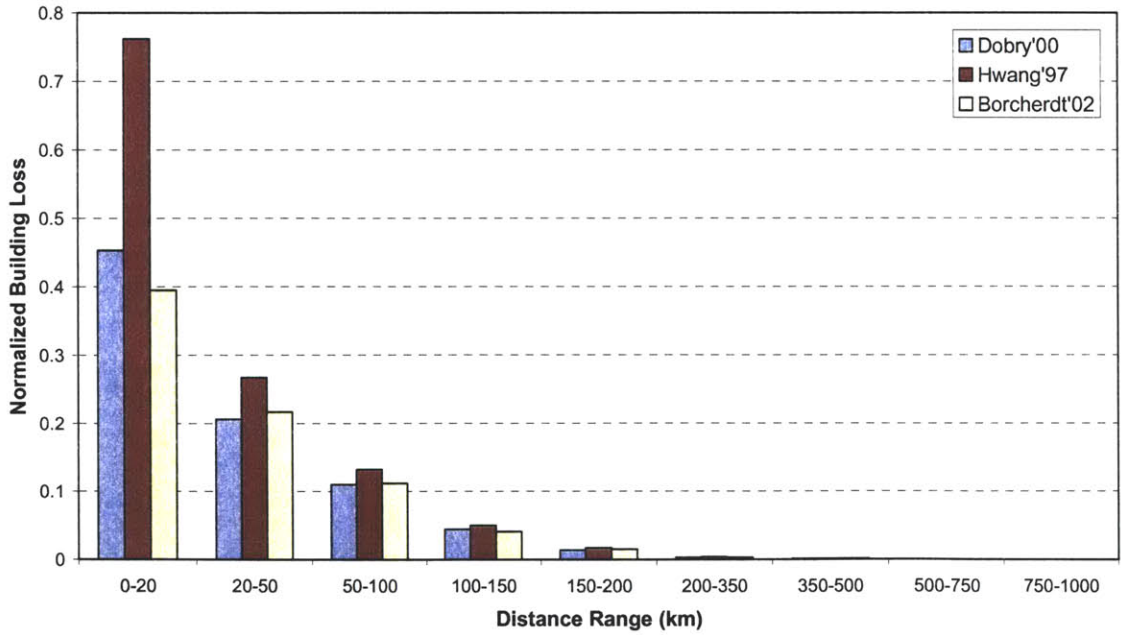

Figure 4-32: Distribution of Normalized Building Losses with Distance for Different Soil Amplification Models

As in the case of building losses, value added losses (see Table 4-18) are highest when the soil amplification factors of Hwang et al (1997) are used. The direct and indirect value added losses in Shelby County and NMSZ are about 35-45% and 25-35% higher, respectively, than in the baseline scenario. These percent increases are slightly higher than for building losses. The value added losses from Borcherdt (2000) are only slightly higher than the corresponding baseline scenario losses except for the NMSZ where the value added losses from Dobry et al (2000) are higher. In this case, the percent difference in the value added losses is lower than that for building losses, as the slight increase in building damage does not cause much change in building functionality.

Figures 4-33 and 4-34 show the distribution with distance of direct value added losses and normalized direct value added losses. Results are similar to those for building losses; see Figures 4-31 and 4-32. The reason is that direct value added losses are closely related to building damage. As in the case of building losses, most of the difference in direct value added losses comes from Shelby County (20-50km distance range). The normalized direct value added loss for this region is between 0.29 and 0.39 depending on the amplification model used. In the epicentral region, the normalized direct value added loss is between 0.6 and 0.8. The difference in normalized direct value added losses among different models is less significant in this distance range compared to the normalized building losses (which ranged from 0.40 to 0.75) mainly due to nonlinearity in the functionality and recovery model. The buildings in this distance range are significantly damaged and additional incremental changes in damage do not cause much change in building functionality/recovery time and hence in the value added losses.

4.2.5 Sensitivity to Soil Conditions

In the baseline scenario, we have used soil conditions obtained from the CUSEC soil classification maps and in the regions that are not covered by these maps we have assumed site class D. In this section, we look at the sensitivity of losses to soil conditions. We consider three additional cases in addition to the baseline scenario, in which we assume uniform soil conditions of type C, D and E. In all cases, we use the soil amplification factors of Dobry et al (2000).The losses obtained from these additional cases are listed in Tables 4-19 and 4-21 together with results from the baseline scenario.

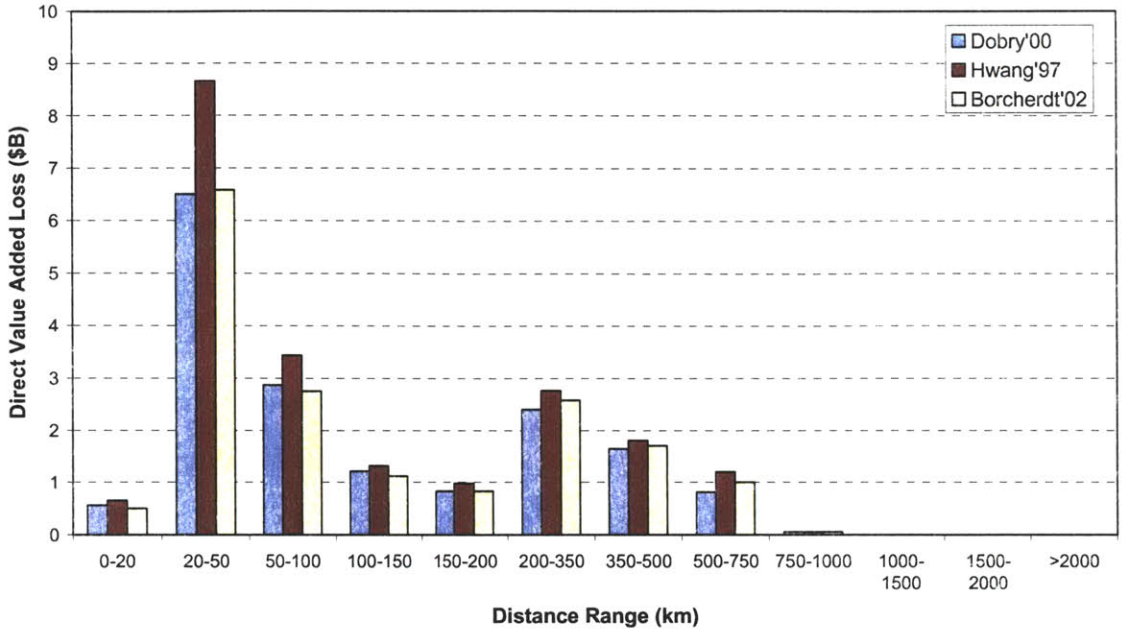

Figure 4-33: Distribution of Value Added Losses with Distance for Different Soil Amplification Models

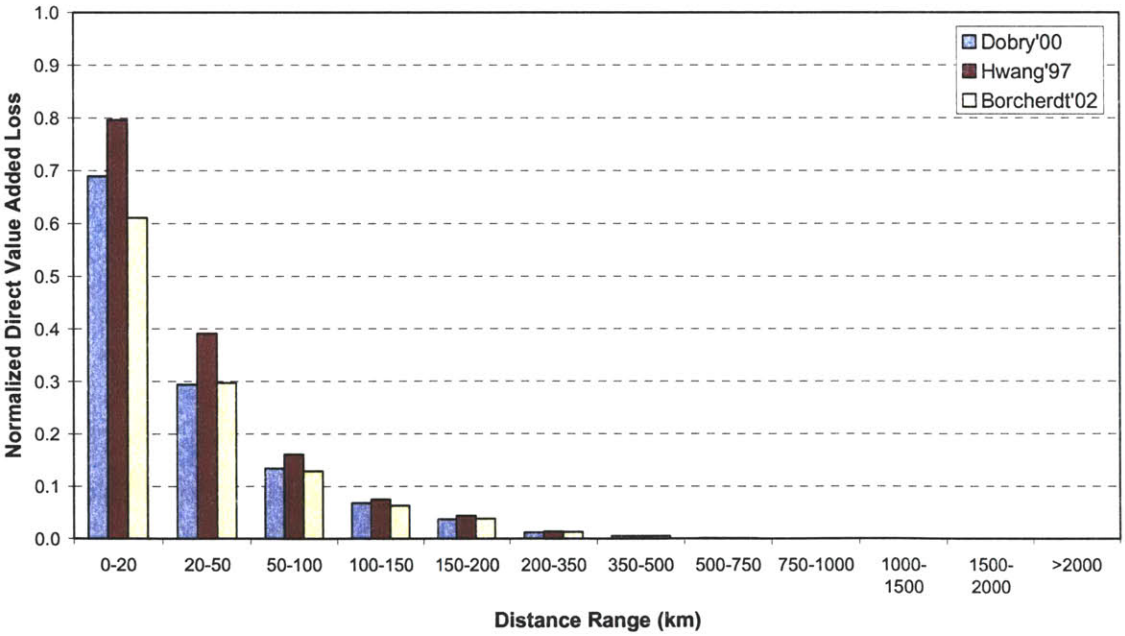

Figure 4-34: Distribution of Normalized Direct Value Added Losses with Distance for Different Soil Amplification Models

Table 4-19: Sensitivity of Building Losses to Soil Conditions

Loss ($M)	Soil Condition			
	CUSEC*	Type C	Type D	Type E
Shelby County				
Building Losses	11,740	8,312	11,017	15,901
Structural	2,238	1,506	2,061	3,127
Non-Str. Drift Sensitive	4,394	2,986	4,070	6,201
Non-Str. Acceleration Sensitive	5,109	3,820	4,886	6,573
Contents	4,480	3,351	4,284	5,760
NMSZ				
Building Losses	21,656	13,285	18,715	30,642
Structural	4,307	2,511	3,634	6,236
Non-Str. Drift Sensitive	8,290	4,917	7,051	12,048
Non-Str. Acceleration Sensitive	9,060	5,857	8,030	12,358
Contents	7,982	5,158	7,072	10,893
CUS				
Building Losses	24,206	14,495	21,268	38,283
Structural	5,045	2,900	4,380	8,209
Non-Str. Drift Sensitive	9,458	5,494	8,229	15,408
Non-Str. Acceleration Sensitive	9,703	6,102	8,659	14,666
Contents	8,553	5,375	7,631	12,945

Table 4-20: Sensitivity of Bridge Losses to Soil Conditions

Bridge Loss ($M)	Soil Condition			
	CUSEC*	Type C	Type D	Type E
Bridge Losses (Network)	269	54	88	311
Bridge Losses (HAZUS)	222	62	121	321

Table 4-21: Sensitivity of Economic Losses to Soil Conditions

Business Loss ($M)	Soil Condition			
	CUSEC*	Type C	Type D	Type E
Shelby				
Production Losses	14,490	8,553	12,297	23,820
Direct	11,740	7,020	10,085	19,039
Indirect	2,750	1,532	2,212	4,780
Value Added Losses	7,789	4,611	6,612	12,784
Direct	6,309	3,779	5,416	10,237
Indirect	1,480	833	1,195	2,547
NMSZ				
Production Losses	27,164	15,190	22,022	41,566
Direct	22,220	12,570	18,190	33,549
Indirect	4,944	2,621	3,831	8,017
Value Added Losses	14,585	8,224	11,870	22,265
Direct	11,908	6,786	9,783	17,979
Indirect	2,677	1,438	2,087	4,286
CUS				
Production Losses	26,867	15,059	22,812	50,524
Direct	31,177	18,233	27,108	51,398
Indirect	-4,310	-3,174	-4,297	-874
Value Added Losses	15,447	8,822	13,229	28,338
Direct	16,891	9,964	14,749	27,845
Indirect	-1,443	-1,142	-1,520	493
US				
Production Losses	-8,827	-5,061	-7,625	-14,113
Direct	31,177	18,233	27,108	51,398
Indirect	-40,004	-23,294	-34,734	-65,511
Value Added Losses	-339	-158	-292	-629
Direct	16,891	9,964	14,749	27,845
Indirect	-17,230	-10,121	-15,041	-28,474

The losses from the baseline scenario fall in between those for soils of uniform type D and E. They are slightly higher than those for type D soil as a significant fraction of the soils from the CUSEC soil maps in NMSZ are of type D (with fractions of types C and E). Also, in the region outside the CUSEC soil maps, soil type D is used by default.

In Shelby County, the losses from assuming type E soils are 50% higher than those when using type D. The percent difference in losses increases to 70% for NMSZ and 80% for CUS. The same percent differences between site classes D and C are 35%, 43% and 48%, respectively. The gradual increase in percentage difference of the estimated losses as one gets farther from the epicenter results in part from the dependence of site amplification on ground motion amplitude. Figures 4-35 and 4-36 show the ratios of NEHRP short and long period soil amplification for adjacent site classes, i.e. for site class E relative to site class D and site class D relative to site class C. For different ground motion amplitudes, the ratios of long period soil amplification are about the same, whereas for short period ground motions there is considerable dependence on ground motion amplitude for site class E. At 0.25 g, the ratio of amplification for site classes E to D is about 1.6 and at 1.0g this ratio decreases to 0.8. In regions far away from the epicenter where ground motion is weak (e.g. regions outside NMSZ), the difference in site amplification for site classes D and E would be more significant, resulting in higher losses for site class E. On the other hand close to the epicenter, (e.g. in Shelby County), the ratio of the losses for site classes D and E is smaller.

The difference in building damage under different soil conditions is reflected in different economic losses. Again, the economic losses for CUSEC soil conditions are between the loss estimates under uniform soil conditions of type D and E. The percent differences in business losses are larger than those for building losses due to a combination of factors including increased functionality reductions with increasing building damage level, nonlinearity of functionality loss, and interactions among different sectors. For example, the value added losses for soil class E are about twice those for soil class D for all regions considered.

The previous observations about the effect of soil conditions on earthquake losses underscore the importance of using appropriate soil classes for loss analysis. Deviation of actual soil conditions from the assumed ones may significantly influence the results. In our case, we did not observe much difference in losses between the baseline case and the assumption of site D conditions (as

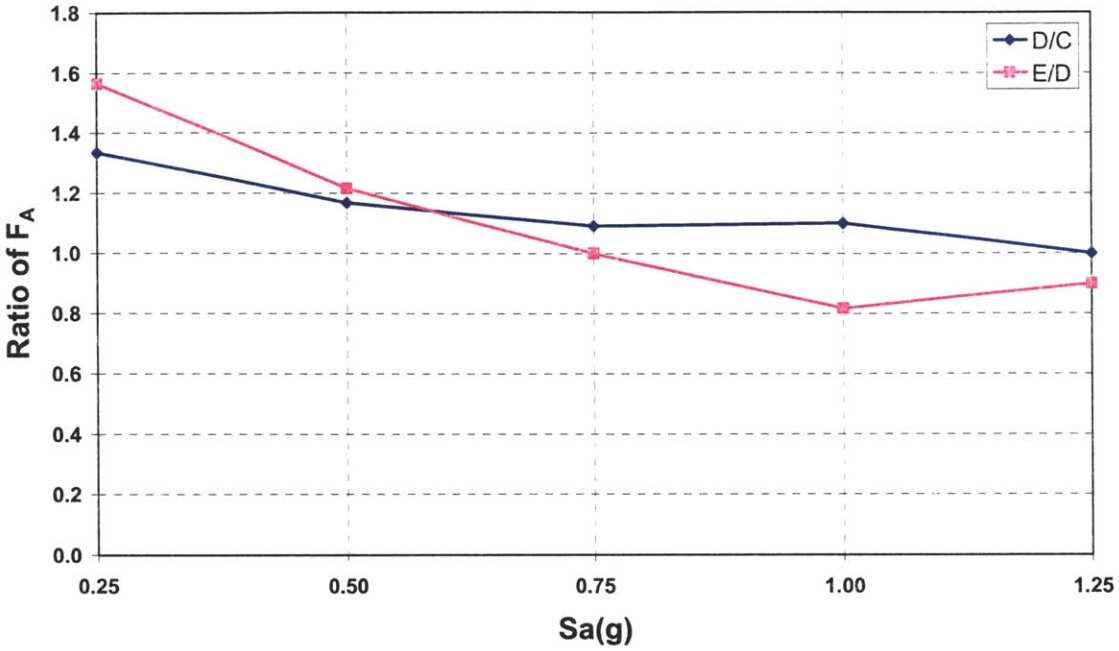

Figure 4-35: Ratio of NEHRP Short Period Soil Amplification Factors

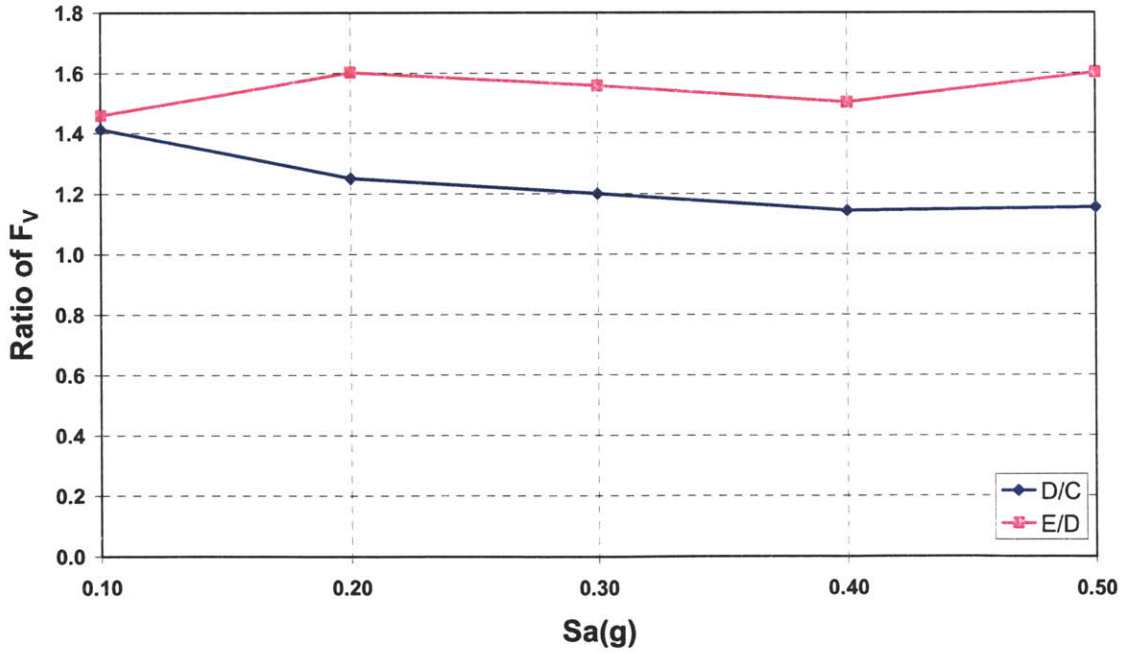

Figure 4-36: Ratio of NEHRP Long Period Soil Amplification Factors

in HAZUS) since most of the analysis regions in NMSZ fall into the type D class. For critical infrastructure, such as bridges, an accurate local evaluation should be made.

4.2.6 Sensitivity to Building Code Levels

The vulnerability of buildings designed for different building code levels is evaluated as explained in Chapter 3. In the baseline scenario, we used the default mapping for Shelby County, which considers the majority of buildings to be in the "moderate code" class with the remaining assigned to "pre-code". Here we investigate three additional cases in which all buildings are either in the pre-code, low-code, or moderate-code level. The results are presented in Tables 4-22 and 4-23.

The regional building losses in Table 4-22 indicate that there are considerable differences in the estimates for moderate, low, and pre-code levels. The results for Shelby County in the baseline analysis are only slightly higher than those for moderate code as most of the buildings were mapped into this code level by default. The building losses in the CUS range from \$20.0B to \$35.2B for pre and moderate code levels, respectively, and between \$10.3B and \$16.1B in Shelby County. The building losses for moderate code level are about 5% lower than those of the baseline scenario. The losses for pre-code level are about 50% to 67% higher than those for the baseline scenario.

Most of the change in building losses arise from changes in structural and drift sensitive nonstructural components rather than the acceleration sensitive nonstructural components. For the latter, the percent increase under pre and low code are about 20% compared to the baseline scenario. For the same design levels, the percent increases for drift sensitive nonstructural components are about 90-120% and 70-90%, respectively. The structural losses are less sensitive, with percent increases of 60-75% and 17-22% for pre-code and low code levels.

Figures 4-37 and 4-38 show the distribution of building and normalized building losses with distance. The 20-100km distance range dominates the building losses, with considerable differences between moderate, low, and pre-code. The normalized building losses in the immediate vicinity of the epicenter range between 0.45 and 0.73. In the 20-50km distance range the mean loss ratio changes from 0.20 to 0.30. Although the percent difference in normalized building loss decreases with distance, the relative difference displays the opposite trend (see

Table 4-22: Sensitivity of Building Losses to Building Code Level

Loss ($M)	Building Code Level			
	Default	Pre-Code	Low-Code	Moderate-Code
Shelby County				
Building Losses	11,740	16,077	14,441	11,386
Structural	2,238	3,616	2,738	2,055
Non-Str. Drift Sensitive	4,394	6,335	5,626	4,211
Non-Str. Acceleration Sensitive	5,109	6,127	6,077	5,120
Contents	4,480	5,346	5,304	4,492
NMSZ				
Building Losses	21,656	30,277	26,751	20,937
Structural	4,307	7,144	5,204	3,922
Non-Str. Drift Sensitive	8,290	12,047	10,564	7,955
Non-Str. Acceleration Sensitive	9,060	11,087	10,983	9,059
Contents	7,982	9,745	9,657	7,982
CUS				
Building Losses	24,206	35,190	29,970	23,256
Structural	5,045	8,828	5,926	4,512
Non-Str. Drift Sensitive	9,458	14,286	12,087	9,073
Non-Str. Acceleration Sensitive	9,703	12,076	11,956	9,671
Contents	8,553	10,626	10,524	8,523

Table 4-23: Sensitivity of Economic Losses to Building Code Level

Loss ($M)	Building Code Level			
	Shelby Co Mapping	Pre-Code	Low-Code	Moderate-Code
Shelby				
Production Losses	14,490	21,104	17,665	12,898
Direct	11,740	16,571	14,044	10,418
Indirect	2,750	4,533	3,622	2,479
Value Added Losses	7,789	11,273	9,455	6,938
Direct	6,309	8,869	7,524	5,608
Indirect	1,480	2,405	1,930	1,330
NMSZ				
Production Losses	27,164	40,404	32,612	23,847
Direct	22,220	31,835	26,130	19,253
Indirect	4,944	8,569	6,482	4,594
Value Added Losses	14,585	21,478	17,403	12,794
Direct	11,908	16,952	13,947	10,336
Indirect	2,677	4,526	3,456	2,458
CUS				
Production Losses	26,867	44,122	29,095	21,928
Direct	31,177	45,021	33,715	26,153
Indirect	-4,310	-898	-4,620	-4,225
Value Added Losses	15,447	24,627	16,581	12,679
Direct	16,891	24,270	18,160	14,202
Indirect	-1,443	357	-1,578	-1,523
US				
Production Losses	-8,827	-14,846	-12,636	-8,303
Direct	31,177	45,021	33,715	26,153
Indirect	-40,004	-59,867	-46,351	-34,456
Value Added Losses	-339	-627	-526	-298
Direct	16,891	24,270	18,160	14,202
Indirect	-17,230	-24,897	-18,686	-14,500

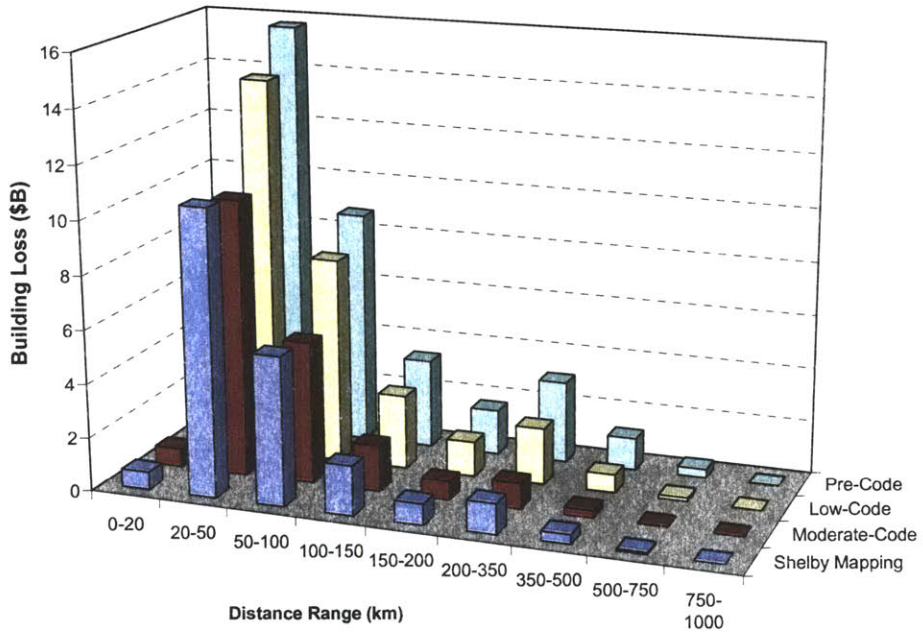

Figure 4-37: Distribution of Building Losses with Distance for Different Building Code Levels

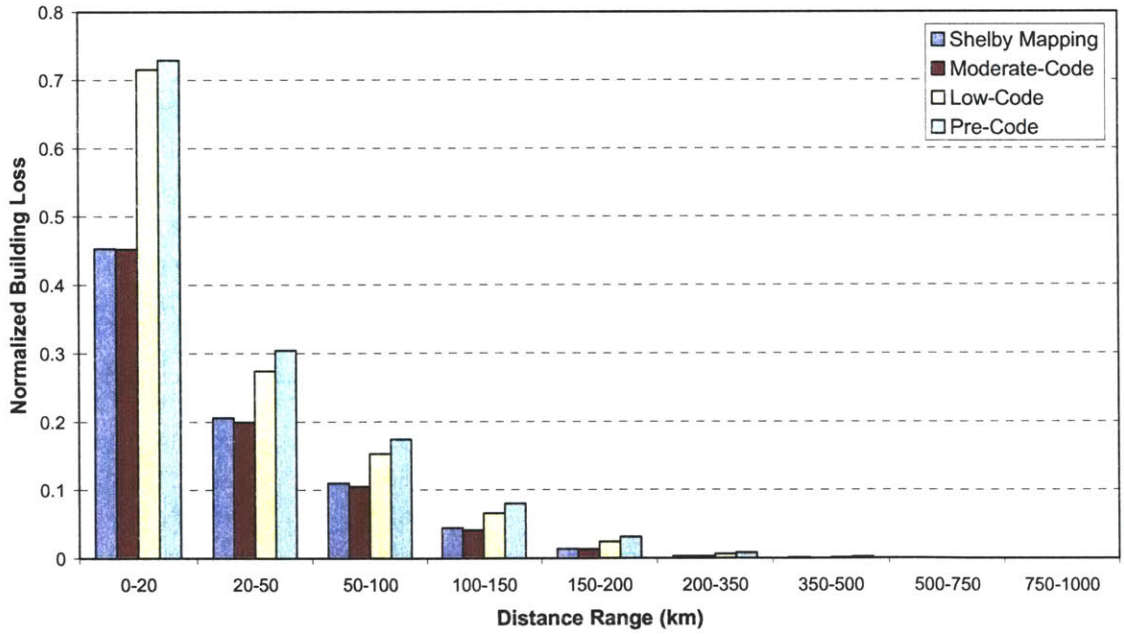

Figure 4-38: Distribution of Normalized Building Losses with Distance for Different Building Code Levels

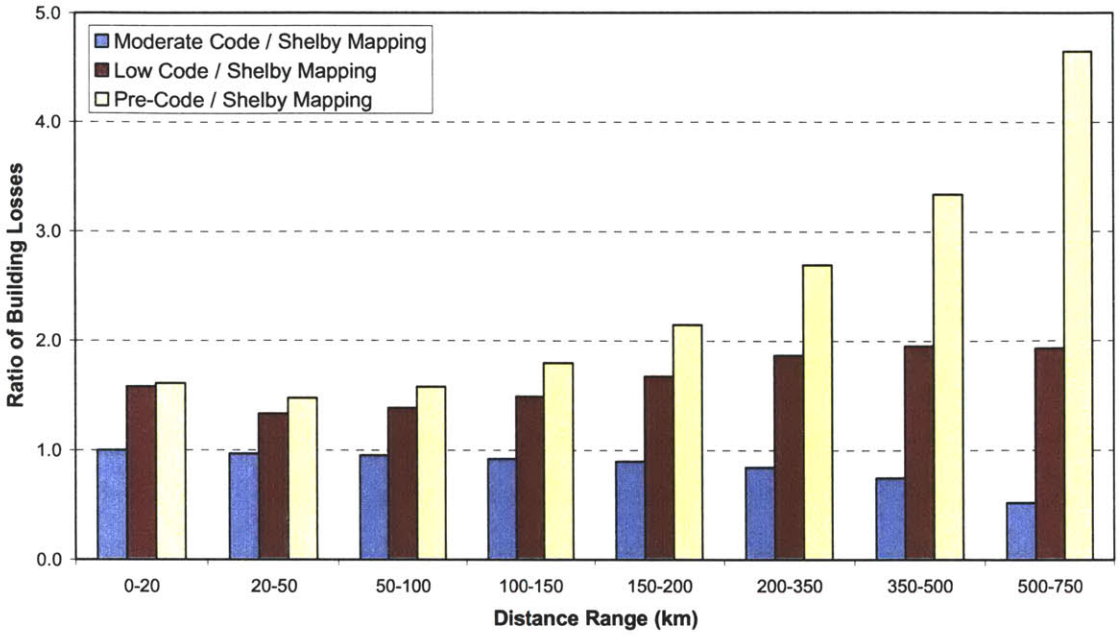

Figure 4-39: Comparison of Building Losses for Different Code Levels to Baseline Scenario at Different Distances

Figure 4-39), as pre-code and low code buildings are more susceptible to damage at low ground motion intensities compared to moderate code levels. For example, in Figure 4-39, comparison of the losses in the 500-750 km distance range shows that the losses for pre-code are about 4.5 times those under the baseline scenario. Also, the losses for moderate code are about half of those from the baseline mapping, as the losses from pre-code buildings contribute more at these low levels of ground motion intensity.

The change in business interruption losses listed in Table 4-23 increases with increasing building loss in a region. For example, the value added losses in Shelby County for pre-code level are 45% higher than in the baseline scenario, whereas those for moderate code level are about 10% lower.

4.2.7 Sensitivity to Expected Mean Building Vulnerability

Next we look at the sensitivity of the losses to the mean of the building vulnerability functions. We increase and decrease the parameters μ_M by $0.25\sigma_M$, where σ_M is the building to building standard deviation of the mean building vulnerability. For example, μ_M for structural

components of residential building class RES-1 is set to 1.340 and 0.886 by changing $\mu_M = 1.113$ by 25% of $\sigma_M = 0.908$. The results are presented in Tables 4-24 and 4-25.

When the mean building vulnerability is increased, the building losses in all regions increase by 25% to 35%, see Table 4-24. When the mean building vulnerability is decreased, the losses decrease by similar amounts. The percent change in losses is about the same for different building components, with drift sensitive nonstructural components being slightly more sensitive than structural and acceleration sensitive nonstructural components.

Figures 4-40 and 4-41 show the distribution of building and normalized building losses. In the epicentral region, the normalized losses are between 0.40 and 0.52. In the 20-50km distance range, the normalized losses decrease to values between 0.16 and 0.26. The percent differences in losses among different cases are observed to increase with distance, see Figure 4-42. In the $\mu_M - 0.25\sigma_M$ case, the percent difference increases steadily from 13% in the 0-20km distance range to 85% in the 350-500km distance range. In the $\mu_M + 0.25\sigma_M$ case, the percent difference in losses decreases steadily from -13% in the 0-20km distance range to -48% for buildings in the 350-500km distance range. In the epicentral region, the ground motion intensity is very high and the resulting damage is less sensitive to building vulnerability. On the other hand, as the epicentral distance increases, the ground motion intensity decreases and the losses become more sensitive to building vulnerability parameters.

As in the case of building losses, the business losses increase when μ_M is reduced and decrease when μ_M is reduced, Table 4-25. The business losses are less sensitive to μ_M compared to building losses. The percent difference in value added losses for Shelby County, NMSZ and CUS regions range between 10% and 30%.

4.2.8 Sensitivity to Variation in Mean Building Vulnerability

To investigate the sensitivity of the losses to the building-to-building standard deviation of the mean of the building vulnerability, we increase and decrease σ_M by 25%.

Increasing the variation in mean building vulnerability increases the losses, see Table 4-26. Similarly, the building losses decrease with decreasing σ_M. For Shelby County and the NMSZ

Table 4-24: Sensitivity of Building Losses to Mean Building Vulnerability

Loss ($M)	Mean Building Vulnerability		
	μ_M	$\mu_M + 0.25\sigma_M$	$\mu_M - 0.25\sigma_M$
Shelby County			
Building Losses	11,740	9,067	14,856
Structural	2,238	1,770	2,782
Non-Str. Drift Sensitive	4,394	3,312	5,694
Non-Str. Acceleration Sensitive	5,109	3,985	6,380
Contents	4,480	3,495	5,595
NMSZ			
Building Losses	21,656	16,371	28,087
Structural	4,307	3,327	5,495
Non-Str. Drift Sensitive	8,290	6,130	10,996
Non-Str. Acceleration Sensitive	9,060	6,914	11,596
Contents	7,982	6,092	10,216
CUS			
Building Losses	24,206	17,794	32,518
Structural	5,045	3,744	6,762
Non-Str. Drift Sensitive	9,458	6,761	13,085
Non-Str. Acceleration Sensitive	9,703	7,288	12,672
Contents	8,553	6,424	11,172

Table 4-25: Sensitivity of Economic Losses to Mean Building Vulnerability

Loss ($M)	Mean Building Vulnerability		
	μ_M	$\mu_M + 0.25\sigma_M$	$\mu_M - 0.25\sigma_M$
Shelby			
Production Losses	14,490	12,870	16,324
Direct	11,740	10,460	13,125
Indirect	2,750	2,409	3,199
Value Added Losses	7,789	6,929	8,758
Direct	6,309	5,631	7,045
Indirect	1,480	1,298	1,713
NMSZ			
Production Losses	27,164	23,832	31,259
Direct	22,220	19,480	25,288
Indirect	4,944	4,352	5,971
Value Added Losses	14,585	12,810	16,726
Direct	11,908	10,459	13,527
Indirect	2,677	2,351	3,199
CUS			
Production Losses	26,867	22,431	35,596
Direct	31,177	25,627	38,846
Indirect	-4,310	-3,196	-3,249
Value Added Losses	15,447	12,862	20,240
Direct	16,891	13,900	21,069
Indirect	-1,443	-1,037	-828
US			
Production Losses	-8,827	-6,406	-12,001
Direct	31,177	25,627	38,846
Indirect	-40,004	-32,033	-50,847
Value Added Losses	-339	-217	-507
Direct	16,891	13,900	21,069
Indirect	-17,230	-14,117	-21,576

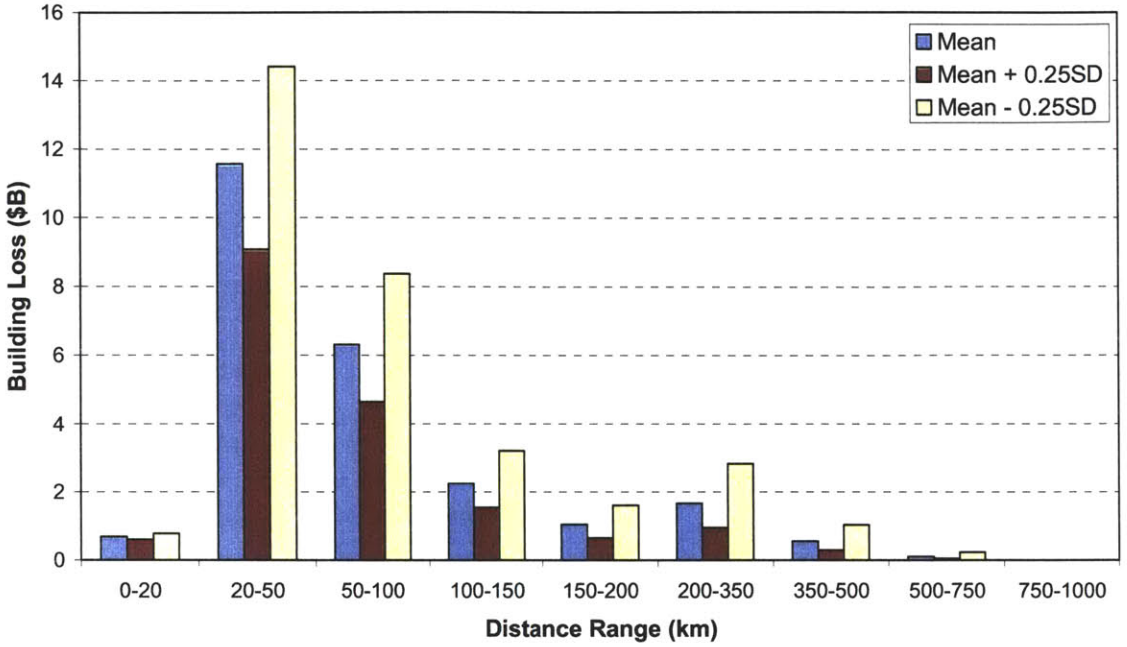

Figure 4-40: Distribution of Building Losses with Distance for Different Mean Seismic Vulnerability

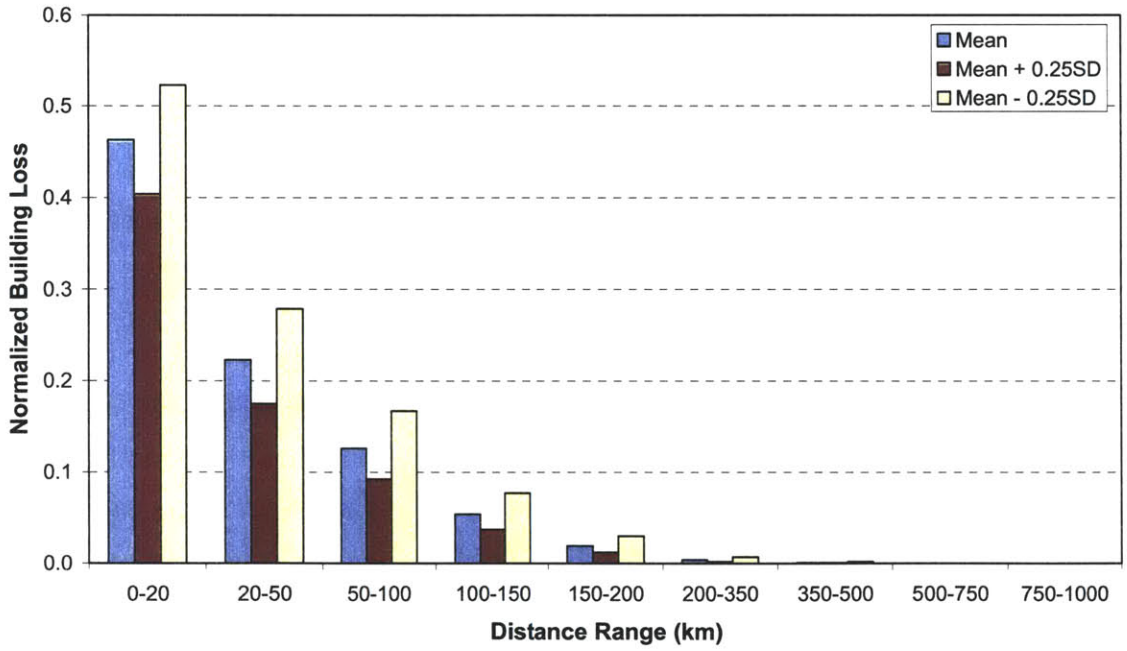

Figure 4-41: Distribution of Normalized Building Losses with Distance for Different Mean Seismic Vulnerability

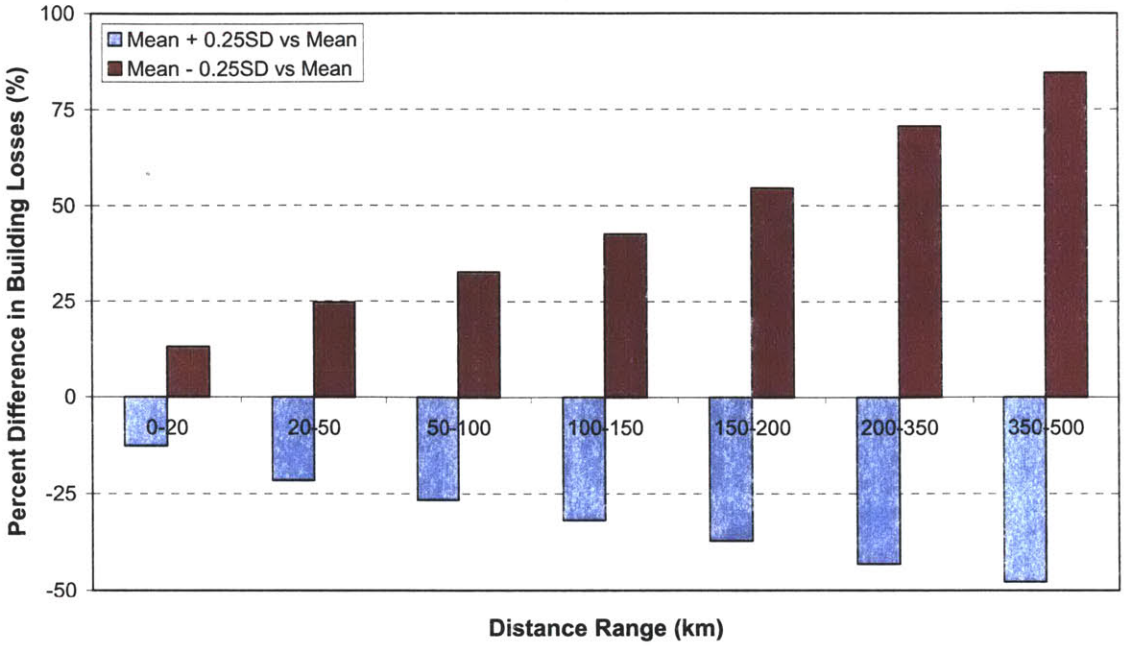

Figure 4-42: Comparison of Building Losses for Different Mean Seismic Vulnerability

region, the change in losses is about 15% and 20%. For CUS, the percent change in losses is 25% and 40% for $\sigma_M - 0.25\sigma_M$ and $\sigma_M + 0.25\sigma_M$, respectively. The losses from acceleration sensitive non structural components are less sensitive to σ_M compared to structural and acceleration sensitive nonstructural components. Figure 4-43 shows the distribution of building losses for the three cases. The building losses are about the same in the heavily damaged 0-20km distance range. The percent differences in losses increase significantly with increasing distance, see Figure 4-44. In the epicentral region, the difference in losses is about 2% but the percent difference in losses gets much larger at distances over 100km.

The business losses follow the patterns observed for building losses, see Table 4-27. However, they are less sensitive to variation in mean building vulnerability than the building losses. The change in business losses for Shelby County and NMSZ region are about 4% to 7%. The percent difference in the losses from the CUS region is approximately 20-25%. Most of the difference in business losses is due to differences in direct business losses, which are more closely related to building losses compared to indirect business losses.

Table 4-26: Sensitivity of Building Losses to Variation in Mean Building Vulnerability

Loss ($M)	Variation in Mean Building Vulnerability		
	σ_M *	$\sigma_M + 0.25\sigma_M$	$\sigma_M - 0.25\sigma_M$
Shelby County			
Building Losses	11,740	13,470	9,973
Structural	2,238	2,548	1,954
Non-Str. Drift Sensitive	4,394	5,254	3,530
Non-Str. Acceleration Sensitive	5,109	5,668	4,489
Contents	4,480	4,971	3,937
NMSZ			
Building Losses	21,656	26,424	17,372
Structural	4,307	5,207	3,551
Non-Str. Drift Sensitive	8,290	10,583	6,274
Non-Str. Acceleration Sensitive	9,060	10,634	7,548
Contents	7,982	9,371	6,649
CUS			
Building Losses	24,206	33,607	18,073
Structural	5,045	7,169	3,763
Non-Str. Drift Sensitive	9,458	14,192	6,543
Non-Str. Acceleration Sensitive	9,703	12,246	7,767
Contents	8,553	10,801	6,844

Table 4-27: Sensitivity of Economic Losses to Variation in Mean Building Vulnerability

Loss ($M)	Variation in Mean Building Vulnerability		
	σ_M *	$\sigma_M + 0.25\sigma_M$	$\sigma_M - 0.25\sigma_M$
Shelby			
Production Losses	14,490	15,117	13,824
Direct	11,740	12,169	11,263
Indirect	2,750	2,949	2,561
Value Added Losses	7,789	8,128	7,425
Direct	6,309	6,544	6,048
Indirect	1,480	1,584	1,377
NMSZ			
Production Losses	27,164	29,012	25,598
Direct	22,220	23,587	20,989
Indirect	4,944	5,425	4,609
Value Added Losses	14,585	15,549	13,749
Direct	11,908	12,630	11,257
Indirect	2,677	2,918	2,491
CUS			
Production Losses	26,867	33,825	21,459
Direct	31,177	38,364	25,966
Indirect	-4,310	-4,539	-4,507
Value Added Losses	15,447	19,339	12,377
Direct	16,891	20,791	14,034
Indirect	-1,443	-1,451	-1,657
US			
Production Losses	-8,827	-14,209	-7,547
Direct	31,177	38,364	25,966
Indirect	-40,004	-52,573	-33,514
Value Added Losses	-339	-607	-280
Direct	16,891	20,791	14,034
Indirect	-17,230	-21,398	-14,314

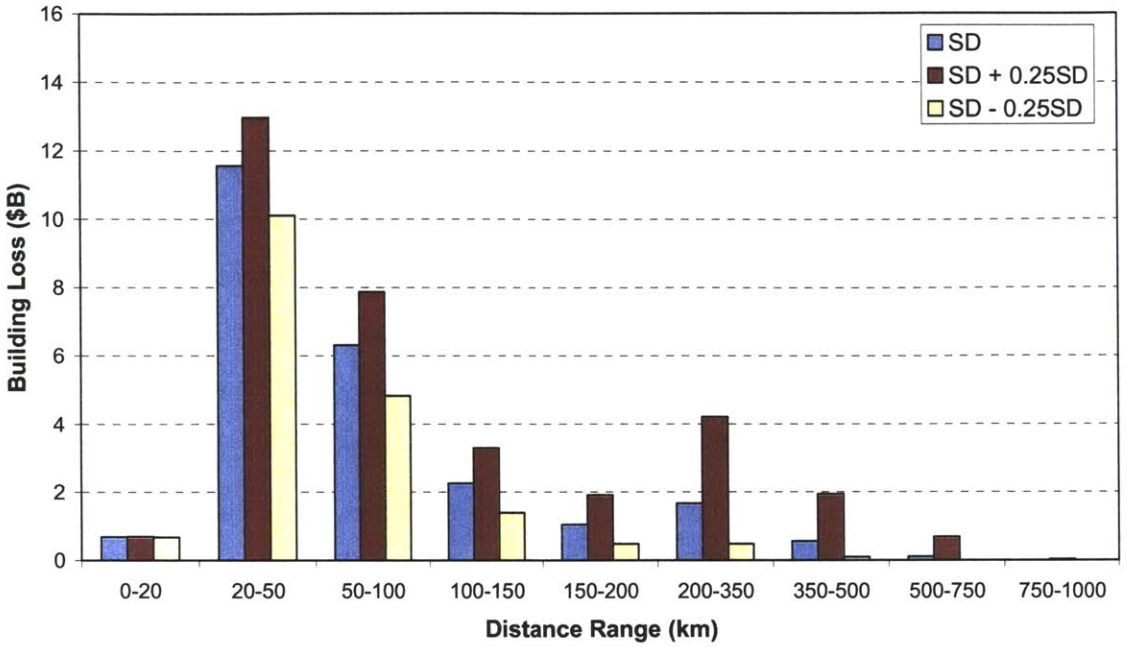

Figure 4-43: Distribution of Building Losses with Distance for Different Variance in Mean Seismic Vulnerability

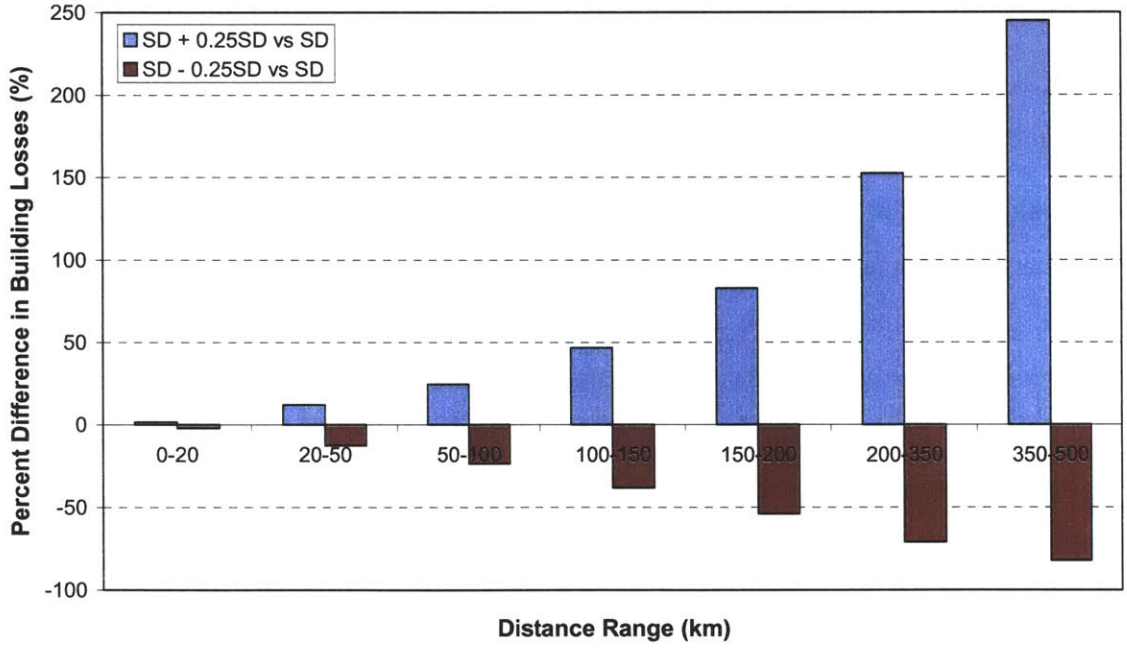

Figure 4-44: Comparison of Building Losses for Different Variance in Mean Seismic Vulnerability

4.2.9 Sensitivity to Functionality of Structural and Nonstructural Building Components

The functionality and recovery time of building occupancy classes depend on the building damage level as explained in Chapter 3. In the baseline scenario, we assumed that the functionality and recovery time of a building occupancy class is determined only by its structural damage level. However, the functionality and recovery rate of a building may depend also on its nonstructural components and contents. Here, we look at the sensitivity of business losses to the weights assigned to structural, acceleration sensitive nonstructural and drift sensitive nonstructural components as well as building contents in determining the building functionality and recovery rate. The baseline scenario assigns weights (1.0, 0.0, 0.0, 0.0) to these components.

Table 4-28 gives the weights to the above building components under each alternative analysis condition and the corresponding business interruption losses. The highest business losses are obtained when more weight is assigned to structural and drift sensitive nonstructural components, as the damage factors for these components are larger than those for acceleration sensitive nonstructural components. The lowest losses are obtained when more weight is assigned to building contents as only half of the building contents are assumed to be susceptible to damage. Assigning more weight to acceleration sensitive nonstructural components results in slightly higher losses than when higher weights are given to building contents.

The total value added or production losses for the US are practically the same for all cases. The reason is that these losses depend mainly on the total building losses and the slack in production capacity. In the presence of slack, undamaged regions make up for reduced productions in the damaged regions and the recovery time of the economic sectors makes little difference in the overall production levels. With slack, the effect of the recovery rate is most pronounced at the local level, for example Shelby County or NMSZ. On the other hand, in the absence of slack, the business interruption losses at all spatial scales are significantly affected by the functionality and recovery time of damaged buildings and industrial facilities.

Table 4-28: Sensitivity of Economic Losses to Weights Assigned to Functionality of Structural and Nonstructural Components

Loss ($M)	Weights Assigned to Functionality of Building Components				
	(1.0, 0.0, 0.0, 0.0)	(0.7, 0.1, 0.1, 0.1)	(0.7, 0.3, 0.0, 0.0)	(0.7, 0.0, 0.3, 0.0)	(0.7, 0.0, 0.0, 0.3)
Shelby					
Production Losses	14,490	12,039	11,194	14,521	10,817
Direct	11,740	9,935	9,289	11,740	9,029
Indirect	2,750	2,104	1,905	2,780	1,788
Value Added Losses	7,789	6,495	6,055	7,802	5,856
Direct	6,309	5,353	5,016	6,309	4,876
Indirect	1,480	1,142	1,039	1,493	980
NMSZ					
Production Losses	27,164	23,035	21,556	27,335	20,722
Direct	22,220	19,063	17,949	22,222	17,419
Indirect	4,944	3,972	3,607	5,113	3,303
Value Added Losses	14,585	12,400	11,635	14,658	11,206
Direct	11,908	10,242	9,664	11,909	9,381
Indirect	2,677	2,157	1,971	2,749	1,825
CUS					
Production Losses	26,867	22,423	20,688	27,226	19,441
Direct	31,177	27,611	26,332	31,179	25,557
Indirect	-4,310	-5,189	-5,644	-3,953	-6,116
Value Added Losses	15,447	13,068	12,162	15,590	11,528
Direct	16,891	15,011	14,337	16,892	13,917
Indirect	-1,443	-1,943	-2,175	-1,301	-2,389
US					
Production Losses	-8,827	-8,830	-8,832	-8,829	-8,825
Direct	31,177	27,611	26,332	31,179	25,557
Indirect	-40,004	-36,441	-35,164	-40,008	-34,382
Value Added Losses	-339	-341	-342	-341	-339
Direct	16,891	15,011	14,337	16,892	13,917
Indirect	-17,230	-15,352	-14,679	-17,232	-14,256

4.2.10 Sensitivity to Functionality and Recovery Interactions

In this section, we investigate the sensitivity of business losses to the functionality and recovery interactions among building occupancy classes (economic sectors), intra-nodal transportation system, and lifelines. As explained in Chapter 3, we use a multiplicative interaction model to quantify the effect of damage to the residential sector, intra-nodal transportation system, and lifelines on the functionality and recovery of the building occupancy classes. The model assumes only one way interactions, with the functionality of building occupancy classes (except the residential class) affected by the functionality of the residential sector, intra-nodal transportation system and lifelines. The functionality of the residential class is affected only by the functionality of the intra-nodal transportation system and lifelines.

We first look at the effect of presence/absence of interaction on the business losses. Table 4-29 lists results for cases with functionality and recovery interactions, only functionality interactions, only recovery interactions, and no interactions. In the presence of functionality and recovery interactions, the value added losses for Shelby Co, NMSZ and CUS are about 27-37% higher than in the case with no interaction. The functionality interactions are more significant than the recovery interactions. When only recovery interactions are considered, the value added losses increase by about 4-8%. The total value added losses for the US are again about the same for all cases due to presence of slack in production capacity.

In Table 4-30, we present results for different combinations of functionality and recovery interactions for the residential sector, intra-nodal transportation, and lifelines. All cases include both functionality and recovery interactions. One can clearly see that the interaction effects of lifelines are much more significant than the effects of residential sector and intra-nodal transportation interactions. The reason is that the functionality interaction coefficients assigned to lifelines were much larger than those of the residential sector and intra-nodal transportation system. Dependence on residential sector functionality has the least influence on business losses partly due to the fact that the functionality of the residential sector itself depends on the functionality of the intra-nodal transportation and lifelines.

Table 4-29: Sensitivity of Economic Losses to Functionality and Recovery Interactions

Loss ($M)	Functionality and Recovery Interactions			
	Functionality and Recovery*	None	Only Recovery	Only Functionality
Shelby				
Production Losses	14,490	10,576	11,418	14,035
Direct	11,740	8,650	9,302	11,291
Indirect	2,750	1,926	2,116	2,744
Value Added Losses	7,789	5,650	6,131	7,516
Direct	6,309	4,612	4,989	6,050
Indirect	1,480	1,038	1,142	1,466
NMSZ				
Production Losses	27,164	21,065	22,615	26,753
Direct	22,220	17,401	18,431	21,508
Indirect	4,944	3,664	4,184	5,246
Value Added Losses	14,585	11,262	12,115	14,296
Direct	11,908	9,276	9,863	11,503
Indirect	2,677	1,986	2,252	2,793
CUS				
Production Losses	26,867	20,825	22,897	27,165
Direct	31,177	26,338	27,373	30,458
Indirect	-4,310	-5,513	-4,476	-3,293
Value Added Losses	15,447	12,131	13,218	15,456
Direct	16,891	14,247	14,837	16,482
Indirect	-1,443	-2,117	-1,619	-1,027
US				
Production Losses	-8,827	-8,835	-8,800	-8,793
Direct	31,177	26,338	27,373	30,458
Indirect	-40,004	-35,173	-36,173	-39,251
Value Added Losses	-339	-343	-327	-323
Direct	16,891	14,247	14,837	16,482
Indirect	-17,230	-14,590	-15,164	-16,806

Table 4-30: Sensitivity of Economic Losses to Selected Functionality and Recovery Interactions

Loss ($M)	Selected Functionality and Recovery Interactions					
	Only Residential	Only Transport.	Only Utilities	No Residential	No Transport.	No Utilities
Shelby						
Production Losses	10,604	10,955	14,263	14,358	14,421	11,025
Direct	8,668	8,940	11,528	11,600	11,669	8,993
Indirect	1,936	2,015	2,734	2,758	2,752	2,033
Value Added Losses	5,665	5,859	7,656	7,709	7,747	5,898
Direct	4,622	4,772	6,189	6,230	6,269	4,801
Indirect	1,043	1,087	1,467	1,479	1,478	1,097
NMSZ						
Production Losses	21,152	21,744	26,860	27,100	27,059	21,903
Direct	17,454	17,905	21,828	21,990	22,053	18,016
Indirect	3,699	3,839	5,032	5,111	5,006	3,887
Value Added Losses	11,308	11,633	14,388	14,520	14,509	11,719
Direct	9,305	9,552	11,688	11,778	11,815	9,613
Indirect	2,003	2,081	2,700	2,742	2,693	2,106
CUS						
Production Losses	20,939	21,549	26,786	27,102	26,821	21,730
Direct	26,392	26,859	30,765	30,943	30,992	26,974
Indirect	-5,453	-5,310	-3,979	-3,841	-4,171	-5,243
Value Added Losses	12,190	12,526	15,330	15,500	15,378	12,623
Direct	14,277	14,532	16,659	16,758	16,787	14,596
Indirect	-2,087	-2,006	-1,329	-1,258	-1,409	-1,973
US						
Production Losses	-8,833	-8,834	-8,825	-8,822	-8,835	-8,834
Direct	26,392	26,859	30,765	30,943	30,992	26,974
Indirect	-35,226	-35,693	-39,590	-39,765	-39,826	-35,808
Value Added Losses	-343	-343	-338	-337	-343	-343
Direct	14,277	14,533	16,659	16,758	16,787	14,596
Indirect	-14,619	-14,875	-16,998	-17,096	-17,130	-14,938

4.2.11 Sensitivity to Rerouting

In the baseline scenario, we used a rerouting parameter of 0.10 to allow a minimum traffic flow (10% of capacity) in the damaged links to account for the effect of secondary routes that are not explicitly modeled. Here, we investigate the sensitivity of the business losses and traffic costs to the rerouting parameter. The results when the rerouting parameter is set to 0.01, 0.05, and 0.10 are given in Table 4-31.

The value added losses are rather insensitive to the rerouting parameter but a slight increase in indirect value added losses is observed with decreasing rerouting parameter. The increase in indirect value added losses is on the order of 1-3% for Shelby County and the NMSZ region, when the rerouting parameter is reduced to 0.01 from 0.10. In the CUS, the percent difference in indirect value added losses, which are negative (gains), is 14%. The value added losses for the US are not affected by the rerouting parameter.

On the other hand, we observe a significant increase of 10% in transportation costs when the rerouting parameter is reduced to 0.01. In this case, the transportation costs increase from $1.34B to $1.48B for the two year period after the earthquake.

4.2.12 Sensitivity to Reconstruction Spending

Table 4-32 shows the effect of reconstruction spending and repayment or reconstruction money on business losses. When there is no reconstruction spending and repayment, we observe production and value added losses in all regions as there is no positive stimulus from reconstruction spending. As an alternative, we look at a hypothetical case in which reconstruction spending is done without any repayment in the future. As expected, there are significant business gains in this scenario. The gains are again observed in regions outside NMSZ as these regions increase their productions to export services and goods.

4.2.13 Sensitivity to Cost of Borrowing

In the baseline scenario, we did not consider any borrowing costs associated with the loans for reconstruction efforts. The sensitivity of business losses to one-time borrowing costs of 1%, 3%, 5% and 10% of total reconstruction spending are investigated here; see Table 4-33.

Table 4-31: Sensitivity of Economic Losses to Rerouting

Loss ($M)	Rerouting		
	0.01	0.05	0.10
Shelby			
Production Losses	14,538	14,520	14,490
Direct	11,740	11,740	11,740
Indirect	2,797	2,780	2,750
Value Added Losses	7,812	7,802	7,789
Direct	6,309	6,309	6,309
Indirect	1,503	1,492	1,480
NMSZ			
Production Losses	27,372	27,329	27,164
Direct	22,222	22,222	22,220
Indirect	5,150	5,107	4,944
Value Added Losses	14,678	14,655	14,585
Direct	11,909	11,909	11,908
Indirect	2,769	2,746	2,677
CUS			
Production Losses	27,299	27,209	26,867
Direct	31,179	31,179	31,177
Indirect	-3,880	-3,971	-4,310
Value Added Losses	15,626	15,582	15,447
Direct	16,892	16,892	16,891
Indirect	-1,265	-1,310	-1,443
US			
Production Losses	-8,824	-8,830	-8,827
Direct	31,179	31,179	31,177
Indirect	-40,003	-40,009	-40,004
Value Added Losses	-338	-341	-339
Direct	16,892	16,892	16,891
Indirect	-17,230	-17,233	-17,230
Transportation Cost	1,485	1,426	1,350

Table 4-32: Sensitivity of Economic Losses to Reconstruction Spending and Repayment

Loss ($M)	Reconstruction Spending and Repayment		
	Spending Repayment	No Spending No Repayment	Spending No Repayment
Shelby			
Production Losses	14,490	14,524	14,531
Direct	11,740	11,740	11,740
Indirect	2,750	2,783	2,791
Value Added Losses	7,789	7,803	7,806
Direct	6,309	6,309	6,309
Indirect	1,480	1,493	1,507
NMSZ			
Production Losses	27,164	27,362	27,398
Direct	22,220	22,222	22,222
Indirect	4,944	5,140	5,176
Value Added Losses	14,585	14,666	14,683
Direct	11,908	11,909	11,909
Indirect	2,677	2,757	2,775
CUS			
Production Losses	26,867	37,998	27,348
Direct	31,177	31,179	31,179
Indirect	-4,310	6,819	-3,831
Value Added Losses	15,447	20,617	15,629
Direct	16,891	16,892	16,892
Indirect	-1,443	3,726	-1,263
US			
Production Losses	-8,827	155	-42,193
Direct	31,177	31,179	31,179
Indirect	-40,004	-31,024	-73,373
Value Added Losses	-339	72	-21,441
Direct	16,891	16,892	16,892
Indirect	-17,230	-16,819	-38,333

Table 4-33: Sensitivity of Economic Losses to Total Borrowing Costs

	Total Borrowing Cost				
Loss ($M)	**0.00**	**0.01**	**0.03**	**0.05**	**0.10**
Shelby					
Production Losses	14,490	14,516	14,538	14,532	14,533
Direct	11,740	11,740	11,740	11,740	11,740
Indirect	2,750	2,776	2,798	2,792	2,793
Value Added Losses	7,789	7,800	7,809	7,807	7,807
Direct	6,309	6,309	6,309	6,309	6,309
Indirect	1,480	1,491	1,500	1,498	1,498
NMSZ					
Production Losses	27,164	27,310	27,430	27,393	27,411
Direct	22,220	22,222	22,222	22,222	22,220
Indirect	4,944	5,088	5,208	5,171	5,191
Value Added Losses	14,585	14,646	14,695	14,684	14,686
Direct	11,908	11,909	11,909	11,909	11,908
Indirect	2,677	2,737	2,786	2,776	2,778
CUS					
Production Losses	26,867	27,152	27,485	27,375	27,542
Direct	31,177	31,179	31,179	31,179	31,177
Indirect	-4,310	-4,027	-3,694	-3,805	-3,635
Value Added Losses	15,447	15,556	15,688	15,656	15,714
Direct	16,891	16,892	16,892	16,892	16,891
Indirect	-1,443	-1,336	-1,204	-1,236	-1,176
US					
Production Losses	-8,827	-8,501	-7,830	-7,160	-5,492
Direct	31,177	31,179	31,179	31,179	31,177
Indirect	-40,004	-39,680	-39,009	-38,340	-36,669
Value Added Losses	-339	-132	291	714	1,768
Direct	16,891	16,892	16,892	16,892	16,891
Indirect	-17,230	-17,024	-16,600	-16,178	-15,122

The production and value added losses for Shelby County and NMSZ are insensitive to the borrowing costs. The change in business losses are more significant for CUS compared to NMSZ. However, the most significant effect of borrowing costs is seen on the business losses for the US. For the baseline scenario with no borrowing costs, the value added losses are negative, i.e. they indicate a gain from reconstruction/repayment. With increasing borrowing costs, these gains decrease and for borrowing costs of 3% and more they become net economic losses. For a 10% borrowing cost, the business losses for the US are $1.77B.

4.2.14 Sensitivity to Slack in Production Capacity

The slack in the production capacity of various economic sectors is an important parameter in determining the value added losses for the US. In the baseline scenario, we assumed a slack of 5% and here we consider as alternatives the values of 0%, 1%, and 2% (see Table 4-34).

The direct and indirect value added losses in Shelby County and the NMSZ region are slightly affected by the slack value. These differences in business losses are mainly a result of different levels of production in the pre-earthquake state due to different values of slack utilized. Figure 4-45 show the slack used at different distance ranges for the above cases. We observe that in all cases slack is almost fully utilized up to 500 km from the epicenter, which implies that in the presence of slack the pre-earthquake and maximum post-earthquake regional productions in this region are higher than in the no slack case. This is why, at a given damage level, one observes higher business losses for higher slack values. The value added losses in Shelby County and NMSZ are quite similar when they are normalized to account for this effect.

The losses for the CUS region are more sensitive to slack as this region extends up to 1000km from the epicenter and for a slack of 2% and 5% there is some excess production capacity or unutilized slack in the 750-1000km and 500-1000km distance ranges, respectively. Regions in these distance ranges would increase their productions to make up for the reduced productions in the damaged regions, which result in reduced indirect economic losses for the CUS. For example, indirect losses in the CUS are negative for 5% slack implying increased productions in certain regions of the CUS, which results in reduced value added losses for CUS compared to other cases.

Table 4-34: Sensitivity of Economic Losses to Available Slack in Production

Loss ($M)	Slack in Production			
	0.0	0.01	0.02	0.05
Shelby				
Production Losses	13,909	14,202	14,211	14,490
Direct	11,186	11,297	11,408	11,740
Indirect	2,723	2,905	2,803	2,750
Value Added Losses	7,468	7,617	7,629	7,789
Direct	6,011	6,071	6,130	6,309
Indirect	1,457	1,547	1,499	1,480
Consumption Losses	696	10	3	3
NMSZ				
Production Losses	26,440	27,510	27,098	27,164
Direct	21,175	21,384	21,593	22,220
Indirect	5,265	6,126	5,505	4,944
Value Added Losses	14,149	14,682	14,496	14,585
Direct	11,346	11,459	11,571	11,908
Indirect	2,803	3,223	2,925	2,677
Consumption Losses	1,585	54	15	13
CUS				
Production Losses	37,256	39,803	38,339	26,867
Direct	29,707	30,001	30,296	31,177
Indirect	7,549	9,802	8,044	-4,310
Value Added Losses	20,141	21,377	20,705	15,447
Direct	16,092	16,252	16,412	16,891
Indirect	4,049	5,125	4,293	-1,443
Consumption Losses	3,620	124	37	33
US				
Production Losses	61,939	3,462	-8,012	-8,827
Direct	29,707	30,001	30,296	31,177
Indirect	32,232	-26,540	-38,308	-40,004
Value Added Losses	35,653	5,642	19	-339
Direct	16,092	16,252	16,412	16,891
Indirect	19,560	-10,611	-16,393	-17,230
Consumption Losses	34,110	6,053	438	80

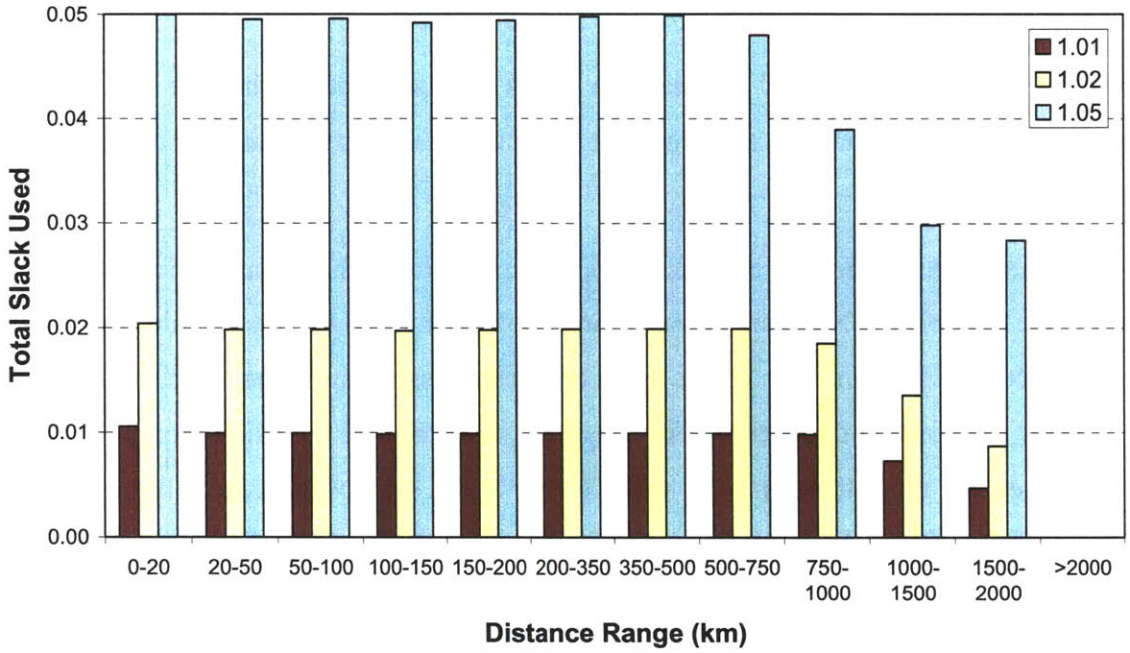

Figure 4-45: Total Slack Used in Pre-earthquake state

The indirect and total value added losses for the US are highly sensitive to the value of slack. In the absence of slack or when the excess production capacity is not able to make up for the lost productions in damaged regions, we observe a much higher value added loss. For example, with 1% slack, the total value added loss for the US decreases from \$35.7B to \$5.6B. In the case of 5%, this becomes a gain due to capacity availability and reconstruction effects. The indirect losses for the US are negative except in the no slack case.

The effect of slack on consumption losses is also significant. This loss quantifies the unsatisfied household demand for commodities or services provided by the various economic sectors. In the presence of slack, there is minimal consumption loss in Shelby County, the NMSZ region, and the CUS, although this loss increases with decreasing slack. When no slack is present, the consumption losses are significant for all these regions and for the entire US they are about the same as the value added losses. The sum of value added and the household demand constitute the GDP and these two values must be equal to each other. In this regard, the loss in value added and household consumption must be identical in the absence of slack. The slight difference in value added and consumption losses in this case arises from the effects of reconstruction spending and repayment.

4.3 Concluding Remarks

In this chapter, we first analyzed in detail the losses for a scenario earthquake when parameters are set to nominal values and investigated sensitivity of the results to a number of earthquake and modeling parameters.

The selected scenario event is a magnitude M7.5 earthquake with epicenter located about 35km northwest of Memphis, TN. A significant portion of the building losses results from buildings within the NMSZ region and about half of these losses are from Shelby County. The contributions of drift and acceleration sensitive nonstructural building components to the building losses are about the same and make up for about 80% of the total building losses. The remaining 20% is due to losses from structural components. The contents losses are about one third of total building losses.

The bridge repair costs for the scenario earthquake is about $0.27B, which is much less than the building losses. Of the 4651 bridges considered, 98 are in the extensive damage state with an additional 59 bridges in the complete damage state. The bridges that are in minor, moderate and extensive damage states recover much faster than the bridges in complete damage state. Therefore, the recovery of transportation link capacity mainly depends on the bridges in the complete damage state. The increase in transportation cost due to damage to transportation links is about $1.3B.

The value added losses from Shelby County and NMSZ are $7.8B and $14.6B, respectively, and are about 65% of the building losses within these regions. About 80% of the value added losses result from direct functionality losses. In the CUS and the US, we observe negative indirect value added losses (i.e. gains) as a result of increased productions in these regions to make up for the lost productions in the damaged regions. The business losses or gains at the national level are sensitive to the slack in production capacity. In particular, business losses increase significantly in the absence of slack.

We looked at the sensitivity of the above building and business losses to various parameters and component models, including ground motion attenuation, soil type, soil amplification model, building code level, and building vulnerability parameters. Other variables that affect transportation costs or business losses include functionality parameters, rerouting along links, reconstruction spending, borrowing costs, and slack in production capacity. In addition, we

investigated the losses for different earthquake locations and magnitudes. Table 4-35 summarizes the sensitivity results for building losses.

For earthquakes with the same magnitude, the distance of the epicenter to Shelby County, where most of the building inventory in the region is located, is the determinant factor. In addition, earthquakes modeled as line sources rather than point sources produce higher losses since there is greater amount of inventory close to a line source compared to a point source.

As one would expect, both building and business losses are significantly affected by the earthquake magnitude. The total building loss for a magnitude M8.0 event is $36.8B, which is about 50% higher than that of a magnitude M7.5 event at the same location. The percent increase in total building loss for magnitude M7.5 event compared to a magnitude M7.0 event is even higher (about 80%). Hence sensitivity to earthquake magnitude is very high.

For the M7.5 scenario earthquake, building loss estimates for different attenuation relations range between $19.7B and $33.8B. The building losses are less sensitive to the soil amplification model than attenuation relations but the assumed soil class significantly changes the estimated losses. For example, losses for type E soil conditions are 2.6 times those obtained for type C conditions.

Building code level is another parameter that significantly affects the building losses. The losses for pre-code level conditions are 50% higher than those for moderate-code conditions. The sensitivity of the building losses to the expected value (μ_M) and standard deviation (σ_M) of the mean building vulnerability is about the same. The building losses increase about 35% when μ_M is decreased or when σ_M is increased by $0.25\sigma_M$.

In general, these trends for building losses apply also to business losses, especially for regions close to the earthquake epicenter such as Shelby County and NMSZ. The reason is that the level of building damage determines the recovery times of buildings and economic sectors. The business losses are more sensitive than the building losses to many of the above parameters. The expected value (μ_M) and standard deviation (σ_M) of mean building vulnerability are exceptions. All other parameters affect the overall building response, whereas these two only determine the intensity and distribution of building damage given a building response.

Table 4-35: Summary of Sensitivity Results for Building Losses

Parameter	% Difference in Building Losses		
	Shelby	NMSZ	CUS
Attenuation Relation	-15%, +21%	-19%, +32%	-20%, +40%
Soil Amplification	+30%	+26%	+27%
Soil Class	-30%, +35%	-39%, +41%	-40%, +58%
Building Code Level	-4%, +50%	-4%, +56%	-5%, +67%
Mean Building Vulnerability	-23%, +27%	-24%, +30%	-26%, +34%
Variation in Building Vulnerability	-15%, +15%	-20%, +22%	-25%, +39%

Business loss at the national level is significantly affected by the slack in production capacity and its magnitude is much smaller than the building loss, as regions outside the immediately affected region increase their productions to make up for lost capacity in the damaged region. However, in a fully constrained economy, i.e. in the case of no slack, the business losses at the national level increase significantly and may even exceed the building losses. Borrowing costs associated with reconstruction spending increase the business losses mainly at the national level. When no borrowing cost is considered an economic gain of 0.3B is observed at the national level, while a loss of 0.7B is estimated for a total borrowing cost of 5% of the reconstruction spending. The functionality and recovery interactions also affect business losses. When no interactions are considered, the value-added losses decrease by 22-27% in Shelby County and NMSZ region. Also, the business losses are more sensitive to functionality interactions compared to recovery interactions. However, the business losses at the national level are insensitive to the interactions due to slack.

The scenario earthquake loss calculation and the sensitivity analysis were intended to shed light on the results of the loss estimation methodology and the relative importance of different components and models. In the next chapter, we use the present results to propagate uncertainty and quantify regional earthquake loss risk.

5 Uncertainty Assessment and Loss-Risk Curves

Following the loss sensitivity analysis for scenario earthquakes, we now turn to the quantification of loss uncertainty. First, we quantify uncertainty on building losses for single scenario earthquakes and then derive risk curves for building loss. This is achieved by analyzing a large number of scenario earthquakes around the NMSZ region and considering the rate of their occurrence. Based on the observation that business losses are closely related to building losses, we also generate total loss risk curves. Finally, we assess the accuracy of a simplified methodology to generate loss risk curves using a limited number of scenario earthquakes and regional seismic hazard data.

5.1 Risk Curves for Building Losses

In this section, we develop building loss risk curves for Shelby County and the NMSZ region. Loss risk curves give the probability of exceeding different loss values and therefore are an important tool of decision analysis.

First, we investigate the uncertainty in building losses for a given scenario earthquake using analysis of variance (ANOVA). Then, we develop loss risk curves for Shelby County and the NMSZ region considering the uncertainty of future earthquakes while fixing all other uncertain parameters to nominal values. Finally, we combine the previous results to generate loss risk curves that include uncertainty in the losses given the location and magnitude as well as uncertainty on the future seismicity.

5.1.1 Uncertainty of Scenario Earthquake Losses

In Chapter 4, we have investigated the sensitivity of building losses to models and parameters including ground motion attenuation, soil amplification, soil type, building code level, and

Table 5-1: Scenario Earthquakes Used in ANOVA

Scenario Earthquake	Magnitude	Latitude	Longitude
M700_3550_9000	7.00	35.50	-90.00
M750_3550_9000	7.50	35.50	-90.00
M800_3550_9000	8.00	35.50	-90.00
M750_3600_9000	7.50	36.00	-90.00

building vulnerability. Here, we assign probabilities to different model/parameter alternatives and run all model/parameter combinations to assess loss uncertainty under a given scenario earthquake. We use ANOVA to analyze the contribution of different sources of variability to the overall uncertainty and to evaluate the importance of interaction effects. We do this for the four scenario earthquakes listed in Table 5-1. For simplicity, we treat as uncertain only four of the six models/parameters and do not include soil type and building code level in this analysis.

The first earthquake in Table 5-1 is the one used for sensitivity analysis in the previous chapter. The following two events are magnitude M8.0 and M7.0 earthquakes at the same location. The fourth scenario earthquake is located 0.5° (approximately 55km) north of the first three earthquakes. These earthquakes have been selected as representative of the highly destructive events that might occur in the region.

We use the same models and sets of parameter values used for sensitivity analysis (see Table 5-2) and perform a full factorial analysis of building losses for Shelby County and the NMSZ region. In analyzing the results through ANOVA, we assign equal weight to all model combinations and calculate the mean, standard deviation, and coefficient of variation (CV) of the losses for the four scenario earthquakes. We also quantify the contribution of each factor to the total variance.

Table 5-3 shows the results for building losses in Shelby County, the NMSZ region, and the CUS region. For the three earthquakes at the same location, the CVs of the total building loss in the CUS region are approximately the same, with values between 0.44 and 0.47. The CVs for the NMSZ region and Shelby County are lower. On the other hand, the CVs for the magnitude M7.50 earthquake at (36.00, 90.00) are larger. For example, for the building losses in CUS, CV=0.59.

Table 5-2: Factors Considered in ANOVA

Model/Parameter	Alternative Models/Parameters Used
Attenuation Relations	Atkinson and Boore (1995)
	Frankel et al (1996)
	Toro et al (1997)
	Somerville et al (2001)
	Campbell (2003)
Site Amplification Factors	Dobry et al (2000)
	Hwang et al (1997)
	Borcherdt et al (2002)
Expected Value of Mean of Building Vulnerability Curves	Nominal (Derived from HAZUS)
	Nominal + 0.25 Standard Deviation
	Nominal - 0.25 Standard Deviation
Standard Deviation of Mean Of Building Vulnerability Curves	Nominal (Derived from HAZUS)
	Nominal + 25% Nominal
	Nominal + 25% Nominal

Figures 5-1 to 5-4 show the importance factors (the fractional contribution of each variable to the total variance) for each scenario earthquake. In all cases, interaction effects are observed to be negligible and first order effects dominate the overall uncertainty. This is an important result as it allows one to use simplified models for uncertainty evaluation only by considering the main effects rather than all possible combinations of the uncertain variables. The soil amplification model is the factor with the smallest contribution to the overall loss uncertainty. The contribution of other factors varies depending on earthquake magnitude and location.

For the three earthquakes at the same location, the importance of the attenuation relation increases with increasing magnitude. For magnitude M7.0, the factors related to building fragility dominate and the fractional contribution of attenuation to the variance is about 0.1. However, for the M8.0 case, uncertainty in attenuation dominates, with an importance factor of approximately 0.6. The importance factors in Figures 5-2 and 5-4 refer to the two M7.5 scenario earthquakes at different locations. These factors are generally in good agreement.

While the analysis has been limited to four earthquakes, there is evidence that the coefficient of variation of building losses is nearly the same for different earthquakes. This fact leads to

Table 5-3: Summary of Results for Scenario Earthquake Uncertainty Assessment

Building Loss ($M)	Scenario Earthquakes			
	35.50N -90.00W M7.00	35.50N -90.00W M7.50	35.50N -90.00W M8.00	36.00N -90.00W M7.50
Shelby County				
Mean	7,263	13,295	19,279	4,867
Standard Deviation	2,523	3,720	5,371	2,613
Coefficient Of Variation	0.347	0.280	0.279	0.537
NMSZ				
Mean	12,373	24,383	38,043	16,083
Standard Deviation	4,940	8,363	13,217	7,337
Coefficient Of Variation	0.399	0.343	0.347	0.456
CUS				
Mean	13,668	28,742	49,290	20,736
Standard Deviation	6,462	12,553	22,684	12,108
Coefficient Of Variation	0.473	0.437	0.460	0.584

simplifications in the analysis of the following sections, where we conservatively assume a constant coefficient of variation of 0.6.

5.1.2 Building Loss Risk Curves from Regional Seismicity

We now develop the loss risk curves for Shelby County and the NMSZ region using a regional seismicity model while keeping all other models and parameters fixed at nominal values, as was done in Chapter 4 in calculating building losses. Specifically, we use the weighted ground motion intensities (as used in the USGS national seismic hazard maps (NSHM)), the soil amplification factors of Dobry et al (2000), and nominal values of the building vulnerability parameters.

5.1.2.1 Regional Seismicity and Earthquake Occurrence Rates

The earthquake recurrence model is an adaptation of the seismicity model of Frankel et al (2002) used to develop the 2002 National Seismic Hazard Maps. For the CUS, Frankel et al used a spatially smoothed "distributed" seismicity model based on historical seismicity and a fault-

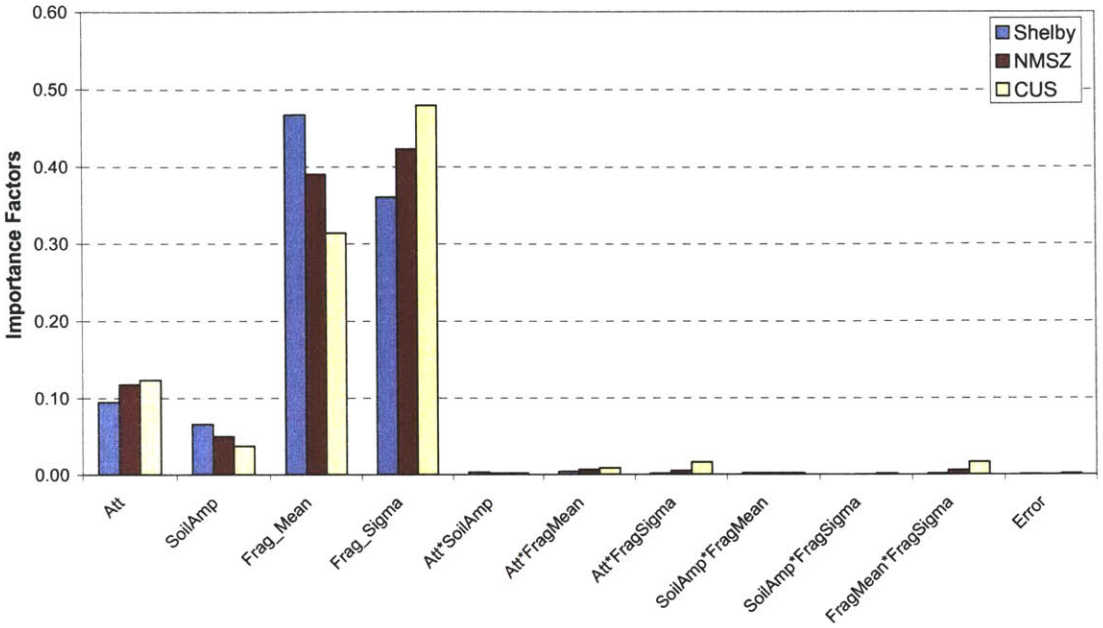

Figure 5-1: Importance Factors for Scenario Earthquake M700_3550_9000

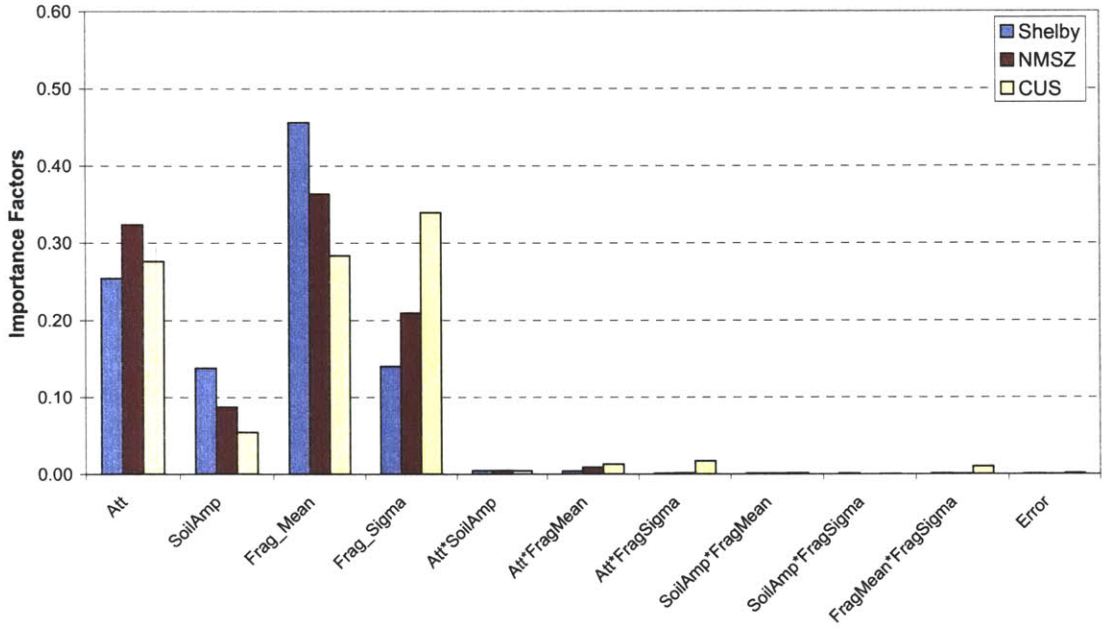

Figure 5-2: Importance Factors for Scenario Earthquake M750_3550_9000

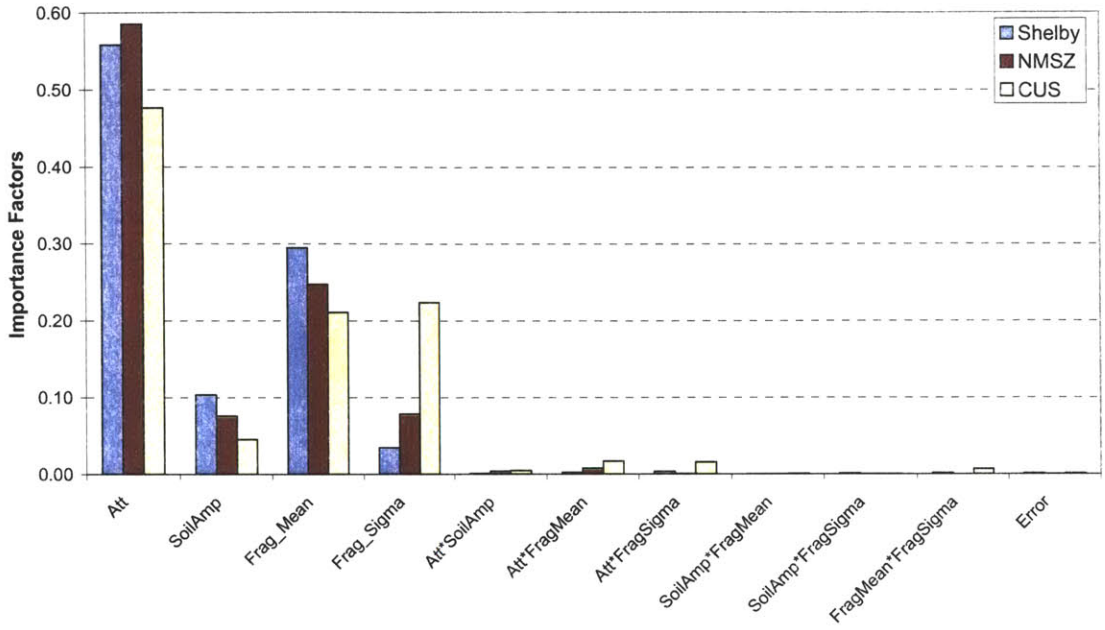

Figure 5-3: Importance Factors for Scenario Earthquake M800_3550_9000

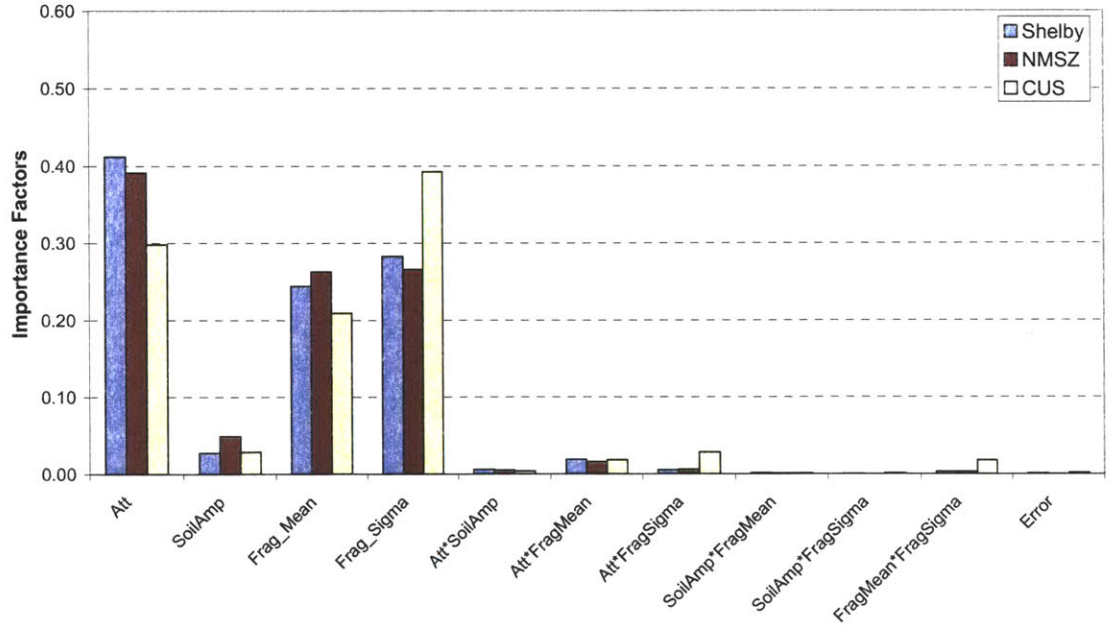

Figure 5-4: Importance Factors for Scenario Earthquake M750_3600_9000

based model for the NMSZ; see Chapter 3. For generating loss risk curves, we use the same seismicity models with some simplifications.

From the Frankel et al model, we have extracted the a-values for the region that extends from -88.0 to -92.0 degrees longitude and from 34.0 to 38.0 degrees latitude. Discretization is at 0.1 degree (approximately 11.1km) intervals. There are 1,681 discretization points inside the defined region. At each of these points, we consider earthquakes with moment magnitudes between M5.0 and M7.5 at magnitude intervals of $\Delta M = 0.5$. We use these large magnitude intervals to limit the number of earthquakes and the computational effort. Hence, a total of 10,086 earthquakes are used to represent the historical or distributed seismicity within the region.

For modeling characteristic earthquakes in NMSZ, we have used the three USGS pseudo faults. These S-shaped faults do not represent real faults but are intended to encompass the area of highest historic seismicity. In the USGS NSHMs, the characteristic earthquakes on these faults have been assigned a combined return period of 500years. The central fault has been given twice the rate of each of the side faults. Thus the effective rates are 1.0e-03 per year for the central fault and 5.0e-4 per year for each side fault. The characteristic magnitudes considered are M7.3, M7.5, M7.7, and M8.0 with assigned weights of 0.15, 0.20, 0.50, and 0.15, respectively. The resulting hazard is approximately equal to that from a single characteristic magnitude of M7.7.

In the development of the USGS NSHMs, it was conservatively assumed that an entire fault ruptures independent of the magnitude. Hence, it was postulated that the characteristic earthquake in NMSZ is not a single event but a sequence of events along the entire length of a fault. In this study, we use the above characteristic earthquakes with the same magnitudes and assigned recurrence rates. However, we assume independence of all the earthquake events and therefore consider partial rupture of the faults. The median fault rupture lengths are calculated from Wells and Coppersmith (1994). This gives rupture lengths of 74, 97, 127, and 190km for M7.3, M7.5, M7.7, and M8.0, respectively. The total fault length ranges from 230 km to 255km for the three faults.

For a given magnitude we discretize location by sliding one end of the rupture zone by increments of 5km along each fault. We assign equal rate to each of these rupture events, which is obtained by dividing the recurrence rate of each fault and each magnitude by the total number of discrete rupture locations along the fault. Hence,

$$\lambda_{eq}(M=m,F=f)=w_M(m)w_F(f)\frac{(L_F-L_{rup})}{\Delta L}\lambda_{eq,NMF} \tag{5.1}$$

where

$w_M(m)$ weight assigned to characteristic magnitude m

$w_F(f)$ weight assigned to fault f

L_F total fault length

L_{rup} rupture length

ΔL incremental distance between consecutive earthquake locations on fault, ($\Delta L = 5km$)

We use the above earthquake rates and the associated calculated building losses to generate loss risk curves and calculate expected annual losses. The expected annual loss, EAL, measures the average yearly loss when one accounts for the frequency and severity of different losses. In our case, EAL is simply calculated from

$$EAL=\sum_{eq=1}^{N_{eq}}\lambda_{eq}L_{eq} \tag{5.2}$$

5.1.2.2 Building Loss Risk Curves with Parameters Fixed to Nominal Values

For each earthquake, we calculate the building losses for Shelby County and the NMSZ region and sort them in ascending order. Starting with the highest loss event, we sum up the occurrence rates of the earthquakes to calculate the loss exceedance rate.

The resulting loss risk curves for Shelby County and NMSZ are shown in Figure 5-5. Also shown in the figures are loss curve approximations using the ground motions from the USGS probabilistic seismic hazard maps for different return periods. When probabilistic hazard maps are used in loss calculation, we used vulnerability parameters derived from HAZUS fragility curves specifically derived for this purpose. These curves are derived without considering the uncertainty in ground motion intensity as this uncertainty component is already included in calculation of the probabilistic ground motions.

For both regions, the losses obtained from our analysis are lower than the losses from USGS PSHMs. For return periods shorter than 500years, the general shape of the curves are in better agreement but the two curves are more dissimilar for return periods longer than 500 years. There are several reasons for these observed differences. First, in generating our loss risk curves we have used the weighted median ground motions obtained from attenuation relations, whereas the USGS hazard curves consider each of these relations separately in calculating the seismic hazard. Second, we have assumed partial rupture of the faults (independent events), wheras USGS hazard curves assumes complete rupture of the NMSZ faults. As the calculated rupture lengths for some of the characteristic earthquakes are much shorter than the total length of the faults, one should expect to have higher losses when using USGS PSHMs. Finally, we have used point sources to represent distributed seismicity, wheras USGS uses finite fault ruptures with random orientation for magnitudes above M6.0. Also, the hazard values combine the effects of different earthquakes.

To investigate the influence of assuming complete rupture of the faults, we have generated a second set of loss risk curves using only 4 earthquakes on each of the NMSZ faults, assuming entire rupture of the faults. The loss risk curves for this case are shown in Figure 5-6. The shape of the loss risk curves changes significantly when assuming full rupture of the faults as was done in the USGS NSHMs and agreement between the two sets of curves improves. However, there are still some differences between our loss-risk curves and the curves obtained from the USGS probabilistic ground motions, especially for the NMSZ. In both cases, the losses for return periods below 500 years are smaller in scenario based loss risk curves. The differences suggest that using weighted ground motion medians rather than the medians from each attenuation relation has a significant effect on the loss risk curve. Also, the use of point rather than finite fault sources for distributed seismicity may contribute to the differences at return periods below 500 years.

Using the loss risk curves, we calculate EAL for the above two cases in which partial or full rupture of the NM faults is assumed; see Table 5-4. When partial rupture of NMSZ faults is assumed, the EAL for Shelby County and the NMSZ are $20.4M/year and $74.6M/year, respectively. Figure 5-7 shows the relative contribution of the seismic sources on EAL of the two regions. The contribution of distributed seismicity to EAL is about 30% for both regions, with

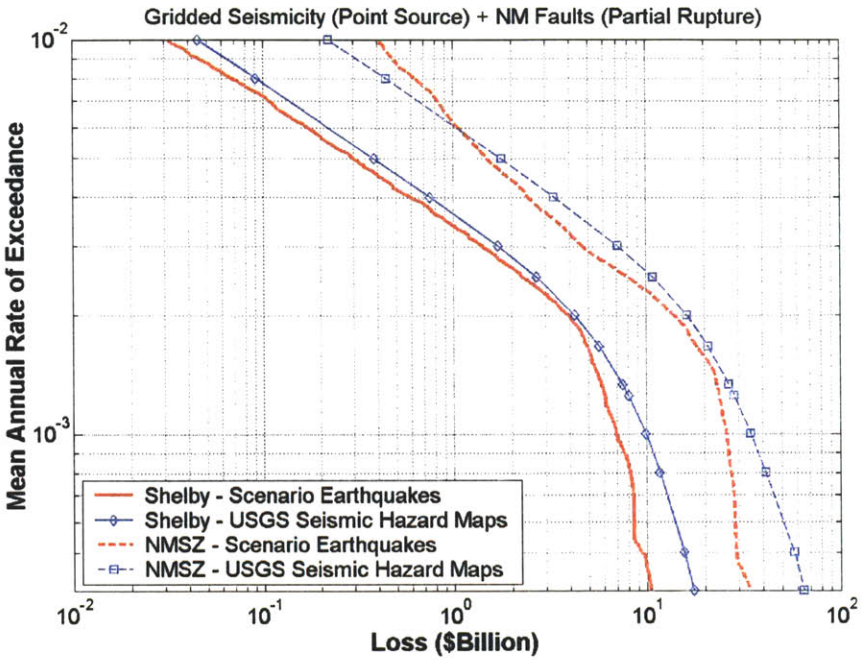

Figure 5-5: Loss Risk Curves for Shelby County and the NMSZ Region - Partial Rupture of NMSZ Faults

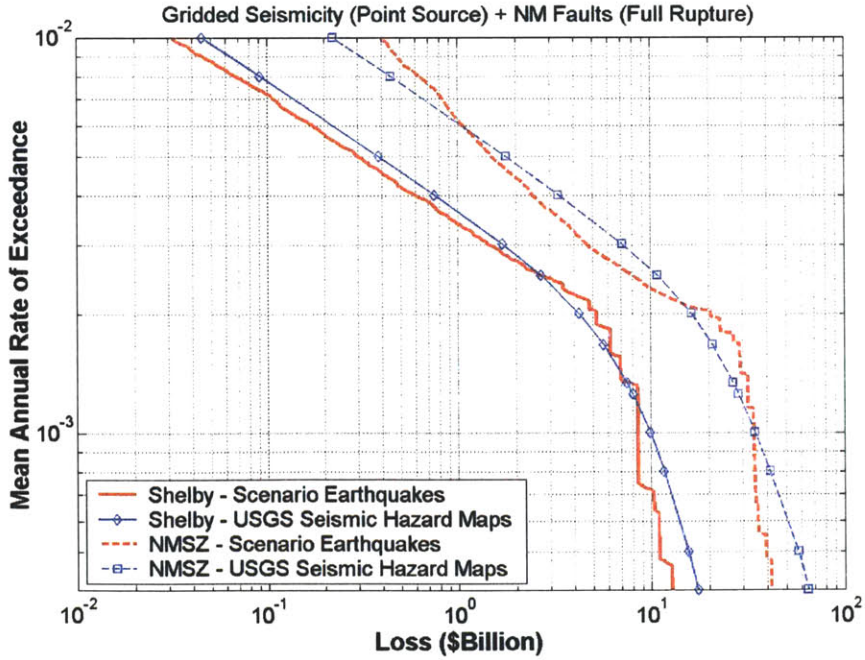

Figure 5-6: Loss Risk Curves for Shelby County and the NMSZ Region– Complete Rupture of NMSZ Faults

Table 5-4: EAL for Shelby County and the NMSZ Region

EAL ($M/year)	Partial Rupture		Complete Rupture	
	Shelby	NMSZ	Shelby	NMSZ
Total	20.361	74.637	24.105	89.973
NMF SE	5.040	14.977	6.996	19.911
NMF Central	6.669	25.367	8.080	32.408
NMF W	2.539	11.744	2.917	15.105
Distributed Seismicity	6.112	22.549	6.112	22.549

the remaining 70% originating from characteristic NMSZ events. Among, the NMSZ faults (NMF), the central one contributes more than the side faults since it is assigned twice the rate than the other two. Also, the relative contribution of the eastern NMF is larger than the western NMF since the eastern fault is closer to Shelby County where there is a large building inventory. Similarly, the relative contribution of the eastern NMF to the EAL of Shelby County is larger than to that of the NMSZ region, 25% vs. 20%, respectively.

Figure 5-8 shows the relative contribution of distributed seismicity earthquakes to EAL of Shelby and the NMSZ regions for different magnitudes. Moment magnitude M7.5 earthquakes account for about 8% of EAL for both regions, while the contributions of earthquakes with smaller magnitudes range between 3.5% and 5%. For characteristic NMSZ events, contribution of earthquakes on three NMFs with different magnitudes to EAL of Shelby County and the NMSZ region are shown in Figures 5-9 and 5-10, respectively. The contributions of NM earthquakes with different magnitudes to EAL are about the same for both regions, with M7.7 events accounting for about 50% of EAL originating only from NM earthquakes or 37% of overall EAL. The contributions of M8.0, M7.5, and M7.3 events are 16%, 11%, and %6, respectively.

When complete rupture of the NMFs is assumed, the EAL of the Shelby County and The NMSZ region increase by about 20% resulting in EALs of $24.1M/year and $90.0M/year, respectively; see Table 5-4. The relative contribution of NMSZ characteristic events to EAL increases from 70% to 75%. Assuming complete rupture of NMFs increases the contributions from NMSZ events for all magnitudes, but the increase in relative contribution of smaller magnitude NM events is larger as the difference between calculated fault rupture lengths and actual fault lengths

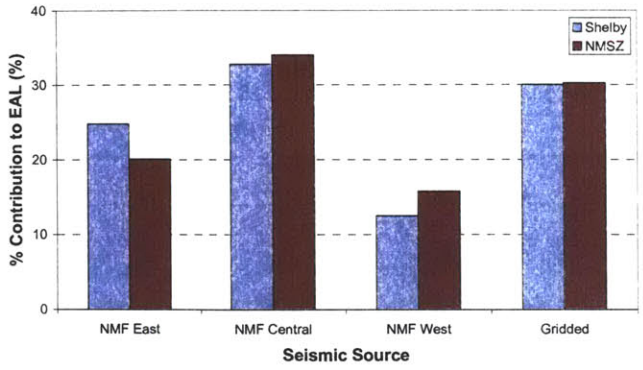

Figure 5-7: Relative Contribution of Seismic Sources to EAL of Shelby County and the NMSZ Region

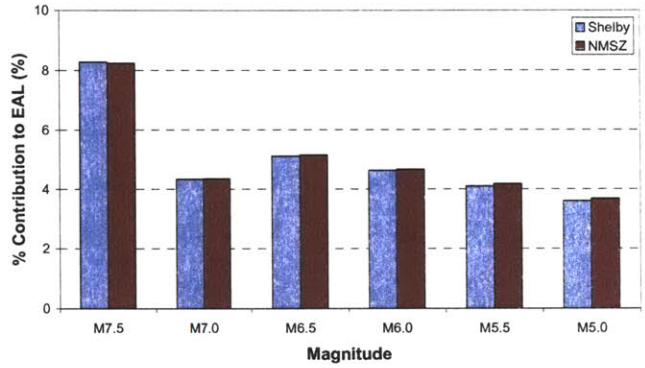

Figure 5-8: Relative Contribution of Distributed Seismicity to EAL of Shelby County and the NMSZ Region

is larger for these earthquakes. For example, the relative contribution of M7.3 events increases from 6% to 7.5% for Shelby County, whereas that of M8.0 events decreases from 16% to 15%; see Figure 5-11.

5.1.3 Building Loss Risk Curves Including Model and Parameter Uncertainty

The loss risk curves in the preceding section use the nominal parameters or component models and account for uncertainty only in earthquake magnitude and location. Here, we develop a new set of loss risk curves by considering uncertainty in the losses produced by given events. This uncertainty was quantified in Section 5.1.1, where it was found that model/parameter uncertainty contributes a random multiplication factor on the loss with a coefficient of variation of about 0.6. Assuming that this random factor has a lognormal distribution and is independent of magnitude and location, we develop a new set of loss risk curves using

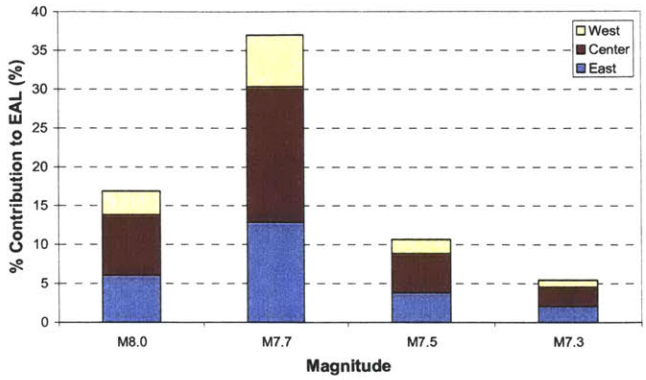

Figure 5-9: Relative Contribution of NMSZ Characteristic Earthquakes to EAL of Shelby County – Partial Rupture of NMSZ Faults

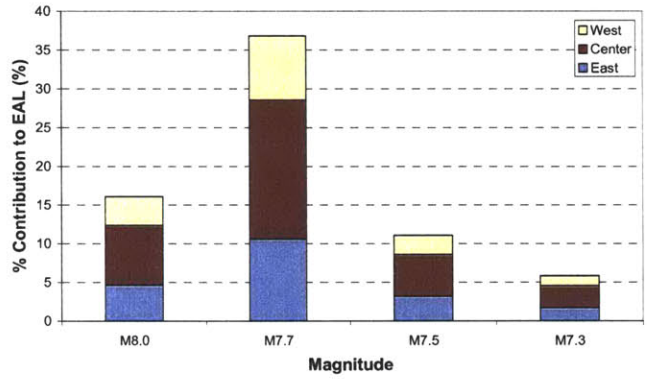

Figure 5-10: Relative Contribution of NMSZ Characteristic Earthquakes to EAL of the NMSZ Region – Partial Rupture of NMSZ Faults

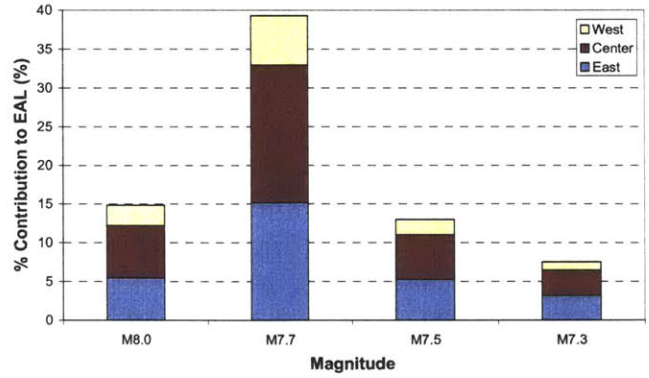

Figure 5-11: Relative Contribution of NMSZ Characteristic Earthquakes to EAL of Shelby County – Complete Rupture of NMSZ Faults

$$\upsilon[L_{Bldg,unc} \geq l] = \int_0^\infty \upsilon[L_{Bldg} \geq l'] f_{LN,Bldg}(l/l')dl' \tag{5.3}$$

where

$\upsilon[L_{Bldg,unc} \geq l]$ is the rate of exceedance of building loss l including model/parameter uncertainty

$\upsilon[L_{Bldg} \geq l']$ is the rate of exceedance of building loss l without model/parameter uncertainty

$f_{LN,Bldg}$ pdf of lognormal distribution of factor for model/parameter uncertainty in building loss

The loss risk curves for Shelby County and NMSZ that include model/parameter uncertainty are shown in Figure 5-12. The inclusion of model/parameter uncertainty results in a higher exceedance rate for a given loss level. The increases are especially significant for return periods above about 500 years. The expected annual loss (EAL) for Shelby County increases 34% from \$20.4M/year to \$27.4M/year. The percent increase in EAL of NMSZ is about the same, \$74.6M/year vs \$100.2M/year.

We also calculated loss risk curves using the results in Figure 5-6 that assume full rupture of the NMSZ faults; see Figure 5-13. The curves with and without model/parameter uncertainty touch each other for a return period of about 500year. The increase in the losses is especially significant for return periods above 750 years. Model/parameter uncertainty results in approximately 32% and 20% higher expected annual losses for Shelby County and the NMSZ region, respectively. The EAL of Shelby County increases from \$24.1M/year to \$32.5M/year and the EAL of NMSZ increases from \$90.0M/year to \$117.4M/year. The observed increases of 30-35% EAL illustrate the significance of model/parameter uncertainty in loss risk analysis.

5.2 Risk Curves for Business Losses

In this section, we develop risk curves for business losses, specifically for value added losses in Shelby County and the NMSZ region. Contrary to what has been done in the previous section for building losses, we do not calculate business losses using a large number of possible future

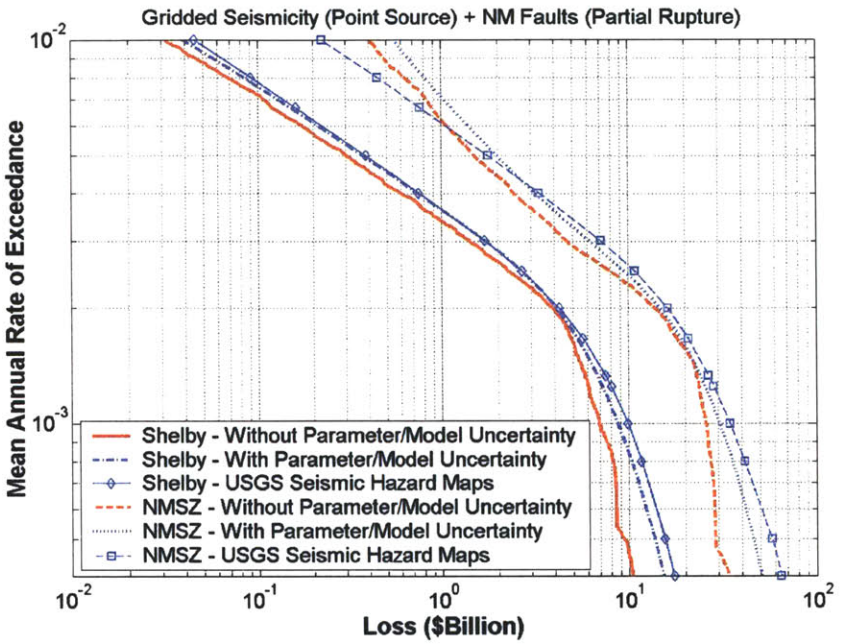

Figure 5-12: Building Loss Risk Curves for Shelby County and the NMSZ Including Parameter/Model Uncertainty (Point Source Distributed Seismicity, Partial Rupture of NMSZ Faults)

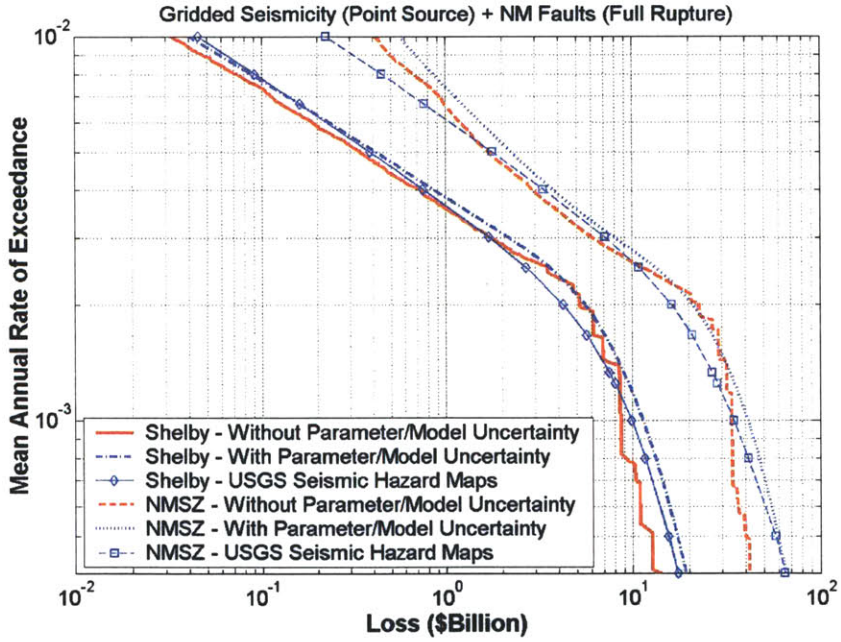

Figure 5-13: Building Loss Risk Curves for Shelby County and the NMSZ Including Parameter/Model Uncertainty (Point Source Distributed Seismicity, Complete Rupture of NMSZ Faults)

earthquakes, as this method is computationally not feasible. Instead, we use an empirical relation between business and building losses to convert risk curves for building losses to risk curves for business losses.

5.2.1 Relation between Business and Building Losses

The regional business losses mainly depend on the recovery time of the damaged local businesses. As the recovery time of the businesses heavily depends on the damage level of the buildings, one may suspect the existence of an approximate relation between regional business losses and regional building losses. Although there are other factors affecting the business losses, the dominant factor is the level of building damage; see Chapter 3.

To check the validity of the assumption, we plot value added loss against building loss in Shelby County and the NMSZ region, for 35 scenario earthquakes with different locations and magnitudes. These scenario earthquakes include events modeled as point sources at different locations within the NMSZ region or as line sources on the three NMSZ faults. The events on the NMSZ faults have magnitudes M7.3, M7.5, M7.7, and M8.0, while the magnitudes of the events modeled as point sources range between M6.0 and M8.0.

The results are shown in Figures 5-14 and 5-15 for Shelby County and the NMSZ region, respectively. Also shown are linear functions fitted to the data, with analytical form

$$L_{VA}^{Shelby} = 0.673(L_{Bldg}^{Shelby}) \tag{5.4}$$

$$L_{VA}^{NMSZ} = 0.696(L_{Bldg}^{NMSZ}) \tag{5.5}$$

In both cases the fit is very good. The total value added losses for Shelby County and the NMSZ region are about 65-70% of the total building losses for the two regions.

Since the evaluation of business losses is much more computationally intensive than the estimation of building losses, we do not perform ANOVA to analyze the contribution of different parameters/models to overall uncertainty in business losses. Rather, we assume that the variation in business loss given building loss can be represented by a multiplicative factor with mean value 1.0 and coefficient of variation 0.6. However, this assumption should be validated through further analysis in future studies.

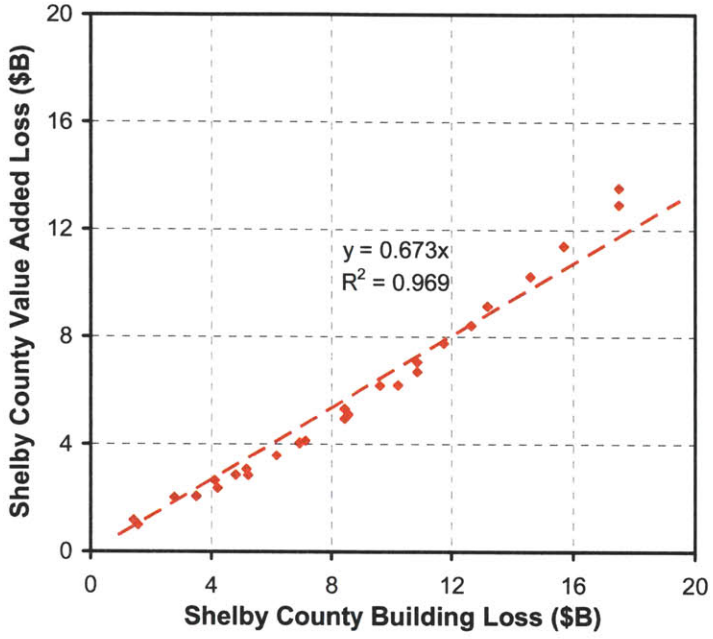

Figure 5-14: Total Value Added Loss vs Total Building Loss in Shelby County

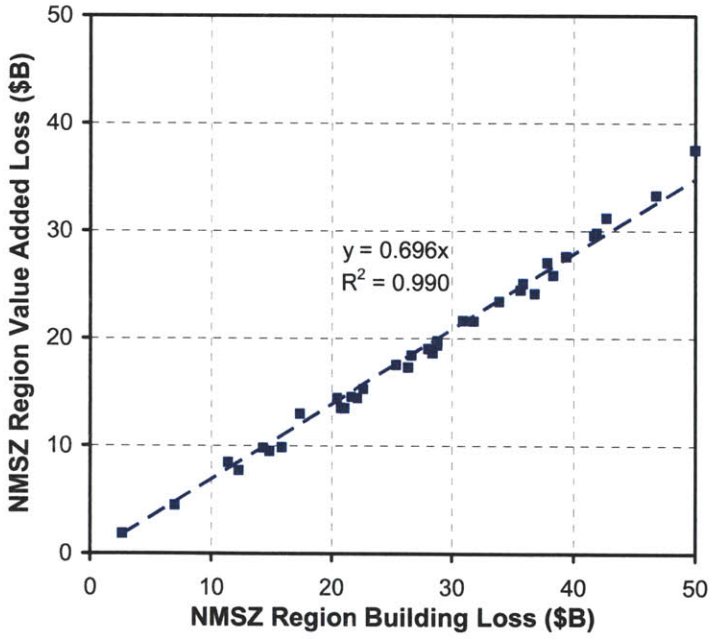

Figure 5-15: Total Value Added Loss vs Total Building Loss in NMSZ Region

5.2.2 Business Loss Risk Curves

Next we use Eqs. (5.4) and (5.5) to develop risk curves for business losses. We assume that model/parameter uncertainty contributes a random multiplication factor on the business loss for given building loss, i.e.

$$L_{VA,unc} = L_{Bldg,unc}\varepsilon_{VA|Bldg} \tag{5.6}$$

where

$\varepsilon_{VA|Bldg}$ is the random multiplication factor for business losses for given building loss with expected value equal to the coefficients in Eqs. (5.4) and (5.5) and coefficient variation 0.6.

Assuming that this random factor has a lognormal distribution and is independent of magnitude and location, we develop a new set of loss risk curves using

$$\upsilon[L_{VA,unc} \geq l] = \int_0^\infty \upsilon[L_{Bldg,unc} \geq l']f_{LN,VA|Bldg}(l/l')dl' \tag{5.7}$$

where

$\upsilon[L_{VA,unc} \geq l]$ is the rate of exceedance of value added loss l including model/parameter uncertainty

$f_{LN,VA|Bldg}$ pdf of $\varepsilon_{VA|Bldg}$

The value added loss risk curves for Shelby County and NMSZ that include model/parameter uncertainty are shown Figure 5-16. The expected annual value-added losses for Shelby County and the NMSZ region are \$25.3M/year and \$86.7M/year, respectively. When complete rupture of the NMSZ faults is assumed (see Figure 5-17) the expected annual value-added losses for the two regions increase to \$30.0M/year and \$103.8M/year. In both cases, the expected annual value-added losses are only slightly less than the expected annual losses for buildings.

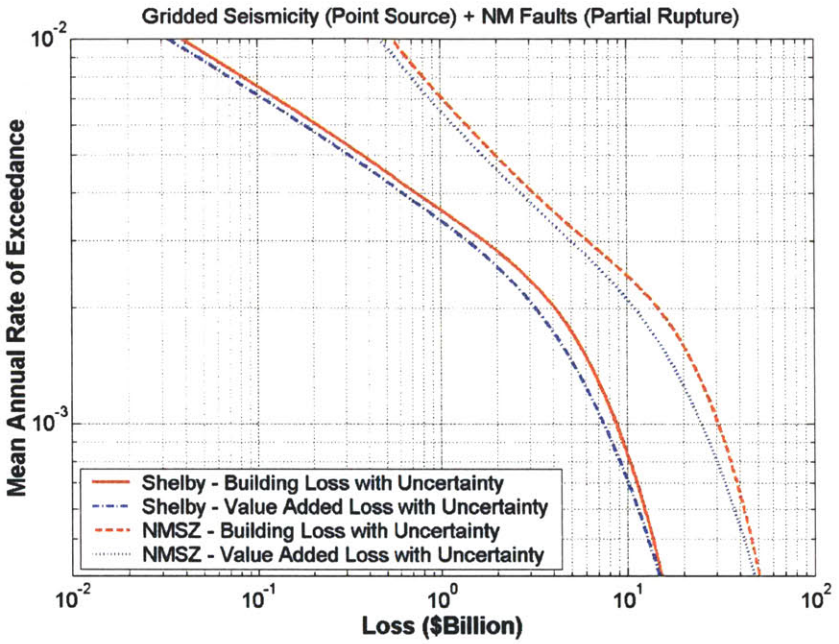

Figure 5-16: Value Added Loss Risk Curves for Shelby County and the NMSZ Including Parameter/Model Uncertainty (Point Source Distributed Seismicity, Partial Rupture of NMSZ Faults)

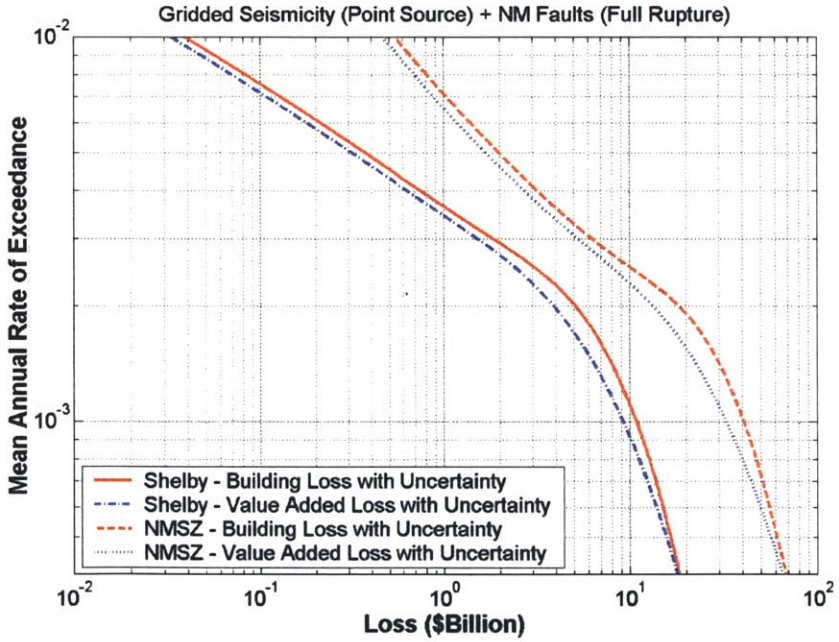

Figure 5-17: Value Added Loss Risk Curves for Shelby County and the NMSZ Including Parameter/Model Uncertainty (Point Source Distributed Seismicity, Complete Rupture of NMSZ Faults)

5.2.3 Total Loss Risk Curves

Having separately developed risk curves for building and value added losses, we develop risk curves for total economic losses. As value added loss is expressed as a fraction of building loss, the total loss is simply

$$L_{Total,unc} = L_{Bldg,unc}(1+\varepsilon_{VA|Bldg}) = L_{Bldg,unc}\varepsilon_{Total|Bldg} \tag{5.8}$$

where

$\varepsilon_{Total|Bldg}$ is the random multiplication factor for total loss for given building loss with $E\left[\varepsilon_{Total|Bldg}\right]=1+E\left[\varepsilon_{VA|Bldg}\right]$ and $Var\left[\varepsilon_{Total|Bldg}\right]=Var\left[\varepsilon_{VA|Bldg}\right]$

Using Eq.(5.8), we develop risk curves for total loss using

$$\upsilon[L_{Total,unc} \geq l] = \int_0^\infty \upsilon[L_{Bldg,unc} \geq l']f_{LN,Total|Bldg}(l/l')dl' \tag{5.9}$$

where

$\upsilon[L_{Total,unc} \geq l]$ is the rate of exceedance of total loss l including model/parameter uncertainty

$f_{LN,Total|Bldg}$ pdf of $\varepsilon_{Total|Bldg}$

The resulting loss risk curves for partial and complete rupture of the NMFs are shown in Figures 5-18 and 5-19 (Figure 5-18 and Figure 5-19). The expected annual total losses for Shelby County for the two cases are \$47.6M/year and \$56.4M/year, respectively. The corresponding expected annual total losses for the NMSZ region are \$174.8M/year and \$226.0M/year. Note that these values are smaller than the sum of the EAL for value added and buildings.

The previous results highlight the importance of the assumption regarding the rupture of the NMSZ faults, i.e. partial vs complete rupture. When complete rupture of the New Madrid faults is assumed, the EAL for Shelby County is 20% higher than when one assumes partial rupture. The corresponding relative increase in EAL of NMSZ is 30%. The differences in EAL between the two cases are significant, which emphasize the importance of more accurately modeling the seismicity of the NMFs that contribute most to the seismic hazard in the region.

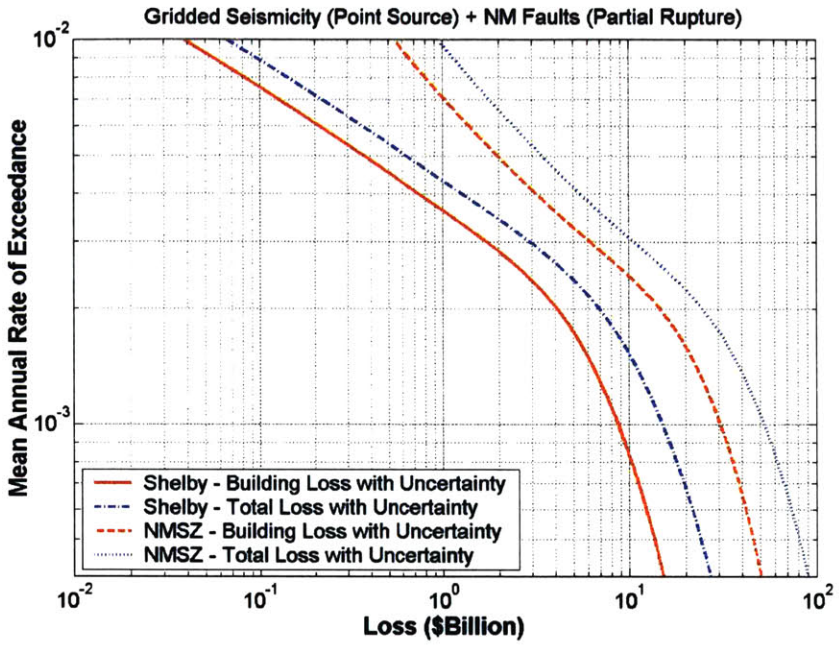

Figure 5-18: Total Loss Risk Curves for Shelby County and the NMSZ Including Parameter/Model Uncertainty (Point Source Distributed Seismicity, Partial Rupture of NMSZ Faults)

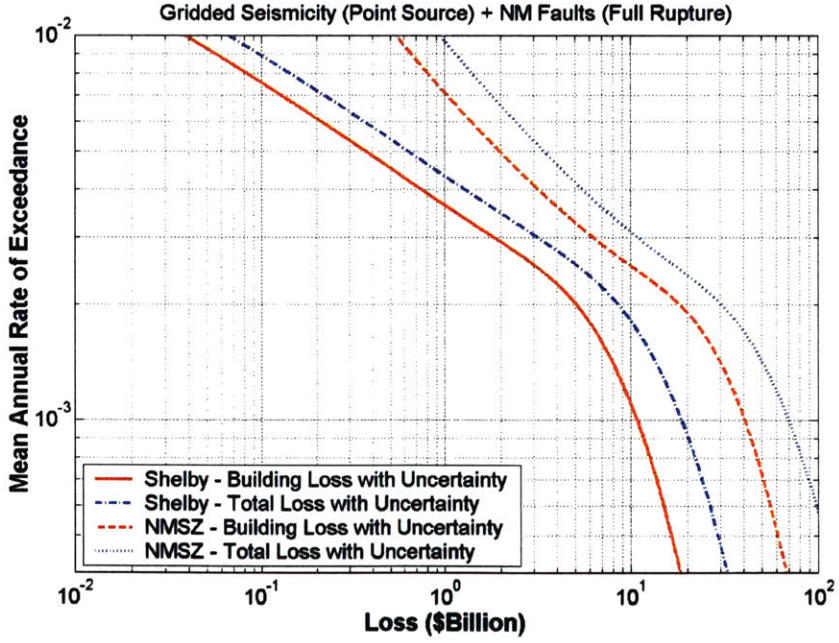

Figure 5-19: Total Loss Risk Curves for Shelby County and the NMSZ Including Parameter/Model Uncertainty (Point Source Distributed Seismicity, Complete Rupture of NMSZ Faults)

5.3 Assigning Hazard Consistent Rates to Scenario Earthquakes

In this section, we use an alternative simplified methodology to generate another set of loss risk curves and compare them with the ones developed in the preceding sections through more detailed analysis. The simplified methodology is built upon the work of Chang et al (2000) and Campbell and Seligson (2003). Limitations of these studies and the modifications and improvements made are discussed later in the text.

The methodology approximately represents seismic hazard in a region using ground motions from a few selected scenario earthquakes. The rates of the scenario earthquakes are assigned to best match seismic hazard at various locations. In doing so one may consider different levels of seismic hazard (e.g. 2%in 50years or 10% in 50 years) and different ground motion parameters (e.g. pga or spectral acceleration). In addition, one may assign weights depending on the losses from different localities in a scenario earthquake. This approach is applied here to evaluate risk curves for building and value added losses in Shelby County and the NMSZ region.

As mentioned above, the present methodology is built upon two previous studies, Chang et al (2000) and Campbell and Seligson (2003).

Chang et al. selected a set of scenario earthquakes to which they assigned hazard consistent rates to approximate regional seismicity. The methodology was applied to the Los Angeles highway network, which is distributed over an area of approximately 100km by 200km. 47 scenario earthquakes with magnitudes between M6.0 and M7.5 were selected along major seismic sources in the region. For each scenario earthquake, the highway system performance was evaluated to obtain a system performance degradation index. Also, the median pga at the centroids of all the census tracts in the region was calculated using attenuation relations.

To represent region seismicity, Chang et al used two sets of regional seismic hazard data, a probabilistic seismic hazard map for 10% in 50 years for peak ground acceleration and a seismic hazard curve for the Los Angeles City Hall. The two data sets provide complementary information, as the former indicates the spatial distribution of the seismic hazard in the region at one specified probability of exceedance and the latter indicates the probability distribution of lower versus higher local ground motion conditions. The methodology does not account for uncertainty in the ground motion attenuation relations.

In assigning the probabilities, Chang et al did not consider all the census tracts within the region but rather used 16 keyed census tracts distributed over the region, which were selected according to some criteria in order to capture the spatial dimension of the seismic events. Then, probabilities were assigned iteratively to the scenario earthquakes such that the resulting ground motion levels at the keyed census tracts conform to the probabilistic seismic hazard map and the ground motions at the Los Angeles City Hall site are consistent with the hazard curve at that site.

The methodology proposed by Campbell and Seligson (2003) is more quantitative and accounts for uncertainty in ground motion attenuation. It is assumed that the majority of the seismic risk comes from major faults, as the scenario earthquakes considered are limited to maximum credible earthquakes (MCE) with moment magnitudes M6.5 and greater. It is also assumed that the relative contribution of each fault to the total system risk can be defined in terms of the recurrence frequency of MCE and the probability of observing the range of ground motion values of interest averaged over all the grid of points of the system. Due to the latter assumption, the methodology was applied to a relatively small system that consists of 40 census tracts in the southeast corner of Los Angeles Basin.

The methodology differs from that of Chang et al, as it considers a number of earthquakes with known recurrence rates and do not assign rates to earthquakes. They, first, find the contribution of each of these earthquakes to different ground motion levels, defined as bins, using attenuation relations and uncertainty in ground motion intensity. Then, average system wide hazard corresponding to a specified ground motion bin and average system wide probability of experiencing a ground motion value in the same bin from each MCE are calculated. For each ground motion bin, only those earthquakes that contribute 5% or more to the average system wide hazard obtained for that ground motion is selected. The result is a different set of scenario earthquakes for each ground motion bin.

As mentioned above, the work of Chang et al does not consider the uncertainty in attenuation relations and only a limited number of census tracts are considered in matching the probabilistic seismic hazard data. They use probabilistic ground motions for a single return period and seismic hazard curve at one location. Trying to match the probabilistic seismic hazard at all locations within the study region for more than one return period may result in assignment of different rates. Although the work of Campbell and Seligson is more objective compared to the work of

Chang et al, the averaging of the hazard and ground motions from scenario earthquakes limits the applicability of the methodology to smaller analysis regions. Moreover, Campbell and Seligson considers only one scenario event along a given fault line. For longer fault lines or for regions close to the fault lines, the uncertainty in location of the seismic events may become quite important.

These two studies are the first attempts to select a limited number of scenario earthquakes so that the seismic risk of spatially distributed systems can be evaluated with reasonable computational effort. But due to limitations mentioned above, there are certain areas that need further improvement in both of the studies. Next we propose some improvements over these methodologies and compare risk results with those from a more exhaustive seismicity model.

5.3.1 Proposed Methodology

The proposed methodology assigns rates to selected scenario earthquakes such that the resulting approximate hazard levels are consistent with the regional probabilistic seismic hazard. The methodology considers uncertainty in ground motion relations, which was not included in the method of Chang et al (2000), and uses probabilistic ground motions for multiple return periods. It is applicable to relatively large regions as the method does not involve averaging of ground motion hazard over the analyzed system as was done by Campbell and Seligson (2003).

As we have done in the initial sections of this chapter, an accurate approach to calculate seismic risk is to evaluate the system performance and losses for all possible future earthquakes. In this case, the expected annual loss is obtained

$$E[L_{Sys}] = \sum_{i=1}^{N_{eq}} L_{Sys}(l_{Sys} \mid q_i) p_i \tag{5.10}$$

where

N_{eq} is the number of all possible earthquakes.

p_i is rate of occurrence of scenario earthquake q_i.

$L_{Sys}(l_{Sys} \mid q_i)$ is total loss of the system for given scenario earthquake q_i.

Since the evaluation of system loss for all possible scenario earthquakes is computationally intensive, the current methodology identifies $\tilde{N}_{eq}$ scenario earthquakes $\tilde{q}_i$ and assigns occurrence rates $\tilde{p}_i$ to approximate seismic risk in the region such that

$$\sum_{i=1}^{\tilde{N}_{eq}} L_{Sys}(l_{Sys} \mid \tilde{q}_i)\tilde{p}_i \approx \sum_{i=1}^{N_{eq}} L_{Sys}(l_{Sys} \mid q_i)p_i \tag{5.11}$$

The set of selected earthquakes and their hazard consistent rates represent in approximation the seismic hazard in the region. Hence, for return periods of interest both the seismic hazard and the earthquake losses should be approximately equal to the values obtained from more detailed analysis.

The proposed methodology assumes that seismic risk is contributed mostly by the main faults within the region. Major faults are identified and a number of scenario earthquakes are defined along each fault line. The number of selected events and their magnitude may depend on the purpose of the study, seismicity of the region, and the properties of the system under investigation.

For each scenario earthquake, one evaluates the ground motion intensities at a set of analysis nodes and the resulting physical damage and economic losses. Then, the methodology assigns rates to the selected earthquakes such that the resulting approximate hazard levels are consistent with the regional probabilistic seismic hazard information. The required seismic hazard information includes probabilistic seismic hazard maps for different rates of exceedance. In addition, seismic hazard curves at specific sites may also be included.

First, ground motion hazard values $Y_j(T_k)$ for different analysis region j and specific return periods T_k are extracted from probabilistic seismic hazard maps of the region. Also, using ground motion attenuation relationships the natural logarithm of the selected ground motion parameter ($\ln y_{ij}$) and its logarithmic standard deviation σ_{ij} for the jth analysis region is calculated for each scenario earthquake $\tilde{q}_i$. The attenuation relationships may be those used in the development of the probabilistic seismic hazard maps.

Assuming a Gaussian distribution for $\ln y_{ij}$, the probability that y_{ij} exceeds $Y_j(T_k)$ is

$$P_{ij}(T_k) = \Pr(y_{ij} > Y_j(T_k)) = 1 - \Phi\left(z = \frac{\ln Y_j(T_k) - \ln y_{ij}}{\sigma_{ij}} \right) \tag{5.12}$$

where $\Phi(z)$ is the cdf of standard normal distribution.

Then, the contribution of earthquake i to the rate at which $Y_j(T_k)$ is exceeded is

$$\tilde{H}_{ij}(T_k) = \tilde{p}_i P_{ij}(T_k) = e^{\tilde{\lambda}_i} P_{ij}(T_k) \tag{5.13}$$

where

$\tilde{p}_i = e^{\tilde{\lambda}_i}$ is the annual occurrence rate assigned to the i th scenario earthquake.

$\tilde{\lambda}_i$ is the log occurrence rate of the i th scenario earthquake.

Summing $\tilde{H}_{ij}(T_k)$ from all scenario earthquakes, the total exceedance rate of $Y_j(T_k)$, $H(T_k)$ is

$$\tilde{H}_j(T_k) = \sum_{i=1}^{N_i} \tilde{H}_{ij}(T_k) = \sum_{i=1}^{N_i} \tilde{p}_i P_{ij}(T_k) = \sum_{i=1}^{N_i} e^{\tilde{\lambda}_i} P_{ij}(T_k) \tag{5.14}$$

One would like $\tilde{H}_{ij}(T_k)$ to be as close as possible to $1/T_k$. We use an optimization formulation to assign the log rates $\tilde{\lambda}_i$ to the scenario earthquakes such that

$$Min\left[\sum_{k=1}^{N_k} w_k \sum_{j=1}^{N_j} \left(\log\left(\tilde{H}_j(T_k)\right) - \log\left(1/T_k\right) \right)^2 \right] \tag{5.15}$$

where

w_k is the weight assigned to return period T_k, and

$\tilde{H}_j(T_k)$ is given by equation (5.14).

Depending on the system analyzed and the objective of the study, different weights can be used to give more importance to ground motions for certain return periods.

Next, we make two modifications to the above formulation and then show an application to the NMSZX region. The first modification assigns loss dependent weights w_j to the analysis regions and the second reduces the number of selected scenario earthquakes.

The above method gives equal weight to each analysis region. Since we are interested in estimating regional earthquake losses, it seems logical to assign different weights to the analysis regions depending on their relative contributions to the total regional loss. Hence we define the regional weights w_j as

$$w_j = \frac{\sum_{i=1}^{N_i} e^{\tilde{\lambda}_i} L_{ij}}{\sum_{j=1}^{N_j} \sum_{i=1}^{N_i} e^{\tilde{\lambda}_i} L_{ij}} \tag{5.16}$$

where

L_{ij} is the loss from the j th analysis region for the i th scenario earthquake.

One might want to reduce the number of scenario earthquakes as much as possible, especially while evaluating losses that require significant computational time as in the case of transportation lossess, while still producing a good fit to the hazard maps. To achieve this, a penalty on the sum of the log occurrence rates of the scenario earthquakes may be introduced, i.e.

$$\sum_{i=1}^{N_i} c_i \tilde{\lambda}_i \tag{5.17}$$

where c_i is the penalty assigned to the log occurrence rate of earthquake i.

With the introduction of above modifications, the optimality criterion becomes

$$Min\left\{\left(\sum_{k=1}^{N_k} w_k \sum_{j=1}^{N_j} w_j \left(\log\left(\tilde{H}_j(T_k)\right) - \log\left(1/T_k\right)\right)^2\right) + \left(\sum_{i=1}^{N_i} c_i \tilde{\lambda}_i\right)\right\} \tag{18}$$

of inserting the expressions for $\tilde{H}_j(T_k)$ and w_j in equations (5.14) and (5.16),

$$Min\left\{\left(\sum_{k=1}^{N_k} w_k \sum_{j=1}^{N_j} \left(\frac{\sum_{i=1}^{N_i} e^{\tilde{\lambda}_i} L_{ij}}{\sum_{j=1}^{N_j} \sum_{i=1}^{N_i} e^{\tilde{\lambda}_i} L_{ij}}\right) \left(\log\left(\sum_{i=1}^{N_i} e^{\tilde{\lambda}_i} P_{ij}(T_k)\right) - \log\left(1/T_k\right)\right)^2\right) + \left(\sum_{i=1}^{N_i} c_i \tilde{\lambda}_i\right)\right\} \tag{19}$$

where $P_{ij}(T_k)$ is given by Eq. (5.12).

A nonlinear programming solution algorithm, such as gradient method, can be used to find the log occurrence rates $\tilde{\lambda}_i$ that satisfy Eq. (19). In the following sections, we make an application to the NMSZ region and Shelby County and compare the approximate risk curves with the exact curves.

5.3.2 Application to NMSZ and Shelby County

To be consistent with the assumptions used in generating the USGS seismic hazard maps, the scenario earthquake selected for this study lie on the three USGS faults. We select a total of 12 scenario earthquakes on these faults and assume complete rupture of the faults. These 12 earthquakes consist of 4 earthquakes on each fault, with moment magnitudes M7.3, M7.5, M7.7, and M8.0. To limit the number of earthquakes, scenario earthquakes on locations other than the NMSZ pseudo faults were not considered. This should be a reasonable selection of scenario earthquakes for regions where most of the seismic hazard is contributed mainly by characteristic NMSZ earthquakes. For example, the contribution of NMSZ events to seismic hazard of Memphis, TN is about 75% for 2500 year return period. This contribution decreases as one gets away from the pseudo fault lines.

For each scenario earthquake, the ground motion intensities at the centroids of the analysis regions are calculated and stored. Building losses from each analysis region are also calculated and stored for weighting of the analysis regions. Building loss is the loss component chosen for weighting of the regions since calculation of building losses for given scenario earthquakes does not require much computational effort. Next section presents results obtained for the NMSZ region and Shelby County, using 2002 seismic hazard maps and PGA as ground motion parameter.

5.3.3 Results for Shelby County and the NMSZ Region

Results for Shelby County and the NMSZ region are summarized in Tables 5-5 and 5-6. We have considered two cases with the same scenario earthquakes. In case 1, we did not impose any constraint, whereas in case 2, we imposed that the total rate of applied scenario earthquakes on the central fault should be twice the value common to the two side faults. In both cases, we set no constraint or weight on the contribution from different magnitudes. We used the USGS

Table 5-5: Hazard Consistent Scenario Earthquake Probabilities

Scenario Earthquake	Loss ($M)		p_i (x10^{-3})		
	Shelby	NMSZ	USGS	Case 1	Case 2
E_M800	17241.74	49477.82	0.075	0.213	0.249
E_M770	13537.77	38955.37	0.250	0.228	0.232
E_M750	11587.49	33208.96	0.100	0.240	0.130
E_M730	9201.16	26199.32	0.075	0.252	0.128
C_M800	10321.36	41001.5	0.150	0.202	0.228
C_M770	7611.83	31318.52	0.500	0.219	0.364
C_M750	6054.84	26375.39	0.200	0.231	0.563
C_M730	4447.76	20466.67	0.150	0.243	0.324
W_M800	8002.26	38739.74	0.075	0.196	0.163
W_M770	5325.20	29534.38	0.250	0.204	0.187
W_M750	4068.41	24587.64	0.100	0.210	0.189
W_M730	2881.35	18469.09	0.075	0.218	0.200
Total			**2.000**	**2.654**	**2.958**

seismic hazard maps for 10%, 5%, and 2% exceedance probability in 50 years, which corresponds to return periods of 475, 975, and 2475 years.

5.3.3.1 Hazard Consistent Probabilities for Selected Earthquakes

Table 5-5 shows the annual rates assigned to each of the scenario earthquakes, whereas Table 5-6 shows the ratios of the weighted average of the calculated hazard exceedance probabilities of the analysis regions to the exceedance probability of the ground motions used, e.g. 10% I n50 years. The total annual occurrence rate of scenario earthquakes is $2.65x10^{-3}$ and $2.96x10^{-3}$ for the two cases, which are both higher than the annual occurrence rate assigned to characteristic earthquakes on the NMSZ in development of seismic hazard maps.

Table 5-6 gives the ratio of the calculated exceedance frequencies to the exceedance frequencies used in representing seismic hazard, e.g. 1/2475 for 2% in 50 year exceedance probability. Although PGA was the ground motion parameter used in application of the methodology, the ratios of calculated to given hazard exceedance probabilities for 0.2sec and 1.0sec spectral accelerations corresponding to assigned probabilities are also given in Table 5-6.

Table 5-6: Ratios of Calculated to Given Ground Motion Exceedance Frequencies

Ratio of Calculated Hazard to Given Hazard	Case 1	Case 2
pga (10% in 50years)	0.872	0.981
pga (5% in 50years)	1.008	1.117
pga (2% in 50years)	1.167	1.267
Sa(0.2sec) (10% in 50years)	0.892	1.003
Sa(0.2sec) (5% in 50years)	1.027	1.142
Sa(0.2sec) (2% in 50years)	1.150	1.252
Sa(1.0sec) (10% in 50years)	0.973	0.981
Sa(1.0sec) (5% in 50years)	1.116	1.117
Sa(1.0sec) (2% in 50years)	1.164	1.267

The ratios of system wide exceedance probabilities to the given ones are better for case 1 as no constraints were included in matching the seismic hazard. As seen from Table 5-6, the pga values for 10% in 50 year exceedance probability is slightly overestimated and the pga values for 2% in 50 year exceedance probability is slightly underestimated for case 1. The results obtained for 0.2sec spectral acceleration are similar to those obtained for pga, but the seismic hazard for 1.0 sec spectral acceleration is slightly higher, which is mainly due to the differences in the attenuation characteristics of short and long period ground motions. Figure 5-20 shows the seismic hazard curve for PGA for Memphis, TN calculated from our analysis together with the values obtained from USGS NSHMs. The two curves are in general agreement especially between the return periods used in the analysis, i.e. 500 to 2500 years. The ground motions for return periods over 2500 years are overestimated whereas the ground motions for return periods below 500 years are underestimated.

In case 2, the ratios of calculated to given exceedance probabilities are higher for return periods other than 475 years. This is a result of the additional constraint applied in this case to limit the weight the occurrence rates on the three faults. As we apply adaptive weighting based on losses calculated in each of the scenario earthquakes, in general we obtain higher weights for the analysis regions in Shelby County since the building inventory and losses from earthquakes are much higher compared to other regions. This is reflected in assignment of the probabilities to scenario earthquakes.

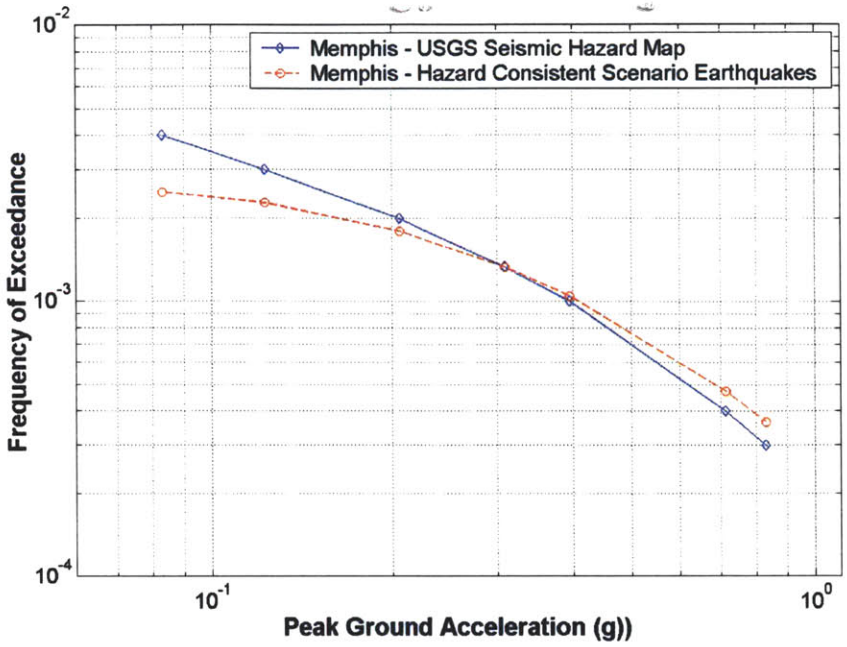

Figure 5-20: Seismic Hazard Curve for Memphis, TN

5.3.3.2 Loss Risk Curves from Hazard-Consistent Earthquake Scenarios

Using the optimized occurrence rates of the selected scenario earthquakes and the corresponding losses, we generate loss risk curves for Shelby County and the NMSZ region for Case 1; see Figure 5-21. Both curves are similar to those obtained by using detailed seismicity. The curves from hazard consistent earthquakes are slightly steeper than the curves obtained from detailed seismicity for lower return periods since only a limited number of earthquake scenarios with large magnitudes are used to represent seismic hazard. If the number of earthquakes were higher and if earthquakes with lower magnitudes were considered in the analysis, a smoother loss risk curve would be obtained.

In addition, there is better agreement between the loss risk curve obtained from limited number of earthquakes and the detailed seismicity in case of Shelby County. As discussed above, this is linked to the use of adaptive weighing in assigning probabilities to scenario earthquakes. Shelby County has a large inventory value and corresponding loss risk. As a result, higher weights are generally assigned to analysis regions in Shelby County compared to other regions in NMSZ. This allows better matching of seismic hazard for Shelby County compared to the NMSZ region through the analysis performed.

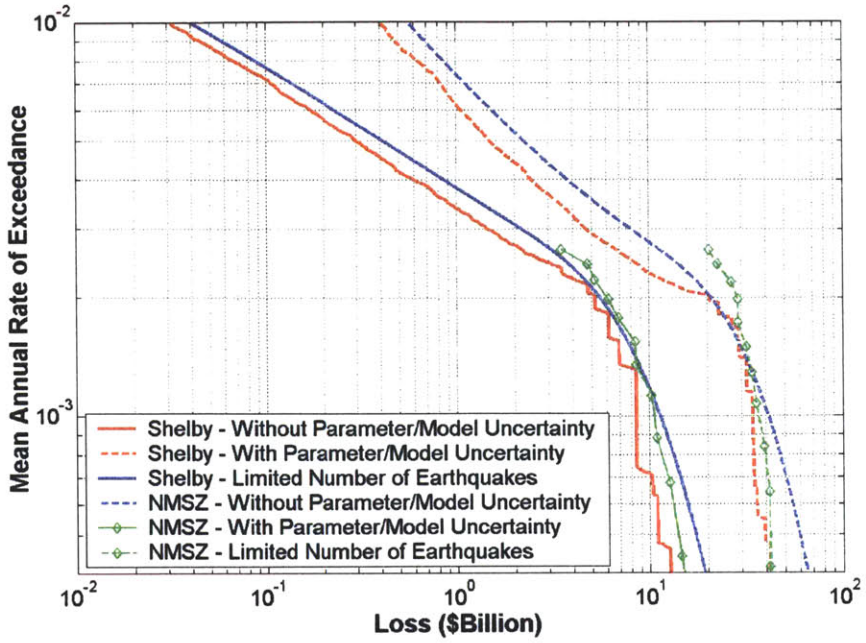

Figure 5-21: Building Loss Risk Curves for Shelby County and the NMSZ Region, Case 1

The EALs for buildings calculated by using the assigned scenario earthquake rates are $26.0M/year and $97.4M/year for Shelby County and the NMSZ region, respectively. The EALs previously obtained in Section 5.1 using the building loss risk curves from distributed seismicity and NMSZ faults were $24.1M/year and $90.0M/year when parameter/model uncertainty was not considered and $32.5M/year and $117.4M/year when parameter/model uncertainty is considered. The EALs are in general agreement as the seismic risk in these regions is dominated by these large magnitude characteristic earthquakes and the proposed analysis was able to provide EAL values closer to the ones calculated from much detailed analysis.

If we calculate expected annual value added loss for Shelby County and the NMSZ region using the assigned occurrence rates and the calculated value added losses for the 12 scenario earthquakes we obtain $15.8M/year and $61.9M/year, respectively (see Figure 5-22). These are much lower than the values calculated in Section 5.2, $30.0M/year and $103.8M/year, which were obtained by making use of building loss risk curves and the relation between value added and building losses. However, they include uncertainty both in building and value added losses, whereas the values calculated in this section do not.

If we generate a new set of loss risk curves for building and value added losses from detailed regional seismicity without considering any model/parameter uncertainty, we get expected

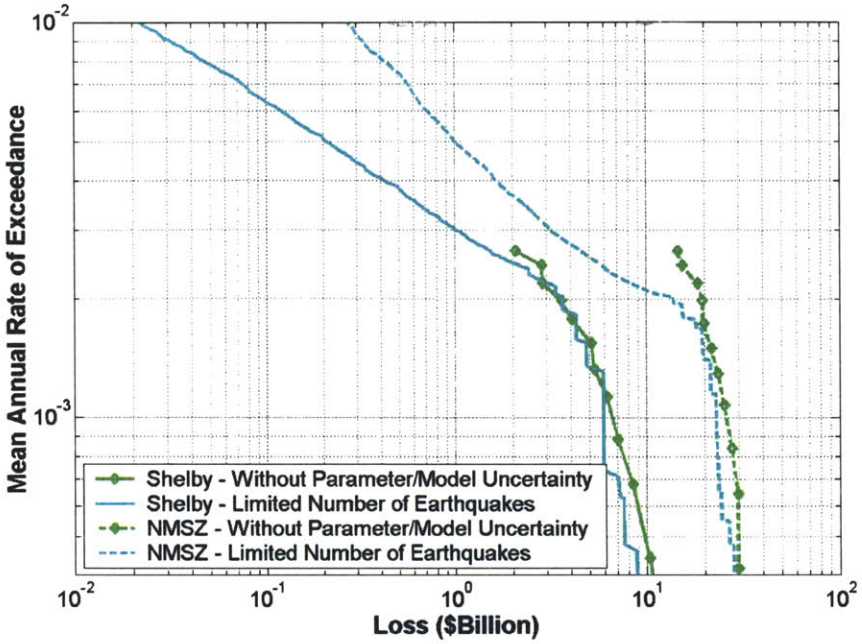

Figure 5-22: Value Added Loss Risk Curves for Shelby County and the NMSZ Region, Case 1

annual value added losses of $16.8M/year and $58.7M/year for Shelby County and the NMSZ region. The EALs obtained both for Shelby County and the NMSZ region are very close to the values obtained in this section. The percent difference among the expected annual value added losses is about 5%. The two sets of value added loss risk curves are shown in Figure 5-22. The risk curves obtained from a limited number of earthquakes match quite good with the curves obtained from more detailed analysis, especially for Shelby County.

Consideration of other scenario earthquakes with smaller magnitudes would allow more accurate representation of the seismicity and the loss risk. This would result in a closer match between the loss risk curves obtained from the proposed methodology and those obtained from more detailed analysis. Similarly, the EAL estimates can be expected to become more accurate with inclusion of increased number of scenario earthquakes.

However, even consideration of a limited number of scenario earthquakes are seen to provide reasonable estimates of EAL and general shape of the loss risk curve, especially for higher return periods. The proposed methodology may be used prior to more detailed analysis of the regional seismic risk in developing a better understanding of the seismic risk within the region

5.4 Concluding Remarks

In this chapter, we developed risk curves for building, value added, and total losses for Shelby County and the NMSZ regions. We first used regional seismicity and our loss estimation methodology with models/parameters at their nominal values to develop risk curves for building losses. Then we added model/parameter uncertainty to building losses using a constant coefficient variation of building losses based on the results of ANOVA for several scenario earthquakes. Then, we made use of a relation between value added losses and building losses to develop risk curves for value added losses in Shelby County and the NMSZ region. This relation was determined from loss results obtained under several scenario earthquakes with different magnitudes and locations. Finally, we combined building and value added losses to obtain total losses including the model/parameter uncertainty. For each case, we calculated expected annual losses. Table 5-7 summarizes the expected annual losses for building, value added, and total losses from Shelby County and the NMSZ region for partial and complete rupture of NM faults.

The results highlight the importance of considering uncertainty in risk assessment. Building losses increase by about 35% when model/parameter uncertainty is included in the analysis. The increase in value added losses is much higher, about 60-80%, since the expected annual value added losses are affected both by uncertainty in models used in building loss estimation and by uncertainty in models/parameters used for business loss estimation.

In addition, the rupture models for the characteristic NMSZ earthquakes are observed to have a significant effect on expected annual losses. Assuming complete rupture of the NM faults results in approximately 20% higher expected annual losses than those calculated by assuming partial rupture of the faults. The results are sensitive to the rupture length of these large magnitude characteristic NM earthquakes since they are the main seismic source contributing to the seismicity of the region. This relatively significant difference in seismic risk underlines the importance of more accurately modeling the seismic events in NMSZ.

In the last part of the chapter, we used another methodology to generate loss risk curves using a small number of scenario earthquakes. We introduced a formulation that assigns occurrence rates to a limited number of seismic events based on seismic hazard in the region so that the hazard generated by the selected events approximately matches the hazard from more detailed analysis. We applied the methodology to a set of 12 earthquakes on the NM faults to obtain hazard

Table 5-7: Summary of EALs for Shelby County and the NMSZ Region

EAL ($M/year)	Partial Rupture		Complete Rupture	
	Shelby	NMSZ	Shelby	NMSZ
Building Loss without Parameter/Model Uncertainty	20.4	74.6	24.1	90.0
Building Loss with Parameter/Model Uncertainty	27.4	100.2	32.5	117.4
Value Added Loss without Parameter/Model Uncertainty	13.7	51.9	16.8	58.7
Value Added Loss with Parameter/Model Uncertainty	25.3	86.7	30.0	103.8
Total Loss without Parameter/Model Uncertainty	34.1	126.5	40.9	148.7
Total Loss with Parameter/Model Uncertainty	47.6	174.8	56.4	226.0

consistent occurrence rates and then developed loss risk curves for building and value added losses using scenario earthquake results. Note that no model/parameter uncertainty is considered in this alternative method other than the ground motion hazard itself. Comparison of the risk curves and expected losses with the more detailed analysis of the previous section (without model/parameter uncertainty) shows that the results are comparable to each other.

This is the first time that the regional loss risk curves are being generated by using a detailed model of regional seismicity. This was made possible by the computational efficiency of the building loss estimation model. The developed loss risk curves matched very well with the ones calculated using the probabilistic seismic hazard maps. The risk curves obtained using a small number of scenario earthquakes also matched well with the previous ones. This approximate analysis may be used to represent seismic hazard for regions, where the regional seismic hazard is contributed by a limited number of seismic sources. It can also be used for systems of interest that are geographically distributed but in a smaller region.

The result that show that the existence of a relation between value added losses and building losses is important that it provides a first order estimate of the business losses without detailed analysis. This almost deterministic relation is valid for regions close to the earthquake epicenter. In these regions, business losses depend mainly on the functionality and recovery of the facilities, which is largely determined by the building damage level.

6 Evaluation of Mitigation Strategies

After developing loss risk curves for buildings and value added losses in the previous chapter, we now evaluate the effectiveness of several pre- and post-earthquake loss mitigation strategies. Pre-earthquake mitigation strategies include the retrofitting of selected building types or the upgrading of bridges on selected links. Post-earthquake mitigation strategies include faster recovery of buildings or bridges. In this study, we focus on the evaluation of the effectiveness of the above mitigation options and ignore the monetary and non-monetary costs of implementing these strategies. In addition, due to computational limitations, we generally evaluate the effectiveness of these alternative mitigation strategies for the scenario earthquake that was used in the sensitivity analysis in Chapter 4. For certain building retrofit strategies, we also look at the effect on building loss risk curves.

6.1 Pre-Earthquake Mitigation Strategies

We consider two main classes of pre-earthquake mitigation strategies: retrofit of buildings and retrofit of bridges. The scenario earthquake considered is a moment magnitude M7.5 event at (35.50W, 90.00N), which is about 35km north of Memphis, TN.

6.1.1 Retrofitting of Buildings

In this mitigation strategy, buildings in the CUS region are upgraded to the high-code design level with the exception of unreinforced masonry (URM) buildings, which are upgraded to high-code reinforced masonry (RM) buildings. To model present vulnerability conditions, we use the code level in HAZUS for Shelby County, which assigns most of the buildings to moderate code and the remaining ones to pre-code. Here, we consider different options including retrofitting all buildings, retrofitting buildings in particular structural classes, or retrofitting buildings in particular occupancy classes.

Table 6-1: Building Inventory Value for Different Building Occupancy and Structural Classes

Building Inventory Value	Shelby County		NMSZ Region	
	Value ($M)	% Total	Value ($M)	% Total
Total	59,845	100.0	202,888	100.0
Residential	49,015	81.9	168,909	83.3
Commercial	8,465	14.1	23,453	11.6
Industrial	1,364	2.3	6,095	3.0
Wood	44,369	74.1	147,891	72.9
Steel	3,201	5.3	10,558	5.2
Concrete	1,117	1.9	3,942	1.9
URM	9,316	15.6	29,450	14.5

Table 6-1 gives the total replacement value of different building occupancy and structural classes for Shelby County and the NMSZ region. Residential buildings account for 82% of the total building value within the two regions. The value of the commercial buildings in Shelby County and the NMSZ region are 14.1% and 11.6% respectively. The contribution of industrial buildings to the total inventory value is about less than 3%. Among various building structural types, wood structures account for the majority of the building value, (74%). URM and concrete buildings make up 15% and 5% of the total building value, respectively. The total value of steel buildings is less than 2%.

Retrofitting of All Building Stock

We first consider the option of retrofitting all building in the CUS region to high-code level (URM to RM). Although this is not a retrofit option that can be realized in short term as it involves billions of dollars worth of building stock, it might be considered as a long term mitigation objective which might be realized over time through changes in building codes. In addition, evaluation of this retrofit option provides a first order estimate of the maximum loss reduction that could be achieved by retrofitting buildings.

The building losses for unretrofitted and retrofitted (high-code level) conditions are given in Table 6-2. We also included the losses for other seismic design levels for comparison. Upgrading buildings to high-code design level results in a building loss reduction of about 35% for Shelby County and the NMSZ. In particular, the total building loss decreases from $24.2B to $15.3B.

Table 6-2: Building Losses for Retrofitted Buildings

Building Loss ($M)	Nominal	Retrofitted
Shelby County		
Building Losses	11,740	7,541
Structural	2,238	882
Non-Str. Drift Sensitive	4,394	2,625
Non-Str. Acceleration Sensitive	5,109	4,034
Contents	4,480	3,552
NMSZ		
Building Losses	21,656	14,006
Structural	4,307	1,834
Non-Str. Drift Sensitive	8,290	5,227
Non-Str. Acceleration Sensitive	9,060	6,945
Contents	7,982	6,125
CUS		
Building Losses	24,206	15,268
Structural	5,045	2,077
Non-Str. Drift Sensitive	9,458	5,915
Non-Str. Acceleration Sensitive	9,703	7,276
Contents	8,553	6,414

The decrease in building loss for Shelby County is $4.2B, which corresponds to 7.0% of the total building value within the region. The decrease in building losses for the NMSZ region, $7.6, is approximately equal to 3.8% of the total building value. The decrease in losses from structural components is about 55-60% and higher than that for drift-sensitive and acceleration sensitive nonstructural components. The latter ranges between 20% and 40%.

For this retrofit option, we also developed reduced loss risk curves for Shelby County and the NMSZ region. Figure 6-1 shows the risk curves before and after retrofit for the two regions. The expected annual building losses for the two regions for the retrofitted condition are $15.4M/year and $59.3M/year. The values before retrofitting were $24.1M/year and $90.0M/year, respectively. The retrofit of buildings results in 36% and 34% reduction in EALs of the two regions. When model/parameter uncertainty is included (see Figure 6-2), the EALs for the two regions increase to $20.7M/year and $77.2M/year, respectively. The corresponding values for the unretrofitted system were $32.5M/year and $117.4M per year. The percent reductions in

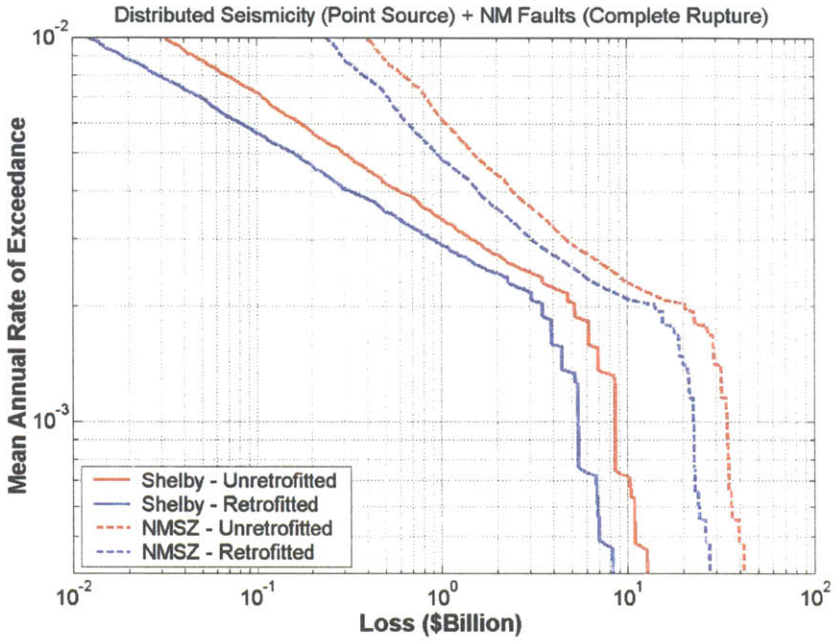

Figure 6-1: Reduced Loss Risk Curves for Shelby County and the NMSZ Region, All Buildings Upgraded to High-Code Level, Complete Rupture of NMSZ Faults

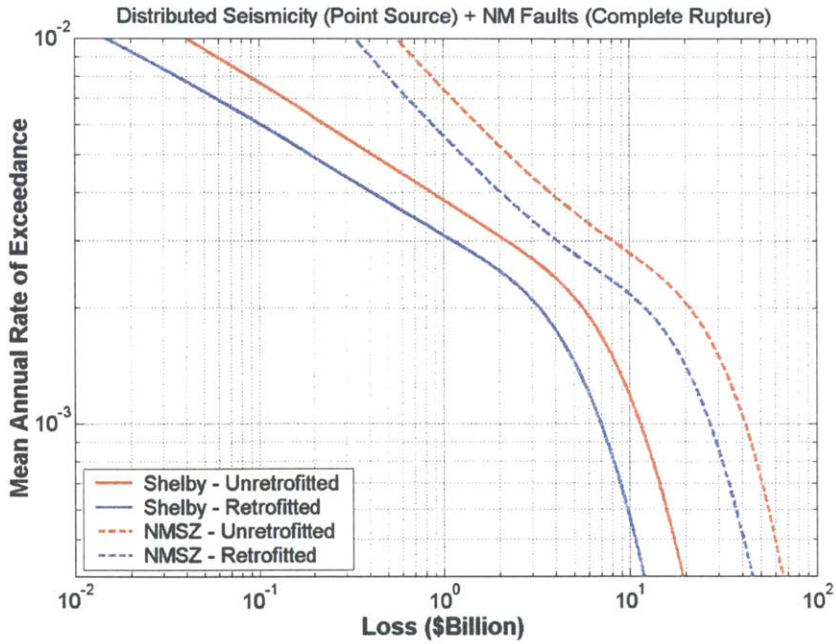

Figure 6-2: Reduced Loss Risk Curves for Shelby County and the NMSZ Region Including Parameter Uncertainty, All Buildings Upgraded to High-Code Level, Complete Rupture of NMSZ Faults

EALs are about the same with the previous case.

Business (value added) losses are shown in Table 6-3. The reduction in value added loss for Shelby County and the NMSZ region is about 45%, while that for the CUS region is about 50%. These percent reductions are much higher than those for building losses (35%). Note that the functionality and recovery rate of a building are evaluated based only on structural damage and that the percent change in the loss from structural building components is about 60%. The ratio of value added losses to building loss under retrofitted condition is about 55-58% for both Shelby County and the NMSZ region. The same ratio was about 65-70% when the default building code classification was used.

Retrofitting of Building Occupancy Classes

After quantifying the maximum loss reduction that can be achieved by retrofitting all the buildings in the CUS region, we now investigate the effect of retrofitting selected building occupancy classes. Retrofitting buildings that house certain industrial and commercial activities rather than all the buildings should be more cost efficient in reducing business losses. Here, we consider retrofitting of general building occupancy classes such as residential, commercial, and industrial without going into the subcategories of these occupancy classes.

The building losses after retrofitting buildings in these three general occupancy classes are given in Table 6-4. Retrofitting residential buildings results in the largest reduction in building losses, 23.7% (5.7% of the value of residential buildings), since residential buildings account for a larger portion of the building stock. Residential buildings are followed by commercial buildings, with a loss reduction of 9.9%, which corresponds to 13.7% of the value of the commercial buildings. The decrease in total building loss when industrial buildings are retrofitted is only 1.0% since these buildings are much fewer, however, the gains normalized by the industrial building value is 8.2%. The retrofitting of buildings for occupancy classes (such as agricultural, educational, and governmental) results in less than 1% total reduction in building losses. Comparing the loss reductions normalized with the value of the corresponding retrofitted buildings show that retrofitting of the commercial buildings (13.7%) is more effective than retrofitting of the residential (5.7%).and industrial buildings (8.2%). Although the highest loss reduction is obtained in case of residential buildings, the normalized gains are the smallest.

Table 6-3: Business Losses for Retrofitted Building Structural Classes

Business Loss ($M)	Nominal	Retrofitted
Shelby		
Production Losses	14,490	7,850
Direct	11,740	6,559
Indirect	2,750	1,292
Value Added Losses	7,789	4,268
Direct	6,309	3,560
Indirect	1,480	708
NMSZ		
Production Losses	27,164	14,984
Direct	22,220	12,570
Indirect	4,944	2,414
Value Added Losses	14,586	8,143
Direct	11,909	6,811
Indirect	2,677	1,331
CUS		
Production Losses	26,867	12,781
Direct	31,177	17,211
Indirect	-4,310	-4,430
Value Added Losses	15,447	7,596
Direct	16,891	9,369
Indirect	-1,443	-1,773
US		
Production Losses	-8,827	-5,493
Direct	31,177	17,211
Indirect	-40,004	-22,704
Value Added Losses	-339	-177
Direct	16,891	9,369
Indirect	-17,230	-9,545

Table 6-4: Building Losses for Retrofitted Building Occupancy Classes

Building Loss ($M)	Nominal	Building Occupancy Class		
		Residential	Commercial	Industrial
Shelby County				
Building Losses	11,740	8,958	10,583	11,628
Structural	2,238	1,469	1,758	2,185
Non-Str. Drift Sensitive	4,394	3,250	3,870	4,363
Non-Str. Acceleration Sensitive	5,109	4,239	4,955	5,080
Contents	4,480	3,760	4,317	4,460
NMSZ				
Building Losses	21,656	16,477	19,799	21,372
Structural	4,307	2,852	3,547	4,180
Non-Str. Drift Sensitive	8,290	6,214	7,505	8,222
Non-Str. Acceleration Sensitive	9,060	7,411	8,746	8,970
Contents	7,982	6,592	7,649	7,920
CUS				
Building Losses	24,206	18,156	22,063	23,868
Structural	5,045	3,275	4,160	4,899
Non-Str. Drift Sensitive	9,458	7,004	8,600	9,384
Non-Str. Acceleration Sensitive	9,703	7,877	9,302	9,585
Contents	8,553	7,016	8,128	8,471

The associated business losses, shown in Table 6-5, display a different pattern. The highest decrease in value added loss for Shelby County, the NMSZ region, and the CUS region occurs when commercial buildings are retrofitted. The reduction in value added losses for Shelby County and the NMSZ region are each about 30%, whereas that for CUS region is about 40%. Commercial buildings are followed by industrial buildings in business loss reduction. The retrofitting of industrial buildings reduces the value added losses by about 13% in each of the above regions. Retrofitting commercial and industrial buildings reduces both direct and indirect business losses.

Upgrading commercial buildings results in a higher loss reduction than upgrading industrial buildings since their damage level is mapped onto the largest economic sector considered in economic analysis including transportation, communications, utilities, services, and government services. This aggregate economic sector accounts for more than half of the total economic activity in the US (See Table 3-7). The functionality of the remaining economic sectors depends

Table 6-5: Business Losses for Retrofitted Building Occupancy Classes

Business Loss ($M)	Nominal	Building Occupancy Class		
		Residential	Commercial	Industrial
Shelby				
Production Losses	14,490	14,573	10,849	11,667
Direct	11,740	11,735	8,872	9,525
Indirect	2,750	2,838	1,977	2,142
Value Added Losses	7,789	7,826	5,383	6,774
Direct	6,309	6,306	4,421	5,512
Indirect	1,480	1,520	962	1,262
NMSZ				
Production Losses	27,164	27,624	20,609	22,074
Direct	22,220	22,204	16,912	18,051
Indirect	4,944	5,419	3,697	4,023
Value Added Losses	14,585	14,789	10,221	12,772
Direct	11,908	11,898	8,413	10,416
Indirect	2,677	2,890	1,808	2,356
CUS				
Production Losses	26,867	30,257	17,779	20,457
Direct	31,177	31,161	22,991	25,573
Indirect	-4,310	-904	-5,213	-5,117
Value Added Losses	15,447	16,991	9,196	13,154
Direct	16,891	16,881	11,501	14,870
Indirect	-1,443	110	-2,305	-1,717
US				
Production Losses	-8,827	-6,534	-8,007	-8,694
Direct	31,177	31,161	22,991	25,573
Indirect	-40,004	-37,695	-30,999	-34,267
Value Added Losses	-339	-213	-288	-327
Direct	16,891	16,881	11,501	14,870
Indirect	-17,230	-17,094	-11,789	-15,197

on the damage level of industrial buildings, except for the agriculture and construction sectors, which are assumed to be unaffected an earthquake.

Although the retrofitting of commercial buildings seems to be the most effective strategy, the decrease in value added loss when industrial buildings are upgraded is also significant (13%) especially considering that retrofit of industrial buildings results in just a 1% decrease in building losses. On the other hand, the 30% reduction in business loss when upgrading commercial buildings is accompanied by a 10% decrease in building losses.

Contrary to intervening on commercial and industrial buildings, the retrofitting of residential buildings results in slightly increased value added losses for Shelby County, the NMSZ region, and the CUS region. This counterintuitive increase in business loss is due to lower post-earthquake reconstruction spending as a result of residential building retrofit. Since residential buildings are not mapped onto any economic sector, retrofitting these buildings does not directly affect the functionality of any economic sector. For example, the direct business losses essentially remain unchanged when residential buildings are retrofitted; see Table 6-5. Although the functionality of residential buildings has some effect on the economic sectors through functionality interactions (see Chapter 3 and Chapter 4), this positive effect is not as significant as the negative effects of reduced reconstruction spending following the earthquake. However, when one considers the total earthquake loss at the national level, which is the sum of the building and value added losses for the US, the retrofitting of residential buildings minimizes the overall losses.

Retrofitting of Building Structural Types

Another pre-earthquake option for mitigation strategy is to retrofit buildings according to structural type. Here we consider upgrading of four different structural building types; wood, concrete, URM, and steel buildings.

Table 6-6 gives the building losses for the above retrofit options. The highest loss reduction is obtained from retrofitting URM buildings, which are relatively more vulnerable to earthquakes than other structural classes and which make up a significant portion of the building stock. The decrease in building loss is about 19%. URM buildings are followed by wood buildings, which account for majority of the building stock. The decrease in loss in this case is about 12%. Note

Table 6-6: Building Losses for Retrofitted Building Structural Classes

Building Loss ($M)	Nominal	Retrofitted Building Structural Class			
		Wood	Concrete	URM	Steel
Shelby County					
Building Losses	11,740	10,389	11,601	9,521	11,452
Structural	2,238	1,944	2,181	1,459	2,092
Non-Str. Drift Sensitive	4,394	4,046	4,321	3,287	4,244
Non-Str. Acceleration Sensitive	5,109	4,399	5,098	4,776	5,116
Contents	4,480	3,868	4,470	4,192	4,487
NMSZ					
Building Losses	21,656	19,088	21,405	17,726	21,113
Structural	4,307	3,737	4,206	2,917	4,031
Non-Str. Drift Sensitive	8,290	7,599	8,170	6,435	8,041
Non-Str. Acceleration Sensitive	9,060	7,752	9,029	8,374	9,041
Contents	7,982	6,832	7,953	7,381	7,966
CUS					
Building Losses	24,206	21,284	23,924	19,525	23,575
Structural	5,045	4,395	4,936	3,312	4,734
Non-Str. Drift Sensitive	9,458	8,606	9,331	7,327	9,193
Non-Str. Acceleration Sensitive	9,703	8,284	9,656	8,887	9,649
Contents	8,553	7,302	8,510	7,836	8,503

that the maximum loss reduction that can be achieved from retrofitting buildings was calculated earlier to be 35%. Wood structures are followed by steel structures in reducing building loss, (2.6%). However, when the loss reduction normalized by the building inventory value of the specific structural classes is considered, retrofitting of URM buildings prove to be the most efficient option, 23.8%. URM buildings are followed by concrete (12.5%) and steel buildings (9.0%). The smallest normalized loss reduction is obtained for wood buildings (3.0%).

In terms of business losses (see Table 6-7), the retrofitting of URM and steel buildings results in the highest loss reductions, 19% and 15%, respectively. Retrofitting wood or concrete buildings results each in a decrease of approximately 6-7% in value added losses. However, when the loss reductions are normalized by the building inventory value of the retrofitted structural classes, retrofitting of concrete and steel buildings are seen to be more effective than the other structural classes. The normalized business loss reductions for concrete and steel buildings are 50% and 38%, respectively. These high values are again due to the fact that concrete and steel buildings

Table 6-7: Business Losses for Retrofitted Building Structural Classes

Business Loss ($M)	Nominal	Retrofitted Building Structural Class			
		Wood	Concrete	URM	Steel
Shelby					
Production Losses	14,490	13,627	13,449	11,782	12,093
Direct	11,740	11,090	10,926	9,678	9,909
Indirect	2,750	2,537	2,524	2,104	2,184
Value Added Losses	7,789	7,261	7,218	6,300	6,589
Direct	6,309	5,916	5,866	5,177	5,391
Indirect	1,480	1,345	1,352	1,123	1,199
NMSZ					
Production Losses	27,164	25,902	25,740	22,613	22,846
Direct	22,220	21,114	20,813	18,562	18,759
Indirect	4,944	4,788	4,927	4,051	4,087
Value Added Losses	14,585	13,781	13,775	12,078	12,410
Direct	11,908	11,243	11,146	9,920	10,170
Indirect	2,677	2,538	2,629	2,158	2,240
CUS					
Production Losses	26,867	26,959	26,291	22,401	22,147
Direct	31,177	30,038	29,703	25,949	26,975
Indirect	-4,310	-3,078	-3,412	-3,549	-4,828
Value Added Losses	15,447	15,236	14,997	12,733	13,043
Direct	16,891	16,206	16,094	14,004	14,789
Indirect	-1,443	-969	-1,097	-1,271	-1,746
US					
Production Losses	-8,827	-7,736	-8,674	-7,074	-8,567
Direct	31,177	30,038	29,703	25,949	26,975
Indirect	-40,004	-37,774	-38,378	-33,024	-35,542
Value Added Losses	-339	-284	-313	-249	-313
Direct	16,891	16,206	16,094	14,004	14,789
Indirect	-17,230	-16,490	-16,407	-14,254	-15,102

account for a significant portion of industrial and commercial facilities. The normalized business loss reduction for URM buildings is about 16%, whereas that for wood buildings is about 1.2% for Shelby County.

6.1.2 Retrofitting of Bridges

A second option we consider is the retrofit of bridges on selected roadways. In this case, we upgrade the seismic design level of the bridges to California conditions. We have considered bridges on four selected routes within and around Shelby County as shown in Figure 6-3. The first route includes interstate highways within Shelby County. The second route is the section of I-40 connecting Memphis, TN to Nashville, TN. The third route is the section of I-40 connecting Memphis, TN to Little Rock, AR. The last route considered is the section of I-55 connecting Memphis, TN to St. Louis, MO, but only till the intersection of I-55 with I-57.

Since the retrofitting of bridges affects only slightly the business losses, here we report only the effect on transportation costs. For calculating transportation costs we first analyze the system in the damaged state and obtain the amount of transported commodities and the corresponding transportation costs. Then, we transport the same amount of commodities in a system in which the transportation link capacities are set at their pre-earthquake values. The difference in the total transportation cost between these two cases is reported as the transportation cost. This method is used rather than comparing the transportation costs with the pre-earthquake level since the economic activity levels following the earthquake are not the same as in the pre-earthquake state.

The transportation costs when different combinations of the above links are retrofitted are given Table 6-8. We have also included the option of upgrading all the network bridges considered in the analysis. When all bridges are retrofitted, a significant reduction in transportation loss can be achieved (a reduction by about 90% compared to the unretrofitted state). In comparison, when the four selected routes are retrofitted, the loss reduction is about 72%.

Among the other cases considered, we see that retrofitting the Memphis Interstate links and Memphis-Little Rock routes results in the maximum decrease in transportation cost, by about 45%. This route is followed by the Memphis-Nashville route in loss reduction. However, we do not observe any decrease in transportation costs when the section of I-50 connecting Memphis to St. Louis is retrofitted. This is a result of the transportation network formulation we use in our

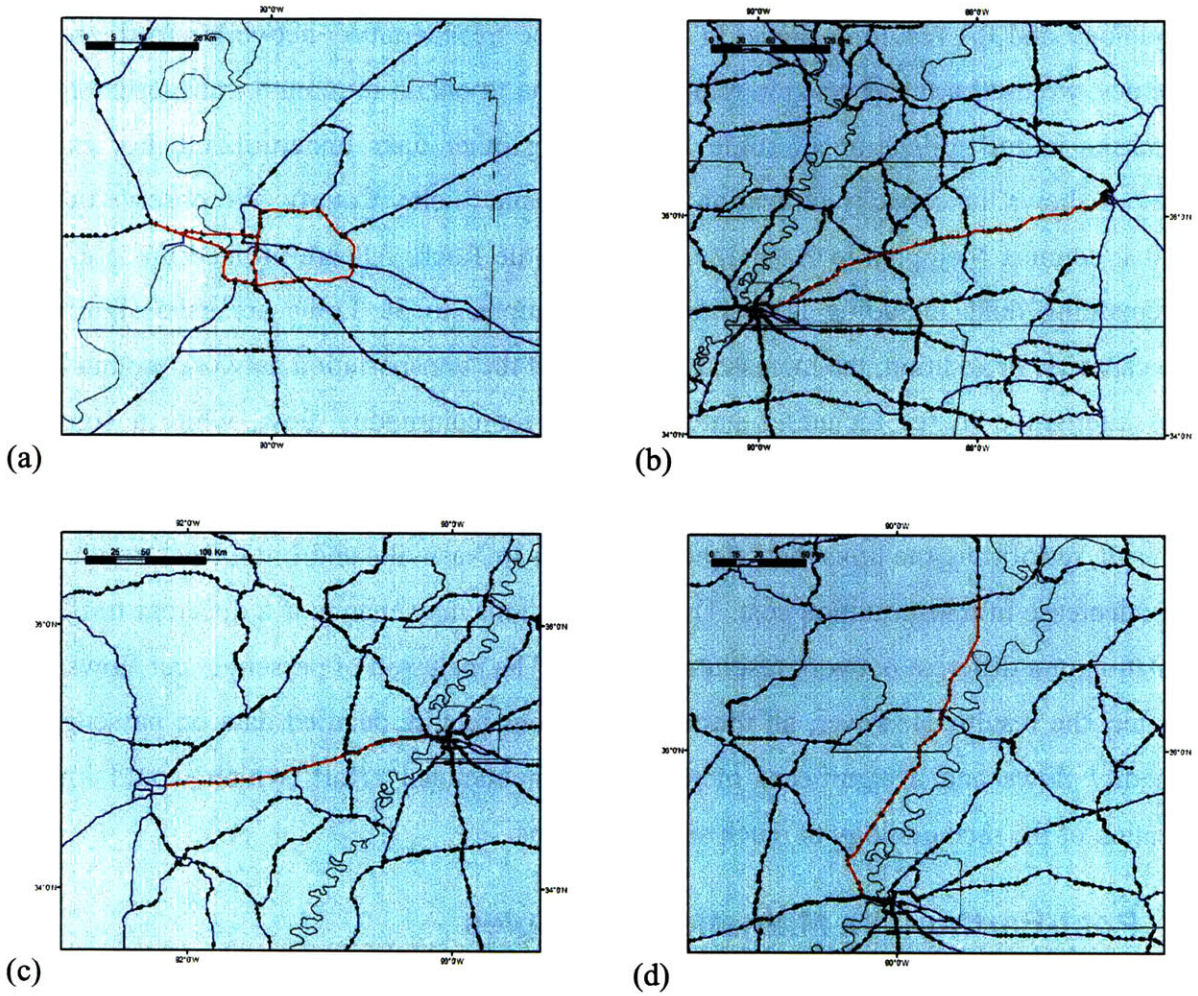

Figure 6-3: Retrofitted Routes (a) Route 1, Memphis Interstate Highway Links, (b) Route 2, Section of I-40 Connecting Memphis to Nashville, (c) Route 3, Section of I-40 Connecting Memphis to Little Rock, AR, and (d) Route 4, Section of I-55 Connecting Memphis to St. Louis, MO.

Table 6-8: Transportation Losses for Retrofitted Bridges on Selected Links

Loss ($M)	Nominal	Retrofitted Links				
		All	1, 2, 3, 4	1, 2	1, 3	1, 4
Transportation Cost	1,350	113	383	1,147	741	1,347

methodology and the resulting flows. In modeling the transportation network and the regional economies, we used a linear programming formulation to obtain minimum transportation costs. This results in full utilization of some links leaving other links underutilized. For example, Figure 6-4 shows the capacity utilization of links around Shelby County. We observe that only links that connect Memphis to Nashville, TN and Little Rock, AR are utilized up to capacity. The remaining links including I-55 connecting Memphis to St. Louis are used significantly below capacity. In addition, the increased resolution of the transportation network around NMSZ creates alternative routes including state highways for commodity flow, while a significant portion of these commodities are transported via interstate highways.

As a result, retrofitting the links that connect Memphis to Nashville and Little Rock results in the highest decrease in transportation cost. These observations may change if a different traffic flow formulation or a different network resolution is used. The inclusion of passenger car flows would also affect the results. However, all these modifications require detailed data on passenger and commodity flows and a significant increase in computational effort, which would limit the application of the methodology to much smaller regions.

6.2 Post-Earthquake Mitigation Strategies

Next, we evaluate the effectiveness of post-earthquake mitigation strategies including faster recovery of functionality for certain building occupancy classes and bridges along selected routes. The recovery rate of buildings and bridges can be increased by allocating more of the available post-earthquake resources to selected economic sectors or transportation links. One mechanism is to provide incentives for repair/restoration projects that are completed ahead of schedule or to provide immediate financial aid or loans to selected economic sectors.

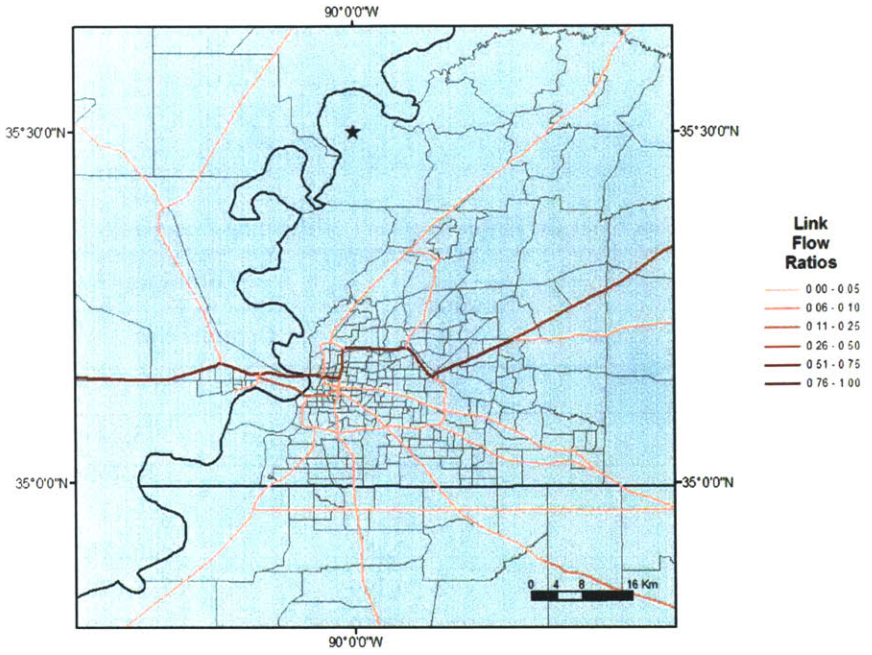

Figure 6-4: Link Capacity Utilization Ratios around Shelby County in Pre-Earthquake State

6.2.1 Faster Recovery of Buildings

In an approach similar to the retrofitting of buildings, we evaluate the effects on business losses of an increased recovery rate for commercial and industrial buildings. In each case, we increase the recovery rate of the buildings by 25% compared to the nominal rate. The results are presented in Table 6-9.

Increasing the recovery rate of commercial buildings is more effective in reducing business losses compared to industrial buildings. The decrease in value added losses for Shelby County, NMSZ, and the CUS region caused by the increased recovery rate of the two occupancy classes is about 15-16% and 5-6%, respectively. The value added losses for these three regions are smaller than those of the baseline scenario due to faster recovery of these sectors, whereas the value added losses at the national level do not change due to the effect of the slack in the economy. As in the case of building retrofit, the decrease in business loss is higher for faster recovery of commercial buildings because of the economic importance of the commercial sector.

Table 6-9: Business Losses for Faster Recovery of Building Occupancy Classes

Business Loss ($M)	Nominal	Building Occupancy Class	
		Commercial	Industrial
Shelby			
Production Losses	14,490	13,240	13,490
Direct	11,740	10,769	11,001
Indirect	2,750	2,471	2,489
Value Added Losses	7,789	6,959	7,428
Direct	6,309	5,670	6,041
Indirect	1,480	1,289	1,387
NMSZ			
Production Losses	27,164	24,771	25,342
Direct	22,220	20,205	20,760
Indirect	4,944	4,565	4,582
Value Added Losses	14,585	12,967	13,935
Direct	11,908	10,581	11,380
Indirect	2,677	2,386	2,555
CUS			
Production Losses	26,867	23,181	24,416
Direct	31,177	27,809	29,072
Indirect	-4,310	-4,627	-4,656
Value Added Losses	15,447	12,920	14,563
Direct	16,891	14,672	16,124
Indirect	-1,443	-1,753	-1,561
US			
Production Losses	-8,827	-8,828	-8,832
Direct	31,177	27,809	29,072
Indirect	-40,004	-36,637	-37,904
Value Added Losses	-339	-340	-342
Direct	16,891	14,672	16,124
Indirect	-17,230	-15,013	-16,466

6.2.2 Faster Recovery of Bridges

Finally, we investigate the effectiveness of increasing by 50% the recovery rate of bridges on the routes used in Section 0. The results for different cases are given in Table 6-10.

When the recovery rates of the network bridges on all links are increased by 50%, the transportation losses decrease by about 32%, to $924.4M. This loss is much higher than that observed from retrofit of all bridges, which was about $113M. The transportation costs do not change as much as when the same bridges are retrofitted. The main reason is that the functionality of a link is governed by the functionality and recovery rate of the bridge with the highest damage. Retrofitting bridges results in significantly reduced damaged ratios and much faster recovery. Note also that there is a significant difference between the damage factors assigned to extensive and complete damage state of bridges, 0.25 vs 1.00. A bridge in a complete damage state takes much longer to repair compared to one in the extensive damage state. Retrofitting bridges results in fewer bridges being in the complete damage state and significantly shortens the recovery time of the links, which cannot be matched by just increasing the recovery rate of bridges by 50%. On the other hand, the retrofitting of bridges would cost much more than increasing their recovery rate.

The results from faster recovery of bridge functionality for different transportation routes are qualitatively similar to those when the same bridges are retrofitted, although the decrease in transportation costs is smaller. Again the route connecting Memphis to Little Rock results in the highest decrease in transportation cost, followed by the section of I-40 connecting Memphis to Nashville. Increasing the recovery rate on the I-55 route connecting Memphis to St. Louis does not change the transportation cost for the reasons given in Section 0. The loss reduction obtained when the recovery rate of bridges on all four routes are increased is more significant (24%) than those obtained for individual routes.

Table 6-10: Transportation Losses for Faster Recovery of Bridges on Selected Links

Loss ($M)	Nominal	Links with Increased Recovery Rate				
		All	1, 2, 3, 4	1, 2	1, 3	1, 4
Transportation Cost	1,350	924	1,023	1,212	1,198	1,349

6.3 Concluding Remarks

The problem of assessing and prioritizing loss mitigation strategies is very complicated due to the difficulty of assessing costs and the social and political difficulties of implementing such measures. Here, we evaluated the effectiveness of several pre and post-earthquake loss mitigation strategies for a selected scenario earthquake without considering the associated costs.

For the selected scenario earthquake, retrofitting all buildings to high-code level results in a building loss reduction of about 35%. The decrease in value added loss for Shelby County and the NMSZ region was higher, about 45%. These values represent the maximum loss reduction that can be achieved by retrofitting buildings. The decrease in building loss for Shelby County is \$4.2B, which corresponds to 7.0% of the total building value within the region. The decrease in building losses for the NMSZ region, \$7.6, is approximately 3.8% of the total building value in that more extended region.

For this building retrofit strategy, we also evaluated the modified loss risk curves. The retrofit of buildings results in 36% and 34% reduction in expected annual losses (EALs) for Shelby County and the NMSZ region. The decrease in EAL for Shelby County is about 8.7M/year (without considering model/parameter uncertainty). Assuming a building lifetime of approximately 50 years, the expected loss reduction over 50 years corresponds to about 0.7% of the total building inventory value in Shelby County. Since the associated retrofit costs would likely far exceed this small percentage, retrofitting of buildings does not seem to be economically justified. However, when the loss reduction in business losses is accounted, retrofitting selected building structural and occupancy types, such as industrial buildings, may become economically feasible. Also, retrofitting might be effective in saving lives and reducing shelter requirements, two consequences that are not considered here.

If one considers loss reductions as fractions of the replacement value of the retrofitted buildings, one finds that retrofitting commercial buildings (13.7%) is more effective than retrofitting residential (5.7%) and industrial buildings (8.2%). The normalized gains are the smallest for residential buildings.

When retrofitting selected building structural types, the highest loss reduction comes from URM and wood buildings, which account for the majority of the building stock, followed by steel and concrete buildings. However, when one normalizes the loss reduction by the building inventory

value of each structural class, retrofitting URM buildings proves to be the most efficient option (23.8%), followed by concrete buildings (12.5%) and steel buildings (9.0%). The lowest normalized loss reduction is obtained for wood buildings (3.0%). In terms of business losses, retrofitting of concrete and steel buildings is the most effective strategy since concrete and steel buildings account for a significant portion of the industrial and commercial facilities. The smallest business loss reduction is obtained by retrofitting wood buildings.

Another pre-earthquake mitigation strategy evaluated was the retrofitting of bridges on selected routes. This action reduces the increase in transportation costs due to network damage. Among the routes considered, the links connecting Memphis to Little Rock and Memphis to Nashville resulted in highest transportation loss reductions. These are the routes with highest truck flows prior to the earthquake. However, this conclusion is sensitive to earthquake location, traffic flow formulation, and transportation network resolution.

Post-earthquake mitigation strategies included faster recovery of functionality for building occupancy classes and bridges. As in the case of building retrofit, increasing the recovery rate of commercial buildings is found to be more effective in reducing business losses compared to industrial buildings. Also, increasing the recovery rate of bridges on the route connecting Memphis to Little Rock results in the highest decrease in transportation costs. The reductions in business or transportation losses through increasing recovery rates are smaller than those achieved through retrofitting buildings or bridges. However, the cost of implementing these post-earthquake strategies is also much lower.

To better evaluate the effectiveness of alternative mitigation options, a more detailed analysis that involves many more scenario earthquakes should be performed. One possible option is to use the simplified methodology described in Chapter 5, which uses only a few scenario earthquakes. These earthquakes may be used to evaluate the system under various conditions and assess risks under mitigated and unmitigated conditions. However, quantification of the associated costs would again be a determinant factor in evaluating the relative and absolute merit of alternative strategies.

7 Summary, Conclusions and Future Work

In this thesis, we developed and used a loss estimation methodology to accomplish three main objectives: (1) evaluate economic losses from scenario earthquakes at regional/national scales with special consideration for the effects of transportation network vulnerability; (2) assess earthquake loss uncertainties at different temporal and spatial scales, and (3) evaluate pre- and post-earthquake loss mitigation measures.

While the developed methodology is conceptually applicable to any region, we have focused our numerical work on the Central U.S. (Chapter 3). The economic consequences include a variety of loss including the cost of building repair, losses due to business interruption, and increased transportation costs. The loss assessment methodology includes spatial interactions (through the transportation network) and business interaction (through an input-output model) and extends geographically to the entire conterminous U.S. The loss evaluation algorithm is however efficient and suitable for sensitivity and uncertainty analysis (Chapter 4). Using a model of regional seismicity and considering many sources of uncertainty, we developed risk curves for building losses, business losses, and total economic losses (Chapter 5). Finally, we evaluated the effectiveness of various pre- and post-earthquake mitigation strategies including retrofitting of buildings or bridges and faster recovery of functionality for various occupancy classes or bridges (Chapter 6).

The following sections summarize the main findings and conclusions of this study and make recommendations for future work.

7.1 Summary and Conclusions

In ***Chapter 3***, we described the general framework of the loss estimation methodology and provided details on its various component models. The methodology is comprehensive in that it involves relatively detailed calculation of building damages and losses, models for loss of functionality and recovery of infrastructure components over time, and integrated analysis of the

transportation network and the regional economies. The calculated quantities include building repair restoration costs, production losses, value added losses, and increased transportation costs. The methodology is unique in that the economic sectors and the transportation network are modeled in an integrated manner and losses are evaluated at different regional scales. In general, due to computational or data requirements, previous studies were limited to the regional scale.

The loss estimation model is flexible and modular, so that alternative models or sets of parameters can be easily used. Also, the calculation of building damages and losses requires much less computation time than similar existing tools such as HAZUS. Since HAZUS runs on a GIS platform, its memory requirements are significant and this limits its applicability to regions smaller than that considered in this study. Also, the evaluation of scenario earthquake losses with HAZUS requires significantly more computational time since the code aggregates and extracts data from GIS databases, while our methodology uses data from pre-prepared input files. In Chapters 4 and 5, we made use of the computational efficiency and flexibility of the algorithm to first perform a detailed sensitivity analysis of earthquake losses and then develop loss risk curves for selected regions of interest.

In ***Chapter 4***, we applied the loss estimation methodology to a scenario earthquake and assessed the sensitivity of the losses to various model components and parameters.

We first presented the results for a moment magnitude M7.5 New Madrid Seismic Zone (NMSZ) earthquake. We specifically discussed the level and spatial distribution of ground motion intensity, building damage and loss, bridge damage and loss, transportation link functionality and flows, and business interruption losses. For the selected scenario earthquake, about half of the total building losses is from buildings within Shelby County. The losses from drift and acceleration sensitive non-structural building components are each about twice the loss from structural building components. Bridge repair costs are much less than the total building loss. The increase in transportation cost due to damage to the transportation network is higher than the direct bridge repair cost. The recovery of transportation capacity is controlled mainly by the bridges in the complete damage state. The value added losses from Shelby County and the NMSZ region are about 65-70% of the building loss within these regions and the majority of these losses are from loss of functionality due to building damage. In the CUS and the US, we observed negative indirect value added losses (i.e. gains) as a result of increased productions in

undamaged regions to make up for the lost production in the damaged regions. The business losses or gains at the national level are sensitive to the slack in production capacity. In particular, business losses increase significantly in the absence of slack.

The subsequent sensitivity analysis investigated the effect on the losses of using alternative models and parameters in various parts of the methodology. The parameters considered include earthquake magnitude and epicentral location, ground motion attenuation, local amplification effects, building vulnerability, the effectiveness of traffic flow rerouting, the functionality of industrial facilities, the borrowing costs for reconstruction spending, functionality interactions, and slack in production.

As one would expect, the building losses are very sensitive to earthquake magnitude and the distance of the epicenter from Shelby County. In addition, earthquakes modeled as line sources rather than point sources produce higher losses since there is greater amount of inventory close to a line source. These sensitivities point at the importance of accurately modeling characteristic earthquakes in the New Madrid Seismic Zone. Attenuation relations, building code level and soil class are all important parameters, while the sensitivity to soil amplification factors and building vulnerability parameters was not as high.

In general, the trends for building losses apply also to business losses, especially for regions close to the earthquake epicenter such as Shelby County and the NMSZ region (see Figure 3-2) since the level of building damage determines the recovery times for buildings and economic sectors. The business losses are more sensitive than the building losses to many of the above parameters. Business loss at the national level is significantly affected by the slack in production capacity and its magnitude is much smaller than the building loss, as regions outside the immediately affected area increase their productions to make up for lost capacity in the damaged region. However, in a fully constrained economy, i.e. in the case of no slack, the business losses at the national level increase significantly and may even exceed the building losses.

In ***Chapter 5***, we quantified uncertainty on the losses and developed risk curves for building, value-added, and total losses for Shelby County and the NMSZ region.

We first used a stochastic regional seismicity model with other models/parameters at their nominal values to develop risk curves for building losses. This is the first time that the regional loss risk curves are being generated by using a detailed model of regional seismicity. This was

made possible by the computational efficiency of the building loss estimation model. We then added the contribution of model/parameter uncertainty to the building losses using a constant coefficient variation of building losses. This was based on the results of analysis of variance (ANOVA) for several scenario earthquakes, where we performed a full factorial analysis of building losses considering alternative attenuation relations, site amplification models and the two building vulnerability parameters. The developed loss risk curves matched very well with those calculated using the probabilistic seismic hazard maps. First, the probabilistic seismic ground motions for each analysis region for different return periods are extracted from seismic hazard maps and then the vulnerability parameters that were derived for use with these ground motions are used to calculate corresponding building losses.

To obtain risk curves for value added losses in Shelby County and the NMSZ region, we used a relation between value added losses and building losses. This relation was determined from loss results obtained under several scenario earthquakes with different magnitudes and locations. This almost deterministic relation is valid for regions close to the earthquake epicenter. In these regions, business losses depend mainly on the functionality and recovery of the facilities, which is largely determined by the building damage level.

The results underline the importance of considering uncertainty in risk assessment. Expected annual building losses and expected annual value-added losses increase significantly when model/parameter uncertainty is included in the analysis. The increase in value added losses is much higher than that in building losses since the business losses are affected by uncertainty on models used in both building and business loss estimation. Also, the rupture models for the characteristic NMSZ earthquakes have a significant effect on expected annual losses. Assuming complete rupture of the NM faults results in approximately 20% higher expected annual losses than when one assumes partial rupture of the faults. This significant difference in seismic risk highlights the importance of more accurately modeling the seismic events in NMSZ.

We compared the results using a detailed seismicity model or alternatively a small number of scenario earthquakes. We assigned nominal occurrence rates to the scenario events so that the hazard generated by the selected events approximately matches the hazard from more detailed analysis. We applied the methodology to a small set of earthquakes on the New Madrid (NM) faults to obtain hazard consistent occurrence rates and then developed loss risk curves for

building and value added losses using the scenario earthquake seismicity model. The risk curves and expected annual are comparable to those from a more detailed model of seismicity.

In **Chapter 6**, we evaluated the effectiveness of alternative pre- and post-earthquake loss mitigation strategies for a selected scenario earthquake. Pre-earthquake mitigation strategies include retrofitting of different types of buildings and the hardening of bridges on selected transportation links. Post-earthquake mitigation strategies include faster recovery of buildings and bridges. We focused on evaluation of the effectiveness of the above mitigation options, without considering the monetary and non-monetary costs of implementing these strategies.

For the selected scenario earthquake of magnitude M7.5 at (35.50°W; 90.00°N), retrofitting all buildings to high-code level results in a building loss reduction of about 35%. The decrease in value added losses for Shelby County and the NMSZ region was much higher, about 45%. The decrease in building loss for Shelby County is $4.2B, which corresponds to 7.0% of the total building value within the region. The decrease in building losses for the NMSZ region, $7.6, is approximately equal to 3.8% of the total building value. For this case, we also developed loss risk curves under retrofitted conditions.

The retrofit of buildings results in 36% and 34% reduction in expected annual losses (EALs) of the Shelby County and the NMSZ region. Assuming a lifetime of approximately 50 years for the buildings, the decrease in EAL of Shelby County over 50 years corresponds to about 0.7% of the building value. This will not justify the retrofitting of buildings as retrofitting costs will be higher than this small percentage. However, when the reductions in contents and business losses are considered, the relative benefit from the retrofitting of buildings will increase, especially when building classes or types that significantly affect business losses (e.g. industrial buildings) are upgraded. Reducing the seismic vulnerability of buildings over time by upgrading seismic design levels may be a more suitable alternative for the CUS region since the cost of constructing new buildings using higher design standards is much lower than that of retrofitting existing buildings.

Among different building occupancy classes upgraded, retrofitting of commercial buildings (13.7%) is more effective than retrofitting of the residential (5.7%).and industrial buildings (8.2%). In case of business losses, retrofitting of commercial buildings resulted in the highest lost reduction (31%), while no loss reduction was observed in case of residential buildings since they are not mapped onto any economic sector. However, when the loss reductions as fractions

of retrofitted building value are considered, industrial buildings (74%) proved to be more effective than commercial buildings (28%).

When retrofitting selected structural types, the highest loss reduction comes from URM buildings, which are seismically more vulnerable than other structural classes and constitute a significant portion of the building stock. When the loss reductions are expressed as fractions of the replacement value of the specific structural classes, retrofitting of URM buildings prove to be the most efficient option, 23.8%, followed by retrofitting of concrete buildings (12.5%) and steel buildings (9.0). The lowest normalized loss reductions are observed in case of wood buildings (3.0%). In terms of business losses, retrofitting of concrete and steel buildings is the most effective strategy since concrete and steel buildings account for a significant portion of industrial and commercial facilities.

Retrofitting of bridges along selected routes reduces the transportation cost due to network damage. This is true mainly for bridges on transportation links with the highest truck flows prior to the earthquake, for example on the route connecting Memphis to Little Rock. These results may be sensitive to the location of the scenario earthquake and may change if more detailed network representation is used or passenger cars are included in the analysis. However, the scenario earthquake analyses provide some useful insight into the effectiveness of bridge retrofit.

For the post-earthquake mitigation option of increasing the recovery rate of buildings, commercial buildings are observed to be more effective in reducing business losses than the industrial buildings. Similarly, increasing the recovery rate of bridges on the routes with higher pre-earthquake truck flows results in the highest decrease in transportation costs. The reductions in business or transportation losses from increasing the recovery rate of buildings or bridges are lower than those achieved through retrofitting of buildings or bridges. However, the costs of implementing these post-earthquake strategies are lower than those of the pre-earthquake mitigation options.

7.2 Future Research Directions

Below is a short list of possible research areas and issues that can be addressed in future studies regarding the methodology and its applications.

Transportation network analysis: We used a linear programming formulation to model only commodity/truck flows without considering passenger flows. Congestion can be modeled by introducing non-linear link cost functions at the expense of additional computational effort. In addition, cross-hauling and passenger flows can be introduced in the model through additional modifications. This would require a path based formulation and detailed data on both commodity and passenger flows. These additional computational and data requirements would limit the geographical scope of the analysis.

Economic analysis and data: The economic data used in this study were obtained at the state level and then disaggregated to the county or census tract level based on population. Obtaining data at finer scales would improve the accuracy of the loss estimates by better representing the spatial distribution of economic activities. However, this should also be accompanied by a refined classification of buildings and, perhaps more importantly, of the economic sectors. Using a more detailed commodity classification would help better model the interactions among different sectors. Since the business losses are shown to be very sensitive to slack in production, this parameter and its effects on the system should be studied in greater detail. Also, the effect of inventory and business relocation may be important.

Sensitivity Analysis: The sensitivity analysis performed here was mainly limited to a single scenario earthquake, although in some cases sensitivity of the loss risk curve was also considered. The analysis may be extended to other earthquake locations and magnitudes to develop a better understanding of the effect of different components. Also different building and economic sector classifications could be used to study the effects of the classification system on the losses.

Uncertainty analysis: In this study, we used detailed models of regional seismicity to model uncertainty in earthquake location and magnitude. We also performed ANOVA to quantify uncertainty in scenario earthquake losses. For this purpose, we evaluated losses for a number of scenario earthquakes through a factorial analysis using all combinations of attenuation relations, soil amplification models, and building vulnerability parameters. The ANOVA results indicate that the interaction effects between the parameters are negligible. These results can be used to further simplify the uncertainty model by considering only main effects.

Evaluation of mitigation strategies: We have evaluated the effectiveness of selected pre- and post-earthquake mitigation strategies mainly using a scenario earthquake. Future studies may consider additional scenarios in the evaluation of these strategies. In addition, the costs of alternative mitigation strategies should be evaluated to provide better support for decision analysis.

REFERENCES

Abrahamson, N.A., and Shedlock, K.M. (1997). "Overview." *Seismological Research Letters*, 68(1), 9-23.

Al-Momani, N.M., and Harrald, J.R. (2003). "Sensitivity of earthquake loss estimation model: How useful are the predictions?" *International Journal of Risk Assessment and Management*, 4(1), 1-19.

ATC (1985). *Report ATC-13: Earthquake Damage Evaluation Data for California*. Redwood City, CA: Applied Technology Council.

ATC (1996). *Report ATC-40: Seismic Evaluation and Retrofit of Concrete Buildings*. Redwood City, CA: Applied Technology Council.

Atkinson, G. (1993). "Source spectra for earthquakes in eastern North America." *Bulletin of Seismological Society of America*, 74(1), 1969-1993.

Atkinson, G., and Mereu (1993). "The shape of ground motion attenuation curves in southeastern Canada." *Bulletin of Seismological Society of America*, 82, 2014-2031.

Atkinson, G.M., and Boore, D.M. (1995). "New ground motion relations for eastern North America." *Bulletin of Seismological Society of America*, 85, 17-30.

Atkinson, G.M., and Boore, D.M. (1997). "Some comparisons between recent ground-motion relations." *Seismological Research Letters*, 68(1), 24-40.

Atkinson, G.M., and Boore, D.M. (1998). "Evaluation of models for earthquake source spectra in Eastern North America." *Bulletin of Seismological Society of America*, 88(4), 917-934.

Bauer, R.A. (1997) *Compilation of Databases and Map Preparation for Regional and Local Seismic Zonation Studies in the CUSEC Region: Collaborative Research*, US Geological Survey Award 1434-HQ-97-GR-03150.

Bazzurro, P. and Luco, N. (2004). "Effects of different sources of uncertainty and correlation on earthquake-generated losses." *IFED - International Forum on Engineering Decision Making*, Stoos, Switzerland, December 5-8.

BEA, (2005). "www.bea.gov" Bureau of Economic Analysis.

Bendimerad, F. (2001). "Loss Estimation: A powerful tool for risk assessment and mitigation." *Soil Dynamics and Earthquake Engineering*, 21, 467-472.

Boore, D., and Atkinson, G.M. (1987). "Stochastic prediction of ground motion and spectral response parameters at hard-rock sites in eastern North America." *Bulletin of Seismological Society of America*, 77, 440-467.

Boore, D., and Joyner, W. (1991). "Estimation of ground motion at deep soil sites in eastern North America." *Bulletin of Seismological Society of America*, 81, 2167-2185.

Borcherdt, R.D., (2002). "Empirical evidence for site coefficients in building code provisions." *Earthquake Spectra*, 18(2), 189-217.

Bozorgnia, Y., and Campbell, K.W. (2004). "Engineering characterization of ground motion." In *Earthquake Engineering - From Engineering Seismology to Performance Based Engineering*. Bozorgnia, Y., and Bertero, V.V (Eds.), CRC Press.

Brookshire, D.S., Chang, S.E., Cochrane, H., Olson, R.A., Rose, A., and Steenson, J. (1997). "Direct and indirect economic losses from earthquake damage." *Earthquake Spectra*, 13(4), 683-701.

BTS (1997). "Truck movements in America: Shipments from, to, within, and through states. BTS/97-TS/1." *U.S. Department of Transportation, Bureau of transportation Statistics,* Washington, DC.

BTS (1998). "Journal of transportation and statistics, special issue on the Northridge earthquake." *U.S. Department of Transportation, Bureau of transportation Statistics,* 1(2).

BTS (1999). *Commodity Flow Survey, 1997*. Bureau of Transportation Statistics, CDROM.

BTS (2002). *National Transportation Atlas Database*. Bureau of Transportation Statistics, CDROM.

Caltrans (1994). "The continuing challenge: the Northridge earthquake of 17 January 1994." *Seismic Advisory Report*, California Department of Transportation, Sacramento, CA.

Campbell, K.W. (2001). *Development of Semi-Empirical Attenuation Relationships for CEUS.* U.S. Geological Survey Award HQGR0011, Final Report.

Campbell, K.W. (2003). "Engineering models of strong ground motion." In *Earthquake Engineering Handbook*. Chen W.F. and Scawthorn C. (Eds.), CRC Press.

Campbell, K.W. (2003). "Prediction of strong ground motion using the hybrid empirical method and its use in the development of ground-motion (attenuation) relations in Eastern North America." *Bulletin of Seismological Society of America*, 93(3): 1012-1033.

Campbell, K.W., and Seligson, H.A. (2003) "Quantitative method for developing Hazard consistent earthquake scenarios." *Advancing Mitigation Technologies and Disaster Response for Lifeline Systems. Proceedings of the Sixth U.S. Conference and Workshop on Lifeline Earthquake Engineering*, August 10-13, 2003, Long Beach, CA, 829-838.

CSSC (1999). "Earthquake risk management: A toolkit for decision-makers." *California Seismic Safety Commission, CSSC Report 99-04,* Sacramento, CA.

Chandler, A. M. and Nelson, T. K. L. (2001). "Performance-based design in earthquake engineering: A multi-disciplinary review." *Engineering Structures*, 23, 1525-1543.

Chang, E., Ziliaskopoulos, A., Boyce, D., and Waller, S.T. (2001). "Solution algorithm for combined interregional commodity flow and transportation network model with link capacity constraints." *Transportation Research Record,* 1771, 114-123, Paper No. 01-2514.

Chang, S.E., Shinozuka, M., and Moore II, J.E. (2000). "Probabilistic earthquake scenarios: extending the risk analysis methodologies to spatially distributed systems." *Earthquake Spectra*, 16(3), 557-572.

Chang, S.E., and Nojima, N. (2001). "Measuring post-disaster transportation system performance: the 1995 Kobe earthquake in comparative perspective." *Transportation Research Part A*, 35, 475-494.

Cho, S., Gordon, P., Richardson, H.W., Moore II, J.E. and Shinozuka, M. (2000). "Analyzing transportation reconstruction network strategies: a full cost approach." *Review of Urban and Regional Development Studies*, 13(3).

Cho, S., Gordon, P., Moore II, J.E., Richardson, H.W., Shinozuka, M., and Chang, S. (2001). "Integrating transportation network and regional economic models to estimate the costs of a large urban earthquake." *Journal of Regional Science*, 41(1), 39-65.

Coburn, A.W., Sspence, R. J. S., Pomonis, A. (1994). "Vulnerability and risk assessment." *Disaster Management Training Programme (DMTP) of the United Nations Development Programme (UNDP),* Cambridge Architectural Research Limited, Cambridge, UK.

Czyzyk, J. Stolarski, M., and Wright, S.J. (1997). *PCx User Guide: Windows 95/NT Supplement.* Technical Report OTC 97/03.

DesRoches, R. (2002). "*Bridge fragility.*" Personal Communication.

Dobry, R., Borcherdt, R.D., Crouse, C.B., Idriss, I.M., Joyner, W.B., Martin, G.R., Power, M.S., Rinne, E.E., and Seed, R.B. (2000). "New site coefficients and site classification system used in recent building seismic code provisions." *Earthquake Spectra*, 16(1), 41-67.

Dowrick, D. (2003). Earthquake Risk Reduction. John Wiley& Sons, West Sussex, England.

EERI (1984). "Glossary of terms for probabilistic seismic-risk and hazard analysis." *Earthquake Spectra*, 1, 33-40.

EERI (1997). "Theme issue: Earthquake loss estimation." *Earthquake Spectra*, 13(4).

EPRI (1993). *Guidelines for Determining Design Basis Ground Motions, Early Site Permit Demonstration Program, RP3302*, Vol.1. Electric Power Research Institute, Palo Alto, CA.

FEMA (1988). *Rapid Visual Screening of Buildings for Potential Seismic Hazards: A Handbook. FEMA 154.* Federal Emergency Management Agency, Washington, D.C.

FEMA (1989). *Estimating Losses from Future Earthquakes. Panel Report (A Non-Technical Summary), FEMA 176,* Federal Emergency Management Agency, Washington, D.C.

FEMA (1992). *NEHRP Handbook for the Seismic Evaluation of Existing Buildings. FEMA-178.* Federal Emergency Management Agency, Washington, D.C.

FEMA (1997). *NEHRP Guidelines for the Seismic Rehabilitation of Buildings, FEMA-273.* Federal Emergency Management Agency, Washington, D.C.

FEMA (1998). *Handbook for the Seismic Evaluation of Buildings –A Prestandard. FEMA 310.* Federal Emergency Management Agency, Washington, D.C.

FEMA (2000). *Prestandard and Commentary for the Seismic Rehabilitation of Buildings. FEMA 356,* Federal Emergency Management Agency, Washington, D.C.

FHWA (2000). *National Bridge Inventory.* Federal Highway Administration, CDROM.

Frankel, A.D., Mueller, C.S., Barnhard, T.P., Perkins, D.M., Leyendecker, E. V., Dickman, N.C., Hanson, S.L., Hopper, M.G. (1996), *National Seismic Hazard Maps: Documentation June 1996*, U.S. Geological Survey, Open File Report 96-532.

Frankel, A.D., Mueller, C.S., Barnhard, T.P., Leyendecker, E.V., Wesson, R.L., Harmsen, S.C., Klein, F.W., Perkins, D.M., Dickman, N.C., Hanson, S.L., and Hopper, M.G. (2000). "USGS national seismic hazard maps." *Earthquake Spectra*, 16(1), 1-19.

Frankel, A.D., Petersen, M.D., Mueller, C.S, Haller, K.M., Wheeler, R.L., Leyendecker, E.V., Wesson, R.L., Harmsen, S.C., Cramer, C.H., Perkins, D.M., and Rukstales, K.S. (2002). *Documentation for the 2002 Update of the National Seismic Hazard Maps*. U.S. Geological Survey, Open File Report 02-420.

Ghobarah, A. (2000). "Seismic assessment of existing RC structures." *Progress in Structural Engineering and Materials*, 2, 60-71.

Grossi, P.A. (2000). "Quantifying the uncertainty in seismic risk and loss estimation." *Proceedings of the Second Euro Conference on Global Change and Catastrophe Risk Management: Earthquake Risks in Europe*. Laxenburg, Austria, July 6-9.

Hawkins, M. (Ed.) (1986). *Seismic Design for Existing Structures. ACI-SCM-14,* American Concrete Institute, MI.

Hwang. H., Lin, H. and Huo, J.R. (1997). "Site coefficients for design of buildings in eastern United States." *Soil Dynamics and Earthquake Engineering*, 16, 29-40.

Hwang, H., Jernigan, J.B., and Lin, Y.W. (2000). "Evaluation of seismic damage to Memphis bridges and highway system." *Journal of Bridge Engineering*, ASCE, 5(4), 322-330.

IBC (2000). *International Building Code*. International Code Council, Falls Church, VA.

Jammalamadaka, P.R.K. (2003). *Uncertainty and Sensitivity in Regional Earthquake Loss Estimation*. MS Thesis, Department of Civil and Environmental Engineering, MIT, Cambridge, MA.

Kim, T.J., Ham, H., and Boyce, D.E. (2002). "Economic impacts of transportation network changes: Implementation of a combined transportation network and input-output model." *Papers in Regional Science*, 81, 223-246.

Kircher, C.A., Nassar, A.A., Kustu, O., Holmes, W.T. (1997). "Development of building damage functions for earthquake loss estimation." *Earthquake Spectra*, 13(4), 663-682.

Kircher, C.A., Reitherman, R.K., Whitman, R.V., and Arnold, C. (1997). "Estimation of earthquake losses to buildings." *Earthquake Spectra*, 13(4), 703-720.

Kramer, S.L. (1996). *Geotechnical Earthquake Engineering*. Prentice Hall, NJ.

Kramer, S.L, and Stewart, J.P. (2004). "Geotechnical aspects of seismic hazards." In *Earthquake Engineering - From Engineering Seismology to Performance Based Engineering*. Bozorgnia, Y., and Bertero, V.V (Eds.), CRC Press.

Krawinkler, H. and Seneviratna, G.D.P.K. (1997). "Pros and cons of a pushover analysis of seismic performance evaluation." *Engineering Structures,* 20 (4), 452-464.

Kunnumkal, S. (2002). *Multi-Resolution Analysis of Earthquake Losses*. MS Thesis, Department of Civil and Environmental Engineering, MIT, Cambridge, MA.

Lawson, A.M., Bersani, K.S., Fahim-Nader, M., and Guo, J. (2002). "Benchmark input-output accounts of the United States, 1997", *Survey of Current Business*, 19-109.

Lee, T-H., and Mosalam, K.M. (2003). "Sensitivity of a seismic demand of a reinforced concrete shear-wall building." *Proceedings of Ninth International Conference on Application of Statistics and Probability in Civil Engineering (ICASP)*, San Francisco, CA, USA, July 6-9.

Marcellini, A., Daminelli, R., Franceschina, G., and Pagani, M. (2001). "Regional and local seismic hazard assessment." *Soil Dynamics and Earthquake Engineering*, 21, 415-429.

McGuire, R.K. (2004). *Seismic Hazard and Risk Analysis*. Oakland, CA. Earthquake Engineering Research Institute.

Newmark, N.M. and Hall, W.J. (1976). "Seismic design spectra for nuclear reactor facilities." *Proceedings of the Fourth World Conference on Earthquake Engineering*, Elsevier Science, Ltd., Oxford.

NIBS (2000). *HAZUS Technical Manuals*. National Institute of Building Sciences, Washington, D.C.

Okuyama,Y., G.J.Hewings, T.J.Kim, D.F.Boyce, H.Ham, and J.Sohn (1999). "Economic Impacts of an Earthquake in the New Madrid Seismic Zone. A Multiregional Analysis." *Proceedings, 5th U.S Conference on Lifeline Earthquake Engineering*, Seattle, WA, U.S Geological Society.

Porter, K.A., Kiremidjian, A.S., and LeGrue, J.S. (2001). "Assembly-based vulnerability of buildings and performance evaluation." *Earthquake Spectra*, 17(2), 291-312.

Porter, K.A. (2002). "Sensitivity of building loss estimates to major uncertain variables." *Earthquake Spectra*, 18 (4): 719-743.

Porter, K.A. (2003). "Seismic vulnerability." In *Earthquake Engineering Handbook*. Chen W.F. and Scawthorn C. (Eds.), CRC Press.

Rojahn, C., King, S.A., Scholl, R.E., Kiremidjian, A.S., Reaveley, L.D., and Wilson, R.R. (1997). "Earthquake damage and loss estimation methodology and data for Salt Lake County, Utah (ATC-36)." *Earthquake Spectra*, 13(4): 623-642.

Rose, A., Benavides, J., Chang, S.E., Szczesniak, P., Lim, D. (1997). "The regional economic impact of an earthquake: Direct and indirect effects of electricity disruptions." *Journal of Regional Science*, 37(3), 437-458.

Scarlat, A.S. (1996). *Approximate methods in structural seismic design*. E&FN Spon, London.

Shinozuka, M., Chang, S.E., Eguchi, R.T., Abrams, D.P., Howard, H.M., and Rose, A. (1997). "Advances in earthquake loss estimation and application to Memphis, Tennessee." *Earthquake Spectra*, 13(4), 739-758.

Silva, W., and Darragh, R.B. (1995). *Engineering Characterization of Strong Ground Motion Recorded at Rock Sites*. EPRI Report TR-102262.

Sohn, J., Hewings, G.J.D., Kim, T.J., Lee, J.S., and Jang, S. (2001). "Economic assessment of earthquake impacts on transportation networks: A scenario analysis". *REAL 01-T-16.*, Regional Economics Laboratory, IL.

Somerville, P.G., Collins, N., Abrahamson, N.A., Graves, R., and Saikia, C. (2001). *Ground Motion Relations for the Central and Unite States*. U.S. Geological Survey Award 99HQGR0098, Final Report.

Toro, G., Abrahamson, N., and Schneider, J. (1993). "Engineering model of string ground motions from earthquakes in central and eastern United States." *Earthquake Spectra*, submitted.

Toro, G.R., Abrahamson, N.A., and Schneider, J.F. (1997). "Engineering model of strong motions from earthquakes in the Central and Eastern United States." *Seismological Research Letters*, 68(1), 41-57.

Veneziano, D., Gupta, U., Kunnumkal, S.M., and Sussman, J.M. (2002). "Earthquake Loss under Limited Transportation Capacity: Assessment, Sensitivity, and Mitigation." *7th National Conference on Earthquake Engineering*, Boston, MA.

Wells, D.L., and Coppersmith, K.J. (1994) "New empirical relationships among magnitude, rupture length, rupture width, rupture area, and surface displacement." *Bulletin of Seismological Society of America*, 84(4), 974-1002.

Werner,S., Taylor, C., Moore, J., and Walton, J. (2000). *A Risk-Based Methodology for Assessing the Seismic Performance of Highway Systems*. Technical Report, Multidisciplinary Center for Earthquake Engineering Research, Buffalo, New York.

Whitman, R.V., Anagnos, T., Kircher, C.A., Lagorio, H.J., Lawson, R.S., and Schneider, P. (1997). "Development of a national earthquake loss estimation methodology." *Earthquake Spectra*, 13(4), 643-661.